THE EFFECTS OF LCN2 AND IRON ON CARDIAC REMODELING AND THE IMPACT ON CARDIAC FUNCTION

HYEKYOUNG SUNG

A DISSERTATION SUBMITTED TO THE FACULTY OF GRADUATE STUDIES IN PARTIAL FULFILLMENT OF THE REQUIREMENTS FOR THE DEGREE OF

DOCTORAL OF PHILOSOPHY

GRADUATE PROGRAM IN BIOLOGY
YORK UNIVERSITY
TORONTO, ONTARIO

AUGUST 2017

ABSTRACT

Lipocalin-2 (Lcn2; also termed neutrophil gelatinase-associated lipocalin (NGAL)) is a proinflammatory factor which is elevated in obese individuals. It has also been implicated in the pathogenesis of heart failure and as a potential biomarker. This thesis exaimed: project 1: Regulation of autophagy by Lcn2 and its functional significance in leading to insulin resistance in cardiomyocytes, project 2: Changes in cardiac function, autophagy and cell death in wild type and Lcn2-knockout mice subjected to chronic myocardial ischemia, and project 3: Effect of iron on insulin sensitivity in cardiomyocytes and mechanistic role of oxidative stress.

Findings from project 1 indicated that Lcn2 treatment caused insulin resistance and use of gain and loss of function approaches elucidated a causative link between autophagy inhibition and regulation of insulin sensitivity in response to Lcn2. Project 2 data demonstrated that Lcn2 attenuated autophagy to worsen the extent of apoptosis induced by chronic myocardial ischemia in mice. Finally, in project I showed that iron directly induced insulin resistance in cardiomyocytes and that this involved regulation of the crosstalk between autophagy and oxidative stress.

In summary, my studies demonstrated that Lcn2 promoted cardiac dysfunction and that lack of Lcn2 in mice was protective against surgically-induced heart failure. Inhibition of autophagy played a central mechanistic role in mediating the detrimental effects of Lcn2 on the heart, which included elevated oxidative stress, cell death and insulin resistance.

ACKNOWLEDGEMENTS

I would like to take this opportunity to first thank Dr. Gary Sweeney, my supervisor, for his constant support, encouragement and advice, I will always be grateful for. It is with his guidance, expertise and patience that I have been able to arrive at this milestone in my academic career. Next, I would like to express my heartfelt gratitude to my committee members: Dr. Chun Peng, Dr. Michael Schied, Dr. Robert Tsushima, Dr. Christopher Perry and Dr. Jonathan Schertzer, for their time and support in the discussion and revision of my thesis.

A very big thank to all past and present members of the Sweeney Lab. Your friendship and day-to-day support have meant so much to me during the past four years and I could not have made it to this point without them. A special thank to Dr. Carol Chan, James Won Suk Jahng and Erica Hee Ho Cho for always being there for me and willing to give a helpful hand, or an attentive ear. Also, to my best friend KyoungMin Kim, who has always been cheering my works, and church friends, Julia SunJin Park, JeongAe Lee and SungYeon Yoon, whom I can always be relied upon to, gave excellent advice, and supported me.

Last but not least, a sincere thank to my loving family. To my parents and parents in law for their love and steadfast support for my efforts, and to my little princess Subin Park for making me happy and giving me energy everyday.

A special thank to my sweet husband, Jin Woo Park, you have always been beside me and supported my career decisions. You were constantly loving, inspiring, motivating and supporting me and I know that you will be with me for the rest of our challenges throughout life. This could not have been possible without you all.

TABLE OF CONTENTS

LIST OF FIGURES

LIST OF ABBREVIATIONS:

Abbreviation	Definition
ACD	Autophagic cell death
Akt (S473)	phosphorylated Akt Serine-473
Akt (T308)	phosphorylated Akt Threonine-308
AMBRA1	Activating molecule in BECN1-regulated autophagy 1
AMPK	Adenosine monophosphate-activated protein kinase
ANOVA	Analysis of variance
APAF1	Apoptotic protease-activating factor 1
ASK	Apoptosis signal-regulating kinase
ATG	Autophagy protein
Atg7KO	Atg7 deficiency mice
BAK	BCL-2 antagonist or killer
BAX	BCL-2-associated X protein
BCA	Bicinchoninic acid
Bcl-2	B cell lymphoma 2
BSA	Bovine serum albumin
CAL	ligation of the left anterior descending coronary artery
CFBHH	Calcium and Bicarconate Free Hanks with Hepes
Chl	Chloroquine
CKD	Chronic kidney disease;
DAPI	4’,6-diamidino-2-phenylyindole
DMEM	Dulbecco’s Modified Eagle’s Medium
DMSO	Dimethyl sulfoxide
DMT-1	Divalent metal ion transporter 1;
EF	Ejection fraction;
ER	Endoplasmic reticulum
ESA	Erythropoietin-stimulating agent
ESC,	European Society of Cardiology
EV	Empty vector

FAIR-HF	Ferinject Assessment in patients with IRon deficiency and chronic Heart Failure
FIP200FAK	Family kinase-interacting protein of 200 kDa
FPN	Ferroportin
NGAL	Neutrophil gelatinase-associated lipocalin
GFP	Green fluorescent protein
GLUT4	Glucose transporter type 4
H9c2	Rat embryonic cardiac myoblasts
Hb	Haemoglobin;
HCP-1	Haem carrierprotein 1
HF	Heart failure
HFpEF	Heart failure with preserved ejection fraction
HFD	High-fat diet
HFrEF	Heart failure with reduced ejection fraction
hiPS-CMs	iCell Cardiomyocytes
ID	Iron deficiency
IFN-γ	Interferon γ
IKKβ	IκB kinase
IOC	Ironoverload cardiomyopathy
IR	Insulin receptor
IRS	Insulin receptor substrate
ISC	Iron-sulfur cluster
LAMP-2A	Lysosome-associated membrane protein type 2A
LC3	Microtubule-associated protein 1A/1B-light chain 3
Lcn2	Lipocalin 2
Lcn2KO	Lipocalin 2 knockout
LMW	Low molecular weight
LTCC	L-type calcium channel
MAPK	Mitogen-activated protein kinase
MCP1	Monocyte chemoattractant protein 1
MI	Myocardial infarction

mTORC2	Mammalian target of rapamycin complex 2
NCOA4	Nuclear receptor co-activator 4
NF-κB	Nuclear factor-κB
NYHA	New York Heart Association;
PAS	Pre-autophagosomal structure
PBS	Phosphate-buffered saline
PDK	Phosphoinositide-dependent kinase
PI3K	Phosphatidylinositol-3-kinase
PINK1	PTEN-induced putative kinase 1
PIP2	Phosphatidylinositol 4,5-bisphosphate
PIP3	Phosphatidylinositol 3,4,5-triphosphate
PKB	Protein kinase B
PKC	Protein kinase C
PTB	Phosphotyrosine-binding
PTEN	Phosphatidylinositol-3,4,5-trisphosphate 3-phosphatase
PVDF	Polyvinylidene fluoride
Rap	Rapamycin
RBP4	Retinol-binding protein 4
RED-HF	Reduction of Events with Darbepoetin α in Heart Failure
RFP	Red fluorescent protein
ROS	Reactive oxygen species
SDS	Sodium dodecyl sulfate
SEM	Standard error of the mean
SH2	Src homology
TEM	Transmission Electron Microscopy
Tf	Transferrin
TfR	Transferrin receptor
TNF-α	Tumour necrosis factor α
TREAT	Trial to Reduce cardiovascular Events with Aranesp (darbepoetin α) Therapy
TSat	Transferrin saturation;

TTCC	T-typecalcium channel
TUNEL	Terminal deoxynucleotidyl transferase dUTP nick end labeling
TZD	Thiazolidinedione
UPR	Unfolded protein response.
wt	Wild type

Chapter One: Introduction

1.1. Heart failure in obesity and diabetes

Obesity and the associated metabolic syndrome (a cluster of chronic symptoms including insulin resistance, hyperglycemia, dyslipidemia, hypertension, and systemic low-grade inflammation) predispose individuals to developing cardiovascular dysfunctions [1-3]. Heart failure is one potential cardiovascular outcome and the consequences in the obese and aging population can be devastating owing to the high risk for mortality or loss of quality of life. However, the mechanisms of obesity and diabetes-induced heart disease are multifaceted and remain to be fully defined [4, 5]. Accordingly, there is currently great interest in resolving the various ways, and stages, via which obesity can influence myocardial remodeling. Central to the pathogenesis of heart failure in obesity are changes in cardiac metabolism and cardiomyocyte cell death [4]. One potentially important mechanism for altered myocardial metabolism is due to altered circulating, or local, adipokine profiles [4, 6, 7]. Various adipokines have also been suggested as potentially useful biomarkers for various aspects of cardiovascular disease. They have proven useful in identifying those at risk for heart failure or its progression and improving prediction of complications.

1.1.1. Lipocalin-2: introduction and changes in obesity, diabetes and heart failure

Lipocalin-2 (Lcn2; also often termed neutrophil gelatinase-associated lipocalin or 24p3) is a small, secreted adipokine and belongs to a diverse family of lipocalins [8-11] (fig1.1). Lcn2 is abundantly produced from adipocytes and recent studies show that Lcn2 is a proinflammatory marker associated with insulin resistance and obesity-related

metabolic disorders [12-17](Fig 1.2). An increased Lcn2 expression in adipose tissue is observed in various experimental models of obesity and in obese humans [14, 18-20]. In mice, the permissive role of Lcn2 in development of aging- and obesity-induced insulin resistance is highlighted by studies indicating that these processes are attenuated by knockout of Lcn2 [16]. Measurement of serum Lcn2 has also been proposed as a useful means for evaluating obesity-related cardiovascular diseases including heart failure, based upon reports of an association between elevated circulating Lcn2 levels and cardiac dysfunction [12, 14, 21]. For example, circulating Lcn2 levels have been shown to increase at an early stage of experimental autoimmune myocarditis and remain high until recovery phase [22]. Elevated Lcn2 content in the myocardium is also induced by ischemia reperfusion, likely via production from infiltrating polymorphonuclear cells [23]. Lcn2 expression is significantly augmented in patients with coronary heart disease and myocardial infarction [15, 24]. Furthermore, measurements of Lcn2 within a few days after ischemic stroke can be used to stratify patients according to mortality risk during the following four-year period [25]. Plasma Lcn2 was increased after carotid artery injury in rats [26] and in a heterotopic mouse transplanted heart after ischemia/reperfusion (I/R) [23]. Finally, it is interesting to note that Lcn2 has bacteriostatic properties and may play a role in linking infection, innate immunity and heart disease [27, 28].

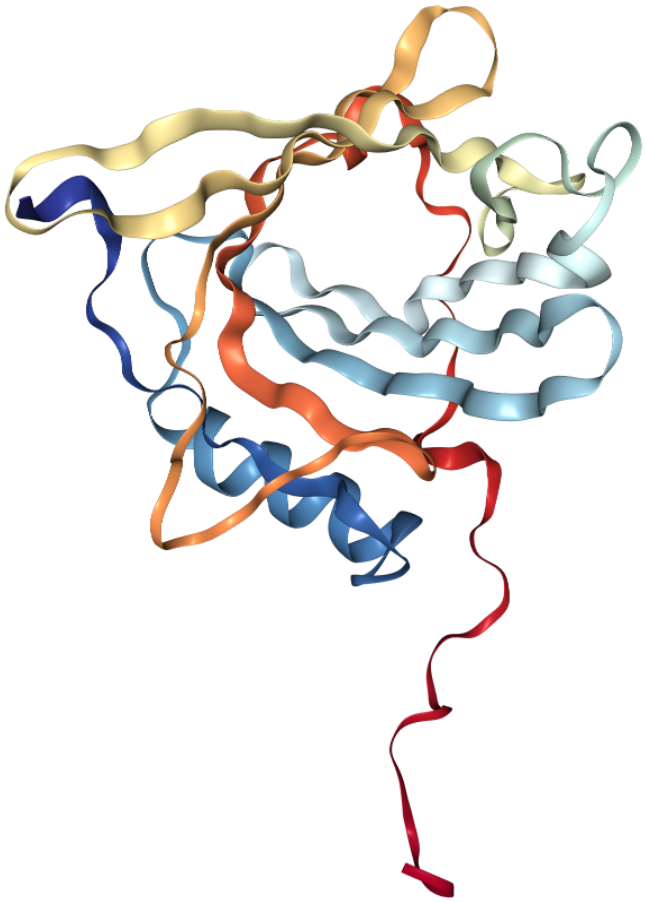

Figure 1.1. The structure for Lcn2. Lcn2 family members have a well conserved structure; 3 dimensional, eight stranded antiparallel beta-barrel with a repeated +1 topology enclosing an internal ligand binding site. Taken from http://www.rcsb.org/pdb/ngl/ngl.do?pdbid=1NGL

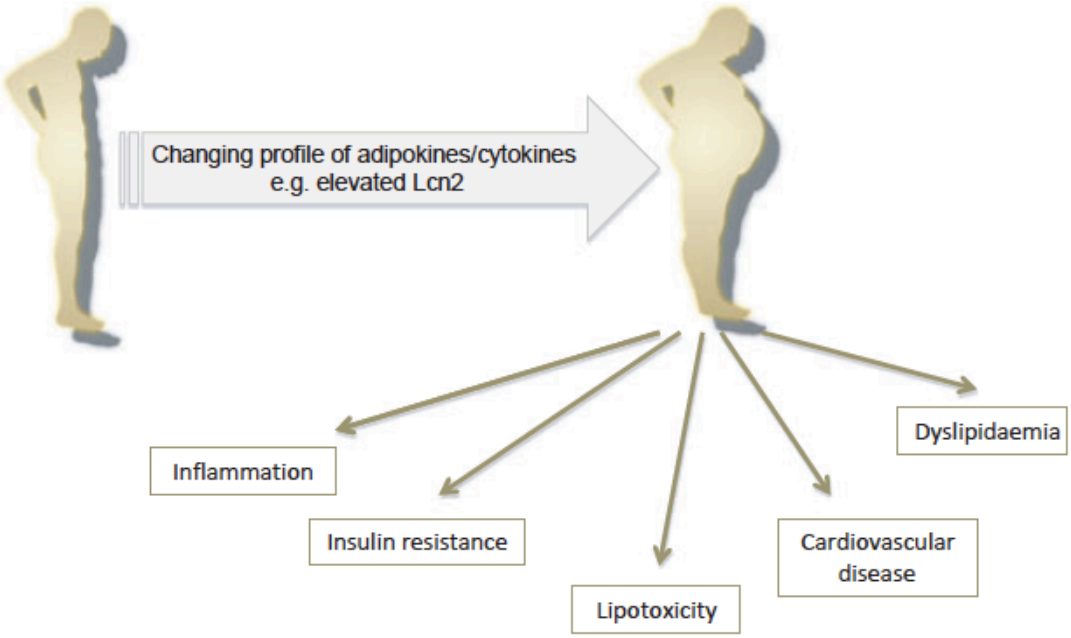

Figure 1.2. Altered profile of Lcn2 in obese individuals.

Schematic diagram indicated that an increase in Lcn2 levels in the body, it altered various health disease such as inflammation, insulin resistance, lipotoxicity, cardiovascular disease and dyslipidemia [12] . (Reprinted from the Clinical and Experimental Pharmacology and Physiology, Vol. 39, Jang *et al., Emerging clinical and experimental evidence for the role of lipocalin-2 in metabolic syndrome*, Page No. 194, Copyright (2012), with permission from John Wiley and Sons)

1.1.2. Evidence linking Lcn2 with metabolic syndrome.

1.1.2.1. Metabolism and inflammation

Numerous human studies have highlighted that serum Lnc2 level was associated with various metabolic parameters and inflammatory markers [14, 18, 29, 30]. Increased Lcn2 concentration clearly correlated with body mass index, body fat percentage, hypertriglyceridaemia, hyperglycaemia and the insulin resistance [14]. Previous research also demonstrated that elevated serum Lcn2 levels occurred in obese patients with metabolic syndrome and there was strong correlation between Lcn2 and insulin resistane in these obese patients. Increased circulating LPS concentrations are sufficient to dysregulate the inflammatory status and initiate the onset of obesity and insulin resistance [31]. Indeed, LPS can induce increases in systemic Lcn2 by 150 fold within 24 hours [32]. Lcn2 deficient mice were shown to have delayed LPS-induced hypoferremia in induced sepsis, indicating a role for Lcn2 in limiting circulating iron levels by enhancing intracellular iron content during inflammatory states [32]. Mice deficient in Lcn2 also had exacerbated endotoxin-induced sepsis, increased immune cell apoptosis and increased mortality [32]. MyD88-dependent signaling is required for the induction of Lcn2 and iron sequestration to maintain the hypoferric response during endotoxemia [33]. Thus, Lcn2 can act as an influencer for the development of endotoxemia and derived metabolic disease by its effect on LPS. As indicated above, elevated Lcn2 levels associated with obesity and insulin resistance [12, 14]. In studies of diabetic patients, it was found that serum Lcn2 concentration significantly associated with fasting triglycerides and insulin and homeostasis model assessment of insulin resistance (HOMA-IR) [29]. Similarly, serum level or adipose tissue Lcn2 content was found to be elevated in overweight

pregnant women and associate with several insulin resistance markers including HOMA-IR, fasting plasma insulin and glucose [34, 35]. Gene and protein expression of Lcn2 increased in visceral adipose tissue of obese compared to lean subjects [36, 37]. Weight loss caused a significant reduction of circulating Lcn2 in overweight/obese women with polycystic ovary syndrome [38], but a similar response was not seen in pre-pubertal children with obesity [39]. One established mechanism via which Lcn2 leads to obesity induced insulin resistance may be its capacity to stimulate the expression of 12-lipoxygenase, an enzyme that metabolizes arachidonic acid, and consequently induces TNFα in adipose tissue [16].

1.1.2.2. Heart failure

In clinical settings, Lcn2 is now regarded as one of the best biomarkers for acute kidney injury, and is also emerging as a promising biomarker for HF [40]. A close interdependent relationship means that renal dysfunction often accompanies cardiac failure; and that cardiac dysfunction is frequently seen with renal failure [40]. Therefore, many biomarkers for kidney or tubular dysfunction, for example, KIM-1 (kidney injury molecule 1), NAG (N-acetyl-beta-D-glucosaminidase) and cystatic C, also predict prognosis and outcomes in patients with HF [41]. However, unlike other renal biomarkers, Lcn2 level was not affected by diuretic withdrawal in patients with chronic systolic HF [42]; and administration of Lcn2 in an animal model of acute ischemic renal injury actually attenuated tubular injury [43]. Moreover, in patients with chronic HF, Lcn2 has been shown to be a more effective marker than creatinine for cardiorenal syndrome; Lcn2 could detect renal injury earlier than creatinine, and was an independent and novel risk predictor

of mortality in chronic HF [44]. Indeed, the elevation of Lcn2 seen in HF and its association with different parameters of HF has affirmed its potential as a HF biomarker. Firstly, serum Lcn2 predicted the outcome of HF, for example, the GALLANT (Lcn2 eva*L*uation *A*long with B-type *N*a*T*riuretic peptide in acutely decompensated heart failure) trial concluded that plasma Lcn2 at the time of discharge was a strong prognostic indicator of 30 days outcomes in patients admitted for acute HF [45]; it independently predicted worse short term prognosis in patients with acute HF [46] and Lcn2 levels correlated well with HF-related functional assessment parameters including the 6 min walk test [47]. Secondly, the CORONA (*CO*ntrolled *RO*suvastatin multi*NA*tional trial in heart failure) study suggested that Lcn2 associated with the severity of HF [48]; the elevated serum Lcn2 in patients with acute post myocardial infarction and chronic HF was found to be associated with more adverse outcome [28]; the Lcn2 level was shown to be correlated with HF severity and hemodynamic improvements after lefy ventricular assist device (LVAD) placement [49]. Thirdly, serum LCN2 predicted severity of chronic HF in terms of NYHA classification and mortality in elderly patients [50]; and plasma Lcn2 also predicted mortality in HF patients with or without CKD [51]. Clearly, there is strong evidence associating Lcn2 with HF in various individual cohorts in terms of HF severity, prognosis and mortality (figure 1.3).

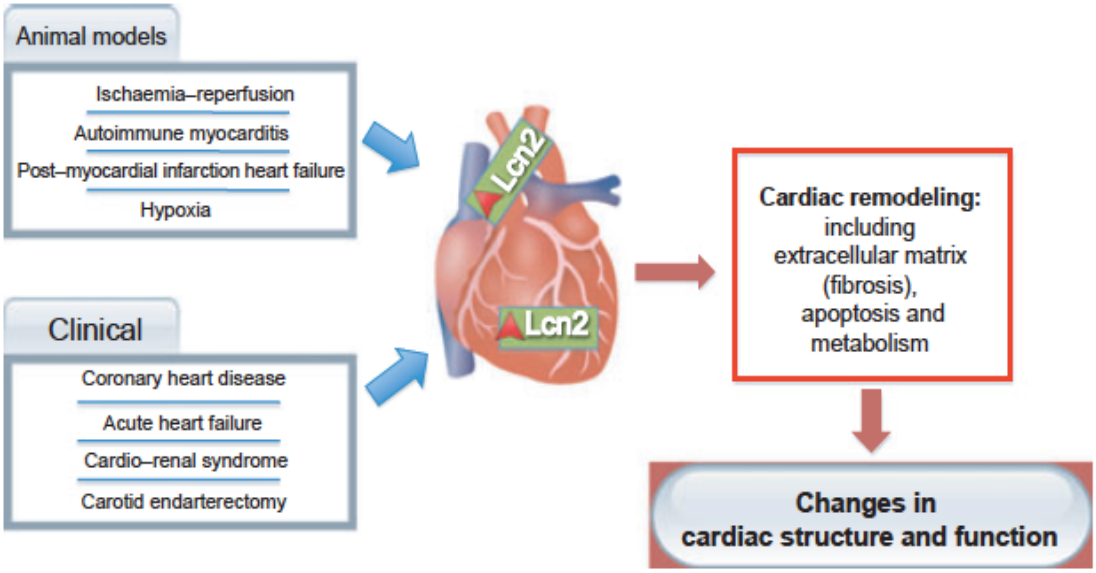

Figure 1.3. Lcn2 is a useful biomarker for evaluating the outcomes in various clinical and basic researches in cardiovascular diseases. Developing clinical and animal model data have been shown that changes in Lcn2 levels in the heart and vasculature under a variety of 'stresses'. This schematic diagram highlighted Lcn2 leads to damaging effects on the cardiovascular system [12]. (Reprinted from the Clinical and Experimental Pharmacology and Physiology, Vol. 39, Jang *et al., Emerging clinical and experimental evidence for the role of lipocalin-2 in metabolic syndrome*, Page No. 194, Copyright (2012), with permission from John Wiley and Sons)

1.2. Cellular mechanisms involved in pathogenesis of heart failure

1.2.1. Insulin signalling

Insulin binds to the insulin receptor (IR), inducing a conformational change that results in the autophosphorylation of tyrosine residues present in the β subunit [52]. Members of the insulin receptor substrate (IRS) family bind to IR via phosphotyrosine binding (PTB) domains [53]. Subsequently, this leads to the phosphorylation of tyrosine residues on IRS proteins and then bind to phosphatidlyinositol-3-kinase (PI3K) through the Src homology 2 (SH2) domain of the p85 regulatory subunit. The catalytic subunit p110 is then activated and phosphorylates phosphatidylinositol 4,5-bisphosphate (PIP2) to phosphatidylinositol 3,4,5-triphosphate (PIP3) at the plasma membrane. PDK1 and Akt are recruited to the plasma membrane by binding to PIP3 through their PH domains. Specifically, interaction with the activating kinase phosphoinositide-dependent kinase-1 (PDK-1) phosphorylates Akt at threonine (308) in its kinase-domain activation loop, causing partial activation of Akt/protein kinase B (PKB). However the complete activation of Akt requires phosphorylation at serine (473), located in the hydrophobic C-terminal domain, by mammalian target of rapamycin complex 2 (mTORC2), previousy known as PDK-2. Another alternative is that Shc recruits Grb2/SOS, which stimulates the MAPK signaling pathway. Substrates activated by the MAPK and PI3K/Akt pathways mediate various downstream biological responses of insulin, including cell survival and glucose metabolism [53].

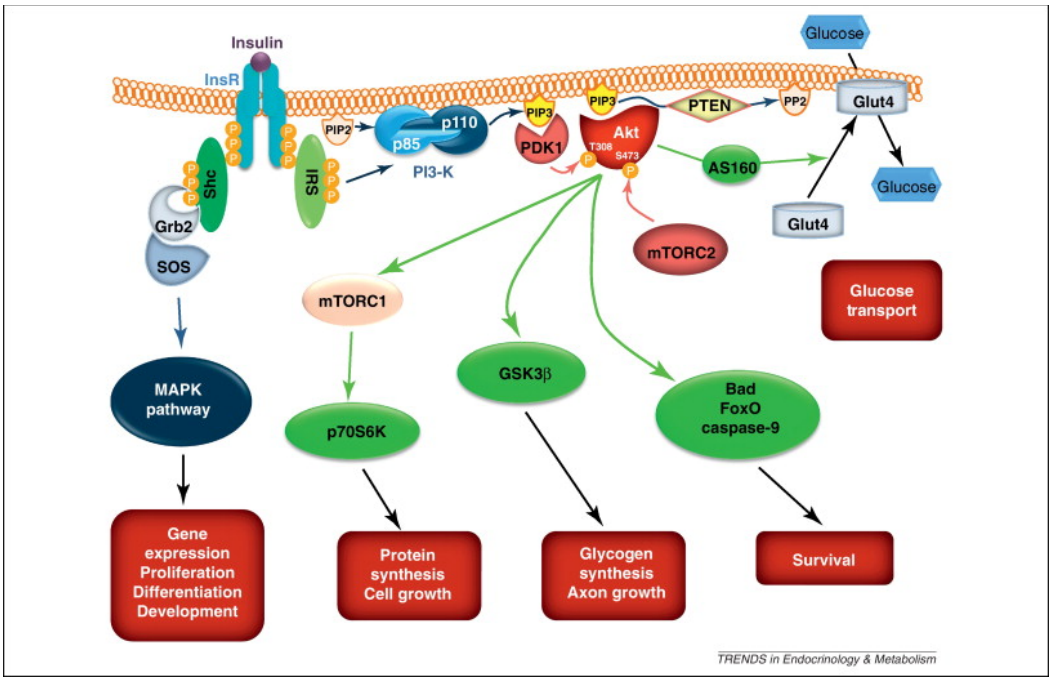

Figure 1.4. Insulin signalling pathway. Insulin stimulates the autophosphorylation of its receptor leading to binding and tyrosine phosphorylation. Phosphorylated tyrosine residues on IRS act as docking sites with SH2 domains such as PI3K, which is central for AKT activation. AKT requires the phosphorylation of threonine residue in the catalytic domain, and serine residue in the hydrophobic motif by PDK1 and the mTORC2 complex, respectively [54]. (Reprinted from the Trends in Endocrinology & Metabolism, Vol. 23, Kim *et al., Insulin resistance in nervous system*, Page No. 133, Copyright (2012), with permission from Elsevier)

1.2.2. Autophagy

Autophagy is a general term now used to describe the processes by which capture of cytoplasmic components for lysosomal degradation occurs [55]. Three types of autophagy have been characterized: macroautophagy, chaperone-mediated autophagy and microautophagy. Macroautphagy has been the most extensively studied form and involves firstly the formation of a double membrane vesicle called the autophagosome. Chaperone-mediated autophagy involves the binding of proteins containing a KFREQ motif to a chaperon protein for translocation to lysosomes where it binds to lysosome-associated membrane protein type 2A (LAMP-2A) receptor and is subsequently internalized and degraded. Lastly, microautophagy involves the direct sequestration of cellular components via the lysosome through the invagination of the lysosomal membrane [56]. Autophagy has been called a "double-edged sword" [57] as it can either be beneficial or detrimental to the cell, depending on the context. The basal autophagy is essential for maintaining cellular homeostasis and for the turnover of cytosolic components, as it degrades long-lived proteins, defective organelles and intracellular pathogens, thus protecting the cell and replacing it with molecules for future anabolic purposes [55, 56].

Autophagosome formation utilizes 18 different Atg proteins and is comprised of three major steps: initiation, nucleation and elongation/enclosure [56]. The initiation step is controlled by the ULK1 (UNC-51-like kinase 1)–FIP200 (FAK family kinase-interacting protein of 200 kDa) ATG13 ATG101 complex. The serine/threonine kinase mammalian target of rapamycin (mTOR) inactivates ULK1 by phosphorylation. Under starvation conditions, autophagy is induced via the inactivation of mTOR that results in ULK1 (Ser757) activation and phosphorylation of Atg13 and FIP200 A. Another pathway is that

AMPK is activated by AMP and activates ULK (Ser555). Anti-apoptotic proteins from the BCL-2 family usually inactivate this complex, but when it is active it enables the nucleation of the isolation membrane. The final elongation and enclosure step requires the recruitment of two ubiquitin-like protein conjugation systems. Firstly, the conjugation of Atg12–Atg5 is mediated by ligases Atg7 and Atg10. Atg5 also associates with Atg16 to form the Atg12–Atg5–Atg16 complex. Second, the microtubule-associated protein light chain 3 (LC3), which is the mammalian homolog of yeast Atg8, is cleaved at its carboxyl terminus by Atg4, giving rise to the soluble, cytosolic form LC3-I, which is then conjugated to phosphatidylethanolamine (PE) through the actions of Atg7 and Atg3. This lipid conjugated form, LC3-II, is localized to the autophagosomal membrane, and allows the closure of the autophagic vacuole [56, 58]. LC3 is to date the only protein that has been identified on the inner membrane of the autophagosome and hence is the most commonly used experimental protein marker for autophagic vacuoles. An increase in LC3-II reflects an increase in autophagsome formation. Another protein important in the assessment of autophagy is P62, which delivers ubiquitinated proteins to the autophagosome for degradation by binding to the polyubiquitin chains and LC3 [56]. P62 is then preferentially degraded by autophagy [59]. Experimentally, autophagic flux is concluded to increase when LC3-II levels increase and P62 levels show a corresponding decrease. Two additional proteins which participate in the recruitment of molecules to the isolation membrane are the transmembrane proteins, ATG9 and vacuole membrane protein 1 (VMP1), which recycle between the golgi, endosomes and autophagosomes, probably shuttling lipids for degradation [60].

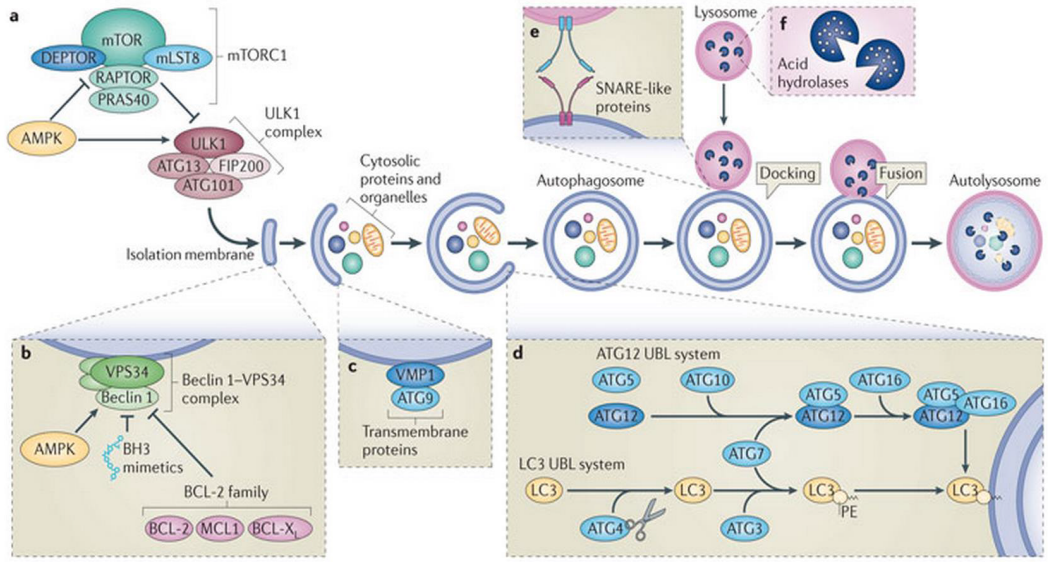

Figure 1.5. The major stages of autophagy. (a) The initiation step of autophagsome formation is controlled by the ULK1-FIP200-ATG13-ATG101 complex, and inhibited by mTOR. (b) VPS34-Beclin 1-class III PI3K complex, which is inactivated by anti-apoptotic BCL-2 family proteins. (c) Transmembrane proteins ATG9 and VMP1 recruit molecules to the isolation membrane. (d) The elongation and enclosure step of autophagosome formation requires two ubiquitin-like protein conjugation systems. (e) Fusion between autophagosomes and (f) various lysosomal enzymes hydrolyse proteins, lipids and nucleic acids in the autolysosome [60]. (Reprinted from the Nature Reviews Molecular Cell Biology, Vol. 15, Marino *et al., Self-consumption: the interplay of autophagy and apoptosis*, Page No. 2, Copyright (2014), with permission from Nature Publishing Group)

1.2.3. Apoptosis

There are different processes that lead to cell death and they must be carefully controlled in order for the organism to survive, grow and carry out its necessary functions. In most cases, unwanted cells are destroyed by programmed cell death in a process called apoptosis. Apoptosis is a highly regulated type of programmed cell death or cell suicide characterized by morphological changes [61]. There are two main pathways in the cell for the initiation of apoptosis: extrinsic pathway and intrinsic pathway [60]. The extrinsic pathways that recruit apoptosis involve transmembrane receptor-mediated interaction. These receptors are members of the tumor necrosis factor (TNF) receptor gene superfamily that contain a cytoplasmic domain of about 80 amino acids termed the "death domain". This death domain plays a critical role in transmitting the death signal from the cell surface to intracellular signaling pathways. The binding of Fas ligand to Fas receptor results in the binding of the adapter protein FADD, and the binding of TNF ligand to TNF receptor results in the binding of the adapter protein TRADD with subsequent recruitment of proteins FADD and RIP. FADD then associates with procaspase-8, leading to caspase 8 dimerization and activation [60]. Once active, caspase 8, an "initiator caspase" [62], can directly cleave and activate "effector or executioner caspases" caspase 3 and caspase 7 [61, 63], leading to caspase-dependent apoptosis. The intrinsic pathway of apoptosis is characterized by one central injurious event – mitochondrial outer membrane permeabilization (MOMP) [60]. Non-receptor-mediated stimuli activate B cell lymphoma 2 (Bcl-2) homology 3 (BH3)-only proteins, which stimulate MOMP by inducing the oligomerization of BCL-2 associated X protein (BAX) and/or BCL-2 antagonist or killer (BAK) in the outer mitochondrial membrane. Cytochrome c is released form damaged

mitochondria and binds apoptotic protease-activating factor 1 (APAF1). Via oligomerization a structure called the apoptosome is formed that recruits and activates an "initiator caspase", caspase 9. Subsequently caspase 9 cleaves and activates "effector or executioner caspases", caspase 3 and caspase 7, leading to caspase-dependent apoptosis.

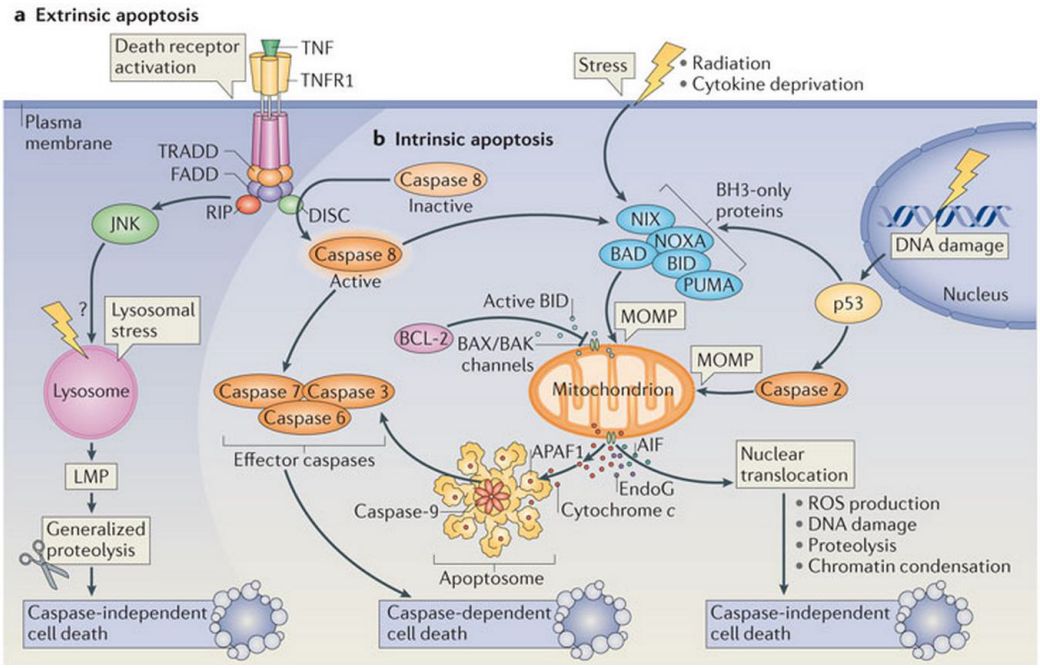

Figure 1.6. The two main pathways for apoptosis. (a) The extrinsic signalling pathways that initiate apoptosis contain transmembrane receptor mediated interactions. (b) The intrinsic signalling pathways that initiate apoptosis involve a various array of non-receptor mediated stimuli that produce intracellular signals that act directly on targets within the cell and are mitochondrial-initiated events. Additional details about the specific information are given in the text [60]. (Reprinted from the Nature Reviews Molecular Cell Biology, Vol. 15, Marino *et al., Self-consumption: the interplay of autophagy and apoptosis*, Page No. 2, Copyright (2014), with permission from Nature Publishing Group)

1.2.4. Oxidative stress

Oxidative stress is a disturbance in the balance between the production of reactive oxygen species (free radicals) and antioxidant defenses [64]. It is thus an altered accumulation of reactive oxygen species (ROS). These ROS can cause pathological alterations in the cell due to DNA damage, oxidation of amino acids, proteins and lipids [64]. ROS designates not only a range of free radicals such as superoxide radical anion ($O_2^{\bullet-}$), carbonate radical anion ($CO_3^{\bullet-}$), hydroperoxyl radical ($HOO^{\bullet}$), hydroxyl radical ($HO^{\bullet}$), peroxyl radical ($ROO^{\bullet}$), and alkoxyl radical ($RO^{\bullet}$), but also non-radicals like hydrogen peroxide (H_2O_2), hypochlorous acid (HClO) and ozone (O_3). Among them, H_2O_2 and $O_2^{\bullet-}$ are the major ROS in living organisms and are continuously produced by cells and in excess must simultaneously be removed by antioxidant enzymes. Neither H_2O_2 nor $O_2^{\bullet-}$ are strong oxidizing agents, but extremely reactive hydroxyl radical $HO^{\bullet}$ can be produced upon reacting with iron or iron-containing molecules through Fenton reaction [65]. H_2O_2 oxidizes Fe^{2+} to Fe^{3+}, producing hydroxyl radical $HO^{\bullet}$ and hydroxide ion OH^- (1); Fe^{3+} is then reduced back to Fe^{2+} by another H_2O_2 molecule, forming a hydroperoxyl radical $HOO^{\bullet}$ and a proton H^+ (2); or by superoxide radical anion ($O_2^{\bullet-}$) to produce oxygen (O_2) (3). In this way, iron acts as a catalyst to generate plentiful amounts of ROS.

$$Fe^{2+} + H_2O_2 \rightarrow Fe^{3+} + HO^{\bullet} + OH^- \quad (1)$$

$$Fe^{3+} + H_2O_2 \rightarrow Fe^{2+} + HOO^{\bullet} + H^+ \quad (2)$$

$$Fe^{3+} + O_2^{\bullet-} \rightarrow Fe^{2+} + O_2 \quad (3)$$

Although ROS has important physiological functions, for example, to combat invading pathogens, excess ROS can result in oxidative stress that damage intracellular protein, lipids and nucleic acid. Indeed, specific parts of the genome were found to be

damaged by Fenton reaction, and are termed “genomic sites vulnerable to the Fenton reaction” [65].

1.3. Iron metabolism and regulation by Lcn2 in cardiomyopathy

1.3.1. Systemic and myocardial iron metabolism

Iron homeostasis is essentially a closed system - iron is acquired from food as inorganic or heme iron, which are primarily absorbed in the duodenum via processes mediated by divalent metal ion transporter 1 (DMT-1) and heme carrier protein 1 (HCP-1), respectively. Iron in the cytoplasm can either be stored as ferritin, or be released to the bloodstream via ferroportin (FPN), where ferrous iron (Fe^{2+}) can be oxidized to ferric iron (Fe^{3+}) by hephaestin to facilitate its binding to transferrin (Tf) and be transported in the circulation. Most cells express transferrin receptor 1 (TfR1) such that holo-Tf can be endocytosed to acquire iron, where the ferric iron gets reduced to ferrous iron by metalloreductase STEAP3. It is then transported across the cell membrane by DMT-1. Hepcidin is a peptide hormone that induces the intracellular degradation of FPN, the only know iron exporter, and therefore is a vital and major iron regulatory hormone that controls plasma iron concentration and tissue iron distribution by inhibiting intestinal iron absorption, iron recycling by macrophages and iron mobilization from hepatic stores [66]. Various processes mediate iron transport in the cardiovascular system. Iron deposition in the heart is a gradual process, and has been suggested to occur in the ventricular myocardium before the atrial myocardium [67]. Sequential appearance has been further documented, beginning initially in the epicardium, then myocardium and eventually endocardium. Myocardial iron levels are normally regulated through transferrin mediated

uptake mechanisms, mainly through TfR1 [68]; although in the case of iron overload where transferrin-mediated transport becomes saturated, non-transferrin bound iron (NTBI) in the circulation increases and can also enter cardiac myocytes through DMT-1, T-type calcium channels (TTCCs), L-type calcium channels (LTCC) [68, 69], ZRT/IRT-like protein 14 (Zip14 or Slc39a14) [70] and also Lcn2 receptor which facilitates the entry of LCN2 bound iron [71]. FPN1 is expressed in cardiomyocytes as an exporter of iron into circulation (Figure 1. 7.)[72].

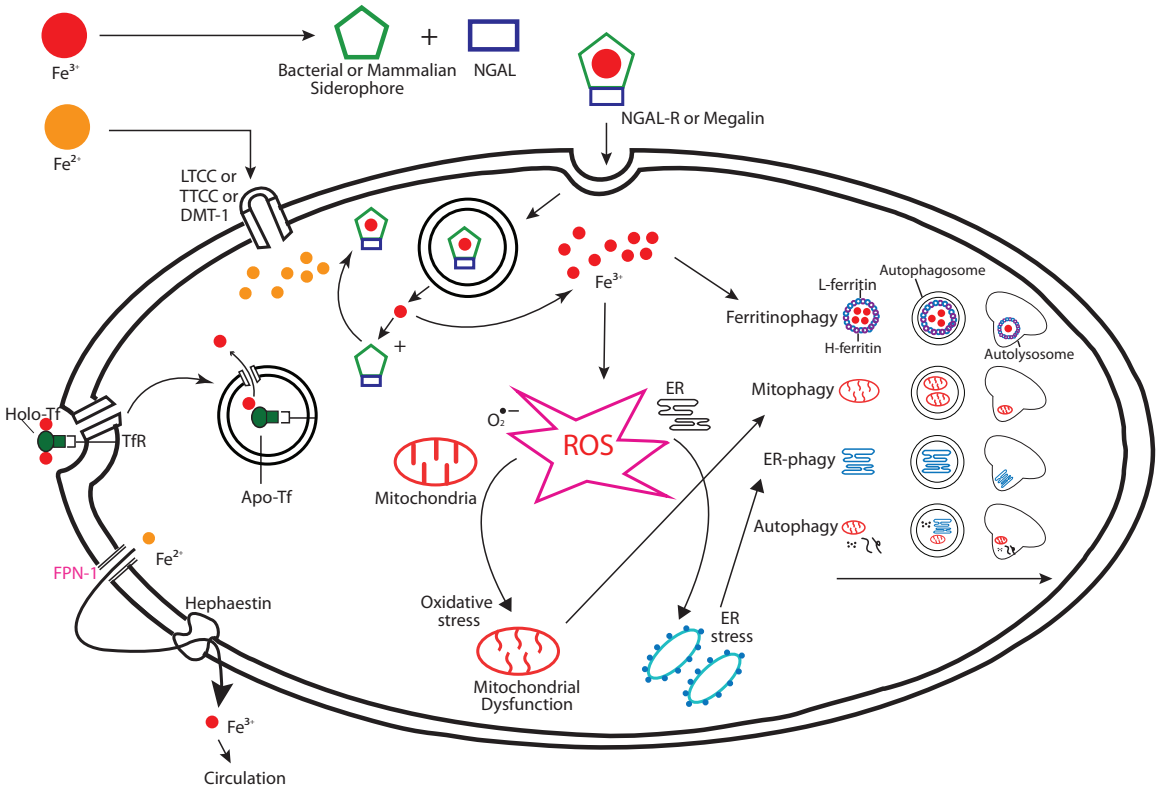

Figure 1.7. Schematic overview of cellular iron transport in cardiomyocytes. The role of DMT-1 as well as other transporters such as LTCC and TTCC as possible portals for iron into cardiomyocytes. In addition Tf binds to TfRs o the external surface of the cell. The role of NGAL(Lcn2) is to donate iron to cell via the NGAL-R. Internalization of NGAL (Lcn2) and its receptor leads to the uptake of iron from siderophore-iorn complex, although the exact mechanism remains unclear. However, accumulation of iron subsequently induces mitochondrial dysfunction, oxidative stress, ER stress and autophagy in cardiomyocyte [73] (Reprinted from Clinical Science, Vol. 129, Chan *et al., Iron metabolism and regulation by neutrophil gelatinase-assocoated lipocalin in cardiomyopathy*, Page No. 851, Copyright (2015), with permission from Portland Press)

1.3.2. Observational changes and diagnosis of iron status in cardiomyopathy

Heart failure (HF) is a highly prevalent chronic progressive condition in which the heart is incapable of pumping enough blood to meet the body's demand. The heart compensates with various remodeling measures including initial enlargement (hypertrophy) to increase pumping capacity [74]. Ejection fraction (EF), the measurement of the amount of blood the left ventricle pumps out in each contraction, is an important indicator for heart function and diagnosis of HF. In patients who have heart failure with reduced ejection fraction (HFrEF), EF drops from a normal range of between 55 and 70% to below 40%; yet half of the patients with HF are observed to have preserved EF (HFpEF) [75]. In the ongoing search for novel treatments of HF, there is strong emerging evidence showing the significance of disturbed iron homeostasis in HF regardless of the degree of change in EF [76], thus establishing excellent therapeutic potential if our understanding of the mechanisms responsible for the association of iron homeostasis and HF can be enhanced.

The normal range of circulating ferritin is from 30-300 μg/L, where <30 μg/L is defined as iron deficiency. However, heart failure has an inflammatory component were serum ferritin, as an acute phase protein, is often elevated without changes in body iron store. Therefore, recently the European Society of Cardiology (ESC) guidelines for diagnosis and treatment of heart failure have recommended a systematic measurement of iron parameters in all patients suspected of having heart failure. Serum ferritin <100 μg/L is regarded as absolute iron deficiency; where serum ferritin 100-299 μg/L and a transferrin saturation of <20% is defined as functional iron deficiency [77]. On the other hand, a serum ferritin >300ug/L and a transferrin saturation of >55% is diagnosed as iron overload cardiomyopathy (IOC). The level of serum ferritin at which iron deposition is

detected in the heart has not yet been conclusively identified. Taking heart biopsy is not only invasive, but technical difficulty often renders the results variable and non-definitive. Both iron overload and iron deficiency have been linked to cardiomyopathy, with the former primarily associated with an enhanced oxidative stress and the latter with mitochondrial dysfunction, impaired heart efficacy [78], hypercoagulable state, increased cardiac burden and also oxidative stress due to anemia [79]. Cardiomyopathy associated with iron overload or deficiency will be reviewed in more detail in the following sections.

1.3.2.1. Iron overload cardiomyopathy (IOC)

IOC is defined as the presence of systolic or diastolic cardiac dysfunction secondary to increased deposition of iron in the heart independent of other concomitant processes [80]. IOC is typically associated with dilated cardiomyopathy with left ventricular hypertrophy and reduced EF [81]. The prevalence of IOC is increasing and is the leading cause of death in patients receiving chronic blood transfusion therapy [82]. While patients may remain asymptomatic in the early disease process, severely overloaded patients can rapidly experience terminal HF. Accumulation of iron in the myocardium may occur via increased iron absorption from gastrointestinal enterocytes (hemochromatosis); excess exogenous iron intake such as by dietary supplements, or blood transfusions (hemosiderosis). The association of IOC with hemochromatosis, an autosomal disorder involving mutation of specific genes involved in iron metabolism that leads to increased gastrointestinal absorption, is well characterized [83]. In fact, this accounts for one third of deaths in hereditary hemochromatosis, especially in young male patients [84]. Chronic blood transfusion is the treatment for hereditary and acquired anemia including

thalassemia and myelodysplastic syndromes. However, since excess body iron cannot be actively excreted, repeated blood transfusion can result in iron deposition in multiple organs. There are numerous mechanisms via which excess iron can reduce cardiac function. Once the antioxidant capacity of cardiomyocytes is exceeded, iron can produce excess oxidative stress by the Fenton reaction (see below) and lead to apoptosis [85]. In addition, excess free iron in blood is suggested to be responsible for the generation of insoluble parafibrin, which is highly resistant to proteolytic dissolution and initiates inflammatory reactions upon deposition on the arterial wall [86]. Association of iron and atherosclerosis is well established in animal studies, for example, iron accumulation is observed in atherosclerotic plaques [87] and decreasing tissue iron by chelating therapy, dietary iron restriction or phlebotomy showed decreased atheroma plaque size with improved stability [88-91]. Such association is also supported in clinical studies – a study involving 12033 men showed increased ferritin concentration was associated with early coronary artery atherosclerosis, independent of traditional cardiovascular risk factors [92]; another study that involved 196 subjects showed a strong association between serum ferritin and pulse wave velocity or aortic stiffness in women [93]. The 6 years long Iron and *A*therosclerosis *ST*udy (FeAST) also established correlations between levels of ferritin, inflammatory biomarkers and mortality in a subset of patients with peripheral arterial disease [94]. Iron availability may have contributed to atherosclerosis by impairing nitric oxide action as demonstrated by improvement in nitric oxide mediated, endothelium-dependent vasodilation in patients with coronary artery disease by chelating iron with deferoxamine [95]. While further mechanisms are yet to be defined, the *A*therosclerosis *R*isk *I*n *C*ommunities (ARIC) study has rejected the hypothesis that excess iron stores would

promote low density lipoprotein (LDL) oxidation [96]. It was shown that dietary iron intake and body iron stores had no direct link to altered structure and function of large arteries in subjects free of cardiovascular disease, cancer or hemochromatosis [97].

1.3.2.2. Iron deficiency (ID) and cardiomyopathy

ID is the most common nutritional deficiency worldwide [98]. It is frequent, has a high occurrence rate from 30% to 50% in patients with HF and presents as an important co-morbidity [99]. Two types of ID can be distinguished – absolute and functional ID. Absolute ID reflects depleted iron stores while iron homeostasis mechanisms and erythropoiesis often remain intact. Absolute ID development in humans can result from inadequate dietary iron intake, impaired gastrointestinal absorption/ transport, drug interactions and gastrointestinal blood loss [100]. On the other hand, functional ID presents a dysregulated iron homeostasis where cells and tissues might be rendered with inadequate iron supply despite normal whole body iron storage. This can be a result of elevated circulating hepcidin concentration, and had been reported in patients with acute phase myocardial infarction [101]. ID is often accompanied by anemia, although both can exist independently and ID usually appears before the onset of anemia. It is important to differentiate anemia from ID – while ID is marked by the insufficiency of iron, anemia is defined by insufficient hemoglobin. ID that is independent of anemia was reported to have a higher risk of death than those with anemia [102, 103]; it has been reported as an independent predictor of mortality and associates with disease severity [104]. In recent years there have been several clinical trials to test whether administration of intravenous iron could improve functional parameters related to HF. One of the most well-known

studies includes the *F*erinject *A*ssessment in patients with *IR*on deficiency and chronic *H*eart *F*ailure (FAIR-HF). It involved 459 patients with iron deficiency and chronic heart failure of New York Heart Association (NYHA) functional class II or III. The treatment with intravenous ferric carboxymaltose over 24 weeks improved NYHA functional class, functional capacity and quality of life in terms of EQ-5D (EuroQol-5 Dimension) and KCCQ (Kansas City Cardiomyopathy Questionnaire) with an acceptable side effect profile [105]. A simplified ferric *C*arboxymalt*O*se evaluatio*N* on per*F*ormance in patients with *IR*on deficiency in co*M*bination with chronic *H*eart *F*ailure (CONFIRM-HF) trial that has enrolled 304 stable, symptomatic HF patients from 41 sites across 9 European countries is currently in progress to confirm the efficacy and safety of iron therapy using intravenous ferric carboxymaltose solution in chronic HF patients with iron deficiency as in the FAIR-HF study [106]. Other clinical trials including the FERRIC-HF [107] and IRON-HF [108] trials have also showed encouraging results with iron therapy using intravenous iron sucrose in improving functional capacity in HF patients with ID. Thus, ID can serve in many cases as a promising therapeutic target for HF. Furthermore, the importance of ID as a marker in the context of HF and its assessment was highlighted and recommended by the ESC [77]. As for anemia, it has also been shown to have a relatively high prevalence (37%) in patients with HF [109]. With less oxygen availability during anemia, the heart compensates by increasing heart rate and stroke volume. Moreover, anemia has been reported to be an independent risk factor for adverse outcomes in HF, both in terms of morbidity and mortality rates [110-117]. Efforts have been made to restore hemoglobin levels as a potential therapeutic approach to HF using erythropoietin-stimulating agents (ESA) and this resulted in improvements in exercise tolerance, peak VO_2, NT-proBNP and

left ventricular performance in patients with HF [118]. However, other studies have also distinguished anemia as being independent from HF [119] – the correction of anemia by ESA darbepoitin alfa demonstrated no difference in the primary end point for HF, and was even associated with elevated embolic and thrombotic events [120]. *Thus, it is suggested that anemia may only serve as a surrogate marker instead of an endpoint target in HF.*

1.3.3. Cellular mechanisms that underlie the association of iron and cardiomyopathy

1.3.3.1. Iron & oxidative stress

Free iron is highly redox reactive and can participate in redox reaction that leads to generation of reactive oxygen species (ROS). Ferroptosis, as the name implies, is a recently identified form of cell death that is morphologically, biochemically and genetically distinct from apoptosis and necrosis and is found to be dependent on intracellular iron, and can be prevented by iron chelators and antioxidants [121]. The use of iron chelator deferoxamine has demonstrated significant reduction of neutrophil-mediated free radical production and amplification of the inflammatory response during cardiopulmonary bypass in human [122] and *in vivo* studies [123-125]. In summary, iron can potently enhance oxidative stress and consequently contribute to cardiomyopathy.

1.3.3.2. Iron and mitochondrial dysfunction

In eukaryotic cells, mitochondria are the main consumers of intracellular iron [126]. With mitochondria being the respiratory centre of the cell, plentiful oxygen can rapidly react with unregulated free iron to produce ROS. To avoid ROS induced damage, mitochondrial iron level and homeostasis is tightly regulated by different transport, storage

and regulatory proteins [127]. Through different biosynthesis pathways, iron is transferred in the mitochondria to its bioactive forms, heme and iron sulphur cluster (ISC). Mitoneet is an ISC-containing protein tethered to the outer mitochondrial membrane that facilitates transfer of iron into the mitochondria [128]. Not only does it play an essential role in redox signaling [129], it also dictates metabolic functions of mitochondria [128, 130-132]. An increased level of mitoneet can lead to accumulation of iron within the mitochondria, which in turn results in dysfunction [133, 134], a hallmark of various diseases. Mitoneet is recognized as a target for the thiazolidinedione class of antidiabetic drugs [129, 135], and its genetic manipulation was shown to have striking antidiabetic effects [136]. Mitochondrial ferritin stores and supplies iron within the mitochondria. Its expression is restricted to highly metabolically active cells such as cardiomyocytes in order to supply iron when demand is increased during active respiration or intense metabolic activities. Frataxin is another mitochondrial protein that handles iron in the mitochondrial matrix assembling ISC [137]. It can either act as a chaperone for ferrous iron, or as an iron storage protein that can mineralize iron as ferrihydrite. There is great interest in improving mitochondrial dysfunction as a potential therapeutic approach for heart failure [138, 139] and the underappreciated contribution of iron homeostasis is worthy of more consideration.

1.3.3.3. Iron & endoplasmic reticulum (ER) stress

Various pathophysiological situations can elevate ER stress. One of the major functions of ER is proper protein folding, and accumulation of misfolded proteins can normally be relieved by cellular responses such as ER-associated protein degradation (ERAD) and unfolded protein response (UPR). These ER stress responses are important

defense mechanisms when the amount of unfolded protein exceeds the folding capacity of ER [140]. ER stress has been strongly implicated in cardiovascular disease. For example, ER stress can lead to cardiomyocyte death *in vivo* and *ex vivo* [141] and in patients with HF [142]. Interestingly, it was suggested that ER stress may be cardioprotective during constriction-induced hypertrophy [143], perhaps by inducing compensatory cellular mechanisms such as autophagy (see below). Similarly, ER stress induction protected cardiomyocytes from oxidative damage [144]. Iron overload induced ER stress was shown *in vivo* in heart under acute and chronic conditions [145], and had been demonstrated in other tissue types including neurons [146] and liver [147]. In reverse, ER stress can modulate iron metabolism. Hepcidin, as mentioned above, degrades the iron efflux transporter FPN, thus leading to a systemic hypoferremic environment. ER stress was found to induce hepcidin expression [148]; the UPR signaling pathway was further shown to increase the transcription of ferroportin and ferritin [149]. Thus, based upon available evidence, ER stress and iron homeostasis appear to have a reciprocal relation such that they can tightly regulate each other. ER stress and UPR related proteins will serve as interesting targets to be studied in future clinical studies

1.3.3.4. Iron & autophagy

Macroautophagy (hereafter referred to as autophagy) is an intracellular degradation system that involves the sequestration of cytoplasmic components within a double-membrane vesicle termed autophagosome, in which the cargo content is degraded by the acidic hydrolases upon the fusion with a lysosome [55]. It has a wide variety of physiological and pathophysiological roles including energy homeostasis, cell survival and

host defense against pathogen invasion [150]. In the heart, autophagy typically occurs at low levels yet is nevertheless important in maintaining cellular homeostasis under normal conditions. Autophagy is typically upregulated in times of stress, for example during ischemia/reperfusion, pressure overload and cardiac toxicity induced by chemicals such as the athracycline doxorubicin [151]. While increased autophagy can promote cell survival by degrading damaged organelles such as mitochondria and protein aggregates to recycle catabolites and maintain ATP production; either excess or lack of autophagy can both result in cell death and cardiac dysfunction. Thus, the role of autophagy can often appear controversial among different studies when different degrees of autophagy, time course and pathological conditions being studied have led to variable observations. *In vivo* data has shown that expression of multiple autophagy related genes were altered in iron overload cardiomyopathy, possibly contributing to cardiac diastolic dysfunction [152].

Specifically, it is now appreciated that iron can regulate autophagy and that autophagy has an important role in iron homeostasis. Nuclear receptor coactivator 4 (NCOA4) was recently identified using quantitative proteomics to be the cargo receptor that mediates autophagy of ferritin - a process termed ferritinophagy. NCOA4 is required for the delivery of ferritin to the lysosome; without NCOA4 cells are malfunctional in ferritin degradation and this can result in a decreased bioavailability of intracellular iron [153]. However, excessive ferritinophagy may result in insufficient ferritin thus reducing its buffering effect on binding intralysosomal low mass iron and can lead to lysosomal fragility and increased sensitivity to oxidative stress [154]. Analysis of autophagy in iron associated cardiomyopathy is relatively new with limited mechanistic and clinical studies;

however we believe this must be rapidly developed since it is of great potential as a therapeutic target.

1.3.4. Regulation of cardiomyopathy by Lcn2

The maintenance of optimal iron levels in the body is largely controlled and influenced by endocrine regulation, and this is likely to be of major significance in cardiomyopathy. In this section I will introduce the importance of Lcn2 in the regulation of iron homeostasis and other possible mechanisms in the context of cardiomyopathy.

1.3.4.1. Possible mechanisms via which Lcn2 may mediate cardiomyopathy

1.3.4.1.1. Iron transport

Lcn2 is most well-known for its participation in innate immunity to limit bacterial growth by sequestrating iron. One way to secure iron from the host by bacteria is by synthesizing and secreting siderophores to extract iron from iron containing compounds such as transferrin and lactoferrin. Lcn2 is secreted by the host to tightly bind to bacterial catecholate-type ferric siderophores to compete for iron and prevent such uptake [155]. Lcn2 saturated with iron (holo form) can increase intracellular iron level by transporting it then releasing iron in the cytoplasm; in contrast, when Lcn2 is iron free (apo-form) it can deplete intracellular iron and transport it to the extracellular space via its receptor LCN2-R [156]. Bacterial infection is often associated with hypoferremia that limits iron availability to pathogens; accordingly, mice deficient in Lcn2 exhibit elevated intracellular labile iron and lowered circulating iron level [32]. Overall, Lcn2, as an iron-trafficking protein, can be regarded as an alternative to transferrin-mediated iron-delivery pathway [157]. Although

limited studies are available, it is speculated that circulating Lcn2 levels may reflect the body iron status, especially in hemodialysis patients. Indeed, it was found that plasma Lcn2 in hemodialysis patients was significantly lower within those who had ID – with transferrin saturation (TSAT) lower than 20%; and that the level of Lcn2 was positively correlated with circulating iron, TSAT and ferritin. Lcn2 was significantly increased after correction of ID with intravenous iron administration [158]. Similar results were also observed in another two studies supporting the potential use of Lcn2 to identify iron deficiency in hemodialysis patients [159, 160]. Likewise, a lowered Lcn2 level was also recorded in patients with iron deficiency anemia [161]; and in patients with chronic HF (both HFpEF and HFrEF), the significantly higher circulating Lcn2 levels also correlated with higher serum iron concentrations in the EPOCARES study [162]. As circulating Lcn2 is often recorded significantly increased in patients experiencing HF [28, 46, 49-51], and that local Lcn2 production in the heart is also increased significantly [22, 28], we believe it will be of great interest to further elucidate the role of Lcn2 in iron associated cardiomyopathy. Interestingly, we previously identified that Lcn2 led to cardiomyocyte apoptosis by causing intracellular iron accumulation [71]. Further mechanistic studies are definitely warranted.

1.3.4.1.2. Proinflammatory actions of Lcn2

As Lcn2 is involved in defending the host during bacterial infection, it comes as little surprise that Lcn2 is regarded as a proinflammatory cytokine. In the fourth Copenhagen Heart Study that involved more than 5000 patients and a follow up period of 10 years, it was shown that plasma Lcn2 strongly associated with all inflammatory markers investigated, including hsCRP, total leukocyte and neutrophil count; increased Lcn2 was

also shown to correspond to increased risk of all-cause mortality and major adverse cardiovascular events [163]. It was suggested that Lcn2 expression and secretion can be induced by IFNγ and TNFα, and that the transcription factors STAT1 and NF-kappa B were shown to bind to the human Lcn2 promotor [164]. Likewise, in elucidating the inflammatory mechanisms of Lcn2 with animal models, Lcn2 mRNA and proteins were upregulated upon vascular injury in an NF-kappa B dependent manner [26]. Lcn2 can enhance cardiac inflammation by promoting macrophage proinflammatory M1 phenotype polarization [165]. Thus, a vicious cycle exists whereby Lcn2 can intensify inflammation by inducing the expressions of TNFα and other pro-inflammatory mediators [166]. Interestingly, preventing the clearance of Lcn2 from the circulation was shown to promote vascular inflammation and endothelial dysfunction [167]. In both HFpEF and advanced HFrEF, elevated systemic and local inflammations with increased circulating TNFα have indispensable roles in disease pathogenesis [168]. It will be interesting to explore how Lcn2 contributes to cardiomyopathy in an inflammation dependent and independent manner.

1.4. HYPOTHESIS AND RESEARCH AIMS

The preceding discussion indicating that a variety of remodeling events occur throughout the progressive development of heart failure in obesity [4, 169]. These include changes in inflammation, mitochondrial dysfunction, autophagy, fibrosis, cell death, endoplasmic reticulum (ER) stress, oxidative stress and insulin sensitivity. I hypothesized that Lcn2 is an important component of the cardiac response to myocardial infarction, directly regulates cardiac remodeling and contributes to development of heart failure. The research aim of this project was to elucidate the effects of Lcn2 on cardiac remodeling, the impact of these changes on cardiac function, and Lcn2 mechanism of action.

My specific research objectives are:

- Aim 1: To examine the effect of Lcn2 on cardiomyocyte insulin sensitivity and what is the mechanism of action.
- Aim 2: To use Lcn2-knockout mice and investigate whether lack of Lcn2 protects against cardiac remodelling and dysfunction induced by chronic myocardial ischemia and the mechanisms via which this occurs.
- Aim 3: To investigate whether iron directly caused insulin resistance in cardiomyocytes and the mechanisms via which this occurred, with a focus on oxidative stress.

Chapter Two: Study1

Lipocalin-2 inhibits autophagy and induces insulin resistance in H9c2 cells

Yee Kwan Chan[#], Hye Kyoung Sung[#], James Won Suk Jahng, Grace Ha Eun Kim, Meng Han & Gary Sweeney

Department of Biology, York University, Toronto, Ontario, Canada

Published: ***Mol Cell Endocrinol.*** **2016 Jul 15;430:68-76**

Author contributions:

HK Sung performed all experiments with contributions form co-authors mentioned below, wrote the partial manuscript daft and performed all revisions necessary for publication**.**

YK Chan contributed to write first draft of manuscript and figure 2.2.C & figure 2.4.F.

JWS Jahng & GHE Kim performed figure 2.3.

M Han performed contributed to maintenance of H9c2 cells for experiments, and assisted with figure 2.1.

G Sweeney provided funding for project, designed experimental outline and edited the manuscript text.

2.1. Summary

Lipocalin-2 (Lcn2; also known as neutrophil gelatinase associated lipocalin, NGAL) levels are increased in obesity and diabetes and associate with insulin resistance. Correlations exist between Lcn2 levels and various forms or stages of heart failure. Insulin resistance and autophagy both play well-established roles in cardiomyopathy. However, little is known about the impact of Lcn2 on insulin signaling in cardiomyocytes. In this study, we treated H9c2 cells with recombinant Lcn2 for 1 hour followed by dose- and time-dependent insulin treatment and found that Lcn2 attenuated insulin signaling assessed via phosphorylation of Akt and p70S6K. We used multiple assays to demonstrate that Lcn2 reduced autophagic flux. First, Lcn2 reduced pULK1 S555, increased pULK1 S757 and reduced LC3-II levels determined by Western blotting. We validated the use of DQ-BSA to assess autolysosomal protein degradation and this together with MagicRed cathepsin B assay indicated that Lcn2 reduced lysosomal degradative activity. Furthermore, we generated H9c2 cells stably expressing tandem fluorescent RFP/GFP-LC3 and this approach verified that Lcn2 decreased autophagic flux. We also created an autophagy-deficient H9c2 cell model by overexpressing a dominant-negative Atg5 mutant and found that reduced autophagy levels also induced insulin resistance. Adding rapamycin after Lcn2 could stimulate autophagy and recover insulin sensitivity. In conclusion, our study indicated that acute Lcn2 treatment caused insulin resistance and use of gain and loss of function approaches elucidated a causative link between autophagy inhibition and regulation of insulin sensitivity by Lcn2.

2.2. Introduction

Lipocalin 2 (Lcn2), also termed 24p3 and neutrophil gelatinase-associated lipocalin (NGAL), is a proinflammatory hormone predominantly expressed by adipose tissue [12]. Various studies have previously reported the close association of circulating Lcn2 levels with hyperglycemia and insulin resistance [14, 16]. Elevated Lcn2 levels in obese or diabetic individuals were normalized by rosiglitazone and this correlated significantly with improved insulin sensitivity and inflammatory status [14]. Similarly, Lcn2 was also found associated with insulin resistance in other *in vitro* [18] or *in vivo* [17] studies and clinical settings [29, 170]. More recently, elevated Lcn2 was observed in patients with heart failure [51]. Furthermore, Lcn2 was shown capable of predicting the severity and mortality of acute and chronic heart failure [46, 50, 51, 171-173]. Lcn2 was also implicated in higher thrombotic risks in patients with atherosclerosis [26, 174]. Currently used as an excellent biomarker for acute kidney damage [175], Lcn2 has also been proposed as an attractive and promising biomarker for heart failure [171-173].

Obesity and diabetes increase the incidence of myocardial infarction and heart failure at least in part via insulin resistance [74, 176]. Cardiac insulin resistance is well established to influence heart failure via multiple mechanisms, including regulation of glucose and fatty acid uptake and metabolism, protein synthesis and vascular function [176, 177]. More recently, numerous studies have shown that autophagy can play a critical role in cardiac metabolic health [178] as well as regulating insulin sensitivity [179, 180]. Disruption of autophagy by cardiac-specific knockdown of Atg5 in adult mice leads to cardiomyopathy [181]. The dogma arising from studies in rodent or pig models is that

autophagy, triggered by various forms of cardiac stress, is a protective mechanism by which apoptosis is inhibited and the detrimental effects of cardiac ischemia are limited [182, 183]. However prolonged activation of autophagy can result in cell death [183] and cardiomyocyte dysfunction [184, 185]. Interestingly, patients with longstanding idiopathic cardiomyopathy show accumulation of autophagosomes in cardiomyocytes [186]. Aortic banding has been shown to induce autophagic activity which peaked at 48 hours and remained significantly elevated for at least 3 weeks [184]. This was attenuated by heterozygous disruption of the gene coding for Beclin 1, a protein required for early autophagosome formation. Subsequent studies have shown increases in markers including LC3-II and p62 levels in the heart 8 weeks post-banding [187, 188]. The role of autophagy in heart failure is clearly complex to study and is likely to influence cardiac remodeling in different ways depending on the magnitude of changes in autophagic flux and timing during the progression of heart failure.

Although elevated Lcn2 levels correlate with heart failure and insulin resistance can contribute to development and progression of heart failure, the impact of Lcn2 on cardiac insulin sensitivity remains unclear. Furthermore, little is known about the mechanisms of action via which Lcn2 impacts upon cardiac function. In this study, we first established that Lcn2 blunted insulin signaling in H9c2 cells, derived from rat heart ventricle. We used multiple assays to assess the effect of Lcn2 on autophagic flux and then used gain and loss of function strategies to determine the functional significance of Lcn2-induced alterations in autophagy. These studies will be important in developing our understanding of cardiac insulin resistance in obesity and diabetes and other inflammatory conditions.

2.3. Materials and methods

2.3.1. Cell culture

H9c2 (ATCC® CRL-1446) rat cardiomyoblasts were grown in Gibco® normal glucose Dulbecco's Modified Eagle's Medium (DMEM) supplemented with 10% fetal bovine serum (FBS) and 1% (v/v) penicillin streptomycin at 37°C and 5% CO_2. For microscopy assays (except TEM), cells were grown on cover slips and treated with or without recombinant apo-lipoclain 2 (Lcn2) (1μg/ml) in DMEM with 0% FBS mimicking starvation at approximately 80% confluency (unless specified otherwise) for 1 hour. A dose response using 1-5μg/ml was previously studied and 1μg/ml was selected based upon preliminary results and used in several publications since (Law, et al. 2010; Xu, et al. 2012). For other assays, cells were grown and treated the same way on 6 or 12 well plates without coverslips. Where appropriate, rapamycin (Sigma) (250nM) was post treated for 30 minutes after incubation with Lcn2.

2.3.2. Recombinant Lcn2 production

The expression of His-tagged Lcn2 (University of Hong Kong) in BL21 Competent *E. Coli* (NEB Biolab) was induced by SOC growth medium (NEB Biolab). Lcn2 was purified from bacterial lysates using the HIS-select® nickel affinity gel (Sigma) according to the manufacturer's protocol. The purity of Lcn2 was confirmed using SDS-PAGE gel. *E. Coli* strain B21 lack siderophore enterobactin, thus Lcn2 derived from this strain lacks iron (apo-Lcn2), as contrast to those purified from *E. Coli* strain XL1 Blue that constitutively expressing siderophore enterobactin that could derive iron loaded Lcn2 (holo-Lcn2) [156].

2.3.3. Western blotting

H9c2 cells were grown to 90% confluency in 6 well plates. After the experimental endpoint, cells were washed in PBS and solubilized in 1x Lysis buffer (50mM Tris, 150mM NaCl, 0.1% SDS 1% Triton X-100 and 0.5% sodium deoxycholate) containing protease inhibitor cocktail – complete ULTRA Tablets, Mini (Roche). Lysates were centrifuged at 12,000 rpm for 5 min at 4°C. Supernatant was collected, heated at 90°C for 5 min and equivalent amounts of lysate were loaded to an SDS-PAGE gel, followed by protein transfer onto PVDF membrane (Bio-Rad). Membranes were first blocked in 3% BSA for 1 hour, incubated in primary antibody at 4°C overnight, washed, incubated in appropriate horse-radish peroxidase (HRP)-linked secondary antibody for 1 hour, washed, then followed by chemiluminescence enhancement using Western Lightning *Plus* ECL (Perkin Elmer) before developing and exposing the membrane to CL-XPosure Film (Thermo Scientific). The band intensities were quantified using Image J. The following primary antibodies were used: pAkt T308, pAkt S473, pULK1 S555, pULK1 S757, LC3B, p70S6K T389 and β-actin (1:1000, Cell Signaling). The following secondary antibodies were used; anti-rabbit IgG HRP-linked antibody and anti-mouse IgG HRP-linked antibody (1:10,000, Cell Signaling).

2.3.4. RT-PCR analysis of autophagy genes expression

H9c2 cells were grown to 90% confluency in 6 well plates. After the experimental time point, RNA was isolated using the RNeasy® Mini Kit (Qiagen) following the manufacturer's protocol, quantified using NanoDrop^{TM} (Thermo Scientific) followed by reverse transcriptionwith GoScript Reverse Transcriptase (Promega). The 20µl reaction

mixture containing a total of 60ng cDNA and primers at a final concentration at 5μM were prepared for real-time PCR using the iQ™ SYBR® Green Supermix (Bio-Rad). Real-time PCR was conducted using Real-Time PCR Detection System (CFX96, Bio-Rad), with a hot start at 95°C for 2min, 40 cycles of denaturation at 95°C for 5s, annealing at 60°C for 5s and extension at 72°C for 5s, followed by a final extension at 72°C for 1 min. The melting curve analysis was done by a serial increment of 1°C from 55°C to 95°C. 18S was used as the reference gene for calculating the relative target gene expression using the delta delta CT method. The primer sequences were in-house designed with the 5' to 3' sequences as follow: Atg5 – Forward: TAGAGCCAATGCTGGAAACC; Reverse: TGTTGCCTCCACTGAACTTG; Atg7 – Forward: CGAAGGTCAGGAGCAGAAAC; Reverse; AGGCACCCAAAGACATCAAG; Atg8 – Forward: GTCTGGAGCATTGGACTTGC; Reverse: AGCCACACCCTTTCACTCAG; Atg9 – Forward: GGAATCTACCATCGCATCC; Reverse: CGGGTGAAGAAGACAACCTC; and Atg12 – Forward: TGACCTGGAACAGGAGTGTG; Reverse: GGGATGAGCCAGAAATGAAC.

2.3.5. Analysis of autophagic degradation by DQ-BSA assay using flow cytometry

H9c2 cells were seeded in 6-well plates, and underwent starvation for 4 hours. DQ™ green BSA was added in each well at 20ug/mL and incubated for 15 minutes. Cells were harvested and fixed with 4% PFA, and run in flow cytometer machine (Gallios ™, Beckman Coulter Inc.) to analyze green fluorescent (BODIPY) signal intensity in each cell within a population of 10,000.

2.3.6. Analysis of DQ-BSA co-localization with autophagy and lysosomal markers

H9c2 cells were seeded in 12-well plates with cover slips and underwent starvation for 4 hours. DQ™ green BSA was added in each well at 20ug/mL, and incubated for a minimum of 30 minutes after treatment. Cells were fixed with 4% paraformaldehyde (PFA) and quenched with 1% glycine then permeablized with 0.1% Triton X-100 for 5 minutes and blocked with 5% BSA for 1 hour. Cells were incubated with primary antibody at different concentration (LC3B, 1:400, p62, 1:400, and Cathepsin D, 1:250) for 1 hour. After three washes, cells were incubated with corresponding secondary antibody (Goat anti-Rabbit/anti-Mouse secondary antibody, AlexaFluor®594, 1: 800) before mounting on a glass slide. Confocal images were taken using a x60 objective (Olympus, BX51 Microscope).

2.3.7. Lysosomal cathepsin B activity measured using Magic Red

H9c2 cells were grown to 80% confluency on coverslips in 12 well plates. At the experimental endpoint, cells were fixed in 4% paraformaldehyde, quenched in 1% glycine, permeabilized with 0.1% Triton X-100 and blocked with 3% BSA before incubation of Magic red stain (Magic Red™ in vitro Cathepsin B kit, ImmunoChemistry Technologies) as per manufacturers' instructions. Coverslips were mounted with Prolong® Gold antifade reagent and Vectashield with DAPI on glass slides. Images were captured at 600x with confocal microscope (Olympus, BS51). At least 6 images at different fields of view were taken per coverslip. Quantitative analysis of Magic Red or TRIC fluorescence intensity in the cytoplasmic area, normalized by the number of cells, was performed using Definiens Tissue Studio® 3 (Definiens). For FACS analysis H9c2 cells were grown to 90% confluency in 6 well plates. At the experimental endpoint, cells were fixed with 4%

paraformaldehyde, quenched in 1% glycine, permeabilized with 0.1% Triton X-100, blocked with 3% BSA before incubation with Magic red stain. Fluorescence intensities of 10,000 cells per sample were measured by flow cytometry using Gallios™ Flow Cytometer (Beckman Coulter) and analyzed using Flowing Software 2 (Perttu Terho).

2.3.8. Generation of H9c2 cells stably overexpressing tandem fluorescent RFP/GFP-LC3 and analysis of autophagic flux

Stable H9c2 cells expressing tf-RFP/GFP-LC3 were created essentially as described by us previously for another cell type [179]. Cells were grown to 80% confluence on coverslips in 12 well plates. At experimental endpoint, cells were carefully washed with PBS before fixing at 4% paraformaldehyde and washing before mounting with Prolong® Gold antifade reagent and Vectashield with DAPI on glass slides. At least 6 images at different fields of view were taken per coverslip with confocal microscope (LSM 700, ZEISS). Quantitative analysis of the RFP:GFP ratio was performed using ZEN software (blue edition, 2012).

2.3.9. Transmission electron microscopy (TEM)

H9c2 cells were grown on 6 well plate to 80% confluency. After the experimental endpoint, cells were washed with PBS and immediately fixed with 2.5% glutaraldehyde in 0.1M sodium cacodylate buffer followed by post-fixation with 1% osmium tetroxide for 1 hour at room temperature. Cells were then dehydrated with ascending concentration of ethanol (50% to 100%) and embedded in Spurr's Epoxy resin. Thin sections at 60 – 80nm were cut with an ultramicrotome (Porter Blum, Ivan Sorvall Inc.) and mounted on copper

mesh grids. The sections were contrasted with 1% uranyl acetate and lead citrate before examining with a transmission electron microscope (CM100, FEI). At least 10 random fields of view were taken per sample using the Kodak Megaplus camera.

2.3.10. Generation of H9c2 cells stably overexpressing a dominant negative ATG5 (K130R) mutant

We generated an autophagy-deficient cell model by generating H9c2 cells stably expressing dominant negative ATG5 mutant in which lysine 130 was mutated to arginine, essentially as described by us previously for another cell type [179]. Cells were grown to >90% confluence in 6 well plate before treatment with insulin (10 or 100nM) for 10min and preparation of protein lysate for Western blotting as described above.

2.3.11. Statistics

Data are presented as mean ± SEM. Effect of Lcn2 was calculated with student unpaired t test and Mann-Whitney test for parametric and non-parametric data respectively (GraphPad Prism). Values of $P<0.05$ were considered significant.

2.4. Results

2.4.1. Lcn2 attenuated dose- and time-dependent insulin signaling

We first showed that H9c2 ventricular cardiomyocyte cells responded dose dependently to insulin as shown by increased phosphorylation of Akt T308 (Figure 2.1.A), Akt S473 (Figure 2.1.B) and 70S6K (Figure 2.1.C) and that these responses to insulin were attenuated in cells pretreated with Lcn2 (Figure 2.1.).

2.4.2. Lcn2 inhibited initiation of autophagy

As shown in Figure 2A and B, Lcn2 directly elicited significant up and down regulation of phosphorylation of ULK1 at Ser757 and Ser555, respectively (Figure 2.2. A&B). These observations on regulation of proteins involved in autophagy initiation corresponded with reduced levels of LC3-II after Lcn2 treatment (Figure 2.2. A&B). The short term time period of Lcn2 treatment used in this study had no significant effects in altering the gene expressions of various autophagy related genes (Figure 2.2. C).

2.4.3. Measurement of lysosmal degradative activity with DQ Green BSA

To further investigate the effects of Lcn2 on autophagic flux we developed a novel assay to investigate protein degradation via autolysosomal activity using DQ Green BSA. DQ-BSA is a derivative of BSA that is heavily conjugated with BODIPY® dye that confers self-quenching, yet releases fluorophores upon enzymatic cleavage in acidic intracellular lysosomal compartments. We first confirmed that BODIPY signals from exogenously added DQ-BSA strongly co-localized with autophagy markers LC3B and p62

as well as the lysosomal marker cathepsin D (Figure 2.3.A). This indicated that DQ-BSA de-quenching occurred at subcellular locations relevant to autophagosome and lysosome. The intensity of BODIPY signals from DQ-BSA was measured quantitatively by flow cytometry and also by immunofluorescence. The intensity of BODIPY signals in 10,000 cells, with or without starvation to induce autophagy, was plotted and the population of green fluorescence shifted rightward in H9c2 cells with starvation (Figure 2.3.B). Importantly, this shift which reflects elevated levels of protein degradation was reduced in autophagy-deficient Atg5K130R cells. Immunofluorescent analysis of cells pulsed with DQ-BSA supported the conclusion that significant green puncta appeared in H9c2 cells after starvation yet this response was attenuated in ATG5K130R cells (Figure 2.3.B & C).

2.4.4. Lcn2 decreased lysosomal enzyme activity and autophagic flux

After verifying the use of DQ-BSA, it was observed using this approach that Lcn2 significantly reduced the autolysosomal activity in H9c2 cells (Figure 2.4.A, B). Magic red dye was then used as a well-established approach to measure cathepsin B activity. Both immunofluorescence (Figure 2.4.C&E) and flow cytometry (Figure 2.4.D&E) analysis of MagicRed indicated a reduction in response to Lcn2. To further assess autophagic flux, we generated H9c2 cardiomyoctyes stably overexpressing tandem fluorescent RFP-GFP-LC3. Given that GFP and RFP have different pH stability, only GFP weakens in acidic environment, the degradation of autophagic vacuoles can be inferred from a lower RFP/GFP ratio. As shown in Figure 4F, an increase in yellow LC3 puncta was observed after the addition of Lcn2. In contrast, addition of rapamycin restored the autophagic flux as shown by a significant increase in red puncta (Figure 2.4.F).

The gold standard technique to visualize autophagic vacuoles in mammalian cells is by transmission electron microscopy (TEM). In H9c2 cardiomyocytes, plentiful autophagic vacuoles including autophagosomes and autolysosomes were observed in the control conditions (Figure 2.5.) yet only a few, and mostly autophagosomes were seen upon the treatment with Lcn2 (Figure 2.5.). This observation correlated well with our above mentioned results.

2.4.5. Regulation of insulin signaling by alterations in autophagy and effect of Lcn2

Based on the observations that Lcn2 inhibited both insulin signaling and autophagy, we investigated if crosstalk occurred between the two. We first generated autophagy-deficient H9c2 cells by stably overexpressing a mutant inactive Atg5 (Atg5K). While we observed a dose dependent increase in phosphorylation of Akt T308 in wild type (WT) H9c2 cells upon stimulation with an increasing dose of insulin this response was significantly decreased in Atg5K cells (Figure 2.6.A&B). We then further examined the potential contribution of autophagy to insulin sensitivity regulation by restoration of autophagy with rapamycin in Lcn2 treated cells. As shown in Figure 2.6.C/D/E, while Lcn2 inhibited insulin-stimulated phosphorylation of Akt T308 and Akt S473, post-treatment with rapamycin significantly increased their phosphorylation by insulin.

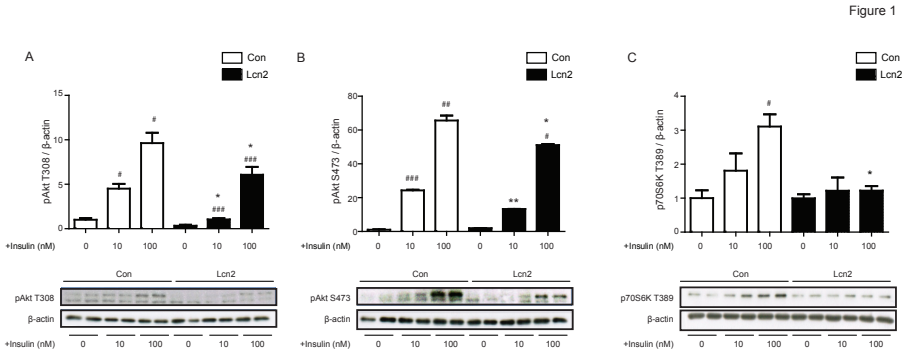

Figure 2.1. Insulin signaling in cardiomyocytes was decreased by Lcn2 as indicated by decreased dose-dependent insulin-stimulated phosphorylation of Akt T308, Akt S473 and p70S6K. H9c2 cells pretreated without (con) or with Lcn2 (1μg/ml, 1 hour) were then treated with insulin (0, 10 or 100nM) for 10 minutes. Representative Western blots showing pAkt T308 (A), pAkt S473(B) and p70S60K T389 (C) and the respective reference protein β-actin and their quantification $^{\#}$ indicates significant difference from control H9c2 cells without insulin; * indicates significant difference from the control with respective insulin dosage. $^{\#}$ $p<0.05$, $^{\#\#}$ $p<0.01$, $^{\#\#\#}$ $p<0.001$; *$p<0.05$, **$p<0.01$. $n \geq 3$.

Figure 2

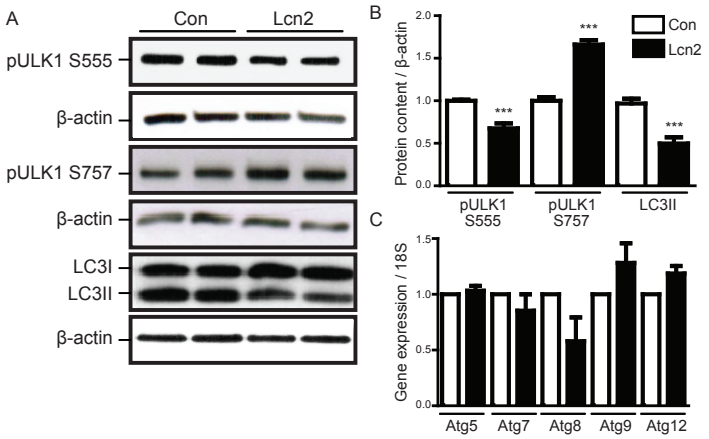

Figure 2.2. Initiation of autophagy was inhibited by Lcn2 in cardiomyocytes. H9c2 cells were treated with Lcn2 (1μg/ml) (Lcn2) or without (Con) for 1 hour. Western blots showing pULK1 S555, pULK1 S757, LC3II and the reference protein β-actin (A) and their quantifications (B). Gene expression of autophagy related genes Atg5, Atg7, Atg8 (LC3), Atg9 and Atg12 by qPCR was quantified with 18S as the reference gene using the delta delta CT method (C). ***$p<0.001$. $n \geq 3$.

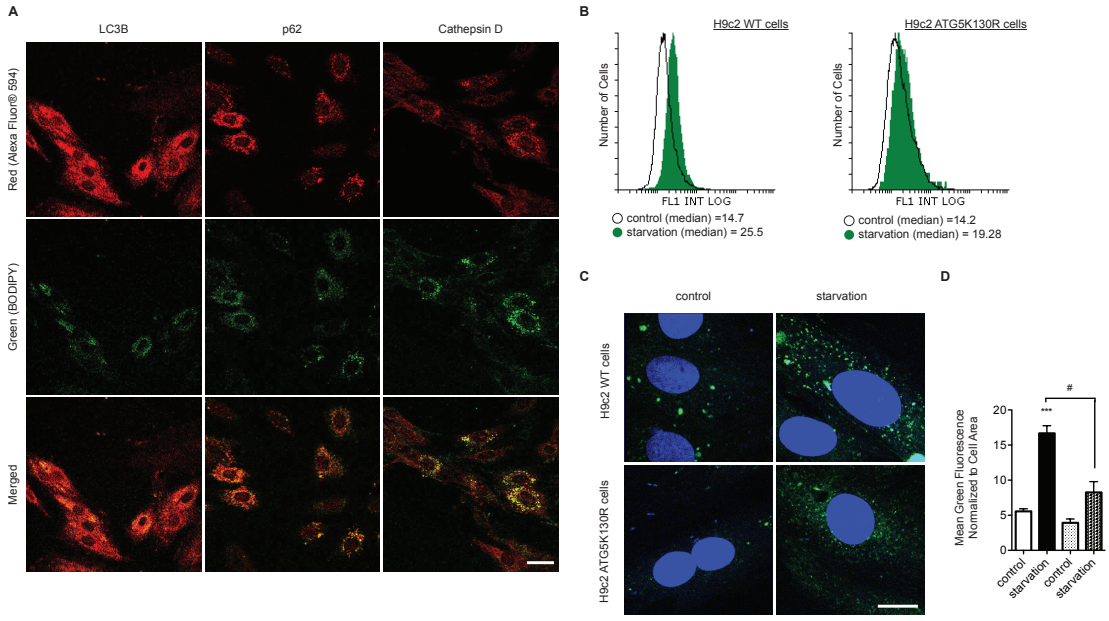

Figure 2.3. Validation of DQ-BSA degradation as a measure of proteolytic autophagy. Representative confocal images of H9c2 cells labelled with LC3B/p62/Cathepsin D and DQ-BSA (20ug/mL) which was pulsed for ≥ 30 minutes (A). Distribution of green fluorescence (BODIPY) intensity of 10,000 H9c2 cells (WT, wild type, and ATG5K130R H9c2 cells) pulsed with DQ-BSA ± starvation (B). Representative confocal images of H9c2 cells (WT and ATG5K130R H9c2 cells) pulsed with DQ-BSA ± starvation (C) and quantification (D). Results are represented as mean ± SEM (n=10 images). *p<0.05 **p<0.01 versus control. Scale bar = 20 um.

Figure 4

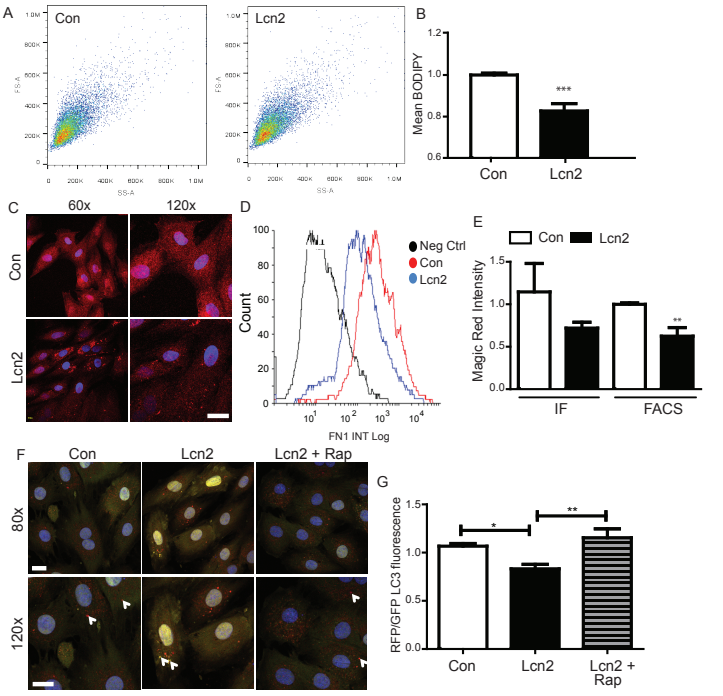

Figure 2.4. Lcn2 decreased lysosomal cathepsin B activities and autophagic flux. H9c2 cells were treated with Lcn2 (1µg/ml) (Lcn2) or without (Con) for 1 hour. The overall proteolysosomal activity was examined by quantifying fluorophore released by DQ-BSA using flow cytometry and representative data are shown in (A) and quantified in (B). The lysosomal cathepsin B activity was further examined using the Magic red dye with immunofluorescence microscopy (C), flow cytometry (D) and these data were both quantitated as shown in (E). Autophagic flux was further evaluated using the RFP/GFP ratio of LC3 puncta in the tf-GFP/RFP-H9c2 cell line. Rapamycin, an inducer of autophagy, was used as a positive control and both representative images and quantitative data are shown in (F). * indicates significant difference from the control. **p<0.01; ***p<0.001. Scale bar = 50µm in C; 20 µm in F. n ≥ 3.

Figure 5

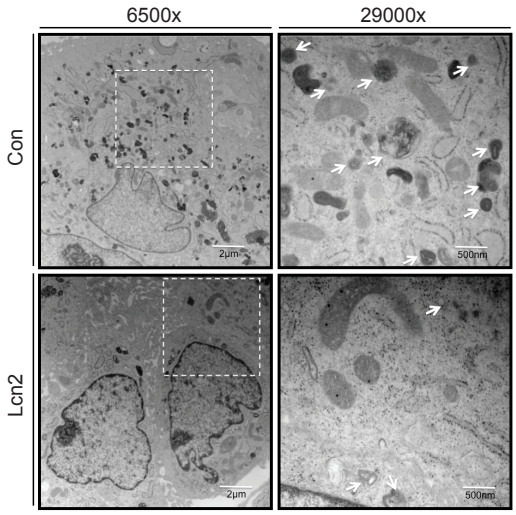

Figure 2.5. Lcn2 decreased number of autophagosomes and autolysosomes in cardiomyocytes. H9c2 cells were treated with Lcn2 (1μg/ml) (Lcn2) or without (Con) for 1 hour. Autophagy was evaluated using transmission electron microscopy. Selected areas from lower magnification (6500x) images were magnified to 29000x with white arrows indicating the presence of autophagic vacuole structures. Shown here is one representative image for each treatment, at different magnifications, from multiple independent samples.

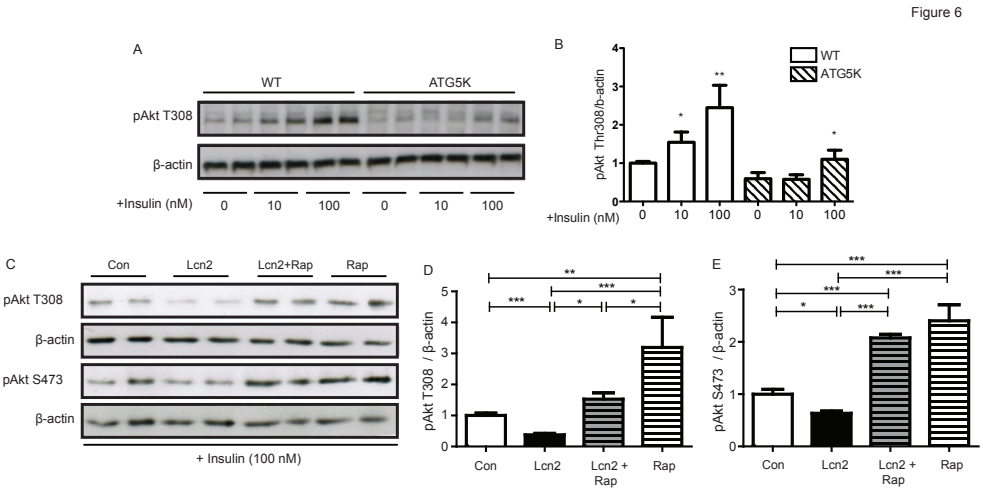

Figure 2.6. Inhibiting autophagy decreased and elevating autophagy rescued insulin signaling in cardiomyocytes. Insulin sensitivity was decreased in autophagy deficient cells overexpressing mutant Atg5, as indicated by decreased phosphorylation of Akt T308; representative Western blots in (A) and quantification in (B). Wild type H9c2 cells were treated with Lcn2 (1μg/ml) (Lcn2) or without (Con) for 1 hour and rapamycin (Rap) (250nM) was added 30 minutes after Lcn2 treatment for the final 30 minutes of treatment. Rap elevated insulin signaling indicated by increased phosphorylation of Akt T308 and Akt S473 in Western blots (C) and quantification (D). * indicates significant differences. *$p<0.05$, **$p<0.01$, ***$p<0.001$. $n \geq 3$

2.5. Discussion

Strong rationale for this study comes from observations of an increased circulating Lcn2 level and increased expression in adipose tissue of various experimental models of obesity and in obese humans [12]. For instance, a study with 2519 subjects showed that serum Lcn2 was significantly higher in those with impaired fasting glucose and/or impaired glucose tolerance even after adjusting for anthropometric measures, genetic predispositions, life style and other diabetic associated biomarkers [189]. Type 2 diabetic patients were shown to have a significant elevation of serum Lcn2 that associated with declining pancreatic beta cell function [190] and a cross sectional study showed that insulin resistance and hyperglycemia were positively correlated with elevated circulating Lcn2 [14]. Rosiglitazone treatment decreased circulating Lcn2 and this correlated significantly with improved insulin sensitivity [14]. Further studies in mice demonstrated the permissive role of Lcn2 in the development of obesity- and aging-induced insulin resistance since these processes were attenuated in Lcn2-KO mice [16]. Measurement of serum Lcn2 has also been proposed as a useful means for evaluating obesity-related cardiovascular diseases including heart failure [171-173], however the direct effects of Lcn2 on cardiomyocyte insulin sensitivity and its possible mechanisms of action remain unclear.

We first investigated whether Lcn2 altered insulin sensitivity in a cell line derived from rat heart ventricle and found that 1 hour treatment with Lcn2 reduced insulin sensitivity. Cardiac insulin resistance is well established to influence heart failure via multiple mechanisms such that exacerbated cardiomyopathy may occur in an insulin-insensitive myocardium [176]. In fact, in type 2 diabetes insulin resistance can be present

for several years before hyperglycaemia develops and at this time contribute to adverse cardiac remodeling [191]. We observed that Lcn2 reduced insulin stimulated signaling to Akt and p70S6K.

Although little is known about the mechanisms of Lcn2 action in cardiomyocytes, previous work has included evidence for a role of increasing intracellular iron levels [71]. Our current study indicates that inhibition of autophagy, by Lcn2 or by generating an autophagy-deficient cell line, can serve as an important contributor to insulin resistance in cardiomyocytes. This is important both from the perspective of our current realization of the critically important role autophagy plays in heart failure [192] and also in emerging evidence that autophagy can regulate insulin sensitivity and metabolism [179, 180].

Autophagy is the major intracellular degradation process where cytoplasmic materials get delivered to lysosomes for degradation and recycling [178, 181, 183, 193]. The entire dynamic process of autophagosome synthesis, fusion with lysosome and the degradation of the autophagic substrates is termed “autophagic flux”, and is important to measure as a reliable indicator of autophagic activity [194]. Several studies have now shown that the degree of autophagy changes in the failing heart and directly in response to ischemia and/or reperfusion [195-198], although the functional significance is still somewhat uncertain. Indeed, autophagy may be regarded as a double edged sword with potential beneficial and detrimental effects in the heart [199]. At low levels autophagy is important in recycling damaged organelles and nutrients, however excessive autophagy contributes to tissue dysfunction [184, 199-202]. Our current study is the first to

demonstrate attenuation of autophagy by Lcn2 in cardiomyocytes and only one previous study examined Lcn2-induced changes in autophagy [203]. These authors investigated autophagy as one potential mechanism underlying its tumorigenic effects. They generated mouse embryonic fibroblasts (MEFs) from WT and Lcn2-/- mice, and immortalized these cells. By Western blotting they found a significant decrease in total LC3 in Lcn2-/- MEFs compared to the WT MEF cells. No further markers of autophagy were analyzed and the authors concluded that Lcn2 is an important regulator in autophagy, possibly via an indirect mechanism. Accurate experimental analysis is critical to allow conclusions on alterations in autophagic flux [192, 200]. Thus, we took an extensive approach using numerous assays designed to examine different stages of autophagic flux in order to carefully characterize the effect of Lcn2. Our conclusion of reduced flux is based on several lines of evidence; increased pULK1 S757, reduced pULK1 S555 and reduced LC3II levels detected by Western blotting, reduced degradation of DQ-BSA, reduced cathepsin B activity, reduced appearance of red puncta in cells stably expressing tandem fluorescent RFP/GFP-LC3, and an overall of reduction in autophagosome and autolysosome content observed by transmission electron microscopy. Thus, our data showing that Lcn2 inhibits autophagic flux are of great interest given the above evidence on the critical role of autophagy in the heart and our need to further understand its regulation and significance.

We further investigated the mechanistic role of autophagy in cardiac insulin sensitivity. First, we stably transfected H9c2 cells to overexpress a dominant-negative Atg5 mutant (Atg5K) [204] to create an autophagy-deficient cell line. This is accepted as a

preferred means of generating reduced levels of autophagy [200] and we confirmed these cells had lower basal LC3II levels (data not shown). Furthermore, disruption of autophagy by cardiac-specific knockdown of Atg5 in adult mice leads to cardiomyopathy [202]. In the current study, we found that when autophagy was impaired in Atg5K H9c2 cells, insulin signaling was subsequently reduced. This was in keeping with the observation that inhibition of autophagy by Lcn2 correlated with insulin resistance. Similarly, defective insulin signaling was observed as a result of Atg7 suppression, the restoration of which enhanced systemic glucose tolerance in obese mice [205]. Numerous studies have shown that increased autophagy improved insulin sensitivity [179, 201, 206, 207]; for example resulting in insulin-stimulated glucose transport in cardiomyocytes [208]. These are in keeping with our observations that reducing autophagic flux led to insulin resistance and when we used rapamycin, commonly used as an activator of autophagy [192] post-Lcn2 treatment we found that increased autophagy correlated with increased insulin signaling.

The results of this study are likely to have important physiological significance. It is likely that the elevated circulating Lcn2 levels found in obesity, diabetes and upon inflammation contribute to adverse cardiac remodeling leading to heart failure by virtue of reducing levels of autophagy and inducing insulin resistance. Furthermore, it is conceivable that elevated Lcn2 is both a causative factor in inducing myocardial infarction and a primary constituent of the response to it. Indeed, Lcn2 levels have been shown to be elevated rapidly after myocardial ischemia [23, 24]. Future studies to determine whether Lcn2 influences stress-induced alterations in cardiac autophagy and their functional

significance will need to be performed. Use of both Lcn2-KO and autophagy deficient mice will be necessary to further establish the significance of these effects.

In conclusion, we treated H9c2 cells with recombinant Lcn2 and observed reduced insulin-stimulated Akt and p70S6K. With autophagy initiated using a serum starved condition, we used multiple approaches, including Western blotting for LC3II, TEM, DQ-BSA degradation, MagicRed assay of cathepsin B activity and tandem fluorescent RFP/GFP-LC3, to demonstrate that Lcn2 reduced autophagic flux. We also generated an autophagy deficient H9c2 cell line by overexpressing a dominant-negative Atg5 mutant and again found that reduced autophagy correlated with lower insulin sensitivity and that adding rapamycin to acutely stimulate autophagic flux restored insulin action. This indicated that autophagy can be beneficial to the myocardium in terms of its insulin sensitizing effect. Thus, an acute effect of Lcn2 on H9c2 cells is to decrease insulin sensitivity and this can occur via its inhibitory effect on autophagic flux.

Chapter Three: Study2

Lipocalin-2 (NGAL) attenuates autophagy to exacerbate cardiac apoptosis induced by myocardial ischemia.

Hye Kyoung Sung[1*], Yee Kwan Chan[1], Meng Han[1], James Won Suk Jahng[1], Erfei Song[1], Danielson Eric[2], Thorsten Berger[3], Tak W. Mak[3] & Gary Sweeney[1#]

[1]Department of Biology, York University, Toronto, ON, Canada, [2]Department of Pharmacology and Toxicology, Medical College of Wisconsin, Milwaukee, Wisconsin, USA & [3]The Campbell Family Institute for Breast Cancer Research and Ontario Cancer Institute, University Health Network, Toronto, ON, Canada.

Published: *J Cell Physiol.* 2017 Aug 232(8);2125-2134

HK Sung performed all experiments with contributions form co-authors mentioned below, wrote the manuscript for publication.

YK Chan performed surgery in wt and Lcn2KO mice.

M Han contributed to maintenance of H9c2 cells for experiments and contributed to figure 3.1.

JWS Jahng performed experiment in figure 3.3.

E Song performed experiment in figure 3.1.D

Eric Danielson contributed to analysis of images in figure 3.5.F &I

Thorsten Berger & Tak W. Mak provided Lcn2 KO mice for experiments.

G Sweeney provided funding for project, designed experimental outline and edited the manuscript text.

3.1. Summary

Lipocalin-2 (Lcn2; also termed neutrophil gelatinase-associated lipocalin (NGAL)) levels correlate positively with heart failure yet mechanisms via which Lcn2 contributes to the pathogenesis of HF remian unclear. In this study we used coronary artery ligation surgery to induce ischemia in wild type (wt) mice and this induced a significant increase in myocardial Lcn2. We then compared wt and Lcn2 knockout (KO) mice and observed that wt mice showed greater ischemia-induced caspase-3 activation and DNA damage measured by TUNEL than Lcn2KO mice. Analysis of autophagy by LC3 and p62 Western blotting, LC3 immunohistochemistry and transmission electron microscopy (TEM) indicated that Lcn2 KO mice had a greater ischemia-induced increase in autophagy. Lcn2KO were protected against ischemia-induced cardiac functional abnormalities measured by echocardiography. Upon treating a cardiomyocyte cell line (h9c2) with Lcn2 and examining AMPK and ULK1 phosphorylation, LC3 and p62 by Western blot as well as tandem fluorescent RFP/GFP-LC3 puncta by immunofluorescence, MagicRed assay for lysosomal cathepsin activity and TEM we demonstrated that Lcn2 suppressed autophagic flux. Lcn2 also exacerbated hypoxia-induced cytochromc c release from mitochondria and caspase-3 activation. We generated an autophagy-deficient h9c2 cell model by overexpressing dominant-negative Atg5 and found significantly increased apoptosis after Lcn2 treatment. In summary, our data indicate that Lcn2 can suppress the beneficial cardiac autophagic response to ischemia and that this contributes to enhanced ischemia-induced cell death and cardiac dysfunction.

3.2. Introduction

Sustained ischemia leads to myocardial infarction (MI) which is often fatal [209], [210, 211]. Lcn2 levels have been positively associated with heart failure [12, 14, 21]] yet little is known about direct effects of lipocalin-2 on cardiac remodeling, and in particular autophagy [8-11, 13, 212]. Lcn2 has been shown to have pro-inflammatory effects and to induce insulin resistance and metabolic dysfunction [15, 16, 23, 24, 213, 214]. Ischemia and/or reperfusion elevated Lcn2 content in the heart, most likely via production from infiltrating neutrophils and macrophages [215]. Lcn2 expression is also significantly augmented in patients with coronary heart disease and myocardial infarction [156, 216]. Lcn2-KO mice showed improved functional recovery and reduced infarction size after hypoxia compared to wild type [179].

During prolonged ischemia, lack of oxygen and nutrients leads to myocardial cell death [217]. Cardiac regeneration is rare and so irreversible loss of cardiomyocytes will lead to reduced ability to sustain contractile function and progression to heart failure. Extensive research and clinical efforts have developed our understanding of structural and functional changes in the heart after MI, yet the role of Lcn2 and mechanisms via which it acts remain to be fully defined. Previous work has shown that Lcn2 can directly induce cardiomyocyte apoptosis [71] and attenuate autophagy leading to insulin resistance in h9c2 cells [218]. Numerous studies have shown that autophagy plays an important role in heart failure [219]. Autophagy is induced by various stressors and maintains an optimal cellular environment through removing protein aggregates and damaged organelles [55, 57, 60, 220]]. Inadequate autophagy leads to adverse effects in the myocardium and subsequent cardiac dysfunction [221, 222].

In this study, we hypothesized that Lcn2 is induced by ischemia and is an important regulator of cardiac remodeling, including inhibition of autophagic flux in cardiomyocytes. Lcn2-KO or wt mice underwent coronary artery ligation (CAL) to induce chronic myocardial ischemia in the left ventricle, or sham surgery, then we performed analysis of cardiac function, apoptosis and autophagy. We also exposed H9c2 cells to hypoxia in the presence or absence of Lcn2 to test direct effects on autophagy and apoptosis. The functional significance of changes in autophagy was investigated via generating autophagy deficient H9c2 cells by overexpressing a dominant-negative mutant of Atg5. Our data contribute to elucidating the role of Lcn2 in ischemia-induced cardiac remodeling and function as well as the mechanisms via which it acts.

3.3. Materials and methods

3.3.1. Animal models

In house bred lipocalin2 knockout (Lcn2KO) mice and age matched C57BL/6 (wild type, WT) mice (The Jackson Laboratory, USA) were fed *ad libitum* on regular chow diet until 6-8 weeks of age and randomly separated into treatment groups (n=4-8 per group) (C57 Sham, n=6; C57 CAL, n=6; Lcn2KO Sham, n=6, Lcn2KO CAL, n=8). All animals were kept in temperature and humidity-control rooms (21 ± 2°C, 35-40%) with a daily 12:12h light-dark cycle in the animal care facility of York University in accordance to the guidelines of the Canadian Council on Animal Care. All study protocols were approved by the Animal Care Committee of York University.

3.3.2. Induction of ischemia via coronary artery ligation surgery

Myocardial infarction (MI) was induced with ligation of the left anterior descending coronary artery (CAL) as previously described [213]. Briefly, left anterior descending coronary artery was ligated with a 8-O suture at 3mm below the tip of the left atrium for 24 hours, resulting in an infarct area of ~30-40% of the left ventricle. The sham animals underwent the same procedure except for the suture ligation around the coronary artery. Mice were sacrificed 24hours after MI.

3.3.3. Analysis of cardiac function using echocardiography

Echocardiography was performed as we previously described [214] using the Vevo2100 system (Visual Sonics, Canada) equipped with an MS550D transducer. Mice were lightly anesthetized using 2.0% isofluorane mixed with 1000% O_2 during the time of imaging. M-mode images of parasternal short-axis view at papillary level was used to calculate cardiac

systolic and diastolic functions. B-mode movie files of parasternal short-axis view were used to perform Speckle-tracking cardiac strain rate analysis. All parameters were averaged at least 5 cardiac cycles for analysis.

3.3.4. Immunofluorescent analysis of LC3 puncta and caspase-3 activation in heart tissue sections

Heart were fixed with 10% buffered formalin and embedded in paraffin. Immunofluorescence staining was performed on 5-µm-thin sections using Abs against cleaved caspase 3 and LC3B (Cell Signaling). Images were captured and analyzed under an Olympus IX71 inverted fluorescent microscope (Olympus Canada, Richmond Hill, ON, Canada).

3.3.5. Cell culture

H9c2 rat embryonic cardiac myoblasts (ATCC® CRL-1446™) were grown in Dulbecco's Modified Eagle's Medium (DMEM) (Gibco®) supplemented with 10% fetal bovine serum and 1% (vol/vol) streptomycin/penicillin (Gibco, Invitrogen) at 37°C and 5% CO_2. When cells reached approximately 80% confluence they were incubated in 0.5% fetal bovine serum-DMEM with or without Lipocalin2 (Lcn2) at 1µg/ml in normoxia and hypoxia condition. Lcn2KO was produced as we previously described [223].

Hypoxia condition was achieved by placing cells in hypoxic chamber filled with pre-analyzed gas mixture of 5% CO2 and 95% N2, and supplemented with Anaeropouch ™(Mitsubishi™, Japan) [215].

3.3.6. Recombinant Lcn2 production

The expression of His-tagged Lcn2 (a kind gift from Aimin Xu and Yu Wang, University of Hong Kong) in BL21 Competent E. Coli (NEB Biolab) was induced by SOC growth medium (NEB Biolab). Lcn2 was purified from bacterial lysates using the HIS-select® nickel affinity gel (Sigma) according to the manufacturer's protocol. The purity of Lcn2 was confirmed using SDS-PAGE gel.

3.3.7. Western blotting

LV heart tissue was snap frozen and pulverized with mortar and pestle in liquid nitrogen. The powdered tissue was then suspended in RIPA lysis buffer as we previously described [216]. H9c2 cells were grown to 90% confluency in 6 well plates. After the experimental endpoint, cells were washed in PBS and solubilized in 1x Lysis buffer (50mM Tris, 150mM NaCl, 0.1% SDS 1% Triton X-100 and 0.5% sodium deoxycholate) containing protease inhibitor cocktail – complete ULTRA Tablets, Mini (Roche). Lysates were centrifuged at 12,000 rpm for 5 min at 4°C. Supernatant was collected , heated at 90°C for 5 min and equivalent amounts of lysate were loaded to an SDS-PAGE gel, followed by protein transfer onto PVDF membrane (Bio-Rad). Membranes were first blocked in 3% BSA for 1 hour, incubated in primary antibody at 4°C overnight, washed, incubated in appropriate horse-radish peroxidase (HRP)-linked secondary antibody for 1 hour, washed, then followed by chemiluminescence enhancement using Western Lightning Plus ECL (Perkin Elmer) before developing and exposing the membrane to CL XPosure Film (Thermo Scientific). The band intensities were quantified using Image J. The following primary antibodies were used: pAMPKα T172, pULK1 S555, LC3B, Caspase 3, β-Actin and GAPDH (1:1000, Cell

Signaling), P62 (BD Biosciences), Lcn2 (University of Hong Kong). The following secondary antibodies were used; anti-rabbit IgG HRP-linked antibody and anti-mouse IgG.

3.3.8. Generation of H9c2 cells stably overexpressing tandem fluorescent RFP/GFP-LC3 and analysis of autophagic flux and autophagy-deficient H9c2-ATG5K130R cells

Stable H9c2 cells expressing tf-RFP/GFP-LC3 were created essentially as described by us previously for another cell type [179]. Cells were grown to 80% confluence on coverslips in 12 well plates. At experimental endpoint, cells were fixed in 4% para formaldehyde (PFA) and quenched with 1% glycine before mounting on a glass slide. Confocal images were taken using a x60 objective (Olympus, BX51 Microscope). Pearson and Overlapping coefficients were calculated using ImageJ with the JACoP plug-in to quantify the extent of GFP and RFP co-localization. To generate H9c2 cells stably over-expressing mutant ATG5 proteins (ATG5K130R), H9c2 cells were transduced with retroviral vector carrying pmCherry-ATG5K130R.

3.3.9. Transmission electron microscopy (TEM)

TEM was performed as described previously [224]. Briefly, LV tissues were cut into small pieces (roughly 1 mm3) and H9c2 cells were grown on 6 well plate to 80% confluency. After the experimental endpoint, cells were washed with PBS and immediately fixed in 2.5% glutaraldehyde in 0.1M sodium cacodylate buffer followed by post-fixation with 1% osmium tetroxide for 1 hour at room temperature. The specimens were then dehydrated with ascending concentrations of ethanol in series (50%–100%) and embedded in Spurr's Epoxy resin.

Afterwards, thin sections (60–80 nm) were cut with an ultramicrotome and mounted on copper mesh grids. The sections were then contrasted with 1% uranyl acetate and lead citrate, and examined with a FEI CM100 TEM and Kodak Megaplus camera.

3.3.10. Analysis of cellular caspase-3/7 activity using immunofluorescence

H9c2 cells were seeded in 12-well plates with cover slip, and treated with/without Lcn2 (1ug/mL) in normoxia or hypoxia condition for 24 hour. After treatment, cells were loaded with CellEvent® Caspase-3/7 Green Detection Reagent according to manufacturer's protocol. Cells were fixed in 4% PFA, quenched with 1% glycine before mounting. Nuclei of cells were countered stained with Vectashield Antifade Mounting Medium with DAPI (Vecotr Laboratories). Images were taken using a 60X objective with confocal microscope (Olympus, BX51).

3.3.11. Analysis of cytochrome C release from mitochondria

H9c2 cells were seeded in 12-well plates with cover slip, and treated with/without recombinant globular Ad (1ug/mL) in normoxia or hypoxia conditions for 48 hour, after treatment, cells were incubated with mitoTracker® Red CMXRos (ThermoFisher Scientific) at 250nM for 30 minutes. Then, Cells were fixed in 4% PFA and quenched with 1% glycine then blocked with 5% BSA. After blocking, cells were incubated with cytochrome C (clone 6H2.B4, BD Pharmingen™, 1:400) followed by Goat anti-Mouse IgG, Alexa Fluor 488 (ThermoFisher, 1:800). Pearson or Manders' Coefficients (M1 & M2) were calculated using ImageJ with the JACoP plug-in to quantify the extent of GFP and RFP co-localization.

Images were taken using a 60X objective with Laser Scanning Microscope (ZEISS, LSM700) and 3D images were using Imaris 3D/4D analysis sofeware.

3.3.12. Statistics

Data was presented as mean±SEM. Statistical significance between treatment groups were calculated using the unpaired Student t test when comparing 2 groups. For comparisons of more than 2 groups, One Way ANOVA followed by Dunnett's posttest and Two Way ANOVA with Bonferroni post-test were performed to adjust multiple comparisons. *P* value <0.05 was considered statistically significant.

3.4. Results

3.4.1. Lipocalin-2 deficiency attenuated ischemia-induced apoptosis

We first assessed the expression of Lcn2 and found a significant increase in the total expression of Lcn2 in the ischemic myocardium (Figure 3.1.A&B). Using both Western blotting and immunofluorescent detection we showed that myocardial cleaved caspase 3 was significantly increased after ischemia in wt, although to a lesser extent in Lcn2KO mice and was further decreased with the Lcn2KO (figure 3.1.A-C).

3.4.2. Lipocalin-2 contributes to suppression of autophagy during ischemia

Autophagy flux was assessed by examining cardiac expression of key proteins involved in autophagy: LC3II and P62. LC3II, a marker of autophagosome content, was increased after ischemia in wt mice (Figure 3.2.A&B). Lcn2KO mice showed higher basal levels of LC3II with no further change induced by ischemia (Figure 3.2.A&B). We also examined autophagic flux by testing p62 expression and found this was unaltered in wt mice, but significantly decreased in Lcn2KO mice after ischemia (Figure 3.2.A&C). We used LC3 immunofluorescence to study autophagosome content. The presence of LC3-positive puncta reflects the presence of autophagic vacuoles, whereas a diffuse cytoplasmic staining is indicative of an absence of autophagic vacuoles [225]. We found greater induction of LC3 puncta in Lcn2KO mice (Figure 3.2.D&E). To further investigate whether autophagic structures are altered in wt or Lcn2KO mice hearts after ischemia we used transmission electron microscopy (TEM). Autophagic vacuole content did increase somewhat after ischemia in wt mice, yet this increase was further enhanced in Lcn2 KO mice, as shown in representative images in figure 3.2.F. Another striking change was the markedly increased

mitochondria damage after 24 hours of ischemia in WT mice, which was evidently attenuated in Lcn2 KO mice (Figure 3.2.F).

3.4.3. Adverse remodeling with cardiac dysfunction in Lcn2KO mice after ischemia

Wt and Lcn2KO mice were subjected to ligation of the left anterior descending coronary artery (CAL) to induce MI, and compared with sham surgery. 1 day after the surgery, wt mice developed systolic dysfunction, increase in end systolic diameter and volume. However, changes in end systolic diameter and volume are comparable between sham and ischemic groups in Lcn2KO mice (Figure 3.3.A). To provide additional details on regional cardiac dysfunction induced by ischemia, we used speckle tracking echocardiography to calculate 3-dimentional strain rate, an indicator of how much the myocardial tissue has physically disabled. Radial strain rate at systole and diastole significantly decreased after the surgery in wt mice yet such change was not observed in Lcn2KO mice (Figure 3.3.B). As visualized clearly in representative images of circumferential strain rate of six segmented wall regions, the synchronicity of two opposing walls (anterior/posterior) of endocardium were disrupted in wt mice whereas the synchronicity was maintained in Lcn2KO mice after ischemia (Figure 3.3.C).

3.4.4. Lipocalin-2 attenuated autophagic flux in cardiomyocytes

As seen in Figure 3.4.A-C, Lcn2 was shown to decrease autophagy initiation by its down regulation of phosphorylation of AMPK and ULK1 S555. Furthermore, Lcn2 decreased the amount of LC3II (Figure 3.4.A&D), the lipidated form of LC3 that is a marker of autophagosome formation. In a complete autophagic pathway or autophagic flux,

autophagosomes will eventually fuse with lysosomes to form autolysosomes where cargo materials get degraded. We used P62 which is a widely used marker as autophagic cargo protein and we found that hypoxia induced P62, and this was exacerbated after treatment with Lcn2 (Figure 3.4.A&E). To directly assess autophagic flux, we transfected H9c2 cardiomyoctyes with tandem fluorescence (RFP-GFP)-LC3. GFP-loses fluorescence due to lysosomal acidity but RFP does not. Thus, increased degradation of autophagosomes can be interpreted via a lower RFP/GFP ratio and appear more red in colour. Under the control conditions, most LC3 punctae appeared red; while an increase in yellow punctate was observed with the addition of Lcn2 (Figure 3.4.F&G). To visualize autophagic structures, mitochondria and endoplasmic reticulum (ER) we used transmission electron microscopy (TEM) of H9c2 cardiomyocytes. Numerous autophagic vacuoles including autophagosomes and autolysosomes were observed after 24 hours of hypoxia conditions (Figure 3.4.H). In particular, we found a large number of autophagic vacuoles, swollen ER and a large number of damaged mitochondria after 24 hours hypoxia with Lcn2 treatment (Figure 3.4.H).

3.4.5. Regulation of apoptosis by alterations in autophagy and effect of lipocalin-2

We investigated Lcn2-induced apoptosis and the role of reduced autophagy in cardiomyocytes via generating autophagy-deficient H9c2 cells by stably overexpressing a mutant inactive Atg5 (ATG5K130R). Cells transduced with retrovirus with empty vector (EV) were used as control. EV and ATG5K130R H9c2 cells underwent 48hr hypoxia treatment, with or without Lcn2 and then we observed caspase 3 levels by Western blotting and activity of caspase-3/7 using activatable fluorescent substrates, respectively (Figure 3.5.A-D). After 48 hours of hypoxia, the expression of cleaved forms of capsase-3 was significantly increased

in both EV and ATG5K130R cells, especially in the latter and with Lcn2 treatment (Figure 3.5.A&B). As indicated by representative confocal images and quantification of green intensity, there was a significant increase in caspase-3 activity in ATG5K130R cells following long term hypoxia and Lcn2 treatment (Figure 3.5.C&D). We then further examined the cellular mechanisms of Lcn2-induced caspase-3 activation by studying cytochrome C colocalization with mitochondria (Mitotracker) (Figure 3.5.E&F). Upon hypoxia treatment (48 hour) or Lcn2, cytochrome C and mitochondrial colocazation decreased (Figure 3.5.H&I). In ATG5K130R cells neither hypoxia nor Lcn2 alone caused significant release of cytochrome c from mitochondria.

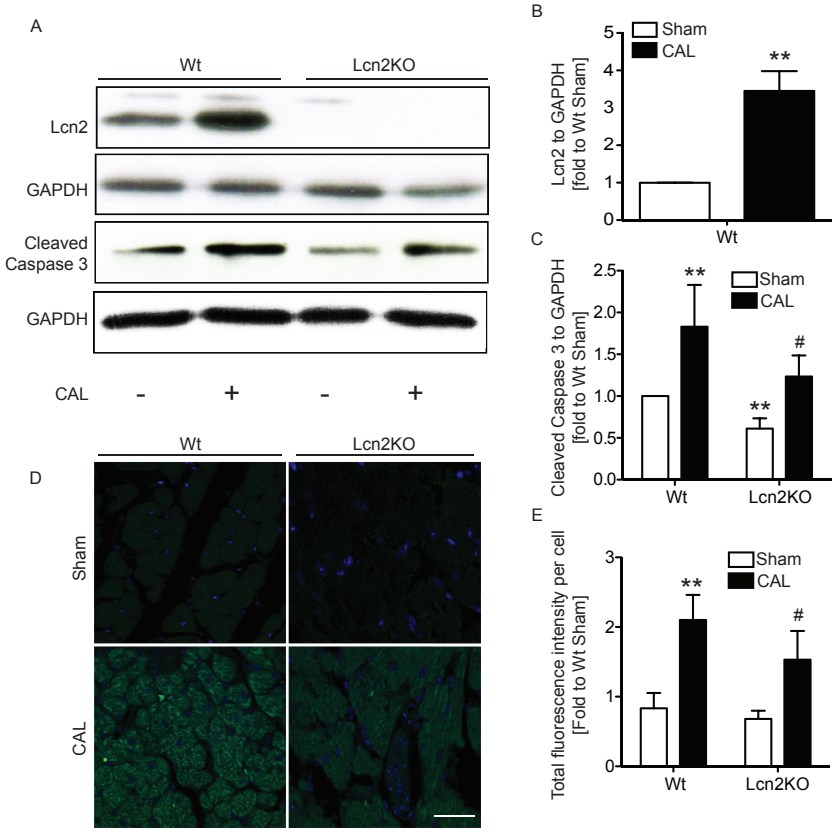

Figure 3.1. Myocardial infarction induced cell death and apoptosis in Wt but less in Lcn2KO mice. (A) Western blotting was performed to examine the protein levels of Lcn2 and apoptosis was analyzed by examining the protein expression of cleaved caspase 3 in heart tissue homogenates from from WT and Lcn2KO mice that have undergone either sham or CAL surgery. (B, C) Densitometric quantifications of Wwestern blots in A. (D) Immunofluorescence was performed for cleaved capase 3 in heart tissue sections collected from WT and Lcn2KO mice subjected to either sham or CAL surgery and (E) quantification. Quantitative data in graphs are shown as mean ± SEM (n=3-5). *P<0.05 versus corresponding Wt sham, # P<0.05 versus corresponding Lcn2KO sham. Scale bar = 50 μm.

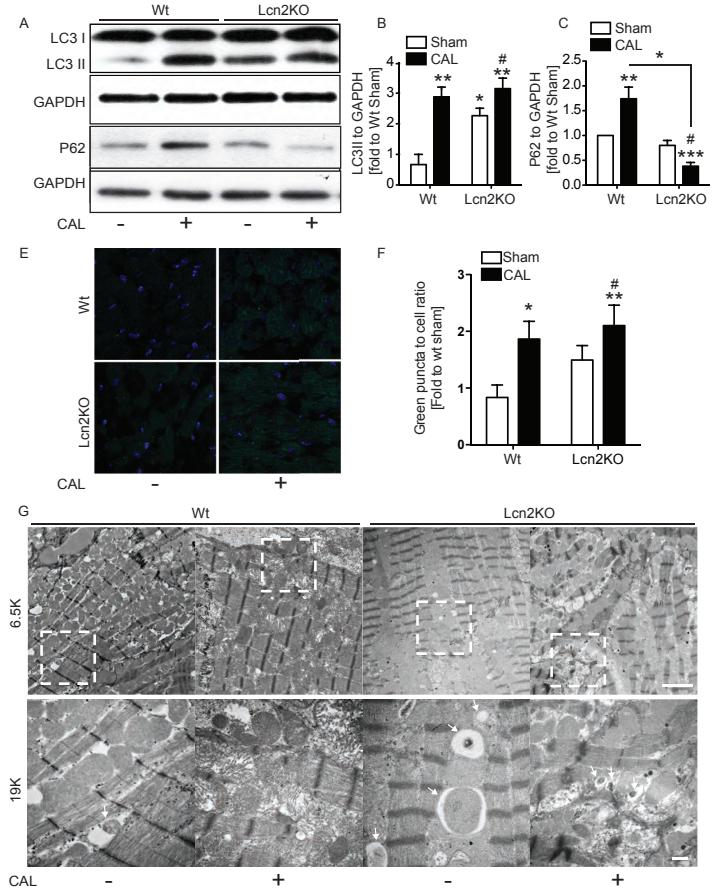

Figure 3.2. Lcn2 deficiency accelerated autophagy. (A) Autophagic flux was analyzed by examining the protein expression of LC3II and P62 in heart tissue lysates from WT and Lcn2KO mice that have undergone either sham or CAL surgery. (B) Densitometric quantifications of Western blots in A. (C) Immunofluorescence was performed for LC3II in heart tissue sections collected from WT and Lcn2KO mice subjected to either sham or CAL surgery. (D) Densitometric quantifications of Western blots in C. (E) Autophagic vacuoles were evaluated using TEM from heart tissue of WT and Lcn2KO mice that had undergone either sham or CAL surgery. Quantitative data in graphs are shown as mean ± SEM (n=3-5). *P<0.05 versus corresponding Wt, # P<0.05 versus corresponding Lcn2KO. Low: 6,500 and high magnification 19,000, Scale bar = 2 μm and 500nm.

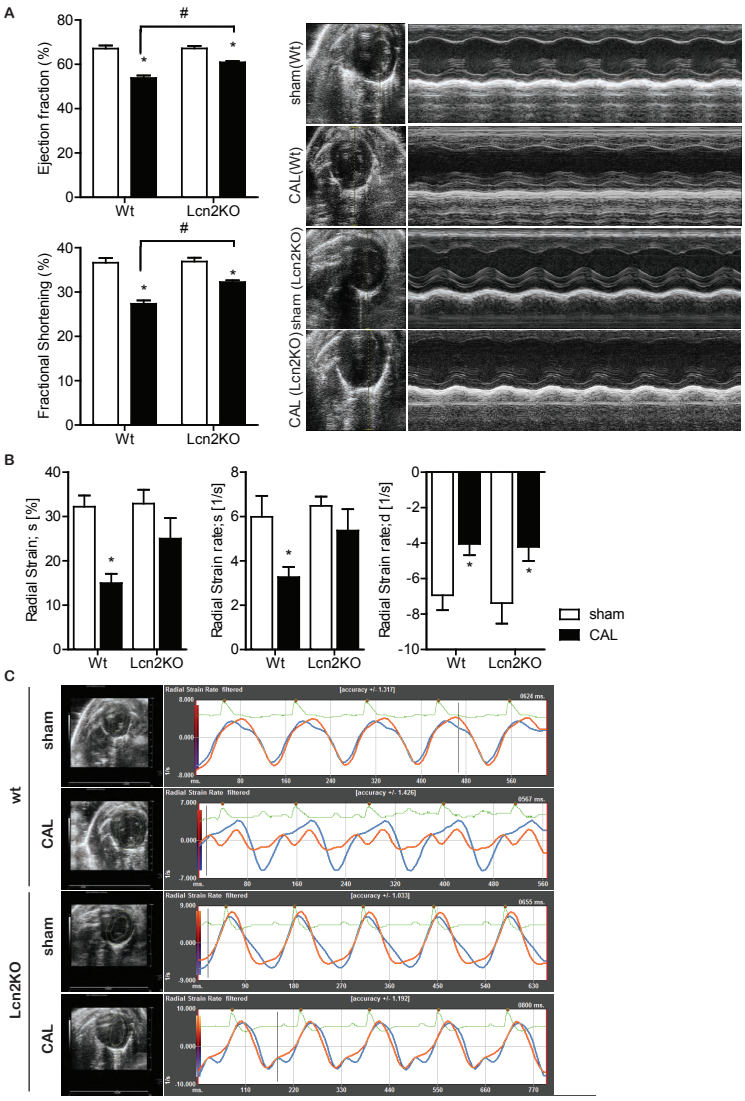

Figure 3.3. Ischemia-induced cardiac dysfunction was reduced in Lcn2KO mice. A. Cardiac function parameters ejection fraction and fractional shortening analyzed 24hrs after CAL surgery using echocardiography. B. Changes in radial strain and peak strain rate (/s) at systole and diastole 24hrs after CAL. C. Representative images of radial strain rate changes between two segments (anterior/posterior apex) during four cardiac cycles. PL: pre-ligation. Results are presented as mean ± SEM (n=4 for wt and n=4 for Lcn2KO mice). [a]P<0.05 vs corresponding sham. [b]P<0.05 vs PL. *P<0.05, vs corresponding sham. #p<0.05 vs wt CAL

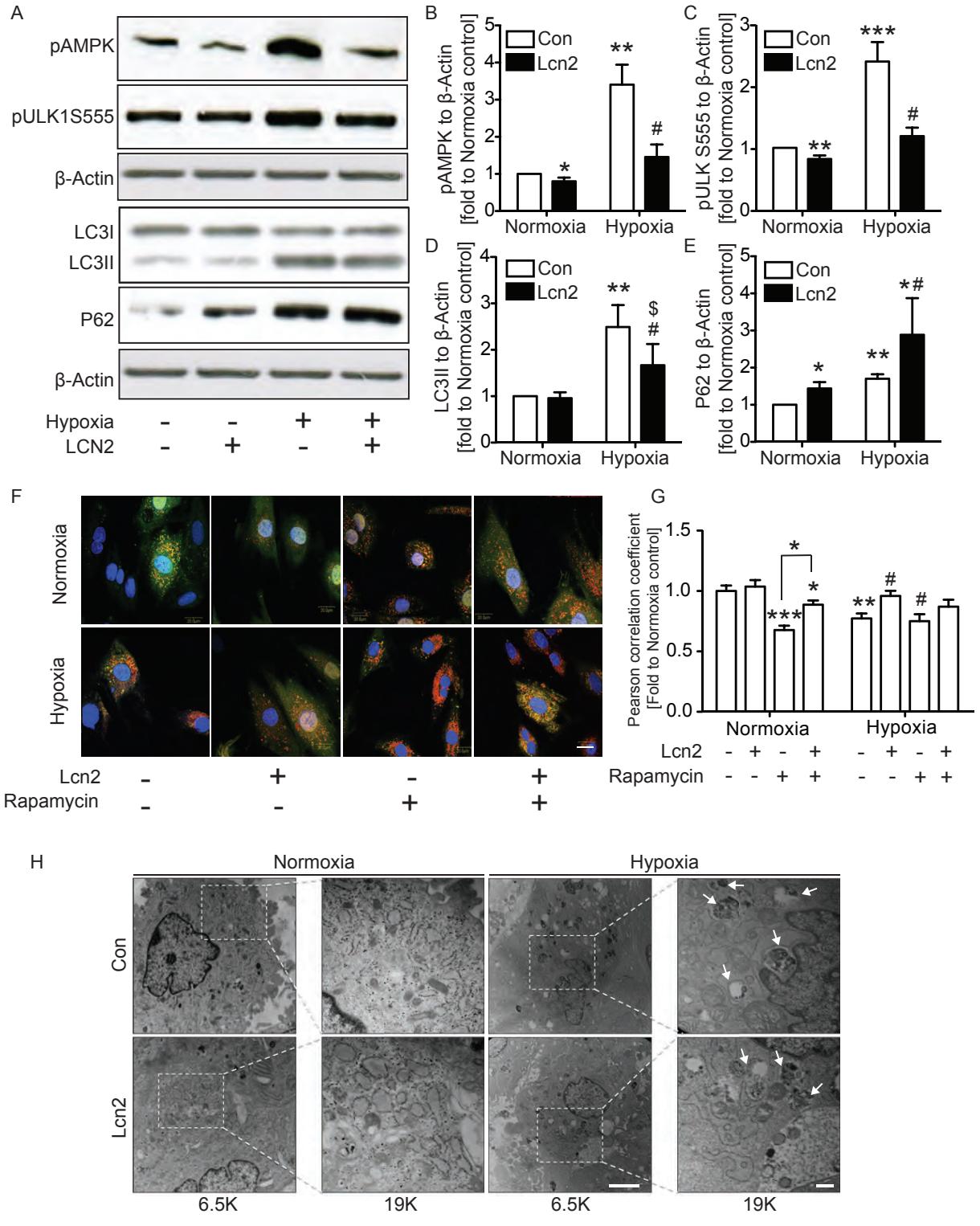
A
pAMPK
pULK1S555
β-Actin
LC3I
LC3II
P62
β-Actin
Hypoxia - - + +
LCN2 - + - +
B
pAMPK to β-Actin [fold to Normoxia control]
Con
Lcn2
Normoxia
Hypoxia
C
pULK S555 to β-Actin [fold to Normoxia control]
D
LC3II to β-Actin [fold to Normoxia control]
E
P62 to β-Actin [fold to Normoxia control]
F
Normoxia
Hypoxia
Lcn2 - + - +
Rapamycin - - + +
G
Pearson correlation coefficient [Fold to Normoxia control]
Lcn2 - + - + - + - +
Rapamycin - - + + - - + +
H
Normoxia
Hypoxia
Con
Lcn2
6.5K
19K
6.5K
19K

Figure 3.4. **Lcn2 and hypoxia reduced autophagic flux in cardiomyocytes.** H9c2 cells were treated with recombinant Lcn2 (1ug/ml) or without (Con) for 24hour in normoxic or hypoxic conditions. (A) Western blots showing protein expression of pAMPK, pULK1S555, LC3II, P62, GAPDH and (B-E) their quantifications. (F) Autophagic flux was evaluated by looking at the RFP/GFP ratio of the LC3 puncta in the tf-GFP/RFP-H9c2 cells and (G) quantification. Scale bar = 20μm. (H) Autophagy was evaluated using transmission electron microscopy. Selected areas were magnified, with white arrows indicating the presence of autophagolysosome. Low: 6,500 and high magnification 19,000, Scale bar = 2 μm and 500nm.

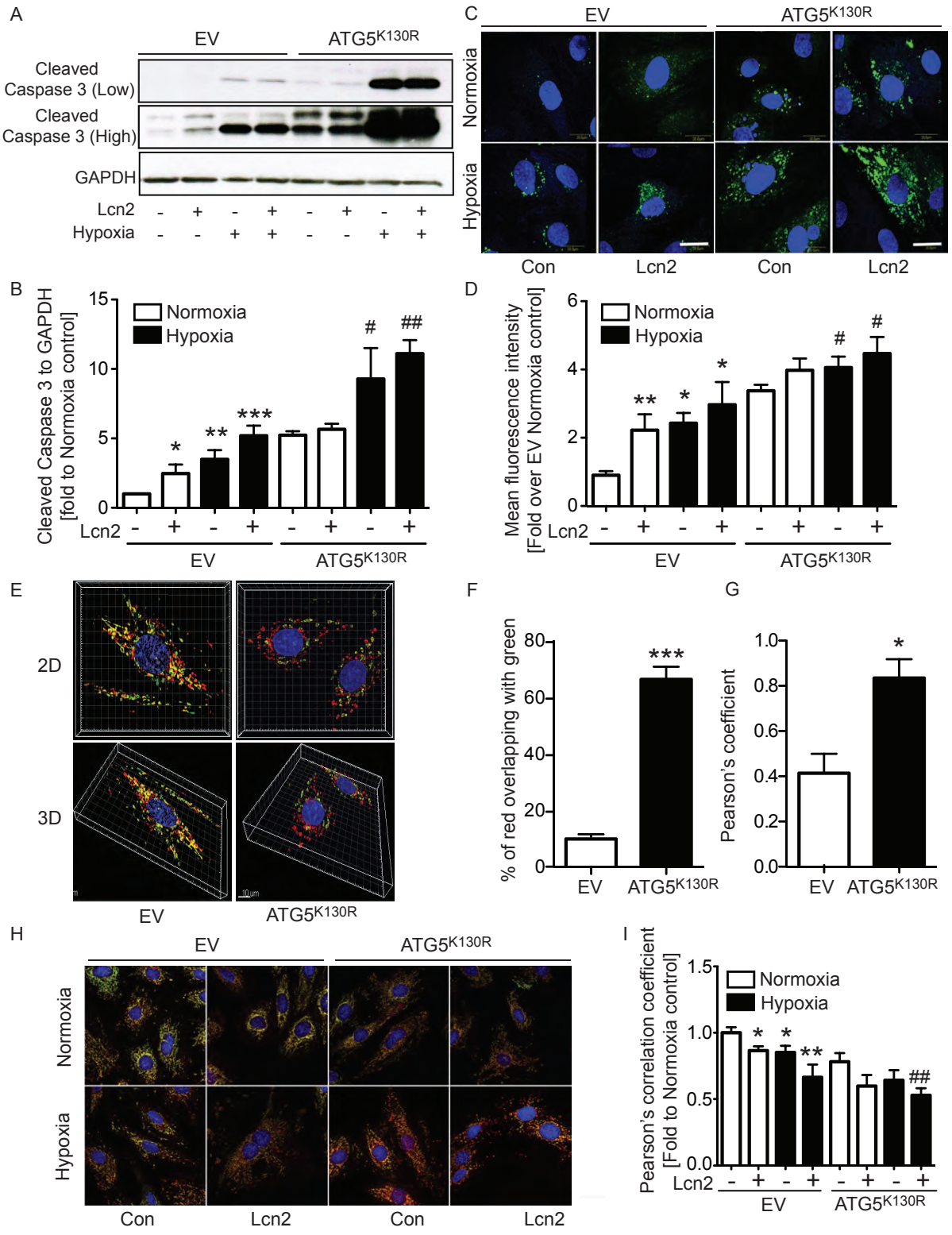
A
EV
ATG5K130R
Cleaved Caspase 3 (Low)
Cleaved Caspase 3 (High)
GAPDH
Lcn2 - + - + - + - +
Hypoxia - - + + - - + +
C
EV
ATG5K130R
Normoxia
Hypoxia
Con
Lcn2
Con
Lcn2
B
Cleaved Caspase 3 to GAPDH [fold to Normoxia control]
Normoxia
Hypoxia
Lcn2 - + - + - + - +
EV
ATG5K130R
D
Mean fluorescence intensity [Fold over EV Normoxia control]
Normoxia
Hypoxia
Lcn2 - + - + - + - +
EV
ATG5K130R
E
2D
3D
EV
ATG5K130R
F
% of red overlapping with green
EV
ATG5K130R
G
Pearson's coefficient
EV
ATG5K130R
H
EV
ATG5K130R
Normoxia
Hypoxia
Con
Lcn2
Con
Lcn2
I
Pearson's correlation coefficient [Fold to Normoxia control]
Normoxia
Hypoxia
Lcn2 - + - + - + - +
EV
ATG5K130R

Figure 3.5. Reduced autophagy exacerbated cell death in H9c2 cells. (A) Western blot analysis of cleaved caspase 3 level in WT and ATG5K cells after long-term hypoxia (48 hour) ± treatment with Lcn2 (1ug/mL) and (B) quantification. (C) Representative confocal images of caspase 3/7 activity and (D) quantification. (E) Representative 3D confocal images of WT and ATG5K cells immunolabeled with cytochrome C (green), stained with mitotracker (red) and (F, G) quantifications. (H) Representative confocal images of WT and ATG5K cells showing cytochrome C and mitotracker ± hypoxia and ± Lcn2 and (I) quantitative and statistical analysis of green/red co-localization coefficients. Experiments were performed at least three times and results are presented as mean ± SEM. *P<0.05 versus EV normoxia control and $^{\#}$ P<0.05 versus ATG5^{K130R} normoxia control, Scale bar = 20μm.

3.5. Discussion

Although clinical studies have established a strong correlative relationship between Lcn2 levels and cardiac dysfunction [12, 73] there have been few studies examining the direct effects of Lcn2 action on the myocardium. In this case we first of all used an ischemic model of heart failure and using echocardiography confirned that mice lacking Lcn2 fared better than wt mice [23], suggesting an important permissive role for Lcn2 in ischemia-induced cardiac dysfunction. Importantly, we showed here that cardiac Lcn2 content increased significanctly after ischemia but not sham surgery.

To investigate mechanisms via which Lcn2 may induce heart failure we focused on autophagy, and cardiomyocyte cell death as an end point. Rationale for this focus comes from recent work by ourselves and others showing that Lcn2 inhibited autophagic flux in H9c2 cells or hepatic chaperone-mediated autophagy [218, 226]. Translating our previous in vitro studies to the animal model of cardiac ischemia used here, we found that ischemia-induced autophagy was exaggerated in mice lacking Lcn2, perhaps reflecting endogenous suppression of autophagy by Lcn2. This is significant since cardiac autophagy is thought to be induced in response to various stressors and act as a protective cellular mechanism [227, 228]. Indeed, we found that the reduced levels of ischemia-induced autophagy correlated with enhanced cell death. Collectively, the data indicated that Lcn2KO mice had enhanced autophagic flux with reduced cell death and cardiac dysfunction after ischemia.

To further investigate this relationship between autophagy and cell death and their regulation by Lcn2 we again used H9c2 cardiomyoblasts and exposed them to hypoxic stress,

with or without presence of Lcn2. Via observing responses such as reduced AMPK(Thr172) and ULK1(Ser555) phosphorylation, reduced LC3-II and increased P62 levels and less evident autophagosomal structures using TEM we concluded that autophagic flux decreased when Lcn2 and hypoxia were used in combination. These data supported our observations in cardiac tissue of mice with ischemia, and to more accurately conclude that these conditions restricted autophagic flux we transduced cells with tandem fluorescent RFP/GFP-LC3 [218] expressing retroviral constructs. Using this approach, cells express LC3 tagged with both GFP and RFP and thus autophagosomes appear as yellow puncta. Upon fusion with lysosome, the acidic pH quenches green but not red fluorescence allowing flux to be viewed by more red puncta. Confocal microscopy analysis showed that Lcn2 reduced appearance of red puncta, indicating that Lcn2 reduced autophagic flux by attenuating autophagosome to lysosome fusion. This suppression of autophagic flux by Lcn2 was also evident when we used a pharmacological stimulant of autophagy, rapamycin [229]. Overall, these multiple approaches also support the conclusion that Lcn2 attenuates autophagic flux.

Apoptosis is established as a cardiac remodeling event which contributes to heart failure and as such is a potentially important therapeutic target [230, 231]. Indeed, previous research [232] showed attenuation of myocardial injury brought by a caspase inhibitor. We next further investigated the mechanistic role of autophagy in Lcn2- and hypoxia-induced cardiomyocyte cell death. To do so, we stably transfected H9c2 cells to overexpress a dominant-negative Atg5 mutant to create an autophagy-deficient cell line [179, 218]. Previous studies showed that Lcn2 induced Bax translocation to mitochondria, caspase-3 activation and apoptosis in primary cardiomyocytes and H9c2 cells [71]. Hypoxia has also been shown to

independently cause activation of intrinsic apoptotic cell death [233]. First of all, we observed that autophagy deficiency mimicked Lcn2 in that elevated caspase-3 activation was observed, and no further increase was observed when Lcn2 was added. Interestingly, hypoxia-induced caspase-3 activation was still observed in autophagy-deficient cells. We also analyzed cytochrome c release from mitochondria as a measure of intrinsic apoptosis and found that in normal cells this was induced by both Lcn2 and hypoxia which together had a synergistic effect. Autophagy-deficiency reduced cytochrome c and mitochondria colocalization and although there was an apparent further reduction by Lcn2 or hypoxia, these were not statistically significant. Therefore, we conclude that attenuation of cardiomyocyte autophagy by Lcn2 or molecular engineering of cells confers increased susceptibility to stress-induced cell death. This is in keeping with literature in which mouse models of autophagy deficiency develop agre-related cardiomyopathy [234], show enhanced hemodynamic stress induced dysfunction [202] and angiotensin-II stimulated inflammation and injury [235].

In summary, our study indicates that Lcn2 is an important suppressor of cardiomyocyte autophagic flux and that this contributes to intrinsic apoptosis. In a mouse model of cardiac ischemia, Lcn2 levels increase and contribute to attenuation of cardiac autophagy with increased cell death and dysfunction. Mice lacking Lcn2 are able to elicit a higher autophagic response after ischemia and are protected from cell death and cardiac dysfunction. These dats suggest that further studies are warranted to investigate the usefulness of Lcn2 as both a biomarker and therapeutic target in heart failure.

Chapter Four: Study 3

Iron induces insulin resistance in cardiomyocytes via regulation of oxidative stress.

Hye Kyoung Sung[1*], Erfei Song[1] & Gary Sweeney[1#]

[1]Department of Biology, York University, Toronto, ON, Canada

Running head: Iron, oxidative stress, autophagy and insulin resistance

HK Sung performed all experiments with contributions form co-authors mentioned below, and wrote the text presented in this thesis chapter.

E Song isolated primary cardiomyocyte cells for experiment in figure 4.2

G Sweeney provided funding for project, designed experimental outline and edited text.

4.1. Summary

Inadequate supply of iron can elicit health defects yet there is also strong evidence that too much iron induces detrimental cellular effects. Accordingly, disturbed iron homeostasis is associated with various pathological conditions, including diabetes and heart failure. Insulin resistance is an established contributor to heart failure and in this project I tested the hypothesis that iron induces cardiomyocyte insulin resistance via oxidative stress. In primary adult and neonatal cardiomyocytes as well as H9c2 cells, derived from rat heart ventricle, iron ($FeSO_4$, 100μM/ml 4hours) induced insulin resistance as determined by Western blotting and immunofluorescent detection of Akt phosphorylation. Using CellROX Deep Red assay we also observed that iron increased generation of reactive oxygen species (ROS), and that anti-oxidant pretreatment attenuated iron-induced insulin resistance. I used multiple assays to monitor autophagic flux and observed that iron suppressed autophagy. First, we determined pULK1(S757), LC3II and P62 levels by Western blotting and immunofluorescence. The increase autopahgosome content was validated by an increase in puncta detected using Cyto ID assay. To study the functional significance of changes in autophagy we created an autophagy-deficient cell model by overexpressing a dominant-negative Atg5 mutant in H9c2 cells and autophagy deficiency both induced insulin resistance. In conclusion, our study indicated that iron reduced autophagy and stimulated ROS production, causing insulin resistance in cardiomyocytes. Future studies will further investigate mechanisms via which iron regulates cardiac remodeling and their physiological significance. I anticipate that our findings will provide new knowledge relevant to current diagnostics and therapeutics related to altered iron status in clinical settings.

4.2. Introduction

Iron is an essential micronutrient and its crucial role in many physiological functions is often underestimated [236]. Altered iron metabolism is implicated in a vast array of diseases, including type 2 diabetes [236], neurodegenerative diseases [237], cardiovascular diseases [79], cancer [238], osteoporosis [239] and many more. In particular, both iron deficiency (ID) and iron overload (IO) have been associated with cardiomyopathy [79, 81]. Recently iron overload cardiomyopathy (IOC) has been presented to define a secondary form of cardiomyopathy resulting from the accumulation of iron in the myocardium mainly because of genetically determined disorders of iron metabolism or multiple transfusions [81, 240]. Iron is a vital structural component of haemoglobin, myoglobin, oxidative enzymes and respiratory chain proteins that are collectively responsible for oxygen transport, storage and energy metabolism [78]. Iron-overload cardiomyopathy is the most common reason of mortality in patients with secondary iron-overload or patients with genetic hemochromatosis [241-247]. In essence, altered iron homeostasis leads to uncontrolled iron deposition in different organs, including the heart, leading to progressive tissue damage [67, 248]. Iron-induced oxidative stress plays an important role in the pathogenesis of iron-overload mediated heart disease [249-251]. The formation of labile NTBI alters the pro-oxidant/antioxidant balance, leading to a pro-oxidant state with increased free radical production, oxidative stress and cellular damage [250, 252, 253]. Previous studies indicated that oxidative stress can lead to mitochondrial dysfunction and accumulation of lipotoxic metabolites which have been shown to contribute to insulin resistance.

Autophagy is the major intracellular degradation process where cytoplasmic materials get delivered to lysosomes for degradation and recycling [178, 183, 193, 254]. Several studies have now shown that the degree of autophagy changes in the failing heart and directly in response to ischemia and/or reperfusion [195] [196-198], although the functional significance is still somewhat uncertain. Indeed, autophagy may be regarded as a double edged sword with potential beneficial and detrimental effects in the heart [199]. At low levels autophagy is important in recycling damaged organelles and nutrients, however excessive autophagy contributes to tissue dysfunction and non-apoptotic programmed cell death in pathological myocardial remodeling [184, 199-202]. Recent evidence indicated that dysregulation of autophagy resulted in ER stress, insulin resistance and glucose intolerance [255]. Our own research also has shown that induction autophagy can be beneficial to the myocardium in terms of its insulin sensitizing effect and reducing apoptosis [218, 256]. In various tissue types it has been found that ROS production results in increased autophagy [257]. In the heart, elevated autophagy is activated post-ischemia in association with ROS upregulation and this is thought to be an endogenous self-protective mechanism [258]. ROS also play an early role in the development of insulin resistance [259, 260]. Evidence suggested that downstream of the PI3K/Akt insulin signaling pathway may be the target of exogenous inducers of autophagy [261].

The precise molecular mechanisms of iron-overload cardiomyopathy have not been elucidated yet. In this study, I test the hypothesis that iron induces insulin resistance in cardiomyocytes, and that this involves regulation of autophagy and/or oxidative stress and crosstalk between them. To do so I used primary adult or neonatal cardiomyocytes, human

stem cell derived cardiomyocytes and H9c2 cells as cellular models and treated with iron for up to 24h and tested ROS production, autophagic flux and insulin sensitivity.

4.3. Materials and methods

4.3.1. Cell culture

H9c2 (ATCC® CRL-1446) rat cardiomyoblasts were grown in Gibco® normal glucose Dulbecco's Modified Eagle's Medium (DMEM) supplemented with 10% fetal bovine serum (FBS) and 1% (v/v) penicillin streptomycin at 37 °C and 5% CO_2. For microscopy assays (except TEM), cells were grown on cover slips and treated with or without recombinant $FeSO_4$ 2 (100 μM/ml) in DMEM with 0% FBS mimicking starvation at approximately 80% confluency (unless specified otherwise) for 1, 4 and 24hrs.

Primary cells; The left ventricles of 1-3 day Wistar rat pups were isolated by decapitation, and a small ventricle incision through the sternum. Hearts were perfused in CFBHH (Calcium and Bicarconate Free Hanks with Hepes) buffer, and torn apart into small pieces with fine tweezers. Samples were transferred to a flat bottom 50ml conical tube with 10ml of trypsin (1:250) and a small stir bar. Heart pieces were stirred in the fume hood for 10 min. The supernatant was collected and neutralized with 10ml of 10% FBS DMEM (1% PenStep, 50mg/L gentamycin sulfate). 10ml of trypsin was added to the remaining sample and was repeated until all tissue was digested. Supernatant was spun down at 2000RPM for 10min, supernatant was removed, and pellet was resuspended in 101%FBS DMEM. Cells were plated in a regular coated $10cm^2$ culture dishes for 1 hour in order to separate fibroblasts from cardiomyocytes. After incubation in a CO_2 incubator at 37ºC, supernatant containing

cardiomyocytes was filtered through a 70µm strainer. Filtrate was supplemented with additional 10%FBS DMEM, and plated on primaria coated culture dishes. 24 hours after isolation, cells were washed with PBS, and treatment media was added to begin experiments.

4.3.2. Colorimetric Intracellular Iron Assay

H9C2 cells were grown to 80% confluency on 24-well plates in 10% FBS DMEM with 1% w/v streptomycin/penicillin where they were treated with 100uM of FeSO4 for 1, 4 and 24 hour durations ending simultaneously. After the treatment had ended, each well was washed 3 times with 0.5ml PBS, lysed with 200ul of 50mM NaOH followed by 200ul of 10mM HCL and 200ul of freshly prepared iron releasing agent thereafter. The 24 well plates were sealed in aluminum foil and incubated at 60°C for a duration of 2 hours. Afterward, 60ul of iron detecting reagent was added to each well and left to incubate for 30 minutes at room temperature (RT). 280ul of each mixture was transferred to a 96 well plate and the absorbance of each well was measured at a wavelength of 550nm using a spectrophotometer. Data was normalized by the control treatment without iron.

4.3.3. PG SK Intracellular Iron Assay

H9C2 cells were grown to 80% confluency on coverslips in 12-well plates in 10% FBS DMEM with 1% w/v streptomycin/penicillin where they were treated with 100uM of FeSO4 for 1, 4 and 24 hour durations 30 minutes after treatment with 3uM of PG SK diacetate. Coverslips were washed 4 times with 0.5 ml PBS++, fixed by covering coverslips with 10% formalin solution for 30 minutes, washed again 3 times in PBS++, quenched by covering coverslips in 1% glycine solution for 15 minutes, washed once more 3 times in PBS++ and transferred on slides using DAPI Mounting Media for fluorescence nuclear

staining and ProLong antifade gold standard reagent (in a 1:2 ratio respectively). Prepared slides were viewed via laser scanning microscopy. PG SK fluorescence was viewed using FITC and quantified by average fluorescent intensity per cell by dividing the total green fluorescence by cell number using ImageJ.

4.3.4. Western blotting

H9c2 cells were grown to 90% confluency in 6 well plates. After the experimental endpoint, cells were washed in PBS and solubilized in 1× Lysis buffer (50 mM Tris, 150 mM NaCl, 0.1% SDS 1% Triton X-100 and 0.5% sodium deoxycholate) containing protease inhibitor cocktail – complete ULTRA Tablets, Mini (Roche). Lysates were centrifuged at 12,000 rpm for 5 min at 4 °C. Supernatant was collected, heated at 90 °C for 5 min and equivalent amounts of lysate were loaded to an SDS-PAGE gel, followed by protein transfer onto PVDF membrane (Bio-Rad). Membranes were first blocked in 3% BSA for 1 h, incubated in primary antibody at 4 °C overnight, washed, incubated in appropriate horse-radish peroxidase (HRP)-linked secondary antibody for 1 h, washed, then followed by chemiluminescence enhancement using Western Lightning *Plus* ECL (Perkin Elmer) before developing and exposing the membrane to CL-XPosure Film (Thermo Scientific). The band intensities were quantified using Image J. The following primary antibodies were used: pAkt T308 and β-actin (1:1000, Cell Signaling). The following secondary antibodies were used; anti-rabbit IgG HRP-linked antibody and anti-mouse IgG HRP-linked antibody (1:10,000, Cell Signaling).

4.3.5. CellROX® deep Red Oxidative Stress assay

CellROX® deep Red Oxidative Stress Reagents (Life Technologies) was utilized. The cell-permeable reagents are non-fluorescent or very weakly fluorescent while in a reduced state and upon oxidation exhibit strong fluorogenic signal. Fluorescence signal was then detected with confocal fluorescence microscopy. H9c2 cells were seeded in 6-well plates, and treated 100uM of FeSO4 for 1, 4 and 24hr. CellROX® deep Red was added in each well at 10 ug/mL and incubated for 15 min. Cells were harvested and fixed with 4% PFA, and run in flow cytometer machine (Gallios ™, Beckman Coulter Inc.) to analyze red fluorescent signal intensity in each cell within a population of 100,000. Confocal images were taken using 40 or 60X objective (LSM 700).

4.3.6. Generation of H9c2 cells stably overexpressing tandem fluorescent RFP/GFP-LC3 and analysis of autophagic flux and autophagy-deficient H9c2-ATG5K130R cells

Stable H9c2 cells expressing tf-RFP/GFP-LC3 were created essentially as described by us previously for another cell type [179] Cells were grown to 80% confluence on coverslips in 12 well plates. At experimental endpoint, cells were fixed in 4% para formaldehyde (PFA) and quenched with 1% glycine before mounting on a glass slide. Confocal images were taken using a x60 objective (Olympus, BX51 Microscope). Pearson and Overlapping coefficients were calculated using ImageJ with the JACoP plug-in to quantify the extent of GFP and RFP co-localization. To generate H9c2 cells stably over-expressing mutant ATG5 proteins (ATG5K130R), H9c2 cells were transduced with retroviral vector carrying pmCherry-ATG5K130R.

4.3.7. Cyto-ID® Green autophagy dye staining procedure for autophagy detection

The Cyto-ID® Green autophagy dye was prepared following the protocol from the manufacturer. The 10X assay buffer was allowed to warm to room temperature and then diluted to 1X with 9 ml of deionized H_2O and 1 ml of the buffer. The Cyto-ID® Green autophagy dye solution was prepared by mixing 8 µl of the dye and 4 ml of 1× assay buffer. The sample is shielded from exposure to direct light and incubated for 30 min at 37°C, followed by a wash and resuspension with 500 µl of 1X assay buffer before imaged-based analysis. Confocal images were taken using 40 or 60X objective (LSM 700).

4.3.8. hiPS-CMs cell culture

hiPS-CMs (iCell Cardiomyocytes), cell culture thawing, and maintenance media were purchased from Cellular Dynamics International (Cat. No. CMM-100-120-005). hiPS-CMs were cultured on gelatine-coated 384 well according to the manufacturers protocol. Briefly, iCell cardiomyocytes (hiPS-CMs) were supplied cryopreserved at a density of more than 1.0×10^6/ml and stored at −150°C until use. Cryopreserved cells were thawed in a 37°C water bath without shaking for 5 min, transferred to a 50 ml falcon tube in a drop wise manner, before addition of 9 ml iCell thawing media. Viability was determined using a manual hemocytometer and total cell count determined taking into account the cell lot plating efficiency. Cells were seeded at 4000/well in gelatine-coated 24 well plates, or 120×10^3/coverslip, in iCell thawing media and incubated at 37°C with 5% CO_2 for 48 h. Following this, cells were washed twice with 50 µl iCell maintenance media per well and

returned to the incubator for a further 48 h. Following this, iCell maintenance media were then removed and replaced with 50 µl fresh iCell maintenance media.

4.3.9. Analysis of glucose uptake and metabolism

To determine glucose uptake cardiomyocytes were seeded in 24well plates and treated with or without $FeSO_4$ (100µM) for periods of 1, 4 and 24 hr. Where indicated insulin was used at 100 nM for 10 min. Subsequently, glucose transport was assayed essentially as we previously described [262] and results are calculated as pmol of glucose uptake per min per mg protein.

4.3.10. Statistics

Data was presented as mean±SEM. Statistical significance between treatment groups were calculated using the unpaired Student t test when comparing 2 groups. For comparisons of more than 2 groups, One Way ANOVA followed by Dunnett's posttest and Two Way ANOVA with Bonferroni post-test were performed to adjust multiple comparisons. *P* value <0.05 was considered statistically significant.

4.4. Results

4.4.1. Intracellular iron accumulation induced insulin resistance in H9c2 cells

I first determined iron accumulation in H9c2 cells after treatment with 100uM $FeSO_4$ for 1, 4 and 24 hours. PGSK was preloaded into cells 30 minutes before iron treatment and compared to cells cultured for the same time period but not treated with iron. Images of cells were captured after being fixed onto coverslips with mounting solution including DAPI, via confocal microscopy (Figure 4.4.1.A). Total green fluorescence per cell was quantified (Figure 1B) using ImageJ software and by subtracting background signal. Another method was also used to measure intracellular iron accumulation in H9c2 cells treated with 100uM of $FeSO_4$ for 1, 4 and 24 hours (Figure 4.4.1.C). This colorimetric intracellular iron assay was conducted by adding ferrozine to H9c2 cell lysates after iron was liberated from ferritin. Absorbances of lysates were measured using a spectrophotometer set at a wavelength of 550nm. Both assays showed an increase in intracellular iron accumulation after 100uM $FeSO_4$ treatment for 1, 4 and 24 hours. I next examined the effects of iron via Western blotting detection of Akt phosphorylation and the data indicated that the response to insulin was attenuated after iron overload (Figure 4.4.1. D&E).

4.4.2. Iron overload induced insulin resistance in primary cardiomyocytes

After the initial observation that iron induced insulin resistance in H9c2 cells, I examined whether iron blunted insulin signaling in primary cells. I first treated with 100 μM $FeSO_4$ for 1, 4 and 24hr in primary neonatal cardiomyocytes and observed that the response to insulin was attenuated in cells treated with iron by immunofluorescent (Figure 4.4.2. A&B) and Western blotting detection of Akt phosphorylation (Figure 4.4.2.C&D). In addition, the

metabolic significance of these effects was examined by measuring glucose uptake and data indicated that iron reduced insulin-stimulated glucose uptake and metabolism in neonatal cardiomyocyte (Figure 4.4.2. E). Then I further confirmed insulin sensitivity was attenuated in primary adult cardiomyocyte cells via immunofluorescent analysis of Akt phosophorylation (Figure 4.4.2. F&G)

4.4.3. Iron induced reactive oxygen species

I then investigated the effect of iron (1 and 4 hours) on the alteration of intracellular reactive oxygen species (ROS). ROS production was measured in H9c2 cells by confocal microscope (Figure 4.4.3. A&B) and flow cytometry (Figure 4.4.3.C&D) with CellROX® reagent. The result showed that intracellular ROS significantly increased in the H9c2 cells treated with 100 μM FeSO4 as early as 1 hour and more significantly at 4 hours. A similar response was observed in human stem cell derived cardiomyocytes (Figure 4.4.3. D& E).

4.4.4. Iron induced insulin resistance via increased generation of reactive oxygen species (ROS), and enhanced by antioxidant (MnTBAP)

I next evaluated whether iron-induced oxidative stress had an effect on insulin sensitivity. To do so I first verified the effectiveness of the antioxidant reagent MnTBAP (100mM). To H9c2 cells were exposed to iron overload conditions for 4hr with 100 μM $FeSO_4$ and antioxidant 100mM MnTBAP. The data from confocal microscopy (Figure 4.4.4. A&B) and flow cytometry experiments (Figure 4.4.4. C&D) suggested that iron overload conditions led to an increase in ROS which was diminished by MnTBAP. I then examined iron ($FeSO_4$, 100μM) induced insulin resistance via Western blotting detection of Akt

phosphorylation (Figure 4.4.4.F&G) and iron significantly induced insulin resistance and attenuated by MnTBAP in H9c2 cells.

4.4.5. Iron reduced insulin signaling due to inhibition of autophagy

I next examined the regulation of autophagy by iron and it's significance in determining insulin sensitivity. As seen in Figure 4.4.5A, iron caused a significant up regulation of phosphorylation of ULK1 at Ser757 (Figure 4.4.5.A). Furthermore, iron increased the amount of LC3II (Figure 4.4.5.B), the lipidated form of LC3 that is essential for closure of the autophagosome and is widely used as a marker for autophagy. The increase autopahgosome content after iron treatment was validated by a increase in puncta detected using Cyto ID assay and confocal microscopy (Figure 4.4.5.D&E). I also examined autophagic flux by testing p62 expression (Figure 4.4.5.C) and found this was elevated by iron, and chloroquine which is well known inhibitor of late stage autophagy flux. LC3-II and p62 data collectively suggests iron attenuates flux.

Based on the observations that iron both induced insulin resistance and inhibited autophagy, I investigated if there were any causation effects between the two. First, I examined if insulin resistance may be caused by the impairment of autophagy. With the use of Atg5K autophagy deficient H9c2 cells, as expected, there was a does dependent increase in phosphorylation of Akt Thr308 was observed in wild type (WT) H9c2 cells upon stimulation with an increasing dose of insulin, yet the response was significantly decreased in the ATG5K cell line (Figure 4.4.5.F&G). This indicated that an impairment of autophagy could lead to insulin resistance in cardiomyocytes.

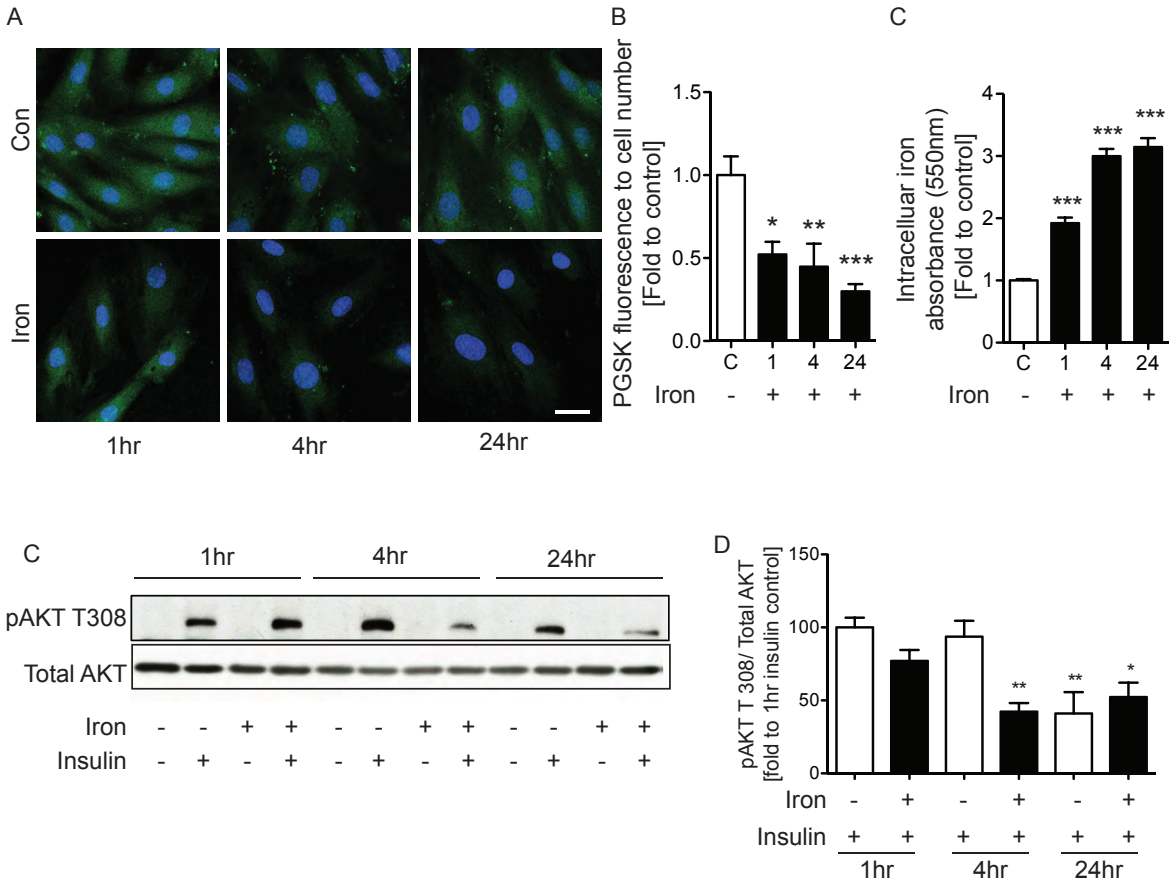

Figure 4.1. Intracellular iron accumulation induced insulin resistance in cardiomyocyte. H9c2 cells were treated with $FeSO_4$ (100µM) or without (Con) for 4 and 24 hr. Characterizing intracellular iron by PGSK assay (A), quantification (B) and Colorimetric assay was evaluated using spectrophotometer (C). H9c2 cells without (con) or with $FeSO_4$ (100µM) were treated with insulin (100nM) for 10 minutes before experimental endpoint. Western blots showing phosphorylation of AKT Thr308 and the reference protein total AKT in H9c2 cells (D) and its quantification (E). *indicates significant difference from control *p<0.05, **p<0.01. n = 5 . Scale bar = 20µm, n ≥ 3.

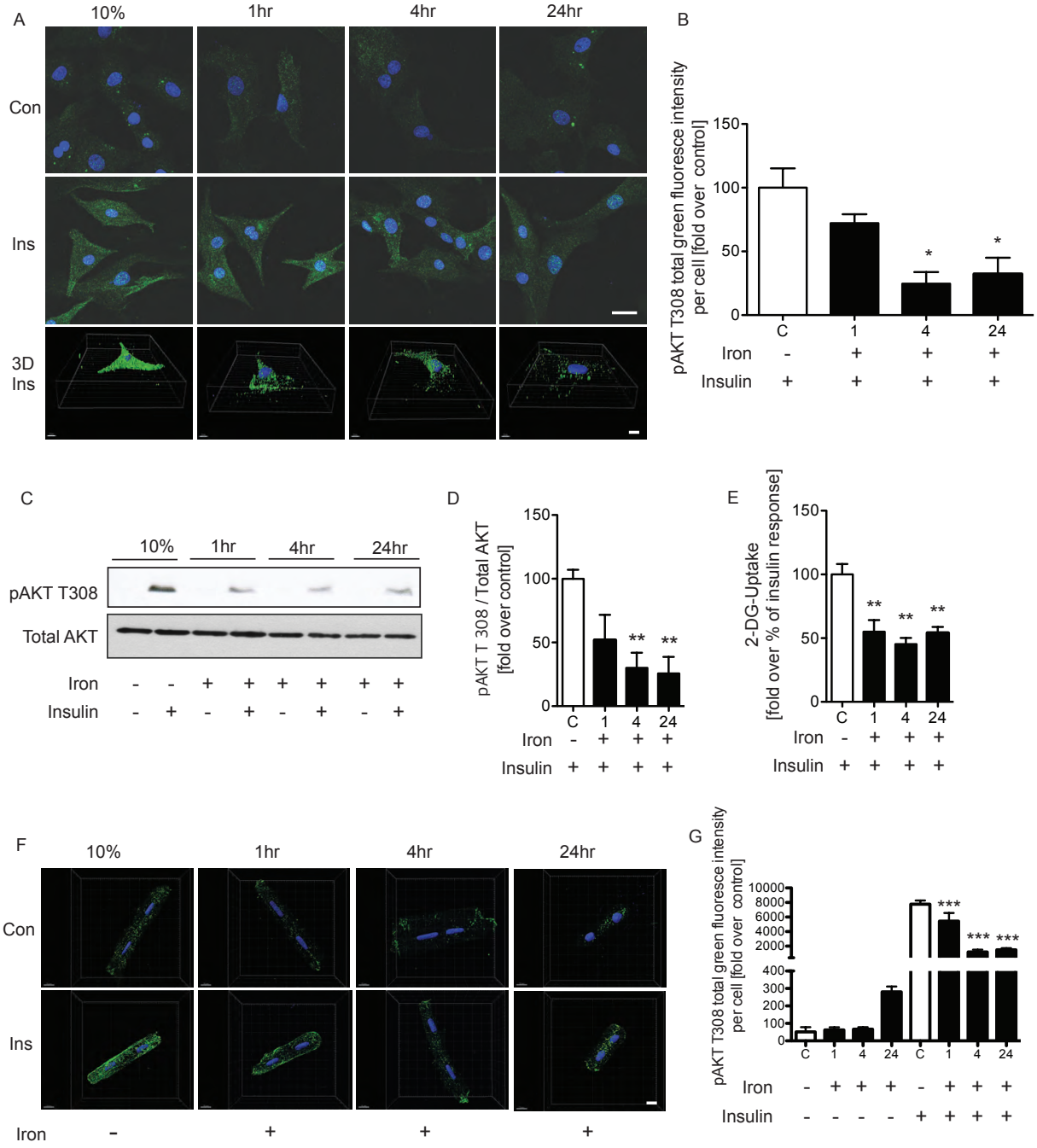
A
10%
1hr
4hr
24hr
Con
Ins
3D Ins
B
pAKT T308 total green fluoresce intensity per cell [fold over control]
150
100
50
0
C 1 4 24
Iron - + + +
Insulin + + + +
C
10%
1hr
4hr
24hr
pAKT T308
Total AKT
Iron - - + + + + + +
Insulin - + - + - + - +
D
pAKT T 308 / Total AKT [fold over control]
150
100
50
0
C 1 4 24
Iron - + + +
Insulin + + + +
E
2-DG-Uptake [fold over % of insulin response]
150
100
50
0
C 1 4 24
Iron - + + +
Insulin + + + +
F
10%
1hr
4hr
24hr
Con
Ins
Iron - + + +
G
pAKT T308 total green fluoresce intensity per cell [fold over control]
10000
8000
6000
4000
2000
400
300
200
100
0
C 1 4 24 C 1 4 24
Iron - + + + - + + +
Insulin - - - - + + + +

Figure 4.2. Insulin signaling in cardiomyocyte indicated by increased phosphorylation of AKT Thr308 was all decreased by iron. In primary adult and neonatal cardiomyocytes, with $FeSO_4$ (100μM) or without (con) were treated with insulin (100nM) for 10 minutes before experimental endpoint. Representative confocal images of phosphorylation of pAKT Thr308 in neonatal (A) and adult cardiomyocyte cells (F) and their quantifications (B&G). Western blots showing phosphorylation of AKT Thr308 and the reference protein total AKT in neonatal cardiomyocyte cells (C) its quantification (D). We examined the effect of $FeSO_4$ (100μM) for 1, 4 and 24 h on glucose uptake (Insulin: 28.30, 1hr $FeSO_4$: 15.62, 4hr $FeSO_4$: 12.00, 24hr $FeSO_4$: 14.48 (pmol/mg/min) (E). * indicates significant difference from control without insulin; # indicates significant difference from the control with respective insulin 100nM. # $p<0.05$, ## $p<0.01$; *$p<0.05$, **$p<0.01$. Scale bar = 20μm, (A &D n = 3, E n=5, F&G n=3).

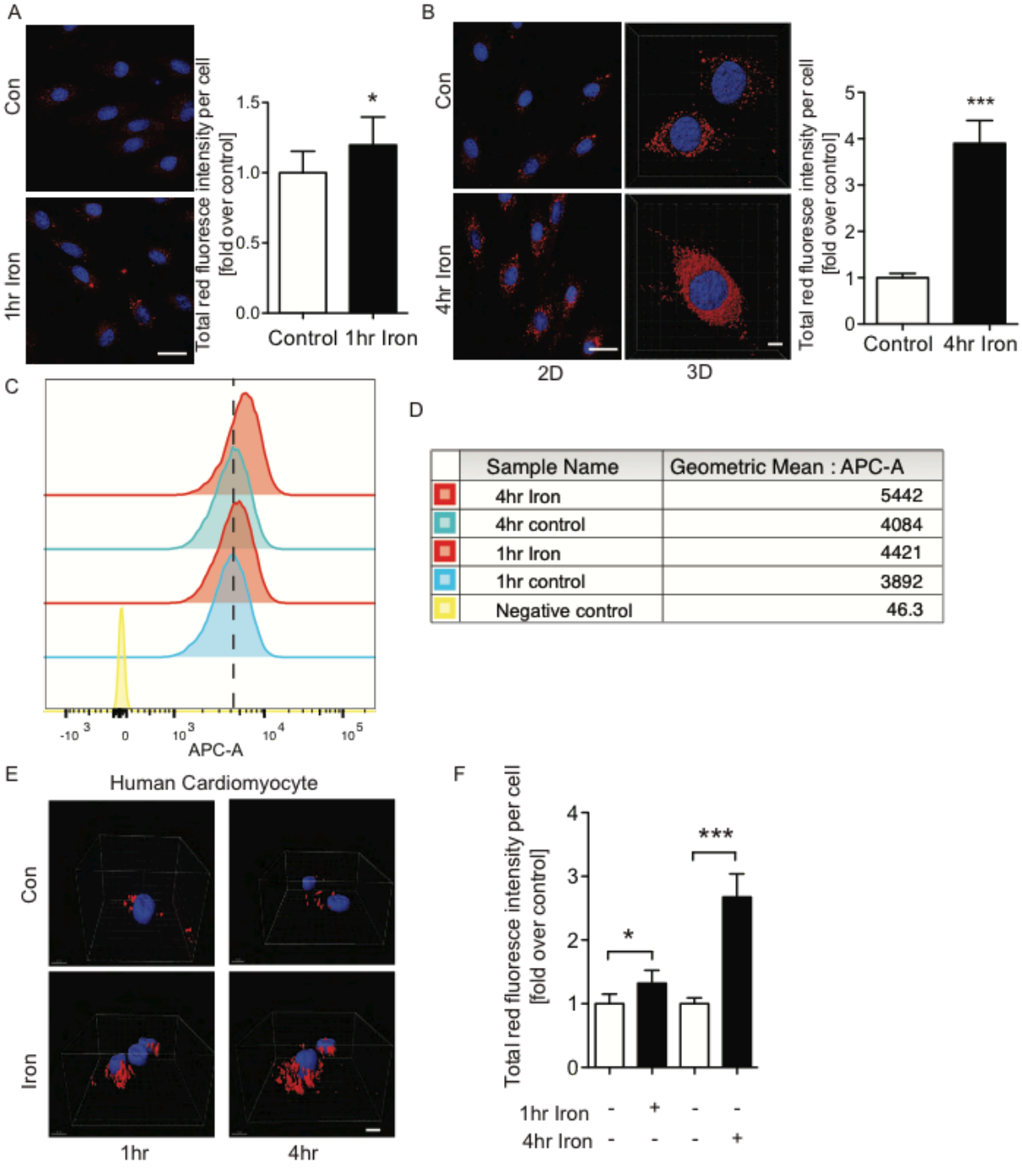
A
Con
1hr Iron
Total red fluoresce intensity per cell [fold over control]
1.5
1.0
0.5
0.0
*
Control
1hr Iron
B
Con
4hr Iron
2D
3D
Total red fluoresce intensity per cell [fold over control]
5
4
3
2
1
0
***
Control
4hr Iron
C
-10 3
0
10 3
10 4
10 5
APC-A
D
Sample Name
Geometric Mean : APC-A
4hr Iron
5442
4hr control
4084
1hr Iron
4421
1hr control
3892
Negative control
46.3
E
Human Cardiomyocyte
Con
Iron
1hr
4hr
F
Total red fluoresce intensity per cell [fold over control]
4
3
2
1
0
*
***
1hr Iron - + - -
4hr Iron - - - +

Figure 4.3. Iron increased reactive oxygen species (ROS) in H9c2 cells at 1 and 4hr. H9c2 cells with $FeSO_4$ or without (con) were treated at 1 and 4hrs by CellROX Red assay by confocal microscope. Representative confocal images of 1hr control and $FeSO_4$ (100μM) in H9c2 cells and quantification (A). 4hr control and FeSO4 (100μM) in H9c2 cells (B). The reactive oxygen species (ROS) production was examined by CellROX red assay using flow cytometry(C) and its quantification (D). Iron increased reactive oxygen species (ROS) in hiPS-CMs (human cardiomyocyte cells). Representative 3D confocal images showed in hiPS-CMs cells (E) and its quantification (F). * indicates significant difference from control $p<0.01$; *$p<0.05$, **$p<0.01$. Scale bar = 20μm, n = 4.

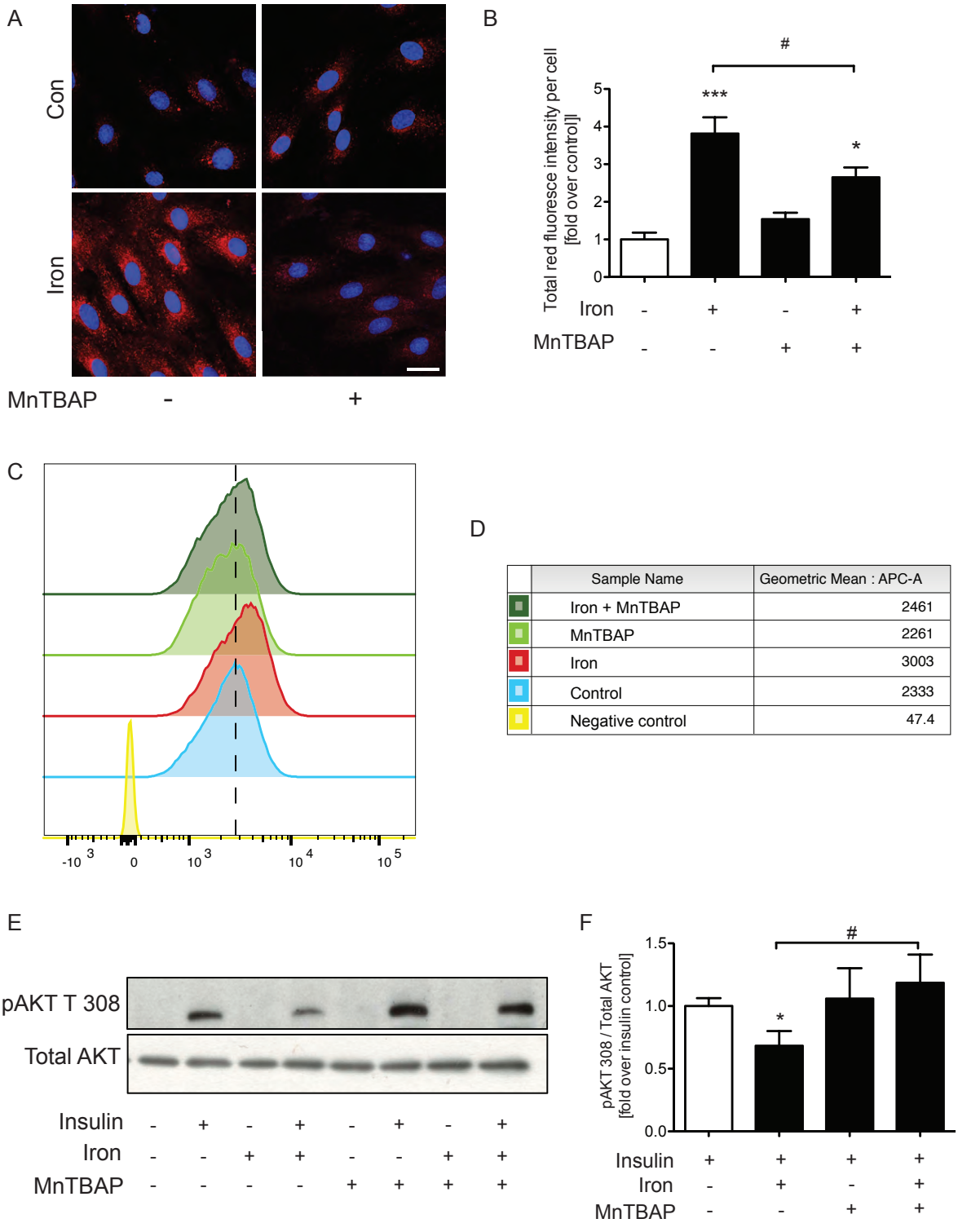
A
Con
Iron
MnTBAP - +
B
Total red fluoresce intensity per cell [fold over control]
#
***
*
Iron - + - +
MnTBAP - - + +
C
-10 3
0
10 3
10 4
10 5
D
Sample Name | Geometric Mean : APC-A
Iron + MnTBAP | 2461
MnTBAP | 2261
Iron | 3003
Control | 2333
Negative control | 47.4
E
pAKT T 308
Total AKT
Insulin - + - + - + - +
Iron - - + + - - + +
MnTBAP - - - - + + + +
F
pAKT 308 / Total AKT [fold over insulin control]
#
*
Insulin + + + +
Iron - + - +
MnTBAP - - + +

Figure 4.4. Iron induced insulin resistance via increased generation of reactive oxygen species (ROS), and enhanced by antioxidant (MnTBAP, 100μM). H9c2 cells were treated at 4hr with $FeSO_4$ (100μM) and ± antioxidant (MnTBAP, 100μM). Representative confocal images of CellROX Red assay (A), flow cytometry (C) and their quantifications (B&D respectively). Western blots showing phosphorylation of pAKT Thr308 and the reference protein total AKT in H9c2 cells (E) its quantification (F). * indicates significant difference from control # indicates significant difference from the $FeSO_4$ (100μM). # $p<0.05$, ## $p<0.01$; *$p<0.05$, **$p<0.01$. Scale bar = 20μm, (A-C n = 3, E&F n=4).

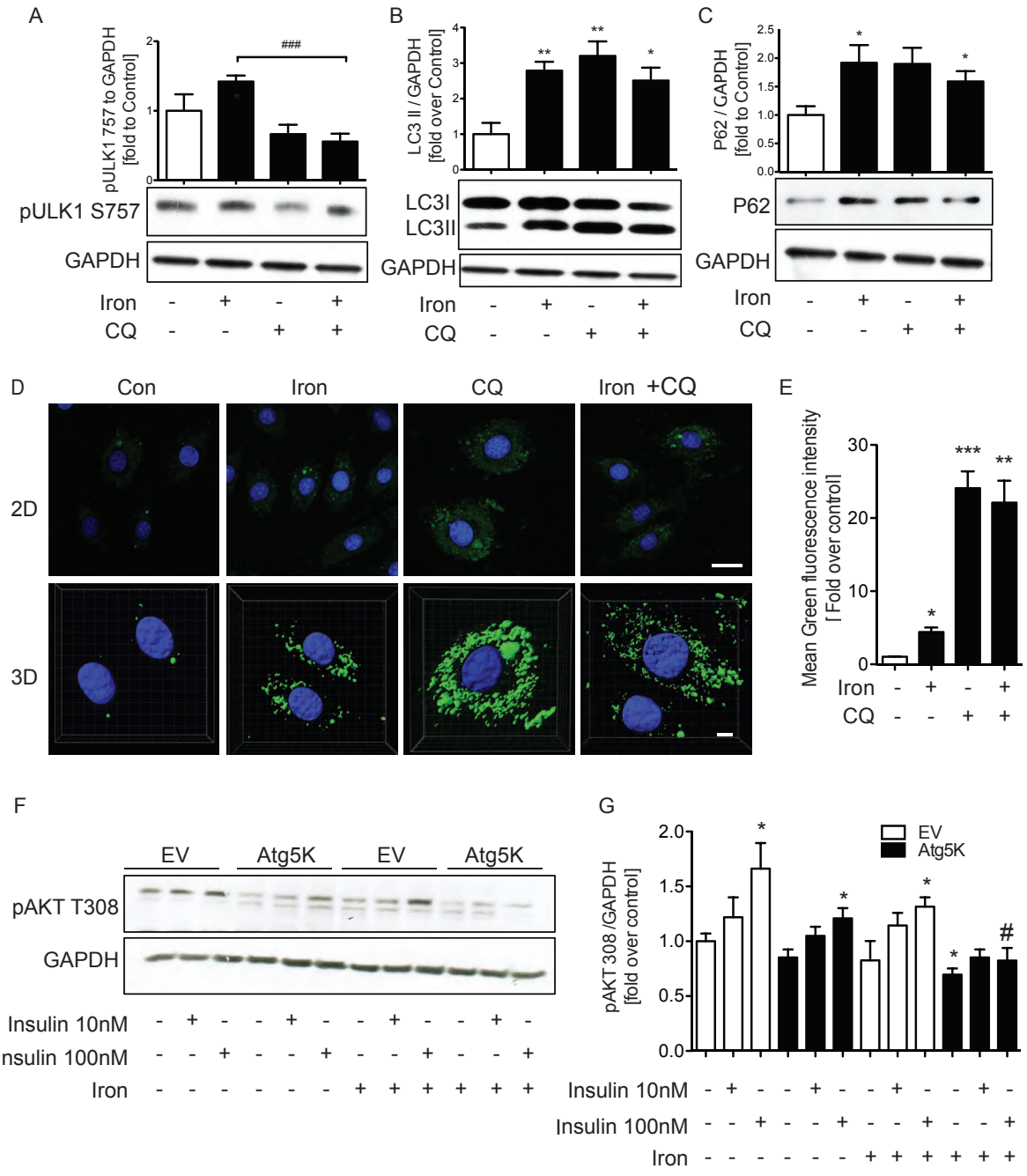
A
pULK1 757 to GAPDH [fold to Control]
###
pULK1 S757
GAPDH
Iron - + - +
CQ - - + +
B
LC3 II / GAPDH [fold over Control]
**
**
*
LC3I
LC3II
GAPDH
Iron - + - +
CQ - - + +
C
P62 / GAPDH [fold to Control]
*
*
P62
GAPDH
Iron - + - +
CQ - - + +
D
Con
Iron
CQ
Iron +CQ
2D
3D
E
Mean Green fluorescence intensity [Fold over control]
***
**
*
Iron - + - +
CQ - - + +
F
EV
Atg5K
EV
Atg5K
pAKT T308
GAPDH
Insulin 10nM - + - - + - - + - - + -
Insulin 100nM - - + - - + - - + - - +
Iron - - - - - - + + + + + +
G
pAKT 308 /GAPDH [fold over control]
EV
Atg5K
*
*
*
*
#
Insulin 10nM - + - - + - - + - - + -
Insulin 100nM - - + - - + - - + - - +
Iron - - - - - - + + + + + +

Figure 4.5. Iron reduced insulin signalling via inhibition of autophagy. H9c2 cells were treated with $FeSO_4$ (100μM) with chloroquine (60nM) and without chloroquine for 4 hr. Western blots showing protein expression of pULK1 S757 (A), LC3II (B), P62(C) and the reference protein GAPDH and their quantifications. The increase autopahgosome by iron was validated by a Cyto ID assay using confocal microscope (D) and its quantification (E). Autophagy was verified essential for insulin signalling by decreasing phosphorylation of AKT T308 in autophagy impaired Atg5K cells dose dependently by western blots (F) and its quantification (G). * indicates significant difference from control # indicates significant difference from the $FeSO_4$ (100μM). # $p<0.05$, ## $p<0.01$; *$p<0.05$, **$p<0.01$. Scale bar = 20μm, (A-E n = 4, F&G n=3).

4.5. Discussion

Iron may play an underappreciated role in the development of insulin resistance and insulin resistance-induced heart failure. Cardiac insulin resistance is well established to influence heart failure via multiple mechanisms such that exacerbated cardiomyopathy may occur in an insulin-sensitive myocardium [34]. In fact, in type 2 diabetes insulin resistance can be present for several years before hyperglycaemia develops and at this time contribute to adverse cardiac remodeling and iron both with insulin resistance and insulin deficiency [263-268]. I first investigated whether iron altered insulin sensitivity in cardiomyocytes and found that iron reduced insulin sensitivity via increased oxidative stress. Iron accumulation in H9c2 cells was done by treating them with 100uM of $FeSO_4$. Using a colorimetric intracellular iron and PGSK assay, it was shown that there was significantly increased intracellular iron after treatment with iron for 1 4 and 24 hours. To assess the effect of iron overload on insulin resistance, pAKT T308 was examined in H9c2 cells after treatment to induce iron overload conditions by Western blotting. We observed same effect of iron in neonatal and adult cardiomyocyte cells and the data showed that reduced phosphrlation of AKT T 308 at 1,4 and 24hours by Western blotting and immunofluorescence.

Although little is known about the mechanisms of iron action in cardiomyocytes, previous work has included evidence iron induced oxidative stress is a key driver in the pathogenesis of myocardial tissue injury and progressive development of iron overload cardiomyopathy [251, 269, 270]. Excess iron promotes oxidative stress via the Fenton reaction, which plays a key pathogenic role in myocardial injury and heart failure [270-273]. Although many studies have described positive relationships between modulation of adipokines and insulin resistance, much importance has been placed on iron-mediated oxidant

stress and the role it plays in the development of insulin resistance [274]. Our study suggested that using CellROX Deep Red assay we also observed that iron increased generation of reactive oxygen species (ROS), and that using anti-oxidant (MnTBAP) to attenuate ROS production reduced iron effect.

Autophagy is the major intracellular degradation process where cytoplasmic materials get delivered to lysosomes for degradation and recycling [178, 181, 183, 193] and many studies have now indicated that the degree of autophagy changes in the failing heart and directly in response to I/R [275-278]. Autophagy typically upregulated in times of stress, for example during ischemia/reperfusion, pressure overload and cardiac toxicity induced by chemicals such as the athracycline doxorubicin [151]. Previous *in vivo* studies also have shown that expression of multiple autophagy related genes were altered in iron overload cardiomyopathy, possibly contributing to cardiac diastolic dysfunction [152].

To do so to study the functional significance of changes in autophagy we created an autophagy-deficient cell model by overexpressing a dominant-negative Atg5 mutant. Our data suggested that iron or autophagy deficiency both induced insulin resistance and autophagy is very important role of regulation insulin resistance in cardiomyocyte. Numerous studies suggested that dysregulation of autophagy leads to increases in oxidative stress [279-283]. For example inhibition of autophagy increased ROS by lysosome inhibitor chloroquine or the cathepsin D inhibitor pestatin A [284-288]. Additionally, disorder of initiation autophagy leads to accumulation of ubiquitiated proteins, induced ROS and mitochondrial dysfunction [289]. Reduction of Atg5 and Atg10 promote ROS via starvation[280].

In conclusion, our study indicated that iron induced insulin resistance in cardiomyocytes and this involved regulation of the crosstalk between autophagy and oxidative stress. Further studies will investigate mechanisms via which iron regulates cardiac remodeling and their physiological significance. We anticipate that our findings will provide new knowledge relevant to current diagnostics and therapeutics related to altered iron status in clinical settings.

Chapter Five: Discussion & Conclusions

5.1 Research summary

Obesity and diabetes increase the incidence of myocardial infarction and heart failure [74, 176]. Lcn2 is most abundantly produced from adipocytes and neutrophils and previous studies showed that Lcn2 is a proinflammatory marker associated with insulin resistance and obesity-related metabolic disorders [7, 10, 155]. My working hypothesis was that Lcn2 induction is an important component of the cardiac response to myocardial infarction, directly regulates cardiac remodeling and contributes to development of heart failure. A variety of remodeling events occur throughout the progressive development of heart failure in obesity [74]. During my PhD studies, I have examined direct effects of Lcn2 on cardiomyocytes and in the heart using mouse mdoels to determine mechanisms via which Lcn2 changes cardiac structure and function. In this concluding chapter I revisit the main results and conclusions from each chapter and bring these together in a unifying discussion.

Project 1: Lcn2 inhibits autophagy leading to insulin resistance in cardiomyocytes.

Data from my first PhD project has been published in the *Journal of Molecular Endocrinology* [218] and forms a strong foundation for the continuation of related work in my thesis. Briefly, I treated H9c2 cardiomyocytes with recombinant Holo-Lcn2 for 1 hour followed by dose and time dependent insulin treatment and found that Holo-Lcn2 induced insulin resistance; assessed via Western blotting for phosphorylation of Akt, ERK and p70S6K. I used multiple assays to monitor autophagic flux and observed that Holo-Lcn2 reduced autophagy. For example, we generated H9c2 cells stably expressing tandem fluorescent RFP/GFP-LC3 and this approach allowed me to demonstrate that Holo-Lcn2

decreased autophagic flux. Importantly, our lab created an autophagy-deficient H9c2 cell model by overexpressing a dominant-negative Atg5 mutant and using this I found that reduced autophagy levels also induced insulin resistance. In summary, this study indicated that Holo-Lcn2 treatment caused insulin resistance and use of gain and loss of function approaches elucidated a causative link between autophagy inhibition and regulation of insulin sensitivity by Holo-Lcn2. Cardiac insulin resistance is well established to influence heart failure via multiple mechanisms such that exacerbated cardiomyopathy may occur in an insulin-insensitive myocardium [176]. In fact, in type 2 diabetes insulin resistance can be present for several years before hyperglycaemia develops and during this time contribute to adverse cardiac remodeling [191]. More recently, numerous studies have shown that autophagy can play a critical role in cardiac metabolic health [178], including regulating insulin sensitivity [179, 180]. Several signalling pathways are also involved in the regulation of autophagy, including insulin signalling via PI3K/Akt/mTOR which leads to the inhibition of autophagy [57]. Indeed, disruption of autophagy by cardiac-specific knockdown of Atg5 in adult mice leads to cardiomyopathy [181]. Furthermore, measuring circulating Lcn2 was shown to be capable of predicting the severity and mortality of acute and chronic heart failure [46, 50, 51, 173, 174, 290], thus making it an attractive and promising biomarker for heart failure. The novel observation from my work that Holo-Lcn2 attenuated autophagy then led me to test the significance of this mechanism in mediating another important effect of Lcn2 in cardiomyocytes that our lab previously established, namely cell death [71].

Project 2: Lcn2 regulates autophagy to control apoptosis upon chronic myocardial ischemia.

Another manuscript, containing data from this project, has been published in *Journal of Cellular Physiology* [256]. In this paper I showed that Holo-Lcn2 attenuates autophagy to worsen the extent of apoptosis induced by chronic myocardial ischemia in mice. Briefly, I used coronary artery ligation surgery to induce ischemia in wild type (wt) and Lcn2 knockout (KO) mice. Lack of Lcn2 protected against ischemia-induced cell death and cardiac dysfunction measured by echocardiography. I used multiple assays to monitor autophagic flux and observed that Lcn2 KO mice had a greater ischemia-induced increase in autophagy versus wt mice. Importantly, these changes correlated with increased cell death and reduced insulin sensitivity in response to Holo-Lcn2. A previous study indicated that Lcn2 KO mice had significantly decreased fasting glucose while their insulin level and sensitivity improved [16]. Moreover, fat mass enlargement, inflammation and accumulation of lipid peroxidation products were significantly attenuated in the adipose tissues of aging or HFD Lcn2 KO mice [16]. As I indicated above, measurement of serum Lcn2 has been proposed as a useful means for evaluating obesity-related cardiovascular diseases including heart failure. Previous literature indicated that mouse models of autophagy deficiency develop age-related cardiomyopathy [234], show enhanced hemodynamic stress induced dysfunction [202] and elevated levels of angiotensin-II stimulated inflammation and injury [235]. This study and project 1 collectively indicated that Holo-Lcn2 attenuated autophagic flux and induced both insulin resistance and cell death in cardiomyocytes; effects which collectively may play an important role in the pathogenesis of heart failure in obesity.

Project 3: Iron induces insulin resistance in cardiomyocytes via regulation of oxidative stress.

Data from my first PhD project indicated that Holo-Lcn2 caused insulin resistance and use of gain and loss of function approaches elucidated a causative link between autophagy inhibition and regulation of insulin sensitivity by Lcn2 [218]. My second project showed that Holo-Lcn2 regulates autophagy to control apoptosis upon chronic myocardial ischemia [256]. Together with our labs previous observation that Lcn2 induced cardiomyocyte apoptosis via elevating intracellular iron levels [71], this led me to appreciate the extensive literature showing that both iron overload and deficiency have been strongly associated with heart failure [92, 101, 106, 109, 179]. Importantly, as I indicated during my thesis introduction, Lcn2 plays important role in regulation of iron homeostasis, promoting iron accumulation in cardiomyocytes, and I thus hypothesized this could be an important mechanism in the context of cardiomyopathy. Circulating Lcn2 is often recorded to be significantly increased in patients experiencing HF [81, 238-240, 291] local Lcn2 produced in the heart is also increased significantly [256]. Hence, I believed it was of great interest to further elucidate the mechanisms of iron-associated cardiomyopathy.

Therefore, in my third project I investigated whether iron caused insulin resistance in cardiomyocytes and the mechanisms via which this occurred, with a focus on oxidative stress. Although little is known about the mechanisms of iron action in cardiomyocytes, previous work has included evidence iron induced oxidative stress is a key driver in the pathogenesis of myocardial tissue injury and progressive development of iron overload cardiomyopathy [251, 269, 270]. Briefly, I used primary adult and neonatal cardiomyocytes as well as H9c2 cells, and observed that iron induced insulin resistance, as determined by Western blotting and immunofluorescent detection of Akt phosphorylation as well as glucose uptake. Using CellROX Deep Red assay I also observed that iron increased generation of reactive oxygen

species (ROS), and that anti-oxidant pretreatment attenuated iron-induced insulin resistance. Furthermore, various complementary assays indicated that iron suppressed autophagy. Although many studies have described positive relationships between modulation of adipokines and insulin resistance, much importance has been placed on iron-mediated oxidant stress and the role it plays in the development of insulin resistance [274]. Autophagy is the major intracellular degradation process where cytoplasmic materials get delivered to lysosomes for degradation and recycling [178, 181, 183, 193] and many studies have now indicated that the degree of autophagy changes in the failing heart and directly in response to I/R [275-278]. Autophagy typically upregulated in times of stress, for example during ischemia/reperfusion, pressure overload and cardiac toxicity induced by chemicals such as the athracycline doxorubicin [151]. Previous *in vivo* studies also have shown that expression of multiple autophagy related genes were altered in iron overload cardiomyopathy, possibly contributing to cardiac diastolic dysfunction [152]. This is in keeping with my Project 3 study which indicated that iron reduced autophagy causing insulin resistance in cardiomyocytes.

5.2 Future directions

Future studies to expand the work presented in this thesis will continue to explore and focus on the mechanistic role of autophagy. Ultimatley, I expect this will have implications in i) establishing Lcn2 as a potential biomarker for the diagnosis of heart failure or it's susceptibility and ii) validating Lcn2 and autophagy as potentially important therapeutic targets in the treatment of heart failure.

As explained above in project 1 and 3, my data led me to place a strong emphasis on the study of autophagy and whether it is regulated by Lcn2 and iron. The pro-apoptotic effect of Lcn2 involved increased intracellular iron levels. It will great interesting point to investigate the role of altered intracellular iron on H/R-induced changes in apoptosis, authopagy, oxidative stress and ER stress. The role of iron in H/R mediated apoptosis is unclear [233, 292] although iron chelation has been proposed as a therapy for various cardiomyopathies [293]. Another study suggested that H/R damage in primary neonatal cardiomyocytes involves oxidative stress via the production of hydroxyl radicals mediated by iron [294]. Similarly to project 3, it would be possible to determine if elevated iron levels contribute to oxidative stress, whether this is part of the mechanism of Lcn2 or H/R-induced cell death and if chelating iron attenuates the apoptotic effects of Lcn2 or H/R. Interestingly, sustained autophagy upon transgenic Atg7 overexpression decreased cardiac fibrosis, hypertrophy and dysfunction [295]. Interestingly, one study showed that patients with longstanding idiopathic cardiomyopathy increased cardiac accumulation of autophagosomes [295]. Accordingly, my experiments are now designed to examine temporal and spatial changes in cardiac autophagy based on the hypothesis that autophagy is induced in the heart

as a protective mechanism in response to I/R and that Lcn2 suppresses this beneficial effect. Lack of Lcn2 may prevent this and allow autophagy to become elevated and confer protection. Furthermore, *Atg7* is required for ATG conjugation mechanism and autophagosome formation. This has important consequences such as amino acid supply in neonates, and starvation-induced bulk degradation of proteins and organelles in mice [296, 297]. *Atg7* deficiency in mice led to multiple cellular abnormalities, such as appearance of concentric membranous structure and deformed mitochondria, and accumulation of ubiquitin-positive aggregates [296]. To examine the autophagy-deficient phenotype, I am currently breeding Atg $7^{F/F}$ with a line of transgenic mice that express the Cre recombinase under the control of a cardiomyocyte specific promoter. These mice will be crossbred onto a background of Lcn2KO mice to create a completely novel mouse model to test our hypothesis. We will subject these mice to surgically induced heart failure (coronary artery ligation to induce ischemia and reperfusion (I/R)) then examine changes in autophagy, cell death, oxidative stress, mitochondrial function, inflammation and fibrosis as well as heart function using techniques well established in our lab [218, 256]. These will allow me to further explore the hypotheses that presence of Lcn2 is permissive in development of cardiac dysfunction whereas lack of Lcn2 may protect mice from I/R-induced dysfunction. Autophagy deficiency is also expected to exacerbate I/R induced heart failure, and we have promising preliminary evidence that lack of autophagy induced cardiac dysfunction. Furthermore, interestingly, whereas I/R induced a large increase in myocardial Lcn2 content in wt mice, it did not in this autophagy-deficient mouse model. This is an unexpected observation and clearly suggests further crosstalk between Lcn2 and autophagy. Previously my study indicated that Lcn2 attenuates autophagy to worsen the extent of apoptosis induced by chronic myocardial ischemia in mice and we observed

significantly increased Lcn2 level after chronic myocardial ischemia. We will also use in vitro studies to further examine direct cellular mechanisms of Lcn2 action with gain and loss of function approaches.

One of the important discoveries made in my thesis was that Lcn2 regulates autophagy and apoptosis upon chronic myocardial ischemia. Now, to further advance this study we will use wt and Lcn2KO mice in which will also restore normal Lcn2 levels by adenoviral delivery, with the specific hypothesis that presence of Lcn2 is permissive in development of cardiac dysfunction whereas lack of Lcn2 may protect mice from I/R-induced dysfunction. This sytudy will be designed to examine mechanisms including autophagy, cell death, oxidative stress, mitochondrial function, inflammation and fibrosis. For example, a novel approach that our lab is developing over the last few months is the use of fluorescent molecular tomography to non-invasively measure autophagy in mice. This is based on the use of a cathepsin-activatable near infra-red probe, is quantitative and will provide spatial and temporal readouts of changes in autophagy in the same mouse over the period of our experimental protocol. We anticipate that in wt, but not Lcn2-KO, there will be sufficient induction of autophagy to limit damage such as cell death or insulin resistance. Reintroduction of Lcn2 to Lcn2-KO by adenovirus will attenuate I/R-induced autophagy and promote dysfunction. This future study also will consider the alternative hypothesis that lack of Lcn2 may allow either too much or - if autophagy is transiently elevated only in the early period or I/R, as was suggested in one recent study - prolonged autophagic induction, both of which may also be detrimental to cellular events such as apoptosis [212]. In addition to examining autophagy, the following experimental measures will also be made: i) Echocardiography to examine cardiac function ii)

Insulin sensitivity iii) Cell death and iv) Fibrosis, all using methods that are established in our lab [9, 10].

5.3 Conclusion

For my PhD studies, I examined effects of Lcn2 on the heart to determine changes in cardiac structure and function. Rationale for this work was based on the fact that obesity and the associated metabolic syndrome (a cluster of chronic symptoms including insulin resistance, hyperglycemia, hypertension, and inflammation) predispose individuals to developing heart failure. The consequences on an obese and aging population can be devastating owing to the high risk for mortality or loss of quality of life.

The most significant observation that I made was that regulation of autophagy was an important mechanism via which Lcn2 altered insulin sensitivity as well as cell death in cardiomyocytes. Furthermore, I demonstrated that iron induced insulin resistance via oxidative stress. These novel cellular mechanistic discoveries led me to propose that future studies will continue to explore and validate the physiological significance of Lcn2-induced heart failure. As I explained above, Lcn2 is a hormone that previous research has suggested could be potentially useful as a biomarker or therapeutic target for heart failure, however much more research is needed to validate either of these possibilities. Knowledge produced by my research will thus have potential to impact improved diagnosis or treatment of heart failure in future.

Bibliography

1. Gaddam, K.K., H.O. Ventura, and C.J. Lavie, *Metabolic syndrome and heart failure--the risk, paradox, and treatment.* Curr Hypertens Rep, 2011. **13**(2): p. 142-8.
2. Mazzone, T., A. Chait, and J. Plutzky, *Cardiovascular disease risk in type 2 diabetes mellitus: insights from mechanistic studies.* Lancet, 2008. **371**(9626): p. 1800-9.
3. Poirier, P., et al., *Obesity and cardiovascular disease: pathophysiology, evaluation, and effect of weight loss: an update of the 1997 American Heart Association Scientific Statement on Obesity and Heart Disease from the Obesity Committee of the Council on Nutrition, Physical Activity, and Metabolism.* Circulation, 2006. **113**(6): p. 898-918.
4. Abel, E.D., S. Litwin, and G. Sweeney, *Cardiac remodeling in obesity.* Physiological reviews, 2008. **In Press**: p. March 2008.
5. Boudina, S. and E.D. Abel, *Diabetic cardiomyopathy, causes and effects.* Rev Endocr Metab Disord, 2010. **11**(1): p. 31-9.
6. Smith, C.C. and D.M. Yellon, *Adipocytokines, cardiovascular pathophysiology and myocardial protection.* Pharmacol Ther, 2011. **129**(2): p. 206-19.
7. Walsh, K., *Adipokines, myokines and cardiovascular disease.* Circ J, 2009. **73**(1): p. 13-8.
8. Schwartz, N., J.S. Michaelson, and C. Putterman, *Lipocalin-2, TWEAK, and other cytokines as urinary biomarkers for lupus nephritis.* Ann N Y Acad Sci, 2007. **1109**: p. 265-74.
9. Kjeldsen, L., et al., *Structural and functional heterogeneity among peroxidase-negative granules in human neutrophils: identification of a distinct gelatinase-containing granule subset by combined immunocytochemistry and subcellular fractionation.* Blood, 1993. **82**(10): p. 3183-91.
10. Flower, D.R., *The lipocalin protein family: structure and function.* Biochem J, 1996. **318 (Pt 1)**: p. 1-14.

11. Cowland, J.B. and N. Borregaard, *Molecular characterization and pattern of tissue expression of the gene for neutrophil gelatinase-associated lipocalin from humans.* Genomics, 1997. **45**(1): p. 17-23.

12. Jang, Y., et al., *Emerging clinical and experimental evidence for the role of lipocalin-2 in metabolic syndrome.* Clin Exp Pharmacol Physiol, 2012. **39**(2): p. 194-9.

13. Taube, A., et al., *Inflammation and metabolic dysfunction: links to cardiovascular diseases.* Am J Physiol Heart Circ Physiol, 2012. **302**(11): p. H2148-65.

14. Wang, Y., et al., *Lipocalin-2 is an inflammatory marker closely associated with obesity, insulin resistance, and hyperglycemia in humans.* Clin Chem, 2007. **53**(1): p. 34-41.

15. Choi, K.M., et al., *Implication of lipocalin-2 and visfatin levels in patients with coronary heart disease.* Eur J Endocrinol, 2008. **158**(2): p. 203-7.

16. Law, I.K., et al., *Lipocalin-2 deficiency attenuates insulin resistance associated with aging and obesity.* Diabetes, 2010. **59**(4): p. 872-82.

17. Guo, H., et al., *Lipocalin-2 deficiency impairs thermogenesis and potentiates diet-induced insulin resistance in mice.* Diabetes, 2010. **59**(6): p. 1376-85.

18. Yan, Q.W., et al., *The adipokine lipocalin 2 is regulated by obesity and promotes insulin resistance.* Diabetes, 2007. **56**(10): p. 2533-40.

19. van Dam, R.M. and F.B. Hu, *Lipocalins and insulin resistance: etiological role of retinol-binding protein 4 and lipocalin-2?* Clin Chem, 2007. **53**(1): p. 5-7.

20. Catalan, V., et al., *Increased adipose tissue expression of lipocalin-2 in obesity is related to inflammation and matrix metalloproteinase-2 and metalloproteinase-9 activities in humans.* J Mol Med, 2009. **87**(8): p. 803-13.

21. Latouche, C., et al., *Neutrophil gelatinase-associated lipocalin is a novel mineralocorticoid target in the cardiovascular system.* Hypertension, 2012. **59**(5): p. 966-72.

22. Ding, L., et al., *Lipocalin-2/neutrophil gelatinase-B associated lipocalin is strongly induced in hearts of rats with autoimmune myocarditis and in human myocarditis.* Circ J, 2010. **74**(3): p. 523-30.

23. Aigner, F., et al., *Lipocalin-2 regulates the inflammatory response during ischemia and reperfusion of the transplanted heart.* Am J Transplant, 2007. **7**(4): p. 779-88.

24. Hemdahl, A.L., et al., *Expression of neutrophil gelatinase-associated lipocalin in atherosclerosis and myocardial infarction.* Arterioscler Thromb Vasc Biol, 2006. **26**(1): p. 136-42.

25. Falke, P., A.M. Elneihoum, and K. Ohlsson, *Leukocyte activation: relation to cardiovascular mortality after cerebrovascular ischemia.* Cerebrovasc Dis, 2000. **10**(2): p. 97-101.

26. Bu, D.X., et al., *Induction of neutrophil gelatinase-associated lipocalin in vascular injury via activation of nuclear factor-kappaB.* Am J Pathol, 2006. **169**(6): p. 2245-53.

27. Sommer, P. and G. Sweeney, *Functional and mechanistic integration of infection and the metabolic syndrome.* Korean Diabetes J, 2010. **34**(2): p. 71-6.

28. Yndestad, A., et al., *Increased systemic and myocardial expression of neutrophil gelatinase-associated lipocalin in clinical and experimental heart failure.* Eur Heart J, 2009. **30**(10): p. 1229-36.

29. Moreno-Navarrete, J.M., et al., *Metabolic endotoxemia and saturated fat contribute to circulating NGAL concentrations in subjects with insulin resistance.* Int J Obes (Lond), 2010. **34**(2): p. 240-9.

30. Rexhepaj, R., et al., *PI3 kinase and PDK1 in the regulation of the electrogenic intestinal dipeptide transport.* Cell Physiol Biochem, 2010. **25**(6): p. 715-22.

31. Cani, P.D., et al., *Metabolic endotoxemia initiates obesity and insulin resistance.* Diabetes, 2007. **56**(7): p. 1761-72.

32. Srinivasan, G., et al., *Lipocalin 2 deficiency dysregulates iron homeostasis and exacerbates endotoxin-induced sepsis.* J Immunol, 2012. **189**(4): p. 1911-9.

33. Layoun, A., et al., *Toll-like receptor signal adaptor protein MyD88 is required for sustained endotoxin-induced acute hypoferremic response in mice.* Am J Pathol, 2012. **180**(6): p. 2340-50.

34. Cesur, S., et al., *Plasma lipocalin-2 levels in pregnancy.* Acta Obstet Gynecol Scand, 2012. **91**(1): p. 112-6.

35. Lou, Y., et al., *The changes of neutrophil gelatinase-associated lipocalin in plasma and its expression in adipose tissue in pregnant women with gestational diabetes.* Diabetes Res Clin Pract, 2014. **104**(1): p. 136-42.

36. Catalan, V., et al., *Increased adipose tissue expression of lipocalin-2 in obesity is related to inflammation and matrix metalloproteinase-2 and metalloproteinase-9 activities in humans.* J Mol Med (Berl), 2009. **87**(8): p. 803-13.

37. Auguet, T., et al., *Upregulation of lipocalin 2 in adipose tissues of severely obese women: positive relationship with proinflammatory cytokines.* Obesity (Silver Spring), 2011. **19**(12): p. 2295-300.

38. Koiou, E., et al., *Weight loss significantly reduces serum lipocalin-2 levels in overweight and obese women with polycystic ovary syndrome.* Gynecol Endocrinol, 2012. **28**(1): p. 20-4.

39. Corripio, R., et al., *Weight loss in prepubertal obese children is associated with a decrease in adipocyte fatty-acid-binding protein without changes in lipocalin-2: a 2-year longitudinal study.* Eur J Endocrinol, 2010. **163**(6): p. 887-93.

40. Shah, B.N. and K. Greaves, *The cardiorenal syndrome: a review.* Int J Nephrol, 2010. **2011**: p. 920195.

41. Peralta, C.A., et al., *Cystatin C identifies chronic kidney disease patients at higher risk for complications.* J Am Soc Nephrol, 2011. **22**(1): p. 147-55.

42. Damman, K., et al., *Volume status and diuretic therapy in systolic heart failure and the detection of early abnormalities in renal and tubular function.* J Am Coll Cardiol, 2011. **57**(22): p. 2233-41.

43. Mishra, J., et al., *Amelioration of ischemic acute renal injury by neutrophil gelatinase-associated lipocalin.* J Am Soc Nephrol, 2004. **15**(12): p. 3073-82.

44. Ahmad, T., et al., *Novel biomarkers in chronic heart failure.* Nat Rev Cardiol, 2012. **9**(6): p. 347-59.

45. Maisel, A.S., et al., *Prognostic utility of plasma neutrophil gelatinase-associated lipocalin in patients with acute heart failure: the NGAL EvaLuation Along with B-type NaTriuretic Peptide in acutely decompensated heart failure (GALLANT) trial.* Eur J Heart Fail, 2011. **13**(8): p. 846-51.

46. Alvelos, M., et al., *Prognostic value of neutrophil gelatinase-associated lipocalin in acute heart failure.* Int J Cardiol, 2013. **165**(1): p. 51-5.

47. Naude, P.J., et al., *Neutrophil Gelatinase-Associated Lipocalin and depression in patients with chronic heart failure.* Brain Behav Immun, 2014. **38**: p. 59-65.

48. Nymo, S.H., et al., *The association between neutrophil gelatinase-associated lipocalin and clinical outcome in chronic heart failure: results from CORONA*.* J Intern Med, 2012. **271**(5): p. 436-43.

49. Pronschinske, K.B., et al., *Neutrophil gelatinase-associated lipocalin and cystatin C for the prediction of clinical events in patients with advanced heart failure and after ventricular assist device placement.* J Heart Lung Transplant, 2014.

50. Bolignano, D., et al., *Increased plasma neutrophil gelatinase-associated lipocalin levels predict mortality in elderly patients with chronic heart failure.* Rejuvenation Res, 2009. **12**(1): p. 7-14.

51. van Deursen, V.M., et al., *Prognostic value of plasma neutrophil gelatinase-associated lipocalin for mortality in patients with heart failure.* Circ Heart Fail, 2014. **7**(1): p. 35-42.

52. Van Obberghen, E., et al., *Surfing the insulin signaling web.* Eur J Clin Invest, 2001. **31**(11): p. 966-77.

53. Lizcano, J.M. and D.R. Alessi, *The insulin signalling pathway.* Curr Biol, 2002. **12**(7): p. R236-8.

54. Kim, B. and E.L. Feldman, *Insulin resistance in the nervous system.* Trends Endocrinol Metab, 2012. **23**(3): p. 133-41.

55. Mizushima, N., *Autophagy: process and function.* Genes Dev, 2007. **21**(22): p. 2861-73.

56. Lavallard, V.J., et al., *Autophagy, signaling and obesity.* Pharmacol Res, 2012. **66**(6): p. 513-25.

57. Shintani, T. and D.J. Klionsky, *Autophagy in health and disease: a double-edged sword.* Science, 2004. **306**(5698): p. 990-5.

58. Mari, M., S.A. Tooze, and F. Reggiori, *The puzzling origin of the autophagosomal membrane.* F1000 Biol Rep, 2011. **3**: p. 25.

59. Tooze, S.A., et al., *Assessing mammalian autophagy.* Methods Mol Biol, 2015. **1270**: p. 155-65.

60. Marino, G., et al., *Self-consumption: the interplay of autophagy and apoptosis.* Nat Rev Mol Cell Biol, 2014. **15**(2): p. 81-94.

61. Galluzzi, L., et al., *Guidelines for the use and interpretation of assays for monitoring cell death in higher eukaryotes.* Cell Death Differ, 2009. **16**(8): p. 1093-107.

62. Dupont-Versteegden, E.E., *Apoptosis in skeletal muscle and its relevance to atrophy.* World J Gastroenterol, 2006. **12**(46): p. 7463-6.

63. Tait, S.W. and D.R. Green, *Mitochondria and cell death: outer membrane permeabilization and beyond.* Nat Rev Mol Cell Biol, 2010. **11**(9): p. 621-32.

64. Sies, H., *Oxidative stress: a concept in redox biology and medicine.* Redox Biol, 2015. **4**: p. 180-3.

65. Toyokuni, S., *Iron and carcinogenesis: from Fenton reaction to target genes.* Redox Rep, 2002. **7**(4): p. 189-97.

66. Nemeth, E. and T. Ganz, *Regulation of iron metabolism by hepcidin.* Annu Rev Nutr, 2006. **26**: p. 323-42.

67. Wood, J.C., *Cardiac iron across different transfusion-dependent diseases.* Blood Rev, 2008. **22 Suppl 2**: p. S14-21.

68. Kumfu, S., et al., *Ferric iron uptake into cardiomyocytes of beta-thalassemic mice is not through calcium channels.* Drug Chem Toxicol, 2013. **36**(3): p. 329-34.

69. Tsushima, R.G., et al., *Modulation of iron uptake in heart by L-type Ca2+ channel modifiers: possible implications in iron overload.* Circ Res, 1999. **84**(11): p. 1302-9.

70. Nam, H., et al., *ZIP14 and DMT1 in the liver, pancreas, and heart are differentially regulated by iron deficiency and overload: implications for tissue iron uptake in iron-related disorders.* Haematologica, 2013. **98**(7): p. 1049-57.

71. Xu, G., et al., *Lipocalin-2 induces cardiomyocyte apoptosis by increasing intracellular iron accumulation.* J Biol Chem, 2012. **287**(7): p. 4808-17.

72. Ge, X.H., et al., *The iron regulatory hormone hepcidin reduces ferroportin 1 content and iron release in H9C2 cardiomyocytes.* J Nutr Biochem, 2009. **20**(11): p. 860-5.

73. Chan, Y.K., H.K. Sung, and G. Sweeney, *Iron metabolism and regulation by neutrophil gelatinase-associated lipocalin in cardiomyopathy.* Clin Sci (Lond), 2015. **129**(10): p. 851-62.

74. Abel, E.D., S.E. Litwin, and G. Sweeney, *Cardiac remodeling in obesity.* Physiol Rev, 2008. **88**(2): p. 389-419.

75. Borlaug, B.A. and W.J. Paulus, *Heart failure with preserved ejection fraction: pathophysiology, diagnosis, and treatment.* Eur Heart J, 2011. **32**(6): p. 670-9.

76. Kasner, M., et al., *Functional iron deficiency and diastolic function in heart failure with preserved ejection fraction.* Int J Cardiol, 2013. **168**(5): p. 4652-7.

77. McMurray, J.J., et al., *ESC Guidelines for the diagnosis and treatment of acute and chronic heart failure 2012: The Task Force for the Diagnosis and Treatment of Acute and Chronic*

Heart Failure 2012 of the European Society of Cardiology. Developed in collaboration with the Heart Failure Association (HFA) of the ESC. Eur Heart J, 2012. **33**(14): p. 1787-847.

78. Jankowska, E.A., et al., *Iron deficiency and heart failure: diagnostic dilemmas and therapeutic perspectives.* Eur Heart J, 2013. **34**(11): p. 816-29.

79. Lapice, E., M. Masulli, and O. Vaccaro, *Iron deficiency and cardiovascular disease: an updated review of the evidence.* Curr Atheroscler Rep, 2013. **15**(10): p. 358.

80. Liu, P. and N. Olivieri, *Iron overload cardiomyopathies: new insights into an old disease.* Cardiovasc Drugs Ther, 1994. **8**(1): p. 101-10.

81. Gujja, P., et al., *Iron overload cardiomyopathy: better understanding of an increasing disorder.* J Am Coll Cardiol, 2010. **56**(13): p. 1001-12.

82. Olivieri, N.F., et al., *Survival in medically treated patients with homozygous beta-thalassemia.* N Engl J Med, 1994. **331**(9): p. 574-8.

83. Chaffers, E., *Death from Suffocation While Inhaling Chloroform: Impaction of False Teeth in Larynx.* Br Med J, 1872. **1**(590): p. 419-20.

84. Hare, J.M., *The dilated, restrictive, and infiltrative cardiomyopathies*, in *Braunwald's heart disease* P. Libby, et al., Editors. 2008, Elsevier: Boston, Massachusetts. p. 1739-1760.

85. Chen, M.P., et al., *Iron Overload and Apoptosis of HL-1 Cardiomyocytes: Effects of Calcium Channel Blockade.* PLoS One, 2014. **9**(11): p. e112915.

86. Lipinski, B. and E. Pretorius, *Iron-induced fibrin in cardiovascular disease.* Curr Neurovasc Res, 2013. **10**(3): p. 269-74.

87. Sullivan, J.L., *Iron in arterial plaque: modifiable risk factor for atherosclerosis.* Biochim Biophys Acta, 2009. **1790**(7): p. 718-23.

88. Minqin, R., et al., *The iron chelator desferrioxamine inhibits atherosclerotic lesion development and decreases lesion iron concentrations in the cholesterol-fed rabbit.* Free Radic Biol Med, 2005. **38**(9): p. 1206-11.

89. Lee, H.T., et al., *Dietary iron restriction increases plaque stability in apolipoprotein-e-deficient mice.* J Biomed Sci, 2003. **10**(5): p. 510-7.

90. Ponraj, D., et al., *The onset of atherosclerotic lesion formation in hypercholesterolemic rabbits is delayed by iron depletion.* FEBS Lett, 1999. **459**(2): p. 218-22.

91. Lee, T.S., et al., *Iron-deficient diet reduces atherosclerotic lesions in apoE-deficient mice.* Circulation, 1999. **99**(9): p. 1222-9.

92. Sung, K.C., et al., *Ferritin is independently associated with the presence of coronary artery calcium in 12,033 men.* Arterioscler Thromb Vasc Biol, 2012. **32**(10): p. 2525-30.

93. Lee, K.R., et al., *Serum ferritin is linked with aortic stiffness in apparently healthy Korean women.* Crit Pathw Cardiol, 2010. **9**(3): p. 160-3.

94. Depalma, R.G., et al., *Ferritin levels, inflammatory biomarkers, and mortality in peripheral arterial disease: a substudy of the Iron (Fe) and Atherosclerosis Study (FeAST) Trial.* J Vasc Surg, 2010. **51**(6): p. 1498-503.

95. Duffy, S.J., et al., *Iron chelation improves endothelial function in patients with coronary artery disease.* Circulation, 2001. **103**(23): p. 2799-804.

96. Iribarren, C., et al., *Lack of association between ferritin level and measures of LDL oxidation: the ARIC study. Atherosclerosis Risk in Communities.* Atherosclerosis, 1998. **139**(1): p. 189-95.

97. Vergnaud, A.C., et al., *Dietary iron intake and serum ferritin in relation to 7.5 years structure and function of large arteries in the SUVIMAX cohort.* Diabetes Metab, 2007. **33**(5): p. 366-71.

98. Milman, N., *Anemia--still a major health problem in many parts of the world!* Ann Hematol, 2011. **90**(4): p. 369-77.

99. Cohen-Solal, A., et al., *Iron deficiency: an emerging therapeutic target in heart failure.* Heart, 2014.

100. Nestorowicz, A., *Word about a good medical journal.* Anaesthesiol Intensive Ther, 2012. **44**(3): p. 115-6.

101. Suzuki, H., et al., *Serum hepcidin-20 is elevated during the acute phase of myocardial infarction.* Tohoku J Exp Med, 2009. **218**(2): p. 93-8.

102. Jankowska, E.A., et al., *Iron deficiency: an ominous sign in patients with systolic chronic heart failure.* Eur Heart J, 2010. **31**(15): p. 1872-80.

103. Okonko, D.O., et al., *Disordered iron homeostasis in chronic heart failure: prevalence, predictors, and relation to anemia, exercise capacity, and survival.* J Am Coll Cardiol, 2011. **58**(12): p. 1241-51.

104. Klip, I.T., et al., *Iron deficiency in chronic heart failure: an international pooled analysis.* Am Heart J, 2013. **165**(4): p. 575-582 e3.

105. Anker, S.D., et al., *Ferric carboxymaltose in patients with heart failure and iron deficiency.* N Engl J Med, 2009. **361**(25): p. 2436-48.

106. Mathiasen, A.B., et al., *Rationale and design of the first randomized, double-blind, placebo-controlled trial of intramyocardial injection of autologous bone-marrow derived Mesenchymal Stromal Cells in chronic ischemic Heart Failure (MSC-HF Trial).* Am Heart J, 2012. **164**(3): p. 285-91.

107. Okonko, D.O., et al., *Effect of intravenous iron sucrose on exercise tolerance in anemic and nonanemic patients with symptomatic chronic heart failure and iron deficiency FERRIC-HF: a randomized, controlled, observer-blinded trial.* J Am Coll Cardiol, 2008. **51**(2): p. 103-12.

108. Beck-da-Silva, L., et al., *IRON-HF study: a randomized trial to assess the effects of iron in heart failure patients with anemia.* Int J Cardiol, 2013. **168**(4): p. 3439-42.

109. Groenveld, H.F., et al., *Anemia and mortality in heart failure patients a systematic review and meta-analysis.* J Am Coll Cardiol, 2008. **52**(10): p. 818-27.

110. Ezekowitz, J.A., F.A. McAlister, and P.W. Armstrong, *Anemia is common in heart failure and is associated with poor outcomes: insights from a cohort of 12 065 patients with new-onset heart failure.* Circulation, 2003. **107**(2): p. 223-5.

111. Anand, I., et al., *Anemia and its relationship to clinical outcome in heart failure.* Circulation, 2004. **110**(2): p. 149-54.

112. Kosiborod, M., et al., *Anemia and outcomes in patients with heart failure: a study from the National Heart Care Project.* Arch Intern Med, 2005. **165**(19): p. 2237-44.

113. Go, A.S., et al., *Hemoglobin level, chronic kidney disease, and the risks of death and hospitalization in adults with chronic heart failure: the Anemia in Chronic Heart Failure: Outcomes and Resource Utilization (ANCHOR) Study.* Circulation, 2006. **113**(23): p. 2713-23.

114. Young, J.B., et al., *Relation of low hemoglobin and anemia to morbidity and mortality in patients hospitalized with heart failure (insight from the OPTIMIZE-HF registry).* Am J Cardiol, 2008. **101**(2): p. 223-30.

115. Silverberg, D.S., et al., *The correction of anemia in patients with the combination of chronic kidney disease and congestive heart failure may prevent progression of both conditions.* Clin Exp Nephrol, 2009. **13**(2): p. 101-6.

116. Mak, G., N.F. Murphy, and K. McDonald, *Anemia in heart failure: to treat or not to treat?* Curr Treat Options Cardiovasc Med, 2008. **10**(6): p. 455-64.

117. He, S.W. and L.X. Wang, *The impact of anemia on the prognosis of chronic heart failure: a meta-analysis and systemic review.* Congest Heart Fail, 2009. **15**(3): p. 123-30.

118. Beavers, C.J., et al., *Distinguishing anemia and iron deficiency of heart failure: signal for severity of disease or unmet therapeutic need?* Pharmacotherapy, 2014. **34**(7): p. 719-32.

119. van Veldhuisen, D.J., et al., *Randomized, double-blind, placebo-controlled study to evaluate the effect of two dosing regimens of darbepoetin alfa in patients with heart failure and anaemia.* Eur Heart J, 2007. **28**(18): p. 2208-16.

120. Swedberg, K., et al., *Treatment of anemia with darbepoetin alfa in systolic heart failure.* N Engl J Med, 2013. **368**(13): p. 1210-9.

121. Dixon, S.J., et al., *Ferroptosis: an iron-dependent form of nonapoptotic cell death.* Cell, 2012. **149**(5): p. 1060-72.

122. Menasche, P., et al., *Deferoxamine reduces neutrophil-mediated free radical production during cardiopulmonary bypass in man.* J Thorac Cardiovasc Surg, 1988. **96**(4): p. 582-9.

123. Ramu, E., et al., *Dexrazoxane prevents myocardial ischemia/reperfusion-induced oxidative stress in the rat heart.* Cardiovasc Drugs Ther, 2006. **20**(5): p. 343-8.

124. Dendorfer, A., et al., *Deferoxamine induces prolonged cardiac preconditioning via accumulation of oxygen radicals.* Free Radic Biol Med, 2005. **38**(1): p. 117-24.

125. Kontoghiorghes, G.J., *Prospects for introducing deferiprone as potent pharmaceutical antioxidant.* Front Biosci (Elite Ed), 2009. **1**: p. 161-78.

126. Gille, G. and H. Reichmann, *Iron-dependent functions of mitochondria--relation to neurodegeneration.* J Neural Transm, 2011. **118**(3): p. 349-59.

127. Levi, S. and E. Rovida, *The role of iron in mitochondrial function.* Biochim Biophys Acta, 2009. **1790**(7): p. 629-36.

128. Zuris, J.A., et al., *Facile transfer of [2Fe-2S] clusters from the diabetes drug target mitoNEET to an apo-acceptor protein.* Proc Natl Acad Sci U S A, 2011. **108**(32): p. 13047-52.

129. Paddock, M.L., et al., *MitoNEET is a uniquely folded 2Fe 2S outer mitochondrial membrane protein stabilized by pioglitazone.* Proc Natl Acad Sci U S A, 2007. **104**(36): p. 14342-7.

130. Baxter, E.L., P.A. Jennings, and J.N. Onuchic, *Strand swapping regulates the iron-sulfur cluster in the diabetes drug target mitoNEET.* Proc Natl Acad Sci U S A, 2012. **109**(6): p. 1955-60.

131. Wiley, S.E., et al., *MitoNEET is an iron-containing outer mitochondrial membrane protein that regulates oxidative capacity.* Proc Natl Acad Sci U S A, 2007. **104**(13): p. 5318-23.

132. Wiley, S.E., et al., *The outer mitochondrial membrane protein mitoNEET contains a novel redox-active 2Fe-2S cluster.* J Biol Chem, 2007. **282**(33): p. 23745-9.

133. Hausmann, A., et al., *Cellular and mitochondrial remodeling upon defects in iron-sulfur protein biogenesis.* J Biol Chem, 2008. **283**(13): p. 8318-30.

134. Hentze, M.W., M.U. Muckenthaler, and N.C. Andrews, *Balancing acts: molecular control of mammalian iron metabolism.* Cell, 2004. **117**(3): p. 285-97.

135. Colca, J.R., et al., *Identification of a novel mitochondrial protein ("mitoNEET") cross-linked specifically by a thiazolidinedione photoprobe.* Am J Physiol Endocrinol Metab, 2004. **286**(2): p. E252-60.

136. Kusminski, C.M., et al., *MitoNEET-driven alterations in adipocyte mitochondrial activity reveal a crucial adaptive process that preserves insulin sensitivity in obesity.* Nat Med, 2012. **18**(10): p. 1539-49.

137. Cook, J.D., et al., *Molecular details of the yeast frataxin-Isu1 interaction during mitochondrial Fe-S cluster assembly.* Biochemistry, 2010. **49**(40): p. 8756-65.

138. Bayeva, M., M. Gheorghiade, and H. Ardehali, *Mitochondria as a therapeutic target in heart failure.* J Am Coll Cardiol, 2013. **61**(6): p. 599-610.

139. Brown, D.A., H.N. Sabbah, and S.R. Shaikh, *Mitochondrial inner membrane lipids and proteins as targets for decreasing cardiac ischemia/reperfusion injury.* Pharmacol Ther, 2013. **140**(3): p. 258-66.

140. Yoshida, H., *ER stress and diseases.* FEBS J, 2007. **274**(3): p. 630-58.

141. Toth, A., et al., *Targeted deletion of Puma attenuates cardiomyocyte death and improves cardiac function during ischemia-reperfusion.* Am J Physiol Heart Circ Physiol, 2006. **291**(1): p. H52-60.

142. Nadanaka, S., et al., *Role of disulfide bridges formed in the luminal domain of ATF6 in sensing endoplasmic reticulum stress.* Mol Cell Biol, 2007. **27**(3): p. 1027-43.

143. Okada, K., et al., *Prolonged endoplasmic reticulum stress in hypertrophic and failing heart after aortic constriction: possible contribution of endoplasmic reticulum stress to cardiac myocyte apoptosis.* Circulation, 2004. **110**(6): p. 705-12.

144. Vitadello, M., et al., *Overexpression of the stress protein Grp94 reduces cardiomyocyte necrosis due to calcium overload and simulated ischemia.* FASEB J, 2003. **17**(8): p. 923-5.

145. Lou, L.X., et al., *Endoplasmic reticulum stress involved in heart and liver injury in iron-loaded rats.* Clin Exp Pharmacol Physiol, 2009. **36**(7): p. 612-8.

146. Liu, Y., et al., *Mutant HFE H63D protein is associated with prolonged endoplasmic reticulum stress and increased neuronal vulnerability.* J Biol Chem, 2011. **286**(15): p. 13161-70.

147. Tan, T.C., et al., *Excess iron modulates endoplasmic reticulum stress-associated pathways in a mouse model of alcohol and high-fat diet-induced liver injury.* Lab Invest, 2013. **93**(12): p. 1295-312.

148. Vecchi, C., et al., *ER stress controls iron metabolism through induction of hepcidin.* Science, 2009. **325**(5942): p. 877-80.

149. Oliveira, S.J., et al., *ER stress-inducible factor CHOP affects the expression of hepcidin by modulating C/EBPalpha activity.* PLoS One, 2009. **4**(8): p. e6618.

150. Levine, B., N. Mizushima, and H.W. Virgin, *Autophagy in immunity and inflammation.* Nature, 2011. **469**(7330): p. 323-35.

151. Jimenez, R.E., D.A. Kubli, and A.B. Gustafsson, *Autophagy and mitophagy in the myocardium: therapeutic potential and concerns.* Br J Pharmacol, 2014. **171**(8): p. 1907-16.

152. Li, G.H., et al., *The role of autophagy in iron-overload cardiomyopathy: a model of diastolic heart failure ue to oxidative stress* Journal of Cardiac Failure, 2009. **15**(6S Suppl.): p. S42-43.

153. Mancias, J.D., et al., *Quantitative proteomics identifies NCOA4 as the cargo receptor mediating ferritinophagy.* Nature, 2014. **509**(7498): p. 105-9.

154. Terman, A. and U.T. Brunk, *Autophagy in cardiac myocyte homeostasis, aging, and pathology.* Cardiovasc Res, 2005. **68**(3): p. 355-65.

155. Flo, T.H., et al., *Lipocalin 2 mediates an innate immune response to bacterial infection by sequestrating iron.* Nature, 2004. **432**(7019): p. 917-21.

156. Devireddy, L.R., et al., *A cell-surface receptor for lipocalin 24p3 selectively mediates apoptosis and iron uptake.* Cell, 2005. **123**(7): p. 1293-305.

157. Yang, J., et al., *An iron delivery pathway mediated by a lipocalin.* Mol Cell, 2002. **10**(5): p. 1045-56.

158. Ismail, M.I., et al., *Neutrophil gelatinase associated lipocalin (NGAL) as a biomarker of iron deficiency in hemodialysis patients.* Austin J of Nephrol and Hypertens, 2015. **2**(2): p. 1036.

159. Malyszko, J., et al., *Possible relationship between neutrophil gelatinase-associated lipocalin, hepcidin, and inflammation in haemodialysed patients.* Nephron Clin Pract, 2010. **115**(4): p. c268-75.

160. Bolignano, D., et al., *Neutrophil gelatinase-associated lipocalin (NGAL) reflects iron status in haemodialysis patients.* Nephrol Dial Transplant, 2009. **24**(11): p. 3398-403.

161. Malbora, B., et al., *Low serum lipocalin levels in patients with iron deficiency anemia.* J Pediatr Hematol Oncol, 2013. **35**(3): p. 218-20.

162. Emans, M.E., et al., *Neutrophil gelatinase-associated lipocalin (NGAL) in chronic cardiorenal failure is correlated with endogenous erythropoietin levels and decreases in response to low-dose erythropoietin treatment.* Kidney Blood Press Res, 2012. **36**(1): p. 344-54.

163. Lindberg, S., et al., *Plasma neutrophil gelatinase-associated lipocalinin in the general population: association with inflammation and prognosis.* Arterioscler Thromb Vasc Biol, 2014. **34**(9): p. 2135-42.

164. Zhao, P., C.M. Elks, and J.M. Stephens, *The induction of lipocalin-2 protein expression in vivo and in vitro.* J Biol Chem, 2014. **289**(9): p. 5960-9.

165. Cheng, L., et al., *Lipocalin-2 promotes m1 macrophages polarization in a mouse cardiac ischaemia-reperfusion injury model.* Scand J Immunol, 2015. **81**(1): p. 31-8.

166. Jha, M.K., et al., *The pivotal role played by lipocalin-2 in chronic inflammatory pain.* Exp Neurol, 2014. **254**: p. 41-53.

167. Song, E., et al., *Deamidated lipocalin-2 induces endothelial dysfunction and hypertension in dietary obese mice.* J Am Heart Assoc, 2014. **3**(2): p. e000837.

168. Paulus, W.J. and C. Tschope, *A novel paradigm for heart failure with preserved ejection fraction: comorbidities drive myocardial dysfunction and remodeling through coronary microvascular endothelial inflammation.* J Am Coll Cardiol, 2013. **62**(4): p. 263-71.

169. Park, M. and G. Sweeney, *Direct effects of adipokines on the heart: focus on adiponectin.* Heart Failure Reviews, 2012. **E-pub online**.

170. Cakal, E., et al., *Serum lipocalin-2 as an insulin resistance marker in patients with polycystic ovary syndrome.* J Endocrinol Invest, 2011. **34**(2): p. 97-100.

171. Wu, G., et al., *Elevated circulating lipocalin-2 levels independently predict incident cardiovascular events in men in a population-based cohort.* Arterioscler Thromb Vasc Biol, 2014. **34**(11): p. 2457-64.

172. Hasegawa, M., et al., *Urinary neutrophil gelatinase-associated lipocalin as a predictor of cardiovascular events in patients with chronic kidney disease.* Heart Vessels, 2013.

173. Pronschinske, K.B., et al., *Neutrophil gelatinase-associated lipocalin and cystatin C for the prediction of clinical events in patients with advanced heart failure and after ventricular assist device placement.* J Heart Lung Transplant, 2014. **33**(12): p. 1215-22.

174. Yan, L., et al., *The high molecular weight urinary matrix metalloproteinase (MMP) activity is a complex of gelatinase B/MMP-9 and neutrophil gelatinase-associated lipocalin (NGAL). Modulation of MMP-9 activity by NGAL.* J Biol Chem, 2001. **276**(40): p. 37258-65.

175. Haase-Fielitz, A., M. Haase, and P. Devarajan, *Neutrophil gelatinase-associated lipocalin as a biomarker of acute kidney injury: a critical evaluation of current status.* Ann Clin Biochem, 2014. **51**(Pt 3): p. 335-51.

176. Abel, E.D., K.M. O'Shea, and R. Ramasamy, *Insulin resistance: metabolic mechanisms and consequences in the heart.* Arterioscler Thromb Vasc Biol, 2012. **32**(9): p. 2068-76.

177. Peterson, L.R., *Obesity and insulin resistance: effects on cardiac structure, function, and substrate metabolism.* Curr Hypertens Rep, 2006. **8**(6): p. 451-6.

178. Jia, G. and J.R. Sowers, *Autophagy: a housekeeper in cardiorenal metabolic health and disease.* Biochim Biophys Acta, 2015. **1852**(2): p. 219-24.

179. Liu, Y., et al., *Adiponectin stimulates autophagy and reduces oxidative stress to enhance insulin sensitivity during high-fat diet feeding in mice.* Diabetes, 2015. **64**(1): p. 36-48.

180. He, C., et al., *Exercise-induced BCL2-regulated autophagy is required for muscle glucose homeostasis.* Nature, 2012. **481**(7382): p. 511-5.

181. Dong, Y., et al., *Autophagy: definition, molecular machinery, and potential role in myocardial ischemia-reperfusion injury.* J Cardiovasc Pharmacol Ther, 2010. **15**(3): p. 220-30.

182. Yan, L., et al., *Autophagy in chronically ischemic myocardium.* Proc Natl Acad Sci U S A, 2005. **102**(39): p. 13807-12.

183. Cao, D.J., T.G. Gillette, and J.A. Hill, *Cardiomyocyte autophagy: remodeling, repairing, and reconstructing the heart.* Curr Hypertens Rep, 2009. **11**(6): p. 406-11.

184. Zhu, H., et al., *Cardiac autophagy is a maladaptive response to hemodynamic stress.* J Clin Invest, 2007. **117**(7): p. 1782-93.

185. Troncoso, R., et al., *Energy-preserving effects of IGF-1 antagonize starvation-induced cardiac autophagy.* Cardiovasc Res, 2012. **93**(2): p. 320-9.

186. Sugimoto, S., *A novel vacuolar myopathy with dilated cardiomyopathy.* Autophagy, 2007. **3**(6): p. 638-9.

187. Givvimani, S., et al., *Mitochondrial division/mitophagy inhibitor (Mdivi) ameliorates pressure overload induced heart failure.* PLoS One, 2012. **7**(3): p. e32388.

188. Shende, P., et al., *Cardiac raptor ablation impairs adaptive hypertrophy, alters metabolic gene expression, and causes heart failure in mice.* Circulation, 2011. **123**(10): p. 1073-82.

189. Huang, Y., et al., *Lipocalin-2, glucose metabolism and chronic low-grade systemic inflammation in Chinese people.* Cardiovasc Diabetol, 2012. **11**: p. 11.

190. El-Mesallamy, H.O., N.M. Hamdy, and A.A. Sallam, *Effect of obesity and glycemic control on serum lipocalins and insulin-like growth factor axis in type 2 diabetic patients.* Acta Diabetol, 2013. **50**(5): p. 679-85.

191. Laakso, M. and J. Kuusisto, *Insulin resistance and hyperglycaemia in cardiovascular disease development.* Nat Rev Endocrinol, 2014. **10**(5): p. 293-302.

192. Klionsky, D.J., et al., *Guidelines for the use and interpretation of assays for monitoring autophagy in higher eukaryotes.* Autophagy, 2008. **4**(2): p. 151-75.

193. Lavandero, S., et al., *Cardiovascular autophagy: concepts, controversies, and perspectives.* Autophagy, 2013. **9**(10): p. 1455-66.

194. Mizushima, N., T. Yoshimori, and B. Levine, *Methods in mammalian autophagy research.* Cell, 2010. **140**(3): p. 313-26.

195. Hariharan, N., P. Zhai, and J. Sadoshima, *Oxidative stress stimulates autophagic flux during ischemia/reperfusion.* Antioxid Redox Signal, 2011. **14**(11): p. 2179-90.

196. French, C.J., D.J. Taatjes, and B.E. Sobel, *Autophagy in myocardium of murine hearts subjected to ischemia followed by reperfusion.* Histochem Cell Biol, 2010. **134**(5): p. 519-26.

197. Kanamori, H., et al., *Autophagy limits acute myocardial infarction induced by permanent coronary artery occlusion.* Am J Physiol Heart Circ Physiol, 2011. **300**(6): p. H2261-71.

198. Hoshino, A., et al., *p53-TIGAR axis attenuates mitophagy to exacerbate cardiac damage after ischemia.* J Mol Cell Cardiol, 2012. **52**(1): p. 175-84.

199. Gurusamy, N. and D.K. Das, *Is autophagy a double-edged sword for the heart?* Acta Physiol Hung, 2009. **96**(3): p. 267-76.

200. Gottlieb, R.A., et al., *Untangling autophagy measurements: all fluxed up.* Circ Res, 2015. **116**(3): p. 504-14.

201. Matsui, Y., et al., *Distinct roles of autophagy in the heart during ischemia and reperfusion: roles of AMP-activated protein kinase and Beclin 1 in mediating autophagy.* Circ Res, 2007. **100**(6): p. 914-22.

202. Nakai, A., et al., *The role of autophagy in cardiomyocytes in the basal state and in response to hemodynamic stress.* Nat Med, 2007. **13**(5): p. 619-24.

203. Jin, D., Y. Zhang, and X. Chen, *Lipocalin 2 deficiency inhibits cell proliferation, autophagy, and mitochondrial biogenesis in mouse embryonic cells.* Mol Cell Biochem, 2011. **351**(1-2): p. 165-72.

204. Hamacher-Brady, A., N.R. Brady, and R.A. Gottlieb, *Enhancing macroautophagy protects against ischemia/reperfusion injury in cardiac myocytes.* J Biol Chem, 2006. **281**(40): p. 29776-87.

205. Yang, L., et al., *Defective hepatic autophagy in obesity promotes ER stress and causes insulin resistance.* Cell Metab, 2010. **11**(6): p. 467-78.

206. Mellor, K.M., et al., *Myocardial autophagy activation and suppressed survival signaling is associated with insulin resistance in fructose-fed mice.* J Mol Cell Cardiol, 2011. **50**(6): p. 1035-43.

207. Sengupta, A., J.D. Molkentin, and K.E. Yutzey, *FoxO transcription factors promote autophagy in cardiomyocytes.* J Biol Chem, 2009. **284**(41): p. 28319-31.

208. Ginion, A., et al., *Inhibition of the mTOR/p70S6K pathway is not involved in the insulin-sensitizing effect of AMPK on cardiac glucose uptake.* Am J Physiol Heart Circ Physiol, 2011. **301**(2): p. H469-77.

209. Mendis, S., et al., *World Health Organization definition of myocardial infarction: 2008-09 revision.* Int J Epidemiol, 2011. **40**(1): p. 139-46.

210. Thygesen, K., et al., *Universal definition of myocardial infarction.* Circulation, 2007. **116**(22): p. 2634-53.

211. Liu, Q., et al., *Porous nanofibrous poly(L-lactic acid) scaffolds supporting cardiovascular progenitor cells for cardiac tissue engineering.* Acta Biomater, 2015. **26**: p. 105-14.

212. Yang, B., et al., *Improved functional recovery to I/R injury in hearts from lipocalin-2 deficiency mice: restoration of mitochondrial function and phospholipids remodeling.* Am J Transl Res, 2012. **4**(1): p. 60-71.

213. Wilson, G.D., et al., *SELDI-TOF-MS Serum Profiling Reveals Predictors of Cardiac MRI Changes in Marathon Runners.* Int J Proteomics, 2012. **2012**: p. 679301.

214. Jahng, J.W., et al., *Pressure Overload-Induced Cardiac Dysfunction in Aged Male Adiponectin Knockout Mice Is Associated With Autophagy Deficiency.* Endocrinology, 2015. **156**(7): p. 2667-77.

215. Namiki, A., et al., *Hypoxia induces vascular endothelial growth factor in cultured human endothelial cells.* J Biol Chem, 1995. **270**(52): p. 31189-95.

216. Liu, Y., et al., *Adiponectin corrects high-fat diet-induced disturbances in muscle metabolomic profile and whole-body glucose homeostasis.* Diabetes, 2013. **62**(3): p. 743-52.

217. Thygesen, K., et al., *Universal definition of myocardial infarction.* J Am Coll Cardiol, 2007. **50**(22): p. 2173-95.

218. Chan, Y.K., et al., *Lipocalin-2 inhibits autophagy and induces insulin resistance in H9c2 cells.* Mol Cell Endocrinol, 2016. **430**: p. 68-76.

219. Nishida, K., et al., *The role of autophagy in the heart.* Cell Death Differ, 2009. **16**(1): p. 31-8.

220. Maiuri, M.C., et al., *Self-eating and self-killing: crosstalk between autophagy and apoptosis.* Nat Rev Mol Cell Biol, 2007. **8**(9): p. 741-52.

221. Yang, Y.P., et al., *Molecular mechanism and regulation of autophagy.* Acta Pharmacol Sin, 2005. **26**(12): p. 1421-34.

222. Dovey, S.M. and M.W. Tilyard, *Fees charged to a consulting population in general practice.* N Z Med J, 1991. **104**(913): p. 222-4.

223. Palanivel, R., et al., *Globular and full-length forms of adiponectin mediate specific changes in glucose and fatty acid uptake and metabolism in cardiomyocytes.* Cardiovasc Res, 2007. **75**(1): p. 148-57.

224. Eguchi, M., et al., *Diabetes influences cardiac extracellular matrix remodelling after myocardial infarction and subsequent development of cardiac dysfunction.* J Cell Mol Med, 2012. **16**(12): p. 2925-34.

225. Nicotra, G., et al., *Autophagy-active beclin-1 correlates with favourable clinical outcome in non-Hodgkin lymphomas.* Mod Pathol, 2010. **23**(7): p. 937-50.

226. Cai, Y., et al., *The Detrimental Role Played by Lipocalin-2 in Alcoholic Fatty Liver in Mice.* Am J Pathol, 2016. **186**(9): p. 2417-28.

227. Delbridge, L.M., et al., *Myocardial autophagic energy stress responses--macroautophagy, mitophagy, and glycophagy.* Am J Physiol Heart Circ Physiol, 2015. **308**(10): p. H1194-204.

228. Sciarretta, S., et al., *The importance of autophagy in cardioprotection.* High Blood Press Cardiovasc Prev, 2014. **21**(1): p. 21-8.

229. Meijer, A.J., et al., *Regulation of autophagy by amino acids and MTOR-dependent signal transduction.* Amino Acids, 2015. **47**(10): p. 2037-63.

230. Takemura, G., et al., *Cardiomyocyte apoptosis in the failing heart--a critical review from definition and classification of cell death.* Int J Cardiol, 2013. **167**(6): p. 2373-86.

231. Yang, B., D. Ye, and Y. Wang, *Caspase-3 as a therapeutic target for heart failure.* Expert Opin Ther Targets, 2013. **17**(3): p. 255-63.

232. Wu, W., et al., *Pretreatment before ischemia induction with polymerized human placenta hemoglobin (PolyPHb) attenuates ischemia/reperfusion injury-induced myocardial apoptosis.* Artif Cells Blood Substit Immobil Biotechnol, 2011. **39**(1): p. 3-6.

233. Shin, E.J., et al., *Leptin attenuates hypoxia/reoxygenation-induced activation of the intrinsic pathway of apoptosis in rat H9c2 cells.* J Cell Physiol, 2009. **221**(2): p. 490-7.

234. Taneike, M., et al., *Inhibition of autophagy in the heart induces age-related cardiomyopathy.* Autophagy, 2010. **6**(5): p. 600-6.

235. Zhao, W., et al., *Atg5 deficiency-mediated mitophagy aggravates cardiac inflammation and injury in response to angiotensin II.* Free Radic Biol Med, 2014. **69**: p. 108-15.

236. Abbaspour, N., R. Hurrell, and R. Kelishadi, *Review on iron and its importance for human health.* J Res Med Sci, 2014. **19**(2): p. 164-74.

237. Rouault, T.A., *Iron metabolism in the CNS: implications for neurodegenerative diseases.* Nat Rev Neurosci, 2013. **14**(8): p. 551-64.

238. Torti, S.V. and F.M. Torti, *Iron and cancer: more ore to be mined.* Nat Rev Cancer, 2013. **13**(5): p. 342-55.

239. Ebner, N. and S. von Haehling, *Iron deficiency in heart failure: a practical guide.* Nutrients, 2013. **5**(9): p. 3730-9.

240. Murphy, C.J. and G.Y. Oudit, *Iron-overload cardiomyopathy: pathophysiology, diagnosis, and treatment.* J Card Fail, 2010. **16**(11): p. 888-900.

241. Kremastinos, D.T., et al., *Left ventricular diastolic Doppler characteristics in beta-thalassemia major.* Circulation, 1993. **88**(3): p. 1127-35.

242. McLaren, G.D., W.A. Muir, and R.W. Kellermeyer, *Iron overload disorders: natural history, pathogenesis, diagnosis, and therapy.* Crit Rev Clin Lab Sci, 1983. **19**(3): p. 205-66.

243. Wade, J.B., V.A. DiScala, and M.J. Karnovsky, *Membrane structural specialization of the toad urinary bladder revealed by the freeze-fracture technique. I. The granular cell.* J Membr Biol, 1975. **22**(3-4): p. 385-402.

244. Kremastinos, D.T., et al., *Beta-thalassemia cardiomyopathy: history, present considerations, and future perspectives.* Circ Heart Fail, 2010. **3**(3): p. 451-8.

245. Wood, J.C., *History and current impact of cardiac magnetic resonance imaging on the management of iron overload.* Circulation, 2009. **120**(20): p. 1937-9.

246. Pietrangelo, A., *Hereditary hemochromatosis--a new look at an old disease.* N Engl J Med, 2004. **350**(23): p. 2383-97.

247. Porter, J.B., *Concepts and goals in the management of transfusional iron overload.* Am J Hematol, 2007. **82**(12 Suppl): p. 1136-9.

248. Hellstrom-Lindberg, E., *Management of anemia associated with myelodysplastic syndrome.* Semin Hematol, 2005. **42**(2 Suppl 1): p. S10-3.

249. Jensen, P.D., et al., *Evaluation of myocardial iron by magnetic resonance imaging during iron chelation therapy with deferrioxamine: indication of close relation between myocardial iron content and chelatable iron pool.* Blood, 2003. **101**(11): p. 4632-9.

250. Ghoti, H., et al., *Oxidative stress in red blood cells, platelets and polymorphonuclear leukocytes from patients with myelodysplastic syndrome.* Eur J Haematol, 2007. **79**(6): p. 463-7.

251. Oudit, G.Y., et al., *L-type Ca2+ channels provide a major pathway for iron entry into cardiomyocytes in iron-overload cardiomyopathy.* Nat Med, 2003. **9**(9): p. 1187-94.

252. Carpenter, J.P., et al., *On T2* magnetic resonance and cardiac iron.* Circulation, 2011. **123**(14): p. 1519-28.

253. Kremastinos, D.T., et al., *Iron overload and left ventricular performance in beta thalassemia.* Acta Cardiol, 1984. **39**(1): p. 29-40.

254. Hopwood, D., *Application of microwaves to electron microscopy.* Eur J Morphol, 1991. **29**(1): p. 62-3.

255. Hotamisligil, G.S., *Endoplasmic reticulum stress and the inflammatory basis of metabolic disease.* Cell, 2010. **140**(6): p. 900-17.

256. Sung, H.K., et al., *Lipocalin-2 (NGAL) Attenuates Autophagy to Exacerbate Cardiac Apoptosis Induced by Myocardial Ischemia.* J Cell Physiol, 2017. **232**(8): p. 2125-2134.

257. Scherz-Shouval, R. and Z. Elazar, *Regulation of autophagy by ROS: physiology and pathology.* Trends Biochem Sci, 2011. **36**(1): p. 30-8.

258. Gustafsson, A.B. and R.A. Gottlieb, *Autophagy in ischemic heart disease.* Circ Res, 2009. **104**(2): p. 150-8.

259. Ritchie, R.H., *Evidence for a causal role of oxidative stress in the myocardial complications of insulin resistance.* Heart Lung Circ, 2009. **18**(1): p. 11-8.

260. Mellor, K.M., R.H. Ritchie, and L.M. Delbridge, *Reactive oxygen species and insulin-resistant cardiomyopathy.* Clin Exp Pharmacol Physiol, 2010. **37**(2): p. 222-8.

261. Jung, C.H., et al., *mTOR regulation of autophagy.* FEBS Lett, 2010. **584**(7): p. 1287-95.

262. Fang, X., et al., *Hyperglycemia- and hyperinsulinemia-induced alteration of adiponectin receptor expression and adiponectin effects in L6 myoblasts.* J Mol Endocrinol, 2005. **35**(3): p. 465-76.

263. Jouihan, H.A., et al., *Iron-mediated inhibition of mitochondrial manganese uptake mediates mitochondrial dysfunction in a mouse model of hemochromatosis.* Mol Med, 2008. **14**(3-4): p. 98-108.

264. McClain, D.A., et al., *High prevalence of abnormal glucose homeostasis secondary to decreased insulin secretion in individuals with hereditary haemochromatosis.* Diabetologia, 2006. **49**(7): p. 1661-9.

265. Cooksey, R.C., et al., *Dietary iron restriction or iron chelation protects from diabetes and loss of beta-cell function in the obese (ob/ob lep-/-) mouse.* Am J Physiol Endocrinol Metab, 2010. **298**(6): p. E1236-43.

266. Cooksey, R.C., et al., *Oxidative stress, beta-cell apoptosis, and decreased insulin secretory capacity in mouse models of hemochromatosis.* Endocrinology, 2004. **145**(11): p. 5305-12.

267. Mangiagli, A., S. Italia, and S. Campisi, *Glucose tolerance and beta-cell secretion in patients with thalassaemia major.* J Pediatr Endocrinol Metab, 1998. **11 Suppl 3**: p. 985-6.

268. Cheng, K., et al., *Hypoxia-inducible factor-1alpha regulates beta cell function in mouse and human islets.* J Clin Invest, 2010. **120**(6): p. 2171-83.

269. Pennell, D.J., et al., *Cardiovascular function and treatment in beta-thalassemia major: a consensus statement from the American Heart Association.* Circulation, 2013. **128**(3): p. 281-308.

270. Oudit, G.Y., et al., *Taurine supplementation reduces oxidative stress and improves cardiovascular function in an iron-overload murine model.* Circulation, 2004. **109**(15): p. 1877-85.

271. Griendling, K.K. and G.A. FitzGerald, *Oxidative stress and cardiovascular injury: Part II: animal and human studies.* Circulation, 2003. **108**(17): p. 2034-40.

272. Sawicki, K.T., et al., *Increased Heme Levels in the Heart Lead to Exacerbated Ischemic Injury.* J Am Heart Assoc, 2015. **4**(8): p. e002272.

273. Munzel, T., et al., *Pathophysiological role of oxidative stress in systolic and diastolic heart failure and its therapeutic implications.* Eur Heart J, 2015. **36**(38): p. 2555-64.

274. Simcox, J.A. and D.A. McClain, *Iron and diabetes risk.* Cell Metab, 2013. **17**(3): p. 329-41.

275. Loos, B., et al., *At the core of survival: autophagy delays the onset of both apoptotic and necrotic cell death in a model of ischemic cell injury.* Exp Cell Res, 2011. **317**(10): p. 1437-53.

276. Freude, B., et al., *Cardiomyocyte apoptosis in acute and chronic conditions.* Basic Res Cardiol, 1998. **93**(2): p. 85-9.

277. Takemura, G. and H. Fujiwara, *Morphological aspects of apoptosis in heart diseases.* J Cell Mol Med, 2006. **10**(1): p. 56-75.

278. Kajstura, J., et al., *Apoptotic and necrotic myocyte cell deaths are independent contributing variables of infarct size in rats.* Lab Invest, 1996. **74**(1): p. 86-107.

279. Scherz-Shouval, R., et al., *Reactive oxygen species are essential for autophagy and specifically regulate the activity of Atg4.* EMBO J, 2007. **26**(7): p. 1749-60.

280. Bensaad, K., E.C. Cheung, and K.H. Vousden, *Modulation of intracellular ROS levels by TIGAR controls autophagy.* EMBO J, 2009. **28**(19): p. 3015-26.

281. Wu, J.J., et al., *Mitochondrial dysfunction and oxidative stress mediate the physiological impairment induced by the disruption of autophagy.* Aging (Albany NY), 2009. **1**(4): p. 425-37.

282. Takamura, A., et al., *Autophagy-deficient mice develop multiple liver tumors.* Genes Dev, 2011. **25**(8): p. 795-800.

283. Stephenson, L.M., et al., *Identification of Atg5-dependent transcriptional changes and increases in mitochondrial mass in Atg5-deficient T lymphocytes.* Autophagy, 2009. **5**(5): p. 625-35.

284. Rouschop, K.M., et al., *Autophagy is required during cycling hypoxia to lower production of reactive oxygen species.* Radiother Oncol, 2009. **92**(3): p. 411-6.

285. Park, B.C., et al., *Chloroquine-induced nitric oxide increase and cell death is dependent on cellular GSH depletion in A172 human glioblastoma cells.* Toxicol Lett, 2008. **178**(1): p. 52-60.

286. Farombi, E.O., *Genotoxicity of chloroquine in rat liver cells: protective role of free radical scavengers.* Cell Biol Toxicol, 2006. **22**(3): p. 159-67.

287. Park, J., et al., *Reactive oxygen species mediate chloroquine-induced expression of chemokines by human astroglial cells.* Glia, 2004. **47**(1): p. 9-20.

288. Yamasaki, R., et al., *Involvement of lysosomal storage-induced p38 MAP kinase activation in the overproduction of nitric oxide by microglia in cathepsin D-deficient mice.* Mol Cell Neurosci, 2007. **35**(4): p. 573-84.

289. Egan, D.F., et al., *Phosphorylation of ULK1 (hATG1) by AMP-activated protein kinase connects energy sensing to mitophagy.* Science, 2011. **331**(6016): p. 456-61.

290. Hasegawa, M., et al., *Urinary neutrophil gelatinase-associated lipocalin as a predictor of cardiovascular events in patients with chronic kidney disease.* Heart Vessels, 2015. **30**(1): p. 81-8.

291. Li, G.F., et al., *Iron homeostasis in osteoporosis and its clinical implications.* Osteoporos Int, 2012. **23**(10): p. 2403-8.

292. Djavaheri-Mergny, M., M.C. Maiuri, and G. Kroemer, *Cross talk between apoptosis and autophagy by caspase-mediated cleavage of Beclin 1.* Oncogene, 2010. **29**(12): p. 1717-9.

293. Kohgo, Y., et al., *Body iron metabolism and pathophysiology of iron overload.* Int J Hematol, 2008. **88**(1): p. 7-15.

294. Tsukada, M. and Y. Ohsumi, *Isolation and characterization of autophagy-defective mutants of Saccharomyces cerevisiae.* FEBS Lett, 1993. **333**(1-2): p. 169-74.

295. Ma, X., et al., *Impaired autophagosome clearance contributes to cardiomyocyte death in ischemia/reperfusion injury.* Circulation, 2012. **125**(25): p. 3170-81.

296. Tanida, I., et al., *The human homolog of Saccharomyces cerevisiae Apg7p is a Protein-activating enzyme for multiple substrates including human Apg12p, GATE-16, GABARAP, and MAP-LC3.* J Biol Chem, 2001. **276**(3): p. 1701-6.

297. Tanida, I., et al., *Apg7p/Cvt2p: A novel protein-activating enzyme essential for autophagy.* Mol Biol Cell, 1999. **10**(5): p. 1367-79.

Appendices

Appendix A: Publications

1. **Sung HK,** Chan YK, Han M, Jahng JW, Song E, Eric D, Berger T3, Mak TW and Sweeney G.
Lipocalin-2 (NGAL) Attenuates Autophagy to Exacerbate Cardiac Apoptosis Induced by Myocardial Ischemia.
Journal of Cellular Physiology (2017) Aug; 232(8): 2125-2134

2. **Sung HK*,** Chan YK*, Jahng JW, Kim GH, Han M and Sweeney G.
Lipocalin-2 inhibits autophagy and induces insulin resistance in H9c2 cells.
*Molecular and Cellular Endocrinol*ogy (2016) Jul 15; 430:68-76. *co-first author

3. Chan YK, **Sung HK** and Sweeney G.
Iron metabolism and regulation by lipocalin-2 in cardiomyopathy
Clinical Science (2015) 129(10):851-62, APPENDIX B

4. Chan YK, **Sung HK** and Sweeney G.
Regulation of Iron and Its Significance in Obesity and Complications
Korean Journal of Obesity (2014) 23(4): 1-9, APPENDIX C

5. Song E, Jahng J WS, Chong, L, **Sung HK**, Han M, Luo C, Wu D, Boo S, Hinz B, Cooper M, Robertson A, Berger T, Mak T, George I, Schulze CP, Wang Y, Xu A and Sweeney G.
Lipocalin-2 induces NLRP3 inflammasome activation via HMGB1 induced TLR4 signaling in heart tissue of mice under pressure overload challenge
American Journal of translational research (2017) Jun 15; 9(6):2723-2735, APPENDIX D

In preparations:

1. **Sung HK*,** Song E and Sweeney G.

Iron induces insulin resistance in cardiomyocytes via regulation of oxidative stress

2. **Sung HK*,** Jahng JWS*, Chan YK, Cho HH, Song E and Sweeney G.

Adiponectin deficient mice exhibit reduced autophagic flux with exaggerated cardiac dysfunction after chronic myocardial ischemia.

3. Jahng JWS, Palanivel R, **Sung HK** & Sweeney G
Iron induces skeletal muscle cell insulin resistance via regulation of endoplasmic reticulum stress and autophagy.

Appendix B

Iron metabolism and regulation by lipocalin-2 in cardiomyopathy

Chan YK, Sung HK and Sweeney G.

Clinical Science (2015) 129(10):851-62

Clinical Science (2015) **129**, 851–862 doi: 10.1042/CS20150075

Review Article

Iron metabolism and regulation by neutrophil gelatinase-associated lipocalin in cardiomyopathy

Yee Kwan Chan*, Hye Kyoung Sung* and Gary Sweeney*

*Department of Biology, York University, Toronto, Ontario, Canada

Abstract

Neutrophil gelatinase-associated lipocalin (NGAL) has recently become established as an important contributor to the pathophysiology of cardiovascular disease. Accordingly, it is now viewed as an attractive candidate as a biomarker for various disease states, and in particular has recently become regarded as one of the best diagnostic biomarkers available for acute kidney injury. Nevertheless, the precise physiological effects of NGAL on the heart and the significance of their alterations during the development of heart failure are only now beginning to be characterized. Furthermore, the mechanisms via which NGAL mediates its effects are unclear because there is no conventional receptor signalling pathway. Instead, previous work suggests that regulation of iron metabolism could represent an important mechanism of NGAL action, with wide-ranging consequences spanning metabolic and cardiovascular diseases to host defence against bacterial infection. In the present review, we summarize rapidly emerging evidence for the role of NGAL in regulating heart failure. In particular, we focus on iron transport as a mechanism of NGAL action and discuss this in the context of the existing strong associations between iron overload and iron deficiency with cardiomyopathy.

Key words: 24p3, autophagy, cardiomyopathy, ER stress, heart failure, iron deficiency, iron overload, lipocalin 2 (Lcn2), mitochondrial dysfunction, NGAL, oxidative stress.

INTRODUCTION

Iron is an essential micronutrient and its crucial role in many physiological functions is often underestimated [1]. Altered iron metabolism is implicated in a vast array of diseases, including neurodegenerative diseases [2], cardiovascular diseases [3], cancer [4], osteoporosis [5] and many more. In particular, both iron deficiency (ID) and iron overload have been associated with cardiomyopathy [6,7]. With the heart being a highly metabolically active organ, optimal iron homoeostasis is especially vital. Iron is a vital structural component of haemoglobin, myoglobin, oxidative enzymes and respiratory chain proteins that are collectively responsible for oxygen transport, storage and energy metabolism [8]. Although epidemiological studies investigating the role of iron in various diseases are often inconsistent, this is not entirely surprising given the differences in experimental criteria and numerous methods used for assessment of iron status [3]. In the present review, we aim to assess the altered iron status in cardiomyopathy, to discuss the possible cellular mechanisms involved, and to highlight the importance of regulation of iron metabolism by neutrophil gelatinase-associated lipocalin (NGAL).

SYSTEMIC AND MYOCARDIAL IRON METABOLISM

Essential concepts of systemic iron metabolism are briefly reviewed (see Figure 1), although readers are referred to some excellent review articles for further details [9,10]. Iron homoeostasis is essentially a closed system: iron is acquired from food as inorganic or haem iron, which is primarily absorbed in the duodenum via processes mediated by divalent metal ion transporter 1 (DMT-1) and haem carrier protein 1 (HCP-1), respectively. Iron in the cytoplasm can be either stored as ferritin or released to the bloodstream via ferroportin (FPN), where ferrous iron (Fe^{2+}) can be oxidized to ferric iron (Fe^{3+}) by hephaestin to facilitate

Abbreviations: CKD, chronic kidney disease; DMT-1, divalent metal ion transporter 1; EF, ejection fraction; ER, endoplasmic reticulum; ESA, erythropoietin-stimulating agent; ESC, European Society of Cardiology; FAIR-HF, Ferinject Assessment in patients with IRon deficiency and chronic Heart Failure; FPN, ferroportin; Hb, haemoglobin; HCP-1, haem carrier protein 1; HF, heart failure; HFpEF, heart failure with preserved ejection fraction; HFrEF, heart failure with reduced ejection fraction; ID, iron deficiency; IFN-γ, interferon γ; IOC, iron overload cardiomyopathy; ISC, iron-sulfur cluster; Lcn2, lipocalin 2; LTCC, L-type calcium channel; NCOA4, nuclear receptor co-activator 4; NF-κB, nuclear factor κB; NGAL, neutrophil gelatinase-associated lipocalin; NYHA, New York Heart Association; RED-HF, Reduction of Events with Darbepoetin α in Heart Failure; ROS, reactive oxygen species; Tf, transferrin; TfR, transferrin receptor; TNF-α, tumour necrosis factor α; TREAT, Trial to Reduce cardiovascular Events with Aranesp (darbepoetin α) Therapy; TSat, transferrin saturation; TTCC, T-type calcium channel; UPR, unfolded protein response.

Correspondence: Dr Gary Sweeney (gsweeney@yorku.ca).

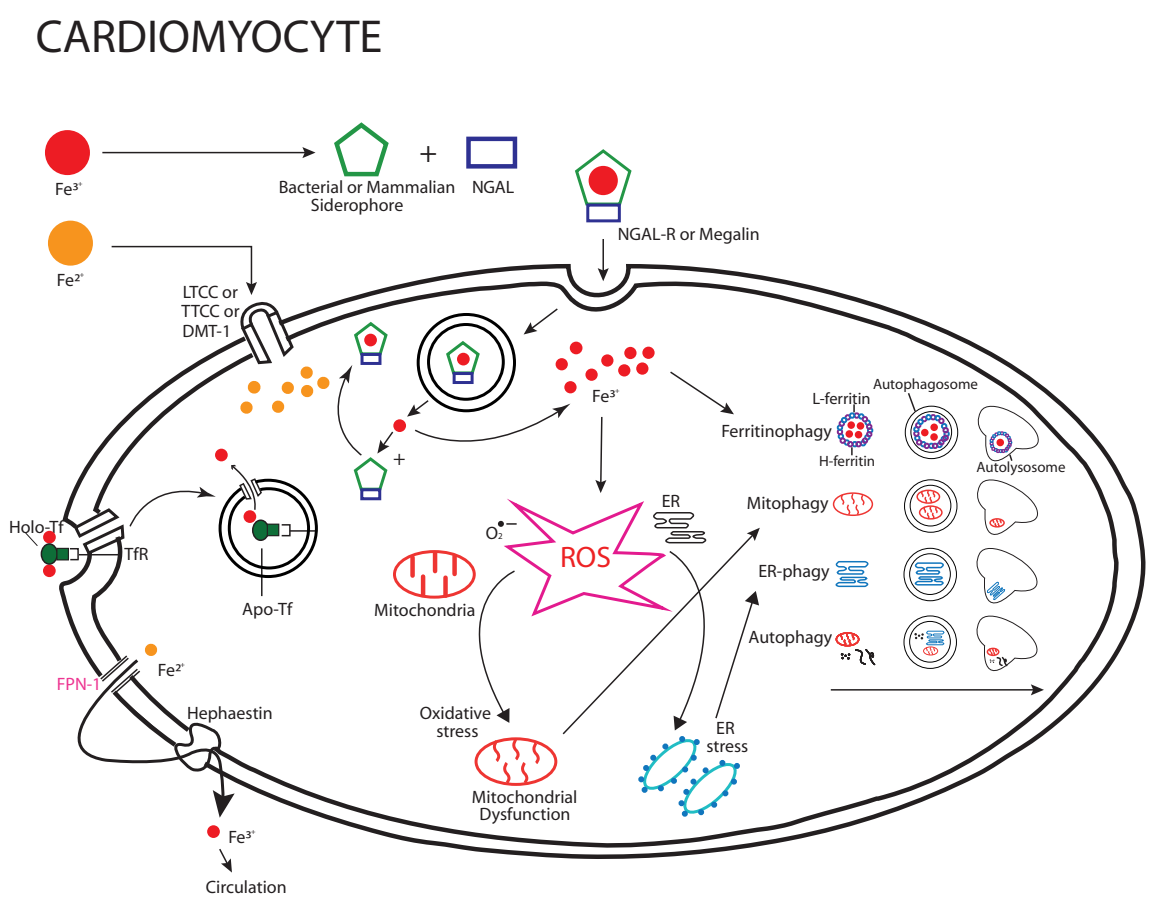

Figure 1 **Schematic overview of cellular iron transport in cardiomyocytes**
The role of DMT-1 as well as other transporters such as LTCC and TTCC as possible portals for iron into cardiomyocytes. In addition Tf binds to TfRs on the external surface of the cell. The role of NGAL is to donate iron to cells via the NGAL-R. Internalization of NGAL and its receptor leads to the uptake of iron from the siderophore–iron complex, although the exact mechanism remains unclear. However, accumulation of iron subsequently induces mitochondrial dysfunction, oxidative stress, ER stress and autophagy in cardiomyocytes. Additional details about the specific information are given in the text.

its binding to transferrin (Tf) and transport in the circulation. Most cells express transferrin receptor 1 (TfR1) such that holo-Tf can be endocytosed to acquire iron, in which the ferric iron is reduced to ferrous iron by the metalloreductase STEAP3. It is then transported across the cell membrane by DMT-1. Hepcidin is a peptide hormone that induces the intracellular degradation of FPN, the only known iron exporter, and therefore it is a vital and major iron-regulatory hormone controlling plasma iron concentration and tissue iron distribution by inhibition of intestinal iron absorption, iron recycling by macrophages and iron mobilization from hepatic stores [11].

Various processes mediate iron transport in the cardiovascular system. Iron deposition in the heart is a gradual process, and has been suggested to occur in the ventricular myocardium before the atrial myocardium [12]. Sequential appearance has been further documented, starting initially in the epicardium, then the myocardium and eventually the endocardium. Myocardial iron levels are normally regulated through Tf-mediated uptake mechanisms, mainly through TfR1 [13], although in the case of iron overload, when Tf-mediated transport becomes saturated, non-Tf-bound iron in the circulation increases and can also enter cardiac myocytes through DMT-1, T-type calcium channels (TTCCs), L-type calcium channels (LTCCs) [13,14], zinc-regulated transporter (ZRT)/iron-regulated transporter (IRT)-like protein 14 (Zip14 or Slc39a14) [15] and also NGAL receptor, which facilitates the entry of NGAL-bound iron [16]. FPN1 is expressed in cardiomyocytes as an exporter of iron into the circulation [17].

OBSERVATIONAL CHANGES AND DIAGNOSIS OF IRON STATUS IN CARDIOMYOPATHY

Heart failure (HF) is a highly prevalent chronic progressive condition in which the heart is incapable of pumping enough blood to meet the body's demand. The ejection fraction (EF), the measurement of the amount of blood that the left ventricle pumps out in each contraction, is an important indicator for heart function and diagnosis of HF. In patients who have HF with reduced ejection fraction (HFrEF), the EF falls from a normal range of between 55% and 70% to <40%, yet half of the patients with HF are

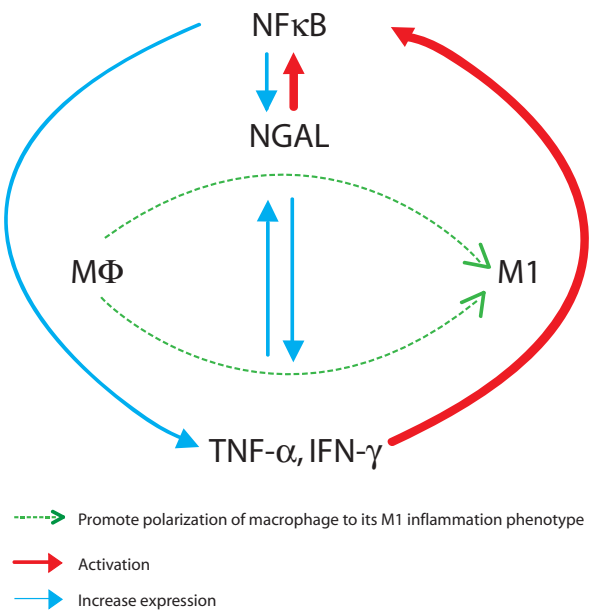

Figure 2 Schematic overview of pro-inflammatory actions of NGAL

NGAL expression is induced by IFN-γ and TNF-α, and one potential mechanism is via an NF-κB-dependent pathway. NGAL itself can also induce NF-κB activation, and further induce IFN-γ and TNF-α expression. In addition it enhances cardiac inflammation by promoting macrophage pro-inflammatory M1 phenotype polarization. Additional details of the various phenomena illustrated are provided in the text.

observed to have preserved EF (HFpEF) [18]. In the ongoing search for novel treatments of HF, strong evidence is emerging to show the significance of disturbed iron homoeostasis in HF, regardless of the degree of change in the EF [19], thus establishing an excellent therapeutic potential if our understanding of the mechanisms responsible for the association of iron homoeostasis and HF can be enhanced.

The normal range of circulating ferritin is from 30 μg/l to 300 μg/l. In healthy individuals, iron deficiency is defined when the circulating ferritin concentration falls to <30 μg/l. However, HF has an inflammatory component in which serum ferritin, as an acute-phase protein, is often elevated without changes in body iron stores. Therefore, it should be noted that there is a difference in the diagnostic criteria for ID between healthy individuals and those with HF (and other chronic diseases). Recently the European Society of Cardiology (ESC) guidelines for diagnosis and treatment of HF have recommended a systematic measurement of iron parameters in all patients suspected of having HF. Serum ferritin <100 μg/l is regarded as absolute iron deficiency; if serum ferritin is 100–299 μg/l and Tf saturation (TSat) <20% this is defined as functional iron deficiency [20]. On the other hand, TSat >55% and serum ferritin >200 μg/l or >300 μg/l in women and men, respectively, is diagnosed as iron overload cardiomyopathy (IOC), as proposed by 2005 American College of Physicians guidelines [21]. The level of serum ferritin at which iron deposition is detected in the heart has not yet been conclusively identified. Not only is it invasive to take a heart biopsy, but technical difficulty also often renders the results variable and non-definitive. Both iron overload and ID have been linked to cardiomyopathy, with the former primarily associated with an enhanced oxidative stress and the latter with mitochondrial dysfunction, impaired heart efficacy [8], hypercoagulable state and increased cardiac burden, and, in addition, oxidative stress due to anaemia [3]. Cardiomyopathy associated with iron overload or ID is reviewed in more detail below.

Iron overload cardiomyopathy

IOC is defined as the presence of systolic or diastolic cardiac dysfunction secondary to increased deposition of iron in the heart independent of other concomitant processes [22]. It is typically associated with dilated cardiomyopathy with left ventricular hypertrophy and reduced EF [7]. Although patients may remain asymptomatic in the early disease process, severely overloaded patients can rapidly experience terminal HF. Accumulation of iron in the myocardium may occur via increased iron absorption from gastrointestinal enterocytes (haemochromatosis), excess exogenous iron intake, such as via dietary supplements, or blood transfusions (haemosiderosis). The association of IOC with haemochromatosis, an autosomal disorder involving mutation of specific genes involved in iron metabolism, leading to increased gastrointestinal absorption, is well characterized [23]. In fact, this accounts for a third of deaths in hereditary haemochromatosis, especially in young male patients [24]. Chronic blood transfusion is the treatment for hereditary and acquired anaemia, including thalassaemia and myelodysplastic syndromes. However, as excess body iron cannot be actively excreted, repeated blood transfusions can result in iron deposition in multiple organs, of which the heart is one of the most sensitive organs to iron toxicity [7]. As the cardiac clinical presentations can vary widely among these patients, a recent review has provided recommendations and clinical guidelines with regard to a decision on chelation therapy by stratifying patients based on the presence or absence of heart dysfunction and heart magnetic resonance imaging T2-weighted values [25].

There are numerous mechanisms via which excess iron can reduce cardiac function. Once the antioxidant capacity of cardiomyocytes has been exceeded, iron can produce excess oxidative stress via the Fenton reaction (see below) and lead to apoptosis [26]. In addition, excess free iron in the blood is suggested as responsible for the generation of insoluble parafibrin, which is highly resistant to proteolytic dissolution and initiates inflammatory reactions on deposition on the arterial wall [27]. The association of iron and atherosclerosis is well established in animal studies, e.g. iron accumulation is observed in atherosclerotic plaques [28], and decreasing tissue iron via chelating therapy, dietary iron restriction or phlebotomy showed decreased atheroma plaque size with improved stability [29–32]. Such association is also supported in clinical studies: a study involving 12 033 men showed that increased ferritin concentration was associated with early coronary artery atherosclerosis, independent of traditional cardiovascular risk factors [33]; another study involving 196 participants showed a strong association between serum ferritin and pulse wave velocity or aortic stiffness in women [34]. The 6-year-long Iron and Atherosclerosis STudy (FeAST) also established correlations of levels of ferritin, inflammatory biomarkers and

mortality in a subset of patients with peripheral arterial disease [35]. Iron availability may have contributed to atherosclerosis by impairing nitric oxide action, as demonstrated by improvement in nitric oxide-mediated endothelium-dependent vasodilatation in patients with coronary artery disease, by chelating iron with desferrioxamine [36]. Although further mechanisms have yet to be defined, the Atherosclerosis Risk In Communities (ARIC) study has rejected the hypothesis that excess iron stores would promote low-density lipoprotein (LDL) oxidation [37]. It was shown that dietary iron intake and body iron stores had no direct link to altered structure and function of large arteries in individuals free of cardiovascular disease, cancer or haemochromatosis [38].

Iron deficiency and cardiomyopathy

Iron deficiency (ID) is the most common nutritional deficiency worldwide [39]. It is frequent, has a high occurrence rate of 30–50% in patients with HF and presents as an important co-morbidity [40]. Two types of ID can be distinguished: absolute and functional. Absolute ID reflects depleted iron stores, whereas iron homoeostatic mechanisms and erythropoiesis often remain intact. Absolute ID development in humans can result from inadequate dietary iron intake, impaired gastrointestinal absorption/transport, drug interactions and gastrointestinal blood loss [41]. On the other hand, functional ID presents a dysregulated iron homoeostasis in which cells and tissues might receive inadequate iron supplies despite normal whole body iron storage. This can be a result of elevated circulating hepcidin concentrations, and has been reported in patients with acute-phase myocardial infarction [42].

ID is often accompanied by anaemia, although both can exist independently and ID usually appears before the onset of anaemia. It is important to differentiate anaemia from ID; although ID is marked by the insufficiency of iron, anaemia is defined by insufficient haemoglobin (Hb). ID that is independent of anaemia was reported to have a higher risk of death than that dependent on anaemia [43,44]; it has been reported as an independent predictor of mortality and is associated with disease severity [45].

In recent years there have been several clinical trials to test whether administration of intravenous iron could improve functional parameters related to HF. One of the most well-known studies includes the Ferinject Assessment in patients with IRon deficiency and chronic Heart Failure (FAIR-HF). This involved 459 patients with ID and chronic heart failure of New York Heart Association (NYHA) functional class II or III. The treatment with intravenous ferric carboxymaltose over 24 weeks improved NYHA functional class, functional capacity and quality of life in terms of EuroQol-5 Dimension and Kansas City Cardiomyopathy Questionnaire with an acceptable side-effect profile [46]. A simplified ferric Carboxymaltose evaluatioN on perFormance in patients with IRon deficiency in combination with chronic Heart Failure (CONFIRM-HF) trial, which has enrolled 304 stable symptomatic HF patients from 41 sites across nine European countries, is currently in progress to confirm the efficacy and safety of iron therapy using intravenous ferric carboxymaltose solution in chronic HF patients with iron deficiency, as in the FAIR-HF study [47]. Other clinical trials including the FERRIC-HF (FERRIC iron sucrose in Heart Failure) [48] and IRON-HF [49] trials have also shown encouraging results with iron therapy, using intravenous iron sucrose in improving functional capacity in HF patients with ID. Thus, ID can serve in many cases as a promising therapeutic target for HF.

Furthermore, the importance of ID as a marker in the context of HF and its assessment was highlighted and recommended by the ESC [20]. As for anaemia, it has also been shown to have a relatively high prevalence (37%) in patients with HF [50]. With less oxygen availability during anaemia, the heart compensates by increasing heart rate and stroke volume. Moreover, anaemia has been reported to be an independent risk factor for adverse outcomes in HF, in terms of both morbidity and mortality rates [51–58]. Efforts have been made to restore Hb levels as a potential therapeutic approach to HF using erythropoietin-stimulating agents (ESAs) and this resulted in improvements in exercise tolerance, peak $\dot{V}O_2$, N-terminus of the prohormone brain natriuretic peptide (NT-proBNP) and left ventricular performance in patients with HF [59]. However, some major clinical trials that evaluated the effect of treating anaemia with the ESA darbepoetin α for cardiovascular events or HF have consistently suggested that darbepoetin α did not significantly improve HF outcomes. One of the earlier trials was the STudy of AneMIa in Heart Failure Trial (STAMINA-HeFT), which involved 319 patients with systemic HF, left ventricular EF <40% and Hb level between 9.0 g/dl and 12.5 g/dl, in which they found a 1-year treatment with darbepoetin α failed to associate with any significant clinical benefits [60]. The Trial to Reduce cardiovascular Events with Aranesp (darbepoetin α) Therapy (TREAT) was initiated in 2004 to provide a robust estimate of the safety and efficacy of darbepoetin α [61]. This event-driven study continued to grow until it reached approximately 1203 patients with Type 2 diabetes, chronic kidney disease (CKD) and anaemia, who have experienced primary events, including the composite end-point of death, cardiovascular morbidity or the need for long-term renal replacement therapy. TREAT initially showed that ESA treatment in diabetic and anaemic patients with CKD did not demonstrate clinical benefits in terms of mortality, morbidity or quality of life [62]; instead, cardiovascular risk was most strongly predicted by age, HF history, and several other established renal and cardiovascular biomarkers [63]. In addition, most of these patients were able to maintain a stable Hb level without having any long-term ESA therapy [64], and long-term (2 years) ESA therapy to treat anaemia did not confer significant benefits [65]. The most recent update from TREAT suggests that the cardiovascular or non-cardiovascular mortality rates, particularly those from sudden death and infection, were associated with lower baseline glomerular filtration rate and higher protein/creatinine ratio in diabetic CKD patients [66].

Another large-scale clinical trial, the Reduction of Events with Darbepoetin α in Heart Failure (RED-HF) trial, was also launched to evaluate the effect of darbepoetin α on mortality and morbidity, and quality of life in patients with HF and anaemia [67]. Over 2600 patients with NYHA class II–IV, EF $\leqslant 40$% and Hb between 9.0 g/dl and 12.0 g/dl were subcutaneously administered darbepoetin α or placebo until the primary end-point was

met [67]. The RED-HF study, compared with other recent clinical trials in HF, had patients who were older, with moderately to markedly symptomatic HF and extensive co-morbidity [68]. The study showed that darbepoetin α did not significantly alter primary or secondary outcomes, concluding that darbepoetin α did not improve clinical outcomes in patients with systolic HF and mild-to-moderate anaemia [69]. Thus, based on all available evidence, it has been suggested that anaemia may serve only as a surrogate marker rather than an end-point target in HF.

CELLULAR MECHANISMS THAT UNDERLIE THE ASSOCIATION OF IRON AND CARDIOMYOPATHY

Iron and oxidative stress

Free iron is highly-redox reactive and can participate in a redox reaction that leads to the generation of reactive oxygen species (ROS). ROS include not only a range of free radicals such as superoxide radical anion ($O_2^{\bullet -}$), carbonate radical anion ($CO_3^{\bullet -}$), hydroperoxyl radical ($HOO^{\bullet}$), hydroxyl radical ($HO^{\bullet}$), peroxyl radical ($ROO^{\bullet}$) and alkoxyl radical ($RO^{\bullet}$), but also non-radicals such as hydrogen peroxide (H_2O_2), hypochlorous acid (HClO) and ozone (O_3). Among them, H_2O_2 and $O_2^{\bullet -}$ are the major ROS in living organisms and are continuously produced by cells and must simultaneously be removed by antioxidant enzymes. Neither H_2O_2 nor $O_2^{\bullet -}$ is a strong oxidizing agent, but the extremely reactive hydroxyl radical $HO^{\bullet}$ can be produced on reaction with iron or iron-containing molecules through the Fenton reaction. H_2O_2 oxidizes Fe^{2+} to Fe^{3+}, producing the hydroxyl radical $HO^{\bullet}$ and hydroxide ion OH^- (eqn 1); Fe^{3+} is then reduced back to Fe^{2+} by another H_2O_2 molecule, forming a hydroperoxyl radical $HOO^{\bullet}$ and a proton H^+ (eqn 2), or by superoxide radical anion ($O_2^{\bullet -}$) to produce oxygen (O_2) (eqn 3). In this way, iron acts as a catalyst to generate plentiful amounts of ROS.

$$Fe^{2+} + H_2O_2 \rightarrow Fe^{3+} + HO^{\bullet} + OH^- \quad (1)$$

$$Fe^{3+} + H_2O_2 \rightarrow Fe^{2+} + HOO^{\bullet} + H^+ \quad (2)$$

$$Fe^{3+} + O_2^{\bullet -} \rightarrow Fe^{2+} + O_2 \quad (3)$$

Although ROS have important physiological functions, e.g. to combat invading pathogens, excess ROS can result in oxidative stress that damages intracellular proteins, lipids and nucleic acids. Indeed, specific parts of the genome were found to be damaged by the Fenton reaction, and are termed 'genomic sites vulnerable to the Fenton reaction' [70]. Ferroptosis, as the name implies, is a recently identified form of cell death that is morphologically, biochemically and genetically distinct from apoptosis and necrosis, and is found to depend on intracellular iron; it can be prevented by iron chelators and antioxidants [71]. The use of the iron chelator desferrioxamine has demonstrated significant reduction of neutrophil-mediated free radical production and amplification of the inflammatory response during cardiopulmonary bypass in humans [72] and in *in vivo* studies [73–75]. In summary, iron can potently enhance oxidative stress and consequently contribute to cardiomyopathy.

Iron and mitochondrial dysfunction

In eukaryotic cells, mitochondria are the main consumers of intracellular iron [76]. With mitochondria being the respiratory centre of the cell, plentiful oxygen can rapidly react with unregulated free iron to produce ROS. To avoid ROS-induced damage, mitochondrial iron level and homoeostasis are tightly regulated by different transport, storage and regulatory proteins [77]. Through different biosynthesis pathways, iron is transferred in the mitochondria to its bioactive forms, haem and iron–sulfur cluster (ISC). MitoNEET is an ISC-containing protein tethered to the outer mitochondrial membrane that facilitates transfer of iron into the mitochondria [78]. Not only does it play an essential role in redox signalling [79], but also it dictates the metabolic functions of mitochondria [78,80–82]. An increased level of mitoNEET can lead to accumulation of iron within the mitochondria, which in turn results in dysfunction [83,84], a hallmark of various diseases. MitoNEET is recognized as a target for the thiazolidinedione class of anti-diabetic drugs [79,85], and its genetic manipulation was shown to have striking anti-diabetic effects [86]. Mitochondrial ferritin stores and supplies iron within the mitochondria. Its expression is restricted to highly metabolically active cells such as cardiomyocytes, in order to supply iron when demand is increased during active respiration or intense metabolic activities. Frataxin is another mitochondrial protein that handles iron in the mitochondrial matrix assembling ISC [87]. It can act either as a chaperone for ferrous iron or as an iron storage protein that can mineralize iron as ferrihydrite. There is great interest in improving mitochondrial dysfunction as a potential therapeutic approach for HF [88,89], and the underappreciated contribution of iron homoeostasis is worthy of more consideration.

Iron and endoplasmic reticulum stress

Various pathophysiological situations can elevate stress in the endoplasmic reticulum (ER). One of the major functions of the ER is proper protein folding, and accumulation of misfolded proteins can normally be relieved by cellular responses such as ER-associated protein degradation (ERAD) and unfolded protein response (UPR). These ER stress responses are important defence mechanisms when the amount of unfolded protein exceeds the folding capacity of the ER [90]. ER stress has been strongly implicated in cardiovascular disease, e.g. ER stress can lead to cardiomyocyte death *in vivo* and *ex vivo* [91], and in patients with HF [92]. Interestingly, it was suggested that ER stress may be cardioprotective during constriction-induced hypertrophy [93], perhaps by inducing compensatory cellular mechanisms such as autophagy (see below). Similarly, ER stress induction protected cardiomyocytes from oxidative damage [94]. Iron overload-induced ER stress was shown *in vivo* in hearts under acute and chronic conditions [95], and had been demonstrated in other tissue types, including neurons [96] and liver [97]. In reverse, ER stress can modulate iron metabolism. Hepcidin, as mentioned above, degrades the iron efflux transporter FPN, thus leading to

a systemic hypoferraemic environment. ER stress was found to induce hepcidin expression [98]; the UPR signalling pathway was further shown to increase the transcription of FPN and ferritin [99]. Thus, based on available evidence, ER stress and iron homoeostasis appear to have a reciprocal relationship such that they can tightly regulate each other. ER stress and UPR-related proteins will serve as interesting targets for future clinical studies.

Iron and autophagy

Macroautophagy (hereafter referred to as autophagy) is an intracellular degradation system that involves the sequestration of cytoplasmic components within a double-membrane vesicle termed an 'autophagosome', in which the cargo content is degraded by the acidic hydrolases on fusion with a lysosome [100]. It has a wide variety of physiological and pathophysiological roles including energy homoeostasis, cell survival and host defence against pathogen invasion [101].

In the heart, autophagy typically occurs at low levels, yet it is nevertheless important in maintaining cellular homoeostasis under normal conditions. Autophagy is typically up-regulated in times of stress, e.g. during ischaemia/reperfusion, pressure overload and cardiac toxicity induced by chemicals such as the athracycline doxorubicin [102]. Although increased autophagy can promote cell survival by degrading damaged organelles, such as mitochondria and protein aggregates, to recycle catabolites and maintain ATP production, either excess or lack of autophagy can result in cell death and cardiac dysfunction. Thus, the role of autophagy can often appear controversial between different studies when different degrees of autophagy, time course and pathological conditions being studied have led to variable observations. *In vivo* data have shown that expression of multiple autophagy-related genes was altered in IOC, possibly contributing to cardiac diastolic dysfunction [103].

Specifically, it is now appreciated that iron can regulate autophagy and that autophagy has an important role in iron homoeostasis. Nuclear receptor co-activator 4 (NCOA4) was recently identified using quantitative proteomics as the cargo receptor that mediates autophagy of ferritin, a process termed 'ferritinophagy'. NCOA4 is required for the delivery of ferritin to the lysosome; without NCOA4, cells are malfunctional in ferritin degradation and this can result in a decreased bioavailability of intracellular iron [104]. However, excessive ferritinophagy may result in insufficient ferritin, thus reducing its buffering effect on binding intralysosomal low-mass iron, and can lead to lysosomal fragility and increased sensitivity to oxidative stress [105]. Analysis of autophagy in iron-associated cardiomyopathy is relatively new with limited mechanistic and clinical studies; however, we believe that this must be rapidly developed because it has great potential as a therapeutic target.

REGULATION OF CARDIOMYOPATHY BY NGAL

The maintenance of optimal iron levels in the body is largely controlled and influenced by endocrine regulation, and this is likely to be of major significance in cardiomyopathy. In this section, we highlight the importance of NGAL in the regulation of iron homoeostasis and other possible mechanisms in the context of cardiomyopathy (see Figure 2).

Neutrophil gelatinase-associated lipocalin

Lipocalins are a diverse family that generally bind small and hydrophobic ligands, but can also bind soluble extracellular macromolecules and specific cell surface receptors [106,107]. NGAL (human orthologue), also termed 'lipocalin 2' (Lcn2) or '24p3' (murine orthologue), is a 25-kDa secretory protein. NGAL was originally identified as a component of neutrophil granules that bound to and prevented the degradation of matrix metalloproteinase-9, and was later found to be secreted by a number of cells including macrophages, endothelial cells [108], epithelial cells [109], cardiomyocytes (Chan, Y.K., Sung, H.K. and Sweeney, G., unpublished work), hepatocytes [110] and adipocytes [111].

Epidemiology of NGAL and heart failure

In clinical settings, NGAL is now regarded as the best biomarker for acute kidney injury, and is also emerging as a promising biomarker for HF. The heart and kidney have numerous similarities and their interdependent relationship makes it understandable that renal dysfunction often accompanies cardiac failure, and that cardiac dysfunction is frequently seen with renal failure [112]. Therefore, many biomarkers for kidney or tubular dysfunction, e.g. kidney injury molecule 1 (KIM-1) and *N*-acetyl-β-D-glucosaminidase, rather than just serving as a means to assess kidney function, also provide insights into the cardiac prognosis in patients with HF. However, unlike other renal biomarkers, the NGAL level was not affected by diuretic withdrawal in patients with chronic systolic HF [113], and administration of NGAL in an animal model of acute ischaemic renal injury actually attenuated tubular injury [114]. Moreover, in patients with chronic HF, NGAL has been shown to be a more effective marker than creatinine for the cardiorenal syndrome; NGAL could detect renal injury earlier than creatinine, and was an independent and novel risk predictor of mortality in chronic HF [115]. Indeed, the elevation of NGAL seen in HF, and its association with different parameters of HF, has affirmed its potential as a HF biomarker. First, serum NGAL predicted the outcome of HF, e.g. the GALLANT (NGAL evaluation Along with B-type NaTriuretic peptide in acutely decompensated heart failure) trial concluded that, at the time of discharge, plasma NGAL was a strong prognostic indicator of 30-day outcomes in patients admitted for acute HF [116]; it independently predicted worse short-term prognosis in patients with acute HF [117], and NGAL levels correlated well with HF-related functional assessment parameters, including the 6-min walk test [118]. Secondly, the CORONA (COntrolled ROsuvastatin multiNAtional trial in heart failure) study suggested that NGAL was associated with the severity of HF [119], the elevated serum NGAL in patients with acute post-myocardial infarction and chronic HF was found to be associated with more adverse outcome [120], and the NGAL level was shown to correlate with HF severity and haemodynamic improvements after placement of a ventricular assist device [121]. Thirdly, serum NGAL predicted severity of chronic HF in terms of NYHA classification and

mortality in elderly patients [122], and plasma NGAL also predicted mortality in HF patients with or without CKD [123], and in community-dwelling older adults independent of traditional risk factors and kidney functions [124]. Clearly, there is strong evidence for NGAL being a useful biomarker to assess severity, prognosis and mortality in HF suggested by various individual cohorts.

Possible mechanisms via which NGAL may mediate cardiomyopathy

Iron transport

NGAL is most well known for its participation in innate immunity to limit bacterial growth by sequestrating iron. One way to secure iron from the host by bacteria is by synthesizing and secreting siderophores to extract iron from iron-containing compounds such as Tf and lactoferrin; NGAL is secreted by the host to tightly bind to bacterial catecholate-type ferric siderophores, competing for iron and preventing such uptake [108]. NGAL saturated with iron (holo-form) can increase intracellular iron levels by transporting and then releasing iron into the cytoplasm; in contrast, when NGAL is iron-free (apo-form), it can deplete intracellular iron and transport it to the extracellular space via its receptor NGAL-R [125]. Bacterial infection is often associated with hypoferrinaemia [126] which limits iron availability to pathogens; accordingly, mice deficient in NGAL exhibit elevated intracellular labile iron and lowered circulating iron levels [127]. Overall, NGAL, as an iron-trafficking protein, can be regarded as an alternative to a Tf-mediated iron-delivery pathway [128].

Although limited studies are available, it is speculated that circulating NGAL levels may reflect the body's iron status, at least in haemodialysis patients [129]. In haemodialysis patients, it was found that plasma NGAL was significantly lower within those who had ID, with TSat $<20\%$, and that the level of NGAL was positively correlated with circulating iron, TSat and ferritin. NGAL was significantly increased after correction of ID with intravenous iron administration [130]. Similar results were also observed in another two studies supporting the potential use of NGAL to identify iron deficiency in haemodialysis patients [129,131]. Likewise, a lowered NGAL level was also recorded in patients with iron deficiency anaemia [132] and, in patients with chronic HF (both HFpEF and HFrEF), the significantly higher circulating NGAL levels also correlated with higher serum iron concentrations in the EPOCARES (ErythroPOietin in the CArdioREnal Syndrome) study [133]. As circulating NGAL is often recorded as significantly increased in patients experiencing HF [117,120–123], and local NGAL production in the heart is also increased significantly (Chan, Y.K., Sung, H.K. and Sweeney, G., unpublished work) [120,134], we believe that it will be of great interest to elucidate the role of NGAL in iron-associated cardiomyopathy further. It is interesting that we previously identified NGAL leading to cardiomyocyte apoptosis by causing intracellular iron accumulation [16]. Further mechanistic studies are definitely warranted.

Pro-inflammatory actions of NGAL

As NGAL is involved in defending the host during bacterial infection, it comes as no surprise that NGAL is regarded as a pro-inflammatory cytokine. In the fourth Copenhagen Heart Study, which involved more than 5000 patients and a follow-up period of 10 years, it was shown that plasma NGAL strongly associated with all inflammatory markers investigated, including high-sensitivity C-reactive protein, and total leucocyte and neutrophil count; increased NGAL was also shown to correspond to an increased risk of all-cause mortality and major adverse cardiovascular events [135]. It was suggested that NGAL expression and secretion can be induced by interferon γ (IFN-γ) and tumour necrosis α (TNF-α), and that the transcription factors, signal transducer and activator of transcription 1 (STAT1) and nuclear factor κB (NF-κB), were shown to bind to the human NGAL promoter [136]. Likewise, in elucidating the inflammatory mechanisms of NGAL with animal models, NGAL mRNA and proteins were up-regulated on vascular injury in an NF-κB-dependent manner [137]. NGAL can enhance cardiac inflammation by promoting polarization of the macrophage pro-inflammatory M1 phenotype [138]. Thus, a vicious cycle exists whereby NGAL can intensify inflammation by inducing the expression of TNF-α and other pro-inflammatory mediators [139]. It is of interest that prevention of the clearance of NGAL from the circulation was shown to promote vascular inflammation and endothelial dysfunction [140]. In both HFpEF and advanced HFrEF, elevated systemic and local inflammation with increased circulating TNF-α have indispensable roles in disease pathogenesis [141]. It will be interesting to explore how NGAL contributes to cardiomyopathy in an inflammation-dependent and -independent manner.

CONCLUSION

Iron is a micronutrient that is integral to the function of many proteins required in cells with high metabolic activity. It is involved in regulating various cellular mechanisms including oxidative stress, mitochondrial dysfunction, ER stress and autophagy, all of which can contribute to cardiac dysfunction when perturbed. NGAL, an adipokine that mediates iron transport through association with a siderophore, can increase or decrease intracellular iron content based on the body iron store and its iron saturation, making it a malleable factor in the maintenance of iron homoeostasis. Indeed, elevation of NGAL is well documented in various instances of HF with strong association to severity of HF and resulting morbidity and mortality. Furthermore, NGAL is an inflammatory biomarker that can be induced by endotoxaemia and myocarditis. It can also contribute to atherosclerosis and insulin resistance. Future work to fully characterize the association of NGAL with iron overload and deficient cardiomyopathy, and in particular to understand the precise mechanisms of NGAL action contributing to cardiac dysfunction, are needed. These would both validate the potential use of NGAL as a biomarker and allow the development of novel therapeutic targets for the treatment of heart failure.

ACKNOWLEDGEMENTS

We thank Hyosik Kim for help with graphic design.

FUNDING

Related work in our group is funded by the Canadian Institutes of Health Research, Heart and Stroke Foundation and Canadian Diabetes Association.

REFERENCES

1 Abbaspour, N., Hurrell, R. and Kelishadi, R. (2014) Review on iron and its importance for human health. J. Res. Med. Sci. **19**, 164–174 PubMed
2 Rouault, T.A. (2013) Iron metabolism in the CNS: implications for neurodegenerative diseases. Nat. Rev. Neurosci. **14**, 551–564 CrossRef PubMed
3 Lapice, E., Masulli, M. and Vaccaro, O. (2013) Iron deficiency and cardiovascular disease: an updated review of the evidence. Curr. Atheroscler. Rep. **15**, 358 CrossRef PubMed
4 Torti, S.V. and Torti, F.M. (2013) Iron and cancer: more ore to be mined. Nat. Rev. Cancer **13**, 342–355 CrossRef PubMed
5 Li, G.F., Pan, Y.Z., Sirois, P., Li, K. and Xu, Y.J. (2012) Iron homeostasis in osteoporosis and its clinical implications. Osteoporos. Int. **23**, 2403–2408 CrossRef PubMed
6 Ebner, N. and von Haehling, S. (2013) Iron deficiency in heart failure: a practical guide. Nutrients **5**, 3730–3709 CrossRef PubMed
7 Gujja, P., Rosing, D.R., Tripodi, D.J. and Shizukuda, Y. (2010) Iron overload cardiomyopathy: better understanding of an increasing disorder. J. Am. Coll. Cardiol. **56**, 1001–1012 CrossRef PubMed
8 Jankowska, E.A., von Haehling, S., Anker, S.D., Macdougall, I.C. and Ponikowski, P. (2013) Iron deficiency and heart failure: diagnostic dilemmas and therapeutic perspectives. Eur. Heart J. **34**, 816–829 CrossRef PubMed
9 Andrews, N.C. (1999) Disorders of iron metabolism. N. Engl. J. Med. **341**, 1986–1995 CrossRef PubMed
10 Wang, J. and Pantopoulos, K. (2011) Regulation of cellular iron metabolism. Biochem. J. **434**, 365–381 CrossRef PubMed
11 Nemeth, E. and Ganz, T. (2006) Regulation of iron metabolism by hepcidin. Annu. Rev. Nutr. **26**, 323–242 CrossRef PubMed
12 Wood, J.C. (2008) Cardiac iron across different transfusion-dependent diseases. Blood Rev. **22** (Suppl. 2), S14–S21 CrossRef PubMed
13 Kumfu, S., Chattipakorn, S., Fucharoen, S. and Chattipakorn, N. (2013) Ferric iron uptake into cardiomyocytes of beta-thalassemic mice is not through calcium channels. Drug Chem. Toxicol. **36**, 329–334 CrossRef PubMed
14 Tsushima, R.G., Wickenden, A.D., Bouchard, R.A., Oudit, G.Y., Liu, P.P. and Backx, P.H. (1999) Modulation of iron uptake in heart by L-type Ca2+ channel modifiers: possible implications in iron overload. Circ. Res. **84**, 1302–1309 CrossRef PubMed
15 Nam, H., Wang, C.Y., Zhang, L., Zhang, W., Hojyo, S., Fukada, T. and Knutson, M.D. (2013) ZIP14 and DMT1 in the liver, pancreas, and heart are differentially regulated by iron deficiency and overload: implications for tissue iron uptake in iron-related disorders. Haematologica **98**, 1049–1057 CrossRef PubMed
16 Xu, G., Ahn, J., Chang, S., Eguchi, M., Ogier, A., Han, S., Park, Y., Shim, C., Jang, Y., Yang, B. et al. (2012) Lipocalin-2 induces cardiomyocyte apoptosis by increasing intracellular iron accumulation. J. Biol. Chem. **287**, 4808–4817 CrossRef PubMed
17 Ge, X.H., Wang, Q., Qian, Z.M., Zhu, L., Du, F., Yung, W.H., Yang, L. and Ke, Y. (2009) The iron regulatory hormone hepcidin reduces ferroportin 1 content and iron release in H9C2 cardiomyocytes. J. Nutr. Biochem. **20**, 860–865 CrossRef PubMed
18 Borlaug, B.A. and Paulus, W.J. (2011) Heart failure with preserved ejection fraction: pathophysiology, diagnosis, and treatment. Eur. Heart J. **32**, 670–679 CrossRef PubMed
19 Kasner, M., Aleksandrov, A.S., Westermann, D., Lassner, D., Gross, M., von Haehling, S., Anker, S.D., Schultheiss, H.P. and Tschope, C. (2013) Functional iron deficiency and diastolic function in heart failure with preserved ejection fraction. Int. J. Cardiol. **168**, 4652–4657 CrossRef PubMed
20 McMurray, J.J., Adamopoulos, S., Anker, S.D., Auricchio, A., Bohm, M., Dickstein, K., Falk, V., Filippatos, G., Fonseca, C., Gomez-Sanchez, M.A. et al. (2012) ESC Guidelines for the diagnosis and treatment of acute and chronic heart failure 2012: the Task Force for the Diagnosis and Treatment of Acute and Chronic Heart Failure 2012 of the European Society of Cardiology. Developed in collaboration with the Heart Failure Association (HFA) of the ESC. Eur. Heart J. **33**, 1787–1847 CrossRef PubMed
21 Schmitt, B., Golub, R.M. and Green, R. (2005) Screening primary care patients for hereditary hemochromatosis with transferrin saturation and serum ferritin level: systematic review for the American College of Physicians. Ann. Intern. Med. **143**, 522–536 CrossRef PubMed
22 Liu, P. and Olivieri, N. (1994) Iron overload cardiomyopathies: new insights into an old disease. Cardiovasc. Drugs Ther. **8**, 101–110 CrossRef PubMed
23 Chaffers, E. (1872) Death from suffocation while inhaling chloroform: impaction of false teeth in larynx. Br. Med. J. **1**, 419–420 CrossRef PubMed
24 Hare, J.M. (2008) The dilated, restrictive, and infiltrative cardiomyopathies. In Braunwald's Heart Disease (Libby, P., Bonow, R.O., Mann, D.L., Zipes, D.P. and Braunwald, E., eds), pp. 1739–1760, Elsevier, Boston, MA
25 Goel, S.S., Tuzcu, E.M., Agarwal, S., Aksoy, O., Krishnaswamy, A., Griffin, B.P., Svensson, L.G. and Kapadia, S.R. (2011) Comparison of ascending aortic size in patients with severe bicuspid aortic valve stenosis treated with versus without a statin drug. Am. J. Cardiol. **108**, 1458–1462 CrossRef PubMed
26 Chen, M.P., Cabantchik, Z.I., Chan, S., Chan, G.C. and Cheung, Y.F. (2014) Iron overload and apoptosis of HL-1 cardiomyocytes: effects of calcium channel blockade. PLoS One **9**, e112915 CrossRef PubMed
27 Lipinski, B. and Pretorius, E. (2013) Iron-induced fibrin in cardiovascular disease. Curr. Neurovasc. Res. **10**, 269–274 CrossRef PubMed
28 Sullivan, J.L. (2009) Iron in arterial plaque: modifiable risk factor for atherosclerosis. Biochim. Biophys. Acta **1790**, 718–723 CrossRef PubMed
29 Lee, H.T., Chiu, L.L., Lee, T.S., Tsai, H.L. and Chau, L.Y. (2003) Dietary iron restriction increases plaque stability in apolipoprotein-e-deficient mice. J. Biomed. Sci. **10**, 510–517 CrossRef PubMed
30 Lee, T.S., Shiao, M.S., Pan, C.C. and Chau, L.Y. (1999) Iron-deficient diet reduces atherosclerotic lesions in apoE-deficient mice. Circulation **99**, 1222–1229 CrossRef PubMed
31 Minqin, R., Rajendran, R., Pan, N., Tan, B.K., Ong, W.Y., Watt, F. and Halliwell, B. (2005) The iron chelator desferrioxamine inhibits atherosclerotic lesion development and decreases lesion iron concentrations in the cholesterol-fed rabbit. Free Radic. Biol. Med. **38**, 1206–1211 CrossRef PubMed
32 Ponraj, D., Makjanic, J., Thong, P.S., Tan, B.K. and Watt, F. (1999) The onset of atherosclerotic lesion formation in hypercholesterolemic rabbits is delayed by iron depletion. FEBS Lett. **459**, 218–222 CrossRef PubMed
33 Sung, K.C., Kang, S.M., Cho, E.J., Park, J.B., Wild, S.H. and Byrne, C.D. (2012) Ferritin is independently associated with the presence of coronary artery calcium in 12,033 men. Arterioscler. Thromb. Vasc. Biol. **32**, 2525–2530 CrossRef PubMed

34 Lee, K.R., Sweeney, G., Kim, W.Y. and Kim, K.K. (2010) Serum ferritin is linked with aortic stiffness in apparently healthy Korean women. Crit. Pathway Cardiol. **9**, 160–163 CrossRef

35 Depalma, R.G., Hayes, V.W., Chow, B.K., Shamayeva, G., May, P.E. and Zacharski, L.R. (2010) Ferritin levels, inflammatory biomarkers, and mortality in peripheral arterial disease: a substudy of the Iron (Fe) and Atherosclerosis Study (FeAST) Trial. J. Vasc. Surg. **51**, 1498–14503 CrossRef PubMed

36 Duffy, S.J., Biegelsen, E.S., Holbrook, M., Russell, J.D., Gokce, N., Keaney, Jr, J.F. and Vita, J.A. (2001) Iron chelation improves endothelial function in patients with coronary artery disease. Circulation **103**, 2799–2804 CrossRef PubMed

37 Iribarren, C., Sempos, C.T., Eckfeldt, J.H. and Folsom, A.R. (1998) Lack of association between ferritin level and measures of LDL oxidation: the ARIC study. Atherosclerosis Risk in Communities. Atherosclerosis **139**, 189–195 CrossRef PubMed

38 Vergnaud, A.C., Bertrais, S., Zureik, M., Galan, P., Blacher, J., Hercberg, S. and Czernichow, S. (2007) Dietary iron intake and serum ferritin in relation to 7.5 years structure and function of large arteries in the SUVIMAX cohort. Diabetes Metab. **33**, 366–371 CrossRef PubMed

39 Milman, N. (2011) Anemia – still a major health problem in many parts of the world!. Ann. Hematol. **90**, 369–377 CrossRef PubMed

40 Cohen-Solal, A., Leclercq, C., Deray, G., Lasocki, S., Zambrowski, J.J., Mebazaa, A., de Groote, P., Damy, T. and Galinier, M. (2014) Iron deficiency: an emerging therapeutic target in heart failure. Heart **100**, 1414–1420 CrossRef PubMed

41 Nestorowicz, A. (2012) Word about a good medical journal. Anaesthesiol. Intensive Ther. **44**, 115–116 PubMed

42 Suzuki, H., Toba, K., Kato, K., Ozawa, T., Tomosugi, N., Higuchi, M., Kusuyama, T., Iso, Y., Kobayashi, N., Yokoyama, S. et al. (2009) Serum hepcidin-20 is elevated during the acute phase of myocardial infarction. Tohoku J. Exp. Med. **218**, 93–98 CrossRef PubMed

43 Jankowska, E.A., Rozentryt, P., Witkowska, A., Nowak, J., Hartmann, O., Ponikowska, B., Borodulin-Nadzieja, L., Banasiak, W., Polonski, L., Filippatos, G. et al. (2010) Iron deficiency: an ominous sign in patients with systolic chronic heart failure. Eur. Heart J. **31**, 1872–1880 CrossRef PubMed

44 Okonko, D.O., Mandal, A.K., Missouris, C.G. and Poole-Wilson, P.A. (2011) Disordered iron homeostasis in chronic heart failure: prevalence, predictors, and relation to anemia, exercise capacity, and survival. J. Am. Coll. Cardiol. **58**, 1241–1251 CrossRef PubMed

45 Klip, I.T., Comin-Colet, J., Voors, A.A., Ponikowski, P., Enjuanes, C., Banasiak, W., Lok, D.J., Rosentryt, P., Torrens, A., Polonski, L. et al. (2013) Iron deficiency in chronic heart failure: an international pooled analysis. Am. Heart J. **165**, 575–582 CrossRef PubMed

46 Anker, S.D., Comin-Colet, J., Filippatos, G., Willenheimer, R., Dickstein, K., Drexler, H., Luscher, T.F., Bart, B., Banasiak, W., Niegowska, J. et al. (2009) Ferric carboxymaltose in patients with heart failure and iron deficiency. N. Engl. J. Med. **361**, 2436–2448 CrossRef PubMed

47 Mathiasen, A.B., Jorgensen, E., Qayyum, A.A., Haack-Sorensen, M., Ekblond, A. and Kastrup, J. (2012) Rationale and design of the first randomized, double-blind, placebo-controlled trial of intramyocardial injection of autologous bone-marrow derived Mesenchymal Stromal Cells in chronic ischemic Heart Failure (MSC-HF Trial). Am. Heart J. **164**, 285–291 CrossRef PubMed

48 Okonko, D.O., Grzeslo, A., Witkowski, T., Mandal, A.K., Slater, R.M., Roughton, M., Foldes, G., Thum, T., Majda, J., Banasiak, W. et al. (2008) Effect of intravenous iron sucrose on exercise tolerance in anemic and nonanemic patients with symptomatic chronic heart failure and iron deficiency FERRIC-HF: a randomized, controlled, observer-blinded trial. J. Am. Coll. Cardiol. **51**, 103–112 CrossRef PubMed

49 Beck-da-Silva, L., Piardi, D., Soder, S., Rohde, L.E., Pereira-Barretto, A.C., Albuquerque, D. de, Bocchi, E., Vilas-Boas, F., Moura, L.Z., Montera, M.W. et al. (2013) IRON-HF study: a randomized trial to assess the effects of iron in heart failure patients with anemia. Int. J. Cardiol. **168**, 3439–3442 CrossRef PubMed

50 Groenveld, H.F., Januzzi, J.L., Damman, K., van Wijngaarden, J., Hillege, H.L., van Veldhuisen, D.J. and van der Meer, P. (2008) Anemia and mortality in heart failure patients a systematic review and meta-analysis. J. Am. Coll. Cardiol. **52**, 818–827 CrossRef PubMed

51 Anand, I., McMurray, J.J., Whitmore, J., Warren, M., Pham, A., McCamish, M.A. and Burton, P.B. (2004) Anemia and its relationship to clinical outcome in heart failure. Circulation **110**, 149–154 CrossRef PubMed

52 Ezekowitz, J.A., McAlister, F.A. and Armstrong, P.W. (2003) Anemia is common in heart failure and is associated with poor outcomes: insights from a cohort of 12 065 patients with new-onset heart failure. Circulation **107**, 223–225 CrossRef PubMed

53 Go, A.S., Yang, J., Ackerson, L.M., Lepper, K., Robbins, S., Massie, B.M. and Shlipak, M.G. (2006) Hemoglobin level, chronic kidney disease, and the risks of death and hospitalization in adults with chronic heart failure: the Anemia in Chronic Heart Failure: Outcomes and Resource Utilization (ANCHOR) Study. Circulation **113**, 2713–2723 CrossRef PubMed

54 He, S.W. and Wang, L.X. (2009) The impact of anemia on the prognosis of chronic heart failure: a meta-analysis and systemic review. Congest. Heart Fail. **15**, 123–130 CrossRef PubMed

55 Kosiborod, M., Curtis, J.P., Wang, Y., Smith, G.L., Masoudi, F.A., Foody, J.M., Havranek, E.P. and Krumholz, H.M. (2005) Anemia and outcomes in patients with heart failure: a study from the National Heart Care Project. Arch. Intern. Med. **165**, 2237–2244 CrossRef PubMed

56 Mak, G., Murphy, N.F. and McDonald, K. (2008) Anemia in heart failure: to treat or not to treat? Curr. Treat. Options Cardiovasc. Med. **10**, 455–464 CrossRef PubMed

57 Silverberg, D.S., Wexler, D., Iaina, A. and Schwartz, D. (2009) The correction of anemia in patients with the combination of chronic kidney disease and congestive heart failure may prevent progression of both conditions. Clin. Exp. Nephrol. **13**, 101–106 CrossRef PubMed

58 Young, J.B., Abraham, W.T., Albert, N.M., Gattis Stough, W., Gheorghiade, M., Greenberg, B.H., O'Connor, C.M., She, L., Sun, J.L. et al. (2008) Relation of low hemoglobin and anemia to morbidity and mortality in patients hospitalized with heart failure (insight from the OPTIMIZE-HF registry). Am. J. Cardiol. **101**, 223–230 CrossRef PubMed

59 Beavers, C.J., Alburikan, K.A., Rodgers, J.E., Dunn, S.P. and Reed, B.N. (2014) Distinguishing anemia and iron deficiency of heart failure: signal for severity of disease or unmet therapeutic need? Pharmacotherapy **34**, 719–732 CrossRef PubMed

60 Ghali, J.K., Anand, I.S., Abraham, W.T., Fonarow, G.C., Greenberg, B., Krum, H., Massie, B.M., Wasserman, S.M., Trotman, M.L., Sun, Y. et al. (2008) Randomized double-blind trial of darbepoetin alfa in patients with symptomatic heart failure and anemia. Circulation **117**, 526–535 CrossRef PubMed

61 Pfeffer, M.A., Burdmann, E.A., Chen, C.Y., Cooper, M.E., de Zeeuw, D., Eckardt, K.U., Ivanovich, P., Kewalramani, R., Levey, A.S., Lewis, E.F. et al. (2009) Baseline characteristics in the Trial to Reduce Cardiovascular Events With Aranesp Therapy (TREAT). Am. J. Kidney Dis. **54**, 59–69 CrossRef PubMed

62 Berns, J.S. (2010) Are there implications from the Trial to Reduce Cardiovascular Events with Aranesp Therapy study for anemia management in dialysis patients? Curr. Opin. Nephrol. Hypertens. **19**, 567–572 CrossRef PubMed

63 McMurray, J.J., Uno, H., Jarolim, P., Desai, A.S., Zeeuw, D., de, Eckardt, K.U., Ivanovich, P., Levey, A.S., Lewis, E.F., McGill, J.B. et al. (2011) Predictors of fatal and nonfatal cardiovascular events in patients with type 2 diabetes mellitus, chronic kidney disease, and anemia: an analysis of the Trial to Reduce cardiovascular Events with Aranesp (darbepoetin-alfa) Therapy (TREAT). Am. Heart J. **162**, 748–755 CrossRef PubMed

64 Skali, H., Lin, J., Pfeffer, M.A., Chen, C.Y., Cooper, M.E., McMurray, J.J., Nissenson, A.R., Remuzzi, G., Rossert, J., Parfrey, P.S. et al. (2013) Hemoglobin stability in patients with anemia, CKD, and type 2 diabetes: an analysis of the TREAT (Trial to Reduce Cardiovascular Events With Aranesp Therapy) placebo arm. Am. J. Kidney Dis. **61**, 238–246 CrossRef PubMed

65 Thamer, M., Zhang, Y., Kshirsagar, O., Cotter, D.J. and Kaufman, J.S. (2014) Erythropoiesis-stimulating agent use among non-dialysis-dependent CKD patients before and after the trial to Reduce Cardiovascular Events With Aranesp Therapy (TREAT) using a large US health plan database. Am. J. Kidney Dis. **64**, 706–713 CrossRef PubMed

66 , Charytan, D.M., Lewis, E.F., Desai, A.S., Weinrauch, L.A., Ivanovich, P., Toto, R.D., Claggett, B., Liu, J., Hartley, L.H., Finn, P. et al. (2015) Cause of death in patients with diabetic CKD enrolled in the Trial to Reduce Cardiovascular Events With Aranesp Therapy (TREAT). Am. J. Kidney Dis. CrossRef PubMed

67 McMurray, J.J., Anand, I.S., Diaz, R., Maggioni, A.P., O'Connor, C., Pfeffer, M.A., Polu, K.R., Solomon, S.D., Sun, Y., Swedberg, K. et al. (2009) Design of the Reduction of Events with Darbepoetin alfa in Heart Failure (RED-HF): a phase III, anaemia correction, morbidity–mortality trial. Eur. J. Heart Fail. **11**, 795–801 CrossRef PubMed

68 McMurray, J.J., Anand, I.S., Diaz, R., Maggioni, A.P., O'Connor, C., Pfeffer, M.A., Solomonm, S.D., Tendera, M., van Veldhuisen, D.J., Albizem, M. et al. (2013) Baseline characteristics of patients in the Reduction of Events with Darbepoetin alfa in Heart Failure trial (RED-HF). Eur. J. Heart Fail. **15**, 334–341 CrossRef PubMed

69 El Tahan, M.R. (2012) Can entropy predict neurologic complications after cardiac surgery? Saudi J. Anaesth. **6**, 426–428 CrossRef PubMed

70 Toyokuni, S. (2002) Iron and carcinogenesis: from Fenton reaction to target genes. Redox Rep. **7**, 189–197 CrossRef PubMed

71 Dixon, S.J., Lemberg, K.M., Lamprecht, M.R., Skouta, R., Zaitsev, E.M., Gleason, C.E., Patel, D.N., Bauer, A.J., Cantley, A.M., Yang, W.S. et al. (2012) Ferroptosis: an iron-dependent form of nonapoptotic cell death. Cell **149**, 1060–1072 CrossRef PubMed

72 Menasche, P., Pasquier, C., Bellucci, S., Lorente, P., Jaillon, P. and Piwnica, A. (1988) Deferoxamine reduces neutrophil-mediated free radical production during cardiopulmonary bypass in man. J. Thorac. Cardiovasc. Surg. **96**, 582–589 PubMed

73 Ramu, E., Korach, A., Houminer, E., Schneider, A., Elami, A. and Schwalb, H. (2006) Dexrazoxane prevents myocardial ischemia/reperfusion-induced oxidative stress in the rat heart. Cardiovasc. Drugs Ther. **20**, 343–348 CrossRef PubMed

74 Dendorfer, A., Heidbreder, M., Hellwig-Burgel, T., Johren, O., Qadri, F. and Dominiak, P. (2005) Deferoxamine induces prolonged cardiac preconditioning via accumulation of oxygen radicals. Free Radic. Biol Med. **38**, 117–124 CrossRef PubMed

75 Kontoghiorghes, G.J. (2009) Prospects for introducing deferiprone as potent pharmaceutical antioxidant. Front. Biosci. (Elite Ed.) **1**, 161–178 PubMed

76 Gille, G. and Reichmann, H. (2011) Iron-dependent functions of mitochondria – relation to neurodegeneration. J. Neural Transm. **118**, 349–359 CrossRef PubMed

77 Levi, S. and Rovida, E. (2009) The role of iron in mitochondrial function. Biochim. Biophys. Acta **1790**, 629–636 CrossRef PubMed

78 Zuris, J.A., Harir, Y., Conlan, A.R., Shvartsman, M., Michaeli, D., Tamir, S., Paddock, M.L., Onuchic, J.N., Mittler, R., Cabantchik, Z.I. et al. (2011) Facile transfer of [2Fe-2S] clusters from the diabetes drug target mitoNEET to an apo-acceptor protein. Proc. Natl. Acad. Sci. U.S.A. **108**, 13047–13052 CrossRef PubMed

79 Paddock, M.L., Wiley, S.E., Axelrod, H.L., Cohen, A.E., Roy, M., Abresch, E.C., Capraro, D., Murphy, A.N., Nechushtai, R., Dixon, J.E. et al. (2007) MitoNEET is a uniquely folded 2Fe 2S outer mitochondrial membrane protein stabilized by pioglitazone. Proc. Natl. Acad. Sci. U.S.A. **104**, 14342–14347 CrossRef PubMed

80 Baxter, E.L., Jennings, P.A. and Onuchic, J.N. (2012) Strand swapping regulates the iron-sulfur cluster in the diabetes drug target mitoNEET. Proc. Natl. Acad. Sci. U.S.A. **109**, 1955–1960 CrossRef PubMed

81 Wiley, S.E., Murphy, A.N., Ross, S.A., van der Geer, P. and Dixon, J.E. (2007) MitoNEET is an iron-containing outer mitochondrial membrane protein that regulates oxidative capacity. Proc. Natl. Acad. Sci. U.S.A. **104**, 5318–5323 CrossRef PubMed

82 Wiley, S.E., Paddock, M.L., Abresch, E.C., Gross, L., van der Geer, P., Nechushtai, R., Murphy, A.N., Jennings, P.A. and Dixon, J.E. (2007) The outer mitochondrial membrane protein mitoNEET contains a novel redox-active 2Fe-2S cluster. J. Biol. Chem. **282**, 23745–23739 CrossRef PubMed

83 Hausmann, A., Samans, B., Lill, R. and Muhlenhoff, U. (2008) Cellular and mitochondrial remodeling upon defects in iron-sulfur protein biogenesis. J. Biol. Chem. **283**, 8318–8330 CrossRef PubMed

84 Hentze, M.W., Muckenthaler, M.U. and Andrews, N.C. (2004) Balancing acts: molecular control of mammalian iron metabolism. Cell **117**, 285–297 CrossRef PubMed

85 Colca, J.R., McDonald, W.G., Waldon, D.J., Leone, J.W., Lull, J.M., Bannow, C.A., Lund, E.T. and Mathews, W.R. (2004) Identification of a novel mitochondrial protein ('mitoNEET') cross-linked specifically by a thiazolidinedione photoprobe. Am. J. Physiol. Endocrinol. Metab. **286**, E252–E260 CrossRef PubMed

86 Kusminski, C.M., Holland, W.L., Sun, K., Park, J., Spurgin, S.B., Lin, Y., Askew, G.R., Simcox, J.A., McClain, D.A., Li, C. et al. (2012) MitoNEET-driven alterations in adipocyte mitochondrial activity reveal a crucial adaptive process that preserves insulin sensitivity in obesity. Nat Med. **18**, 1539–1549 CrossRef PubMed

87 Cook, J.D., Kondapalli, K.C., Rawat, S., Childs, W.C., Murugesan, Y., Dancis, A. and Stemmler, T.L. (2010) Molecular details of the yeast frataxin-Isu1 interaction during mitochondrial Fe-S cluster assembly. Biochemistry **49**, 8756–8765 CrossRef PubMed

88 Bayeva, M., Gheorghiade, M. and Ardehali, H. (2013) Mitochondria as a therapeutic target in heart failure. J. Am. Coll. Cardiol. **61**, 599–610 CrossRef PubMed

89 Brown, D.A., Sabbah, H.N. and Shaikh, S.R. (2013) Mitochondrial inner membrane lipids and proteins as targets for decreasing cardiac ischemia/reperfusion injury. Pharmacol. Ther. **140**, 258–266 CrossRef PubMed

90 Yoshida, H. (2007) ER stress and diseases. FEBS J. **274**, 630–658 CrossRef PubMed

91 Toth, A., Jeffers, J.R., Nickson, P., Min, J.Y., Morgan, J.P., Zambetti, G.P. and Erhardt, P. (2006) Targeted deletion of Puma attenuates cardiomyocyte death and improves cardiac function during ischemia-reperfusion. Am. J. Physiol. Heart Circ. Physiol. **291**, H52–H60 CrossRef PubMed

92 Nadanaka, S., Okada, T., Yoshida, H. and Mori, K. (2007) Role of disulfide bridges formed in the luminal domain of ATF6 in sensing endoplasmic reticulum stress. Mol. Cell. Biol. **27**, 1027–1943 CrossRef PubMed

93 Okada, K., Minamino, T., Tsukamoto, Y., Liao, Y., Tsukamoto, O., Takashima, S., Hirata, A., Fujita, M., Nagamachi, Y., Nakatani, T. et al. (2004) Prolonged endoplasmic reticulum stress in hypertrophic and failing heart after aortic constriction: possible contribution of endoplasmic reticulum stress to cardiac myocyte apoptosis. Circulation **110**, 705–712 CrossRef PubMed

94 Vitadello, M., Penzo, D., Petronilli, V., Michieli, G., Gomirato, S., Menabo, R., Di Lisa, F. and Gorza, L. (2003) Overexpression of the stress protein Grp94 reduces cardiomyocyte necrosis due to calcium overload and simulated ischemia. FASEB J. **17**, 923–925 PubMed

95 Lou, L.X., Geng, B., Chen, Y., Yu, F., Zhao, J. and Tang, C.S. (2009) Endoplasmic reticulum stress involved in heart and liver injury in iron-loaded rats. Clin. Exp. Pharmacol. Physiol. **36**, 612–618 CrossRef PubMed

96 Liu, Y., Lee, S.Y., Neely, E., Nandar, W., Moyo, M., Simmons, Z. and Connor, J.R. (2011) Mutant HFE H63D protein is associated with prolonged endoplasmic reticulum stress and increased neuronal vulnerability. J. Biol. Chem. **286**, 13161–13170 CrossRef PubMed

97 Tan, T.C., Crawford, D.H., Jaskowski, L.A., Subramaniam, V.N., Clouston, A.D., Crane, D.I., Bridle, K.R., Anderson, G.J. and Fletcher, L.M. (2013) Excess iron modulates endoplasmic reticulum stress-associated pathways in a mouse model of alcohol and high-fat diet-induced liver injury. Lab. Invest. **93**, 1295–1312 CrossRef PubMed

98 Vecchi, C., Montosi, G., Zhang, K., Lamberti, I., Duncan, S.A., Kaufman, R.J. and Pietrangelo, A. (2009) ER stress controls iron metabolism through induction of hepcidin. Science **325**, 877–880 CrossRef PubMed

99 Oliveira, S.J., Pinto, J.P., Picarote, G., Costa, V.M., Carvalho, F., Rangel, M., de Sousa, M. and de Almeida, S.F. (2009) ER stress-inducible factor CHOP affects the expression of hepcidin by modulating C/EBPalpha activity. PLoS One **4**, e6618 CrossRef PubMed

100 Mizushima, N. (2007) Autophagy: process and function. Genes Dev. **21**, 2861–2873 CrossRef PubMed

101 Levine, B., Mizushima, N. and Virgin, H.W. (2011) Autophagy in immunity and inflammation. Nature **469**, 323–335 CrossRef PubMed

102 Jimenez, R.E., Kubli, D.A. and Gustafsson, A.B. (2014) Autophagy and mitophagy in the myocardium: therapeutic potential and concerns. Br. J. Pharmacol. **171**, 1907–1916 CrossRef PubMed

103 Li, G.H., Shi, Y., Chen, Y., Sun, M., Couto, G., Fukuoka, M., Wang, X., Dawood, F., Chen, M., Li, M. et al. (2009) The role of autophagy in iron-overload cardiomyopathy: a model of diastolic heart failure due to oxidative stress. J. Card. Fail. **15** (Suppl.), S42–S43 CrossRef

104 Mancias, J.D., Wang, X., Gygi, S.P., Harper, J.W. and Kimmelman, A.C. (2014) Quantitative proteomics identifies NCOA4 as the cargo receptor mediating ferritinophagy. Nature **509**, 105–109 CrossRef PubMed

105 Terman, A. and Brunk, U.T. (2005) Autophagy in cardiac myocyte homeostasis, aging, and pathology. Cardiovasc. Res. **68**, 355–365 CrossRef PubMed

106 Flower, D.R. (1996) The lipocalin protein family: structure and function. Biochem. J. **318**, 1–14 PubMed

107 Flower, D.R., North, A.C. and Sansom, C.E. (2000) The lipocalin protein family: structural and sequence overview. Biochim. Biophys. Acta **1482**, 9–24 CrossRef PubMed

108 Flo, T.H., Smith, K.D., Sato, S., Rodriguez, D.J., Holmes, M.A., Strong, R.K., Akira, S. and Aderem, A. (2004) Lipocalin 2 mediates an innate immune response to bacterial infection by sequestrating iron. Nature **432**, 917–921 CrossRef PubMed

109 Goetz, D.H., Holmes, M.A., Borregaard, N., Bluhm, M.E., Raymond, K.N. and Strong, R.K. (2002) The neutrophil lipocalin NGAL is a bacteriostatic agent that interferes with siderophore-mediated iron acquisition. Mol. Cell **10**, 1033–1043 CrossRef PubMed

110 Xu, M.J., Feng, D., Wu, H., Wang, H., Chan, Y., Kolls, J., Borregaard, N., Porse, B., Berger, T., Mak, T.W. et al. (2015) Liver is the major source of elevated serum lipocalin-2 levels after bacterial infection or partial hepatectomy: a critical role for IL-6/STAT3. Hepatology **61**, 692–702 CrossRef PubMed

111 Zhang, Y., Foncea, R., Deis, J.A., Guo, H., Bernlohr, D.A. and Chen, X. (2014) Lipocalin 2 expression and secretion is highly regulated by metabolic stress, cytokines, and nutrients in adipocytes. PLoS One **9**, e96997 CrossRef PubMed

112 Shah, B.N. and Greaves, K. (2010) The cardiorenal syndrome: a review. Int. J. Nephrol. **2011**, 920195 PubMed

113 Damman, K., Ng Kam Chuen, M.J., MacFadyen, R.J., Lip, G.Y., Gaze, D., Collinson, P.O., Hillege, H.L., van Oeveren, W., Voors, A.A. and van Veldhuisen, D.J. (2011) Volume status and diuretic therapy in systolic heart failure and the detection of early abnormalities in renal and tubular function. J. Am. Coll. Cardiol. **57**, 2233–2241 CrossRef PubMed

114 Mishra, J., Mori, K., Ma, Q., Kelly, C., Yang, J., Mitsnefes, M., Barasch, J. and Devarajan, P. (2004) Amelioration of ischemic acute renal injury by neutrophil gelatinase-associated lipocalin. J. Am. Soc. Nephrol. **15**, 3073–3082 CrossRef PubMed

115 Ahmad, T., Fiuzat, M., Felker, G.M. and O'Connor, C. (2012) Novel biomarkers in chronic heart failure. Nat. Rev. Cardiol. **9**, 347–359 CrossRef PubMed

116 Maisel, A.S., Mueller, C., Fitzgerald, R., Brikhan, R., Hiestand, B.C., Iqbal, N., Clopton, P. and van Veldhuisen, D.J. (2011) Prognostic utility of plasma neutrophil gelatinase-associated lipocalin in patients with acute heart failure: the NGAL EvaLuation Along with B-type NaTriuretic Peptide in acutely decompensated heart failure (GALLANT) trial. Eur. J. Heart Fail. **13**, 846–851 CrossRef PubMed

117 Alvelos, M., Lourenco, P., Dias, C., Amorim, M., Rema, J., Leite, A.B., Guimaraes, J.T., Almeida, P. and Bettencourt, P. (2013) Prognostic value of neutrophil gelatinase-associated lipocalin in acute heart failure. Int. J. Cardiol. **165**, 51–55 CrossRef PubMed

118 Naude, P.J., Mommersteeg, P.M., Zijlstra, W.P., Gouweleeuw, L., Kupper, N., Eisel, U.L., Kop, W.J. and Schoemaker, R.G. (2014) Neutrophil gelatinase-associated lipocalin and depression in patients with chronic heart failure. Brain Behav. Immun. **38**, 59–65 CrossRef PubMed

119 Nymo, S.H., Ueland, T., Askevold, E.T., Flo, T.H., Kjekshus, J., Hulthe, J., Wikstrand, J., McMurray, J., Van Veldhuisen, D.J., Gullestad, L. et al. (2012) The association between neutrophil gelatinase-associated lipocalin and clinical outcome in chronic heart failure: results from CORONA. J. Intern. Med. **271**, 436–443 CrossRef PubMed

120 Yndestad, A., Landro, L., Ueland, T., Dahl, C.P., Flo, T.H., Vinge, L.E., Espevik, T., Froland, S.S., Husberg, C., Christensen, G. et al. (2009) Increased systemic and myocardial expression of neutrophil gelatinase-associated lipocalin in clinical and experimental heart failure. Eur. Heart J. **30**, 1229–1236 CrossRef PubMed

121 Pronschinske, K.B., Qiu, S., Wu, C., Kato, T.S., Khawaja, T., Takayama, H., Naka, Y., Templeton, D.L., George, I., Farr, M.A. et al. (2014) Neutrophil gelatinase-associated lipocalin and cystatin C for the prediction of clinical events in patients with advanced heart failure and after ventricular assist device placement. J. Heart Lung Transplant. **33**, 1215–1222 CrossRef PubMed

122 Bolignano, D., Basile, G., Parisi, P., Coppolino, G., Nicocia, G. and Buemi, M. (2009) Increased plasma neutrophil gelatinase-associated lipocalin levels predict mortality in elderly patients with chronic heart failure. Rejuvenation Res. **12**, 7–14 CrossRef PubMed

123 van Deursen, V.M., Damman, K., Voors, A.A., van der Wal, M.H., Jaarsma, T., van Veldhuisen, D.J. and Hillege, H.L. (2014) Prognostic value of plasma neutrophil gelatinase-associated lipocalin for mortality in patients with heart failure. Circ. Heart Fail. **7**, 35–42 CrossRef PubMed

124 Daniels, L.B., Barrett-Connor, E., Clopton, P., Laughlin, J.H., Ix, G.A. and Maisel, A.S. (2012) Plasma neutrophil gelatinase-associated lipocalin is independently associated with cardiovascular disease and mortality in community-dwelling older adults: the Rancho Bernardo Study. J. Am. Coll. Cardiol. **59**, 1101–1109 CrossRef PubMed

125 Devireddy, L.R., Gazin, C., Zhu, X. and Green, M.R. (2005) A cell-surface receptor for lipocalin 24p3 selectively mediates apoptosis and iron uptake. Cell **123**, 1293–1305 CrossRef PubMed

126 Skaar, E.P. (2010) The battle for iron between bacterial pathogens and their vertebrate hosts. PLoS Pathog. **6**, e1000949 CrossRef PubMed

127 Srinivasan, G., Aitken, J.D., Zhang, B., Carvalho, F.A., Chassaing, B., Shashidharamurthy, R., Borregaard, N., Jones, D.P., Gewirtz, A.T. and Vijay-Kumar, M. (2012) Lipocalin 2 deficiency dysregulates iron homeostasis and exacerbates endotoxin-induced sepsis. J. Immunol. **189**, 1911–1919 CrossRef PubMed

128 Yang, J., Goetz, D., Li, J.Y., Wang, W., Mori, K., Setlik, D., Du, T., Erdjument-Bromage, H., Tempst, P., Strong, R. et al. (2002) An iron delivery pathway mediated by a lipocalin. Mol. Cell **10**, 1045–1056 CrossRef PubMed

129 Bolignano, D., Coppolino, G., Romeo, A., De Paola, L., Buemi, A., Lacquaniti, A., Nicocia, G., Lombardi, L. and Buemi, M. (2009) Neutrophil gelatinase-associated lipocalin (NGAL) reflects iron status in haemodialysis patients. Nephrol. Dial. Transplant. **24**, 3398–2403 CrossRef PubMed

130 Ismail, M.I., Fouad, M., Ramadan, A., Fathy, H., Zidan, A. and Mostafa, E. (2015) Neutrophil gelatinase associated lipocalin (NGAL) as a biomarker of iron deficiency in hemodialysis patients. Austin J. Nephrol. Hypertens. **2**, 1036

131 Malyszko, J., Malyszko, J.S., Kozminski, P., Koc-Zorawska, E., Mysliwiec, M. and Macdougall, I. (2010) Possible relationship between neutrophil gelatinase-associated lipocalin, hepcidin, and inflammation in haemodialysed patients. Nephron Clin. Pract. **115**, c268–c275 CrossRef PubMed

132 Malbora, B., Avci, Z., Gulsan, M., Orhan, B. and Ozbek, N. (2013) Low serum lipocalin levels in patients with iron deficiency anemia. J. Pediatr. Hematol. Oncol. **35**, 218–220 CrossRef PubMed

133 Emans, M.E., Braam, B., Diepenbroek, A., van der Putten, K., Cramer, M.J., Wielders, J.P., Swinkels, D.W., Doevendans, P.A. and Gaillard, C.A. (2012) Neutrophil gelatinase-associated lipocalin (NGAL) in chronic cardiorenal failure is correlated with endogenous erythropoietin levels and decreases in response to low-dose erythropoietin treatment. Kidney Blood Press. Res. **36**, 344–354 CrossRef PubMed

134 Ding, L., Hanawa, H., Ota, Y., Hasegawa, G., Hao, K., Asami, F., Watanabe, R., Yoshida, T., Toba, K., Yoshida, K. et al. (2010) Lipocalin-2/neutrophil gelatinase-B associated lipocalin is strongly induced in hearts of rats with autoimmune myocarditis and in human myocarditis. Circ. J. **74**, 523–530 CrossRef PubMed

135 Lindberg, S., Jensen, J.S., Mogelvang, R., Pedersen, S.H., Galatius, S., Flyvbjerg, A. and Magnusson, N.E. (2014) Plasma neutrophil gelatinase-associated lipocalinin in the general population: association with inflammation and prognosis. Arterioscler. Thromb. Vasc. Biol. **34**, 2135–2142 CrossRef PubMed

136 Zhao, P., Elks, C.M. and Stephens, J.M. (2014) The induction of lipocalin-2 protein expression in vivo and in vitro. J. Biol. Chem. **289**, 5960–5969 CrossRef PubMed

137 Bu, D.X., Hemdahl, A.L., Gabrielsen, A., Fuxe, J., Zhu, C., Eriksson, P. and Yan, Z.Q. (2006) Induction of neutrophil gelatinase-associated lipocalin in vascular injury via activation of nuclear factor-kappaB. Am. J. Pathol. **169**, 2245–2253 CrossRef PubMed

138 Cheng, L., Xing, H., Mao, X., Li, L., Li, X. and Li, Q. (2015) Lipocalin-2 promotes m1 macrophages polarization in a mouse cardiac ischaemia-reperfusion injury model. Scand. J. Immunol. **81**, 31–38 CrossRef PubMed

139 Jha, M.K., Jeon, S., Jin, M., Ock, J., Kim, J.H., Lee, W.H. and Suk, K. (2014) The pivotal role played by lipocalin-2 in chronic inflammatory pain. Exp. Neurol. **254**, 41–53 CrossRef PubMed

140 Song, E., Fan, P., Huang, B., Deng, H.B., Cheung, B.M., Feletou, M., Vilaine, J.P., Villeneuve, N., Xu, A., Vanhoutte, P.M. et al. (2014) Deamidated lipocalin-2 induces endothelial dysfunction and hypertension in dietary obese mice. J. Am. Heart Assoc. **3**, e000837 CrossRef PubMed

141 Paulus, W.J. and Tschope, C. (2013) A novel paradigm for heart failure with preserved ejection fraction: comorbidities drive myocardial dysfunction and remodeling through coronary microvascular endothelial inflammation. J. Am. Coll. Cardiol. **62**, 263–271 CrossRef PubMed

Received 26 January 2015/8 June 2015; accepted 14 July 2015

Version of Record published 28 August 2015, doi: 10.1042/CS20150075

Appendix C

Regulation of Iron and Its Significance in Obesity and Complications

Chan YK, Sung HK and Sweeney G.

Korean Journal of Obesity (2014) 23(4): 1-9

Review

Korean J Obes 2014 December;23(4):222-230
http://dx.doi.org/10.7570/kjo.2014.23.4.222
pISSN 1226-4407 eISSN 2234-7631

KJO
The Korean Journal of Obesity

Regulation of Iron and Its Significance in Obesity and Complications

Yee Kwan Chan, Hye Kyoung Sung, Gary Sweeney*
Department of Biology, York University, Toronto, Canada

Iron is an essential micronutrient with important roles in many critical physiological processes, especially as a structural component of hemoglobin responsible for oxygen transport. Iron homeostasis is tightly regulated, yet perturbations resulting in iron deficiency as well as iron overload are linked with obesity and associated metabolic abnormalities, such as insulin resistance and type 2 diabetes. The endocrine system plays an active role in regulating iron homeostasis and here we have highlighted the importance of lipocalin-2 (Lcn2) and hepcidin. Circulating and adipose tissue expression of the proinflammatory Lcn2 are elevated in obesity and this may be an important, and underestimated, regulator of iron homeostasis. Hepcidin is also markedly elevated during obesity and by inducing the internalization of ferroportin, it leads to an accumulation of tissue iron stores but deficiency in circulating iron, a key feature of functional iron deficiency. Due to the critical importance of iron homeostasis in health and disease, there are currently several well established methods for clinical diagnosis of iron levels and various therapeutics have proven effective in restoring normal iron level in iron deficient or overload conditions. Further explorations in the endocrine regulation of iron homeostasis are warranted to develop a better understanding of the pathophysiological roles of iron in obesity and related metabolic diseases.

Key words: Iron, Iron deficiency, Iron overload, Lipocalin-2

Introduction

Iron is an essential trace element required for various critical processes in the human body. The majority of the iron is used for erythropoiesis in the bone marrow, and any remaining iron can be used for other functions or stored as ferritin in various organs. Disturbed iron homeostasis is associated with various pathological conditions, including obesity. In this review, we will summarize the current literature pertaining to iron overload or deficiency in obesity and discuss endocrine regulatory mechanisms, with a focus on lipocalin-2 (Lcn2) (Fig. 1). We also highlight current diagnostics and therapeutics related to altered iron status in clinical settings.

1. Iron transport

An average adult human contains approximately 3-4 g of iron[1], of which the single largest component is the hemoglobin in erythrocytes. Approximately 90% of iron in the body is recycled by old and damaged erythrocyte phagocytosis with release of iron for new red blood cells synthesis. A small proportion of iron is lost in urine, feces and menstrual blood (1-2 mg/day), and this must be replaced via dietary iron intake. The recommended dietary allowance (RDA) for iron varies with gender and age, with an average of 8 mg/day required by an adult male and 18 mg/day and 8 mg/day for premenopausal and postmenopausal women, respectively.[1] Dietary iron, while coming in many forms, is usually classified as either heme or non-heme iron. Animals are the biggest source of heme iron whereas non-heme iron encompasses many forms of iron from both animal and plant sources. The latter can be better absorbed along with ascorbic acid or vitamin C.[2] The duodenum is the primary site for iron absorption, where divalent metal ion transporter 1 (DMT-1), expressed

Corresponding author Gary Sweeney
Department of Biology, 110 Farquharson Life Science Building, York University, Toronto, M3J 1P3, Ontario, Canada
Tel +1-416-736-2100 **Fax** +1-416-736-5698 **E-mail** gsweeney@yorku.ca

Funding institutions: GS is funded by Canadian Institutes of Health Research (CIHR), Heart & Stroke Foundation of Canada and Canadian Diabetes Association.

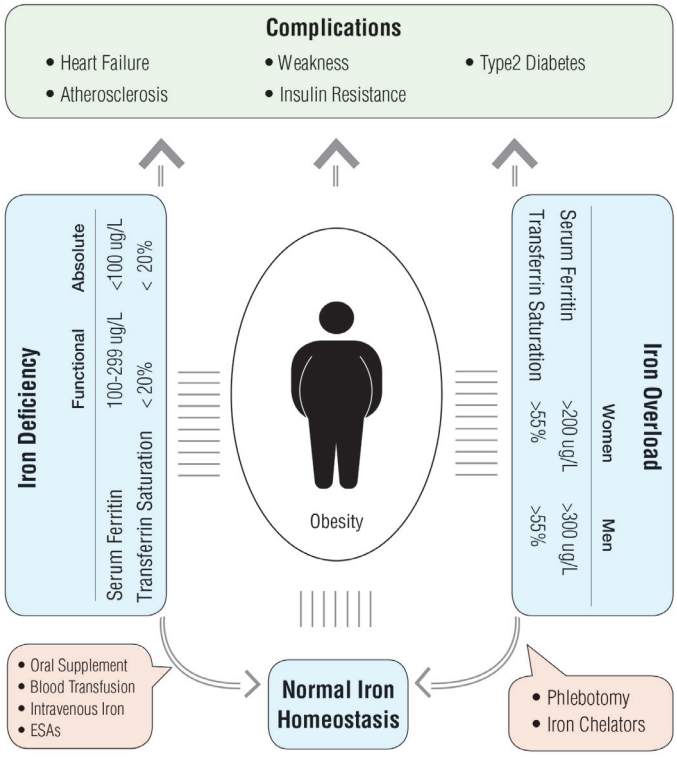

Fig. 1. An imbalance of iron homeostasis has been observed in obesity. Iron overload (blue box, right) and iron deficiency (ID; blue box, left) have both been reported and the latter can be either absolute or functional. Both iron overload and ID have been associated with development of complications which occur in obesity (green box, top). Various therapeutic strategies commonly used to correct iron overload or ID and restore normal iron homeostasis are shown (orange boxes).

on the apical side of duodenal enterocytes, is responsible for the absorption of non-heme iron or inorganic iron. Ferric iron (Fe^{3+}) is reduced by the adjacent duodenal cytochrome B (DcytB) to ferrous iron (Fe^{2+}), which is the substrate of DMT-1 and is internalized in enterocytes. On the other hand, heme iron is likely absorbed through the transporter heme carrier protein 1 (HCP-1). Ferrous iron in the cytoplasm is either stored as ferritin, or transported to the basolateral membrane and released to the bloodstream via ferroportin (FPN). Hephaestin facilitates the conversion of ferrous iron to its ferric form, which is then bound to transferrin (Tf) and transported in circulation. Tf contains two ferric iron binding sites and is approximately 30% saturated with iron under physiological conditions. The high unsaturated apo-Tf confers a high buffering capacity to accommodate any increase in plasma iron and prevent build-up of non-transferrin bound iron (NTBI), which would otherwise promote oxidative injury.[3] At extracellular pH (~7.5), iron-transferrin has a high affinity for transferrin receptor 1 (TfR1). The Tf-TfR1 complex is endocytsed, and ferric iron released from transferrin at the endosomal pH (~6.2). Ferric iron is reduced by Steap family reductases and transported across the endosomal membrane by DMT-1 to reach the ferrous pool in the cytoplasm. Ferrous iron can now be stored as ferritin, incorporated into heme for erythropoiesis, or exported by FPN to circulation to repeat the iron-transferrin cycle described. With FPN as the only known exporter of inorganic iron in mammalian cells, hepcidin, a liver-derived hormone that promotes FPN internalization and lysosomal degradation, plays a key role in iron trafficking and regulation.[4]

2. Iron & obesity

1) Evidence of an association between obesity and iron levels

The first evidence of an inverse correlation between plasma iron and adiposity was reported more than 40 years ago.[5] Subsequent work has validated this phenomenon, for example a study involving 321 children and adolescents showed that low iron levels were present in 38.8% of obese children, in 12.1% of overweight and only 4.4% of those of normal weight children.[6] Another study that involved almost 10,000 children also reported a higher prevalence of iron deficiency in children with increased BMI, concluding that children who were overweight are twice as likely to be iron-deficient than those who were not.[7] Furthermore, obesity or excessive weight gain during pregnancy was found as an independent risk factor for iron deficien-

cy in the newborn.[8]

2) Iron deficiency in obesity

Iron deficiency (ID) is the most common nutritional deficiency worldwide and affects more than one-third of the population.[9] In particular, ID is observed at a high prevalence (between 30% to 50%) in patients with heart failure, and this is often associated with poorer clinical outcomes and greater risk of death, independent of anemia.[10] There are two distinct types of ID – absolute and functional ID.[11,12] Absolute ID reflects depleted iron stores even when iron homeostasis mechanisms and erythropoiesis often remain intact. Absolute ID development in humans can result from inadequate dietary iron intake, impaired gastrointestinal absorption/transport, drug interactions and gastrointestinal blood loss.[11] In contrast, in functional ID iron homeostasis is malfunctional and this renders cells and tissues with an inadequate iron supply despite normal whole body iron storage. For example, iron may be trapped inside cells, especially of the reticuloendothelial system, and thus be unavailable for cellular metabolism.

Serum ferritin, a biomarker that is used to reflect iron store, was found enhanced in obese subjects.[13] Yet, ferritin is an acute phase protein that is elevated during inflammation that does not correspond to iron store, and it was suggested that correction to inflammation should be made if this parameter was to be used to reflect iron deficiency.[14] Soluble transferrin receptor (sTfR), on the other hand, should be preferably used as it is not an acute-phase reactant and is not dynamically affected by the confounding pathologies in obesity.[15] When iron delivery to target tissues does not meet the metabolic demand, expression of TfR increase, leading to a consequent increase in circulating sTfR. Thus, sTfR reflects tissue iron demand and has been found to be significantly higher in obese subjects.[16] Thus, taking transferrin saturation into account will give a better indication to the type of ID present. In that sense, absolute ID is defined when serum ferritin is lower than 100 μg/L, while functional ID is defined as a serum ferritin of 100-299 μg/L accompanied by a transferrin saturation less than 20%.[12]

3) Iron deficiency anemia

ID usually appears before the onset of anemia, yet anemia and ID can exist independently.[17] As mentioned above, ID is related to iron insufficiency in regard to body demand, and can be defined with iron related parameters like ferritin and transferrin saturation; anemia, on the other hand, is related to oxygen carrying capacity and is defined as a blood hemoglobin level less than 13 mg/dL and 12 mg/dL in men and women, respectively.[18] While ID anemia may be the most common form of anemia, there are different forms of anemia, such as those related to vitamin deficiency, chronic disease, bone marrow disease, or those that are inherited such as hemolytic and sickle cell anemia. In general, the main causes of anemia include deficiency in iron, deficient production of erythropoietin (EPO) and resistance to endogenous EPO.[19] EPO resistance may be initiated via the upregulation of proinflammatory cytokines that exert inhibitory effects on erythroid progenitor cells; act negatively on EPO receptors that result in their defective activation and decrease in numbers and elevate hepcidin, thus disrupting iron homeostasis, as well as neocytolysis.[19]

Several theories have been proposed to explain why ID is associated with obesity. Firstly, there may be increased consumption of energy dense but nutrient poor foods with inadequate iron level.[6] It was found that the diet of severely obese patients was unbalanced, with high calorie intake paralleled by insufficient micronutrient intake – only 66.2% of the severely obese patients had an adequate intake of iron.[20] Secondly, obesity inherently translates to increased body mass and blood volume, thus a higher iron requirement. The higher iron need was not met, despite greater food consumption, indicating obese subjects have higher susceptibility to ID.[21] Another widely accepted mechanism is increased hepcidin production as a result of chronic inflammation in obesity.[22] Indeed the iron abnormality in obesity is often characterized by hypoferremia, higher iron body store, lower iron bioavailability and high to normal concentration of serum ferritin that mimics anemia of chronic inflammation.[23] In the obese state, cytokines such as IL-6[24] and leptin[25] increase and elicit upregulated hepatic gene expression and production of hepcidin, such that iron release from macrophages, hepatocytes and enterocytes were blocked, resulting in a functional ID. Mice fed with high fat diet for 24 weeks were shown to display increased hepcidin expression in adipose tissue.[26] While both liver and adipose hepcidin mRNA expressions were increased during obese states, the hepatic expression was ~700 times greater than that of the adipose tissue and is thought to be primarily responsible for the elevated circulating hepcidin levels.[27] Moreover, mRNA and protein expression of the membrane bound hemojuvelin, which can stimulate hepcidin ex-

 http://dx.doi.org/10.7570/kjo.2014.23.4.222

pression through the bone morphogenetic protein (BMP) pathway, was found to be high in adipose tissue from obese individuals.[28] Indeed, this was positively correlated with hepcidin expression levels.[28] Obesity has long been viewed as a major contributor to the development of insulin insensitivity and type 2 diabetes and although many mechanisms have been proposed[29], the role of iron may be underestimated. Iron was found to interfere with insulin action in the liver, such that ferritin levels correlate positively with blood glucose and fasting serum insulin[30] and negatively with insulin sensitivity.[31] Reciprocally, insulin was also shown to cause rapid stimulation of iron uptake by fat cells and hepatocytes.[32]

3. Iron overload

Iron overload is diagnosed when plasma transferrin saturation is greater than 55% and serum ferritin more than 200 μg/L or 300 μg/L for women and men, respectively.[33] Accumulation of iron in tissues may occur via increased iron absorption from the gastrointestinal enterocytes (hemochromatosis); excess exogenous iron intake such as by dietary supplements, or blood transfusions (hemosiderosis). While obesity is primarily associated with ID, it was recently proposed that obesity was a potential consequence of increased availability of iron supplement and fortification in the last several decades.[34] Iron overload, without direct evidence as a cause or result of obesity, is associated to many obesity-related metabolic conditions. For example, iron overload was shown to cause insulin deficiency in ob/ob mice of type 2 diabetes, and upon feeding an iron restricted diet or iron chelator, insulin sensitivity and beta cell functions was significantly increased.[35] An early initiation of removal of iron through phlebotomy in patients with hereditary hemochromatosis, an autosomal disorder involving mutation of specific genes involved in iron metabolism that leads to increased gastrointestinal absorption, was shown effective in ameliorating defective insulin secretion.[36]

1) Iron and bacterial infection

Besides being essential in maintaining daily metabolic functions, iron is also a key regulator of host-pathogen interactions at times of infection. Iron is one of the most important macronutrients required for microbial growth. Iron acts as the global regulator for many cellular and metabolic processes in microbes, including DNA synthesis, electron transport system, heme formation and oxygen transport.[37] The competition for iron between microbes and the human host is a crucial factor for the success of bacterial invasion. Bacteria can acquire iron from the host by either synthesizing high iron affinity binding compounds such as siderophores, or directly capturing iron from iron binding proteins such as transferrin or ferritin. In defending the battle over iron, factors such as lipocalin-2 (Lcn2; also called siderocalin, 24p3, neutrophil gelatinase associated lipocalin [NGAL]) are secreted by the host to sequestrate siderophores and thus limit bacterial growth.[38] Lcn2 is internalized into bacterial infected cells, a process mediated by its putative receptor 24p3R or megalin, where it then intercepts bacterial siderophores and trafficks them to extracellular space. Lcn2 helps to supply iron for non-bacteria infected cells of the host, the Lcn2:mammalian siderophore-iron complex binds to 24p3R, and is endocytosed to the intracellular space then releases iron.[39] Interestingly, an increase in circulating Lcn2 is not only seen in acute immune response, but is also regarded as a biomarker for cardiac disease and other features of metabolic syndrome.[40,41]

4. Endocrine regulation of iron levels in obesity

Iron homeostasis, especially in obesity, is controlled to a large extent by the endocrine system. Here we will highlight and discuss the importance of Lcn2 and hepcidin in iron regulation.

1) Lipocalin-2 (Lcn2)

Lipocalins are a diverse family that generally bind small and hydrophobic ligands, but can also bind soluble macromolecules and specific cell surface receptors.[42] Lcn2 is a 25 kDa secretory protein predominantly expressed in adipose tissue and plays an important role in innate immunity and inflammation, including defense against bacterial invasion by sequestering iron, although more widespread actions in metabolic diseases are now emerging.[41]

Of particular importance here, Lcn2 is crucial in maintaining iron homeostasis during infectious conditions such as endotoxemia or myocarditis. Dysbiosis of the gut microbiota has been found in various disease states, including obesity.[43] In such cases, gut microbial diversity tends to decrease with a relative increase of Gram negative bacteria. Gut epithelial integrity is also disrupted, increasing the chances of bacteria and bacterial products leakage to the circulation, and thus endotoxemia. It has been postulated that increased circulating LPS concentrations are sufficient to dysregulate the inflammatory status and initiate the onset of obesity and insulin resistance.[44] Indeed, LPS can induce increases in systemic Lcn2 by 150

fold within 24 hours.[45] Lcn2 deficient mice were shown to have delayed LPS-induced hypoferremia in induced sepsis, indicating a role for Lcn2 in limiting circulating iron levels by enhancing intracellular iron content during inflammatory states. Mice deficient in Lcn2 also had exacerbated endotoxin-induced sepsis, increased immune cell apoptosis and increased mortality.[45] MyD88-dependent signaling is required for the induction of Lcn2 and iron sequestration to maintain the hypoferric response during endotoxemia.[46] Thus, Lcn2 can act as an influencer for the development of endotoxemia and derived metabolic disease by its effect on LPS.

As indicated above, elevated Lcn2 levels are associated with obesity and insulin resistance. In studies of diabetic patients, it was found that serum Lcn2 concentration significantly associated with fasting triglycerides and LPS binding protein, acutely increased after fat administration and associated with fasting insulin and homeostasis model assessment of insulin resistance (HOMA-IR).[47] Similarly, serum level or adipose tissue Lcn2 content was found to be elevated in overweight pregnant women and associate with several insulin resistance markers including HOMA-IR, fasting plasma insulin and glucose.[48] Gene and protein expression of Lcn2 increased in visceral adipose tissue of obese compared to lean subjects.[49] Inversely, weight loss caused a significant reduction of circulating Lcn2 in overweight/obese women with polycystic ovary syndrome.[50]

One established mechanism via which Lcn2 leads to obesity induced insulin resistance may be its capacity to stimulate the expression of 12-lipoxygenase, an enzyme that metabolizes arachidonic acid, and TNFα in adipose tissue.[51] We propose that Lcn2 can also alter iron homeostasis in adipose tissue, particularly in macrophages, and that this may contribute to iron overload in adipose tissue. As indicated above, obese adipose tissues are marked by infiltration and accumulation of macrophages with a M1, or proinflammatory, phenotype. When comparing to the nonpolarized M0 macrophages, M1 macrophages had repressed ferroportin and induced H-ferritin gene expression that promoted iron sequestration in the reticuloendothelial system.[52] On the contrary, M2 macrophages that possess an anti-inflammatory profile had upregulated ferroportin as well as down-regulated H-ferritin and heme oxygenase that enhanced efficient FPN- mediated iron export.[52] Moreover, it was shown that in obesity, the percentage of adipose tissue macrophages rich in iron was decreased due to impaired capacity to handle iron, and this coincided with adipocyte iron overload in obese mice.[53] Lcn2 can have different effects on macrophages depending on the physiological condition. For example, Lcn2 can amplify M1 polarization in brain microglial cells[54], but can also deactivate macrophages and exacerbate bacterial pneumonia.[55] To our knowledge, the role of Lcn2 on the iron homeostasis of adipose tissue macrophages in obese states has not yet been studied. We hypothesize that the elevated Lcn2 in chronic inflammatory states hampers iron metabolism in macrophages in adipose tissue, and potentially other tissues, and this is associated with iron-induced insulin resistance.

2) Hepcidin

Hepcidin is a systemic iron-regulatory hormone that is primarily produced in liver, but also in other tissues including heart, adipocytes and macrophages.[56-58] It functions to maintain a stable iron concentration through the degradation of the cellular iron exporter – FPN. FPN is found in duodenal enterocyptes and thus increased hepcidin will limit dietary iron absorption. Hepcidin is abundantly expressed in reticuloenothelial macrophages and is particularly important in regulating iron concentration in liver, spleen and bone barrow. While body iron content and hematopoiesis are the principal endogenous regulators of hepcidin synthesis[59], inflammation also acts as a pathological regulator.[60] LPS, IL-6 and leptin are also direct stimulants of hepcidin secretion.[25] Moreover, as mentioned earlier, hepcidin can be upregulated by BMP. Increased expression of hemojuvelin, a co-receptor of BMP, associated with increased hepcidin expression in adipocytes in obesity.[28] As FNP on adipocytes[61] is internalized and degraded by hepcidin, the efflux of iron is reduced, leading to iron overload in adipocytes.[62] Iron overloaded adipocytes can induce dysfunctional endocrine regulation, with one important example being a reduction in adiponectin expression.[61]

5. Iron diagnostics and therapeutics

1) Current diagnostics for iron status – Serology

There are several blood tests that reflect the amount of iron in the body; ferritin level, iron level, total iron binding capacity (TIBC) and transferrin saturation.[63] Blood ferritin levels usually are low in patients with ID anemia and are high in patients with hemochromatosis and other conditions that cause an increase in body iron levels. Since ferritin can also be elevated in certain infections like viral hepatitis and other inflammatory conditions, an elevated ferritin level alone is not sufficient to accurately diagnose chronic iron overload.[64]

 http://dx.doi.org/10.7570/kjo.2014.23.4.222

Serum iron, TIBC and transferrin saturation are often performed together instead. TIBC is a measure of the total amount of iron that can be carried in serum by transferrin, a protein that carries iron in serum from one anatomical location to another. Transferrin saturation value is calculated by dividing serum iron by TIBC, thus reflecting the percentage of the transferrin that is being used to transport iron. In healthy individuals the transferrin saturation is between 20 and 50 percent.[65]

2) Therapeutics – iron deficiency

ID anemia describes a scenario where iron stores have been depleted and the body is unable to maintain levels of haemoglobin in the blood. Too little iron can interfere with these vital functions and lead to morbidity and death. ID patients exhibit symptoms of weakness, fatigue, glossitis, stomatitis, Plummer Vinson syndrome, pica and restless legs syndrome while extreme cases lead to morbidity and mortality.[66]

Oral iron supplementation is commonly recommended as a front line treatment of ID. There are two types of iron supplements; ferrous iron is the most efficiently absorbed form and the majority of iron supplement pills contain ferrous iron in the forms of ferrous sulfate, ferrous fumarate, and ferrous gluconate.[67] Absorption requires an acidic gastric environment and is therefore limited in patients receiving acid-suppression therapy. Hence, although oral iron supplements are commonly used, poor absorption and gastrointestinal intolerance in some individuals limit their use.[68] Blood transfusion is useful in more severely ill patients with chronic ID and Hb less than 7 g/dL.[69,70] However, blood transfusion is not recommended as long-term therapy due to risks such as infection and iron overload.[70] Intravenous iron therapy has been adopted in management of patients with ID and although animal studies showed a resultant increase in indicators of oxidative stress, this has not been observed in clinical trials.[69] Another option for treatment of anemia is erythropoietin stimulating agents (ESAs).[71] As an example, meta-analysis of 11 randomized clinical trials, 9 placebo-controlled and 5 double-blinded, of a total of 794 patients with anemia and heart failure treated with ESAs concluded that there were improvements in functional capacity and a reduction in clinical events. However, another study did not demonstrate an impact of ESAs on heart failure in anemia.[72] Furthermore, ESAs can cause serious side effects, including blood clots, and they are now approved only for treating severely ill anemic patients, such as those with cancer or chronic kidney failure.

3) Therapeutics – iron overload

A common treatment for iron overload in otherwise healthy individuals consists of iron removal via regularly scheduled phlebotomies.[12] When first diagnosed, phlebotomies may be performed once a week until iron levels can be brought to within normal range. Once iron and other markers are within the normal range, phlebotomies may be scheduled every other month or every three months depending upon the patient's rate of iron loading. Some patients treated with phlebotomy are given erythropoietin to maintain erythropoiesis.[72] However, phlebotomies are not recommended for many patients, such as those with Hb level < 10 g/dL, who may develop symptoms of anemia after phlebotomy. Instead, a second approach for removing iron, iron chelating therapy, is recommended for these individuals. Nevertheless, the decision to initiate chelation therapy depends upon several factors, including the patient's overall health, hematologic values and tissue iron level determination. There are three main iron chelating drugs in clinical use at present and these are mainly used for the treatment of transfusional iron overload, namely deferoxamine (DF), deferiprone (L1) and deferasirox (DFRA).[73] DF binds with iron in the bloodstream and enhances its elimination via urine and faeces. Typical treatment for chronic iron overload requires subcutaneous injection over a period of 8-12 hours daily. The other two, L1 and DFRA are newer iron chelating drugs that are licensed for use in patients receiving regular blood transfusions to treat thalasaemia.[74] Beneficial aspects of iron chelation therapy have been shown, such as prevention of complications and early death in iron loading anemia in patients with thalassaemia.[74]

Acknowledgement

We would like to thank Dr. Cheol-Young Park from the Division of Endocrinology and Metabolism, Department of Internal Medicine, Kangbuk Samsung Hospital, Sungkyunkwan University School of Medicine, Republic of Korea for his comments on the manuscript.

References

1. Leong WI, Lönnerdal B. Iron nutrition. In: Anderson GJ, McLaren GD, Editors. Iron physiology and pathophysiology in humans.

New York: Springer; 2012. p. 81-99.
2. Sharp PA. Intestinal iron absorption: regulation by dietary & systemic factors. Int J Vitam Nutr Res 2010;80:231-42.
3. Brissot P, Ropert M, Le Lan C, Loréal O. Non-transferrin bound iron: a key role in iron overload and iron toxicity. Biochim Biophys Acta 2012;1820:403-10.
4. Ganz T. Systemic iron homeostasis. Physiol Rev 2013;93:1721-41.
5. Wenzel BJ, Stults HB, Mayer J. Hypoferraemia in obese adolescents. Lancet 1962;2:327-8.
6. Pinhas-Hamiel O, Newfield RS, Koren I, Agmon A, Lilos P, Phillip M. Greater prevalence of iron deficiency in overweight and obese children and adolescents. Int J Obes Relat Metab Disord 2003;27:416-8.
7. Nead KG, Halterman JS, Kaczorowski JM, Auinger P, Weitzman M. Overweight children and adolescents: a risk group for iron deficiency. Pediatrics 2004;114:104-8.
8. Phillips AK, Roy SC, Lundberg R, Guilbert TW, Auger AP, Blohowiak SE, et al. Neonatal iron status is impaired by maternal obesity and excessive weight gain during pregnancy. J Perinatol 2014;34:513-8.
9. Milman N. Anemia--still a major health problem in many parts of the world! Ann Hematol 2011;90:369-77.
10. Cohen-Solal A, Leclercq C, Deray G, Lasocki S, Zambrowski JJ, Mebazaa A, et al. Iron deficiency: an emerging therapeutic target in heart failure. Heart 2014;100:1414-20.
11. Nestorowicz A. Word about a good medical journal. Anaesthesiol Intensive Ther 2012;44:115-6.
12. McMurray JJ, Adamopoulos S, Anker SD, Auricchio A, Böhm M, Dickstein K, et al. ESC Guidelines for the diagnosis and treatment of acute and chronic heart failure 2012: The Task Force for the Diagnosis and Treatment of Acute and Chronic Heart Failure 2012 of the European Society of Cardiology. Developed in collaboration with the Heart Failure Association (HFA) of the ESC. Eur Heart J 2012;33:1787-847.
13. Gillum RF. Association of serum ferritin and indices of body fat distribution and obesity in Mexican American men--the Third National Health and Nutrition Examination Survey. Int J Obes Relat Metab Disord 2001;25:639-45.
14. Gartner A, Berger J, Bour A, El Ati J, Traissac P, Landais E, et al. Assessment of iron deficiency in the context of the obesity epidemic: importance of correcting serum ferritin concentrations for inflammation. Am J Clin Nutr 2013;98:821-6.
15. Wish JB. Assessing iron status: beyond serum ferritin and transferrin saturation. Clin J Am Soc Nephrol 2006;1 Suppl 1:4-8.
16. Freixenet N, Remacha A, Berlanga E, Caixàs A, Giménez-Palop O, Blanco-Vaca F, et al. Serum soluble transferrin receptor concentrations are increased in central obesity. Results from a screening programme for hereditary hemochromatosis in men with hyperferritinemia. Clin Chim Acta 2009;400:111-6.
17. Beavers CJ, Alburikan KA, Rodgers JE, Dunn SP, Reed BN. Distinguishing anemia and iron deficiency of heart failure: signal for severity of disease or unmet therapeutic need? Pharmacotherapy 2014;34:719-32.
18. World Health Organization. Haemoglobin concentrations for the diagnosis of anaemia and assessment of severity. Vitamin and Mineral Nutrition Information System. Geneva: World Health Organization; 2011. p. 1-6.
19. van der Putten K, Braam B, Jie KE, Gaillard CA. Mechanisms of Disease: erythropoietin resistance in patients with both heart and kidney failure. Nat Clin Pract Nephrol 2008;4:47-57.
20. Correia Horvath JD, Dias de Castro ML, Kops N, Kruger Malinoski N, Friedman R. Obesity coexists with malnutrition? Adequacy of food consumption by severely obese patients to dietary reference intake recommendations. Nutr Hosp 2014;29:292-9.
21. Bertinato J, Aroche C, Plouffe LJ, Lee M, Murtaza Z, Kenney L, et al. Diet-induced obese rats have higher iron requirements and are more vulnerable to iron deficiency. Eur J Nutr 2014;53:885-95.
22. Xu H, Barnes GT, Yang Q, Tan G, Yang D, Chou CJ, et al. Chronic inflammation in fat plays a crucial role in the development of obesity-related insulin resistance. J Clin Invest 2003;112:1821-30.
23. Ausk KJ, Ioannou GN. Is obesity associated with anemia of chronic disease? A population-based study. Obesity (Silver Spring) 2008;16:2356-61.
24. Ganz T. Molecular pathogenesis of anemia of chronic disease. Pediatr Blood Cancer 2006;46:554-7.
25. Chung B, Matak P, McKie AT, Sharp P. Leptin increases the expression of the iron regulatory hormone hepcidin in HuH7 human hepatoma cells. J Nutr 2007;137:2366-70.
26. Gotardo ÉM, dos Santos AN, Miyashiro RA, Gambero S, Rocha T, Ribeiro ML, et al. Mice that are fed a high-fat diet display increased hepcidin expression in adipose tissue. J Nutr Sci Vitaminol (Tokyo) 2013;59:454-61.

 http://dx.doi.org/10.7570/kjo.2014.23.4.222

27. Tussing-Humphreys LM, Nemeth E, Fantuzzi G, Freels S, Guzman G, Holterman AX, et al. Elevated systemic hepcidin and iron depletion in obese premenopausal females. Obesity (Silver Spring) 2010;18:1449-56.
28. Luciani N, Brasse-Lagnel C, Poli M, Anty R, Lesueur C, Cormont M, et al. Hemojuvelin: a new link between obesity and iron homeostasis. Obesity (Silver Spring) 2011;19:1545-51.
29. Kahn SE, Hull RL, Utzschneider KM. Mechanisms linking obesity to insulin resistance and type 2 diabetes. Nature 2006;444:840-6.
30. Tuomainen TP, Nyyssönen K, Salonen R, Tervahauta A, Korpela H, Lakka T, et al. Body iron stores are associated with serum insulin and blood glucose concentrations. Population study in 1,013 eastern Finnish men. Diabetes Care 1997;20:426-8.
31. Dmochowski K, Finegood DT, Francombe W, Tyler B, Zinman B. Factors determining glucose tolerance in patients with thalassemia major. J Clin Endocrinol Metab 1993;77:478-83.
32. Davis RJ, Corvera S, Czech MP. Insulin stimulates cellular iron uptake and causes the redistribution of intracellular transferrin receptors to the plasma membrane. J Biol Chem 1986;261:8708-11.
33. Schmitt B, Golub RM, Green R. Screening primary care patients for hereditary hemochromatosis with transferrin saturation and serum ferritin level: systematic review for the American College of Physicians. Ann Intern Med 2005;143:522-36.
34. Sangani RG, Ghio AJ. Iron, human growth, and the global epidemic of obesity. Nutrients 2013;5:4231-49.
35. Cooksey RC, Jones D, Gabrielsen S, Huang J, Simcox JA, Luo B, et al. Dietary iron restriction or iron chelation protects from diabetes and loss of beta-cell function in the obese (ob/ob lep-/-) mouse. Am J Physiol Endocrinol Metab 2010;298:E1236-43.
36. Creighton Mitchell T, McClain DA. Diabetes and hemochromatosis. Curr Diab Rep 2014;14:488.
37. Saha R, Saha N, Donofrio RS, Bestervelt LL. Microbial siderophores: a mini review. J Basic Microbiol 2013;53:303-17.
38. Flo TH, Smith KD, Sato S, Rodriguez DJ, Holmes MA, Strong RK, et al. Lipocalin 2 mediates an innate immune response to bacterial infection by sequestrating iron. Nature 2004;432:917-21.
39. Sia AK, Allred BE, Raymond KN. Siderocalins: siderophore binding proteins evolved for primary pathogen host defense. Curr Opin Chem Biol 2013;17:150-7.
40. Cruz DN, Gaiao S, Maisel A, Ronco C, Devarajan P. Neutrophil gelatinase-associated lipocalin as a biomarker of cardiovascular disease: a systematic review. Clin Chem Lab Med 2012;50:1533-45.
41. Sommer P, Sweeney G. Functional and mechanistic integration of infection and the metabolic syndrome. Korean Diabetes J 2010;34:71-6.
42. Flower DR. The lipocalin protein family: structure and function. Biochem J 1996;318:1-14.
43. Ley RE, Bäckhed F, Turnbaugh P, Lozupone CA, Knight RD, Gordon JI. Obesity alters gut microbial ecology. Proc Natl Acad Sci U S A 2005;102:11070-5.
44. Cani PD, Amar J, Iglesias MA, Poggi M, Knauf C, Bastelica D, et al. Metabolic endotoxemia initiates obesity and insulin resistance. Diabetes 2007;56:1761-72.
45. Srinivasan G, Aitken JD, Zhang B, Carvalho FA, Chassaing B, Shashidharamurthy R, et al. Lipocalin 2 deficiency dysregulates iron homeostasis and exacerbates endotoxin-induced sepsis. J Immunol 2012;189:1911-9.
46. Layoun A, Huang H, Calvé A, Santos MM. Toll-like receptor signal adaptor protein MyD88 is required for sustained endotoxin-induced acute hypoferremic response in mice. Am J Pathol 2012;180:2340-50.
47. Moreno-Navarrete JM, Manco M, Ibáñez J, García-Fuentes E, Ortega F, Gorostiaga E, et al. Metabolic endotoxemia and saturated fat contribute to circulating NGAL concentrations in subjects with insulin resistance. Int J Obes (Lond) 2010;34:240-9.
48. Lou Y, Wu C, Wu M, Xie C, Ren L. The changes of neutrophil gelatinase-associated lipocalin in plasma and its expression in adipose tissue in pregnant women with gestational diabetes. Diabetes Res Clin Pract 2014;104:136-42.
49. Catalan V, Gómez-Ambrosi J, Rodríguez A, Ramírez B, Silva C, Rotellar F, et al. Increased adipose tissue expression of lipocalin-2 in obesity is related to inflammation and matrix metalloproteinase-2 and metalloproteinase-9 activities in humans. J Mol Med (Berl) 2009;87:803-13.
50. Koiou E, Tziomalos K, Katsikis I, Kandaraki EA, Kalaitzakis E, Delkos D, et al. Weight loss significantly reduces serum lipocalin-2 levels in overweight and obese women with polycystic ovary syndrome. Gynecol Endocrinol 2012;28:20-4.
51. Law IK, Xu A, Lam KS, Berger T, Mak TW, Vanhoutte PM, et al. Lipocalin-2 deficiency attenuates insulin resistance associated with aging and obesity. Diabetes 2010;59:872-82.
52. Recalcati S, Locati M, Marini A, Santambrogio P, Zaninotto F, De

Pizzol M, et al. Differential regulation of iron homeostasis during human macrophage polarized activation. Eur J Immunol 2010;40:824-35.
53. Orr JS, Kennedy A, Anderson-Baucum EK, Webb CD, Fordahl SC, Erikson KM, et al. Obesity alters adipose tissue macrophage iron content and tissue iron distribution. Diabetes 2014;63:421-32.
54. Jang E, Lee S, Kim JH, Kim JH, Seo JW, Lee WH, et al. Secreted protein lipocalin-2 promotes microglial M1 polarization. FASEB J 2013;27:1176-90.
55. Warszawska JM, Gawish R, Sharif O, Sigel S, Doninger B, Lakovits K, et al. Lipocalin 2 deactivates macrophages and worsens pneumococcal pneumonia outcomes. J Clin Invest 2013;123:3363-72.
56. Merle U, Fein E, Gehrke SG, Stremmel W, Kulaksiz H. The iron regulatory peptide hepcidin is expressed in the heart and regulated by hypoxia and inflammation. Endocrinology 2007;148:2663-8.
57. Bekri S, Gual P, Anty R, Luciani N, Dahman M, Ramesh B, et al. Increased adipose tissue expression of hepcidin in severe obesity is independent from diabetes and NASH. Gastroenterology 2006;131:788-96.
58. Sow FB, Florence WC, Satoskar AR, Schlesinger LS, Zwilling BS, Lafuse WP. Expression and localization of hepcidin in macrophages: a role in host defense against tuberculosis. J Leukoc Biol 2007;82:934-45.
59. Ganz T. Hepcidin and its role in regulating systemic iron metabolism. Hematology Am Soc Hematol Educ Program 2006;2006:29-35.
60. Maury E, Noël L, Detry R, Brichard SM. In vitro hyperresponsiveness to tumor necrosis factor-alpha contributes to adipokine dysregulation in omental adipocytes of obese subjects. J Clin Endocrinol Metab 2009;94:1393-400.
61. Gabrielsen JS, Gao Y, Simcox JA, Huang J, Thorup D, Jones D, et al. Adipocyte iron regulates adiponectin and insulin sensitivity. J Clin Invest 2012;122:3529-40.
62. Nemeth E, Tuttle MS, Powelson J, Vaughn MB, Donovan A, Ward DM, et al. Hepcidin regulates cellular iron efflux by binding to ferroportin and inducing its internalization. Science 2004;306:2090-3.
63. Dale JC, Burritt MF, Zinsmeister AR. Diurnal variation of serum iron, iron-binding capacity, transferrin saturation, and ferritin levels. Am J Clin Pathol 2002;117:802-8.
64. Guyatt GH, Oxman AD, Ali M, Willan A, McIlroy W, Patterson C. Laboratory diagnosis of iron-deficiency anemia: an overview. J Gen Intern Med 1992;7:145-53.
65. Piperno A. Classification and diagnosis of iron overload. Haematologica 1998;83:447-55.
66. Jelani QU, Katz SD. Treatment of anemia in heart failure: potential risks and benefits of intravenous iron therapy in cardiovascular disease. Cardiol Rev 2010;18:240-50.
67. Santiago P. Ferrous versus ferric oral iron formulations for the treatment of iron deficiency: a clinical overview. ScientificWorldJournal 2012;2012:846824.
68. Zhu A, Kaneshiro M, Kaunitz JD. Evaluation and treatment of iron deficiency anemia: a gastroenterological perspective. Dig Dis Sci 2010;55:548-59.
69. Silverberg DS, Wexler D, Sheps D, Blum M, Keren G, Baruch R, et al. The effect of correction of mild anemia in severe, resistant congestive heart failure using subcutaneous erythropoietin and intravenous iron: a randomized controlled study. J Am Coll Cardiol 2001;37:1775-80.
70. Mancini DM, Katz SD, Lang CC, LaManca J, Hudaihed A, Androne AS. Effect of erythropoietin on exercise capacity in patients with moderate to severe chronic heart failure. Circulation 2003;107:294-9.
71. Palazzuoli A, Silverberg D, Iovine F, Capobianco S, Giannotti G, Calabrò A, et al. Erythropoietin improves anemia exercise tolerance and renal function and reduces B-type natriuretic peptide and hospitalization in patients with heart failure and anemia. Am Heart J 2006;152:1096. e9-15.
72. Yancy CW, Jessup M, Bozkurt B, Butler J, Casey DE Jr, Drazner MH, et al. 2013 ACCF/AHA guideline for the management of heart failure: a report of the American College of Cardiology Foundation/American Heart Association Task Force on Practice Guidelines. J Am Coll Cardiol 2013;62:e147-239.
73. Kontoghiorghe CN, Kolnagou A, Kontoghiorghes GJ. Potential clinical applications of chelating drugs in diseases targeting transferrin-bound iron and other metals. Expert Opin Investig Drugs 2013;22:591-618.
74. Olivieri NF, Brittenham GM, McLaren CE, Templeton DM, Cameron RG, McClelland RA, et al. Long-term safety and effectiveness of iron-chelation therapy with deferiprone for thalassemia major. N Engl J Med 1998;339:417-23.

 http://dx.doi.org/10.7570/kjo.2014.23.4.222

Appendix D

Lipocalin-2 induces NLRP3 inflammasome activation via HMGB1 induced TLR4 signaling in heart tissue of mice under pressure overload challenge

Song E, Jahng J WS, Chong, L, Sung HK, Han M, Luo C, Wu D, Boo S, Hinz B, Cooper M, Robertson A, Berger T, Mak T, George I, Schulze CP, Wang Y, Xu A and Sweeney G.

American Journal of translational research (2017) Jun 15; 9(6):2723-2735

Am J Transl Res 2017;9(6):2723-2735
www.ajtr.org /ISSN:1943-8141/AJTR0048252

Original Article

Lipocalin-2 induces NLRP3 inflammasome activation via HMGB1 induced TLR4 signaling in heart tissue of mice under pressure overload challenge

Erfei Song[1], James WS Jahng[1], Lisa P Chong[1], Hye K Sung[1], Meng Han[1], Cuiting Luo[2], Donghai Wu[3], Stellar Boo[4], Boris Hinz[4], Matthew A Cooper[5], Avril AB Robertson[5], Thorsten Berger[6], Tak W Mak[6], Isaac George[7], P Christian Schulze[8], Yu Wang[2], Aimin Xu[2], Gary Sweeney[1]

[1]Department of Biology, York University, Toronto, Canada; [2]Department of Pharmacology and Pharmacy, University of Hong Kong, Hong Kong; [3]Guangzhou Institute of Biomedicine & Health, China; [4]Laboratory of Tissue Repair and Regeneration, Matrix Dynamics Group, Faculty of Dentistry, University of Toronto, Toronto, Canada; [5]Institute for Molecular Bioscience, The University of Queensland, Australia; [6]The Campbell Family Institute for Breast Cancer Research and Ontario Cancer Institute, University Health Network, Toronto, Canada; [7]Division of Cardiology, Department of Medicine, Columbia University Medical Center, New York, USA; [8]Department of Internal Medicine I, Division of Cardiology, University Hospital Jena, Friedrich-Schiller-University Jena, Jena, Germany

Received January 6, 2017; Accepted May 5, 2017; Epub June 15, 2017; Published June 30, 2017

Abstract: Lipocalin-2 (also known as NGAL) levels are elevated in obesity and diabetes yet relatively little is known regarding effects on the heart. We induced pressure overload (PO) in mice and found that lipocalin-2 knockout (LKO) mice exhibited less PO-induced autophagy and NLRP3 inflammasome activation than Wt. PO-induced mitochondrial damage was reduced and autophagic flux greater in LKO mice, which correlated with less cardiac dysfunction. All of these observations were negated upon adenoviral-mediated restoration of normal lipocalin-2 levels in LKO. Studies in primary cardiac fibroblasts indicated that lipocalin-2 enhanced priming and activation of NLRP3-inflammasome, detected by increased IL-1β, IL-18 and Caspase-1 activation. This was attenuated in cells isolated from NLRP3-deficient mice or upon pharmacological inhibition of NLRP3. Furthermore, lipocalin-2 induced release of HMGB1 from cells and NLRP3-inflammasome activation was attenuated by TLR4 inhibition. We also found evidence of increased inflammasome activation and reduced autophagy in cardiac biopsy samples from heart failure patients. Overall, this study provides new mechanistic insight on the detrimental role of lipocalin-2 in the development of cardiac dysfunction.

Keywords: Lipocalin-2, pressure overload, NLRP3 inflammasome, HMGB1, toll-like receptor (TLR)-4

Introduction

Heart failure (HF) incidence is increased in patients with obesity and diabetes and inflammation is one underlying mechanism [1]. Lipocalin-2 (LCN2) is a proinflammatory adipokine which is elevated in obesity and diabetes [2] and clinical studies have also established strong positive correlations between circulating LCN2 and various types of HF [3]. Thus, LCN2 has been proposed as an important contributor to the pathophysiology of HF and potentially a useful biomarker for HF. Neutrophils are a major source of LCN2 which is also known as neutrophil gelatinase-associated lipocalin (NGAL) [4]. Mice lacking LCN2 were first shown to exhibit an increased susceptibility to bacterial infections due to lack of antibacterial innate immune response [5] and subsequently shown to be protected from obesity- and aging-associated insulin resistance, endothelial dysfunction and hypertension [6-9]. However, the precise mechanisms via which LCN2 can regulate the progression of HF remain to be resolved.

In contrast to the paucity of information on cardiac effects of LCN2, the pathophysiological role of LCN2/NGAL in kidney dysfunction is much better understood and measurement of LCN2/NGAL has recently become established as a common clinical diagnostic test for acute kidney damage [10]. Inflammation, including

Table 1. Genes detected in fibrosis PCR array

Col1a1	Mmp8
Col3a1	Mmp9
Col4a1	Mmp13
Timp1	Mmp14
Timp2	Gapdh
Timp3	Actb
Mmp1a	MGDC
Mmp2	PPC

NLRP3 (nucleotide-binding domain, leucine-rich-containing family, pyrin domain-containing-3) inflammasome activation, and autophagy have recently been established as important mechanisms regulating cardiac dysfunction [11, 12] although their regulation by LCN2 is unclear. We have recently shown that LCN2 attenuates cardiomyocyte autophagy [13].

We hypothesized that LKO mice would have less pressure overload-induced cardiac dysfunction than wild type (WT) and that reduced autophagy or elevated NLRP3 inflammasome activation may be potential mechanisms of action. To examine this, we induced cardiac pressure overload (PO) in WT and LCN2 knockout mice (LKO) ± restoration of normal circulating LCN2 levels using adenovirus (L2AV). We first examined functional outcomes using echocardiography, then analyzed mechanisms via which LCN2 contributed to cardiac dysfunction by focusing on fibrosis, autophagy and NLRP3 inflammasome activation in these animal models as well as in primary cells isolated from heart of WT and NLRP3-deficient mice.

Material and methods

Animals, induction of pressure overload and analysis of cardiac function

Male WT and LKO mice aged eight weeks with C57BL/6J background were studied using protocols approved by the Animal Care Committee at York University and the Committee on the Use of Live Animals for Teaching and Research of the University of Hong Kong and all methods were performed in accordance with these guidelines and regulations. Pressure overload was induced by transverse aortic banding as described previously [14]. Briefly, surgery was performed on the transverse aortae of mice under general anesthesia (ip; xylazine 0.15 mg/g; ketamine 0.03 mg/g) with a titanium microligation clip using banding calipers calibrated to a 27-g needle. Sham surgery was performed as outlined above without the placement of a ligation clip. The recombinant adenovirus for LCN2 (10^8 plaque-forming units) was injected via tail vein of mice one day prior to surgery to achieve normal circulating levels [7] and echocardiography was performed using the Vevo2100 system (Visual Sonics) [15]. Sera were collected every week from tail vein and hearts were harvested at the ends points (four weeks).

Cardiac biopsy from human subjects with or without heart failure (HF)

Patients with end-stage dilated cardiomyopathy (DCM) who met institutional criteria for LVAD device implantation as a bridge to transplant or as destination therapy at the New York Presbyterian-Columbia Campus were included in this study and processed as previously described [14, 16]. Cardiac biopsy tissue used in this study (n=5) were all male, aged 41.0±21.4 years and HF etiology ischemic or diabetic cardiomyopathy. All tissue obtained at LVAD implantation represented a decompensated heart failure state. Normal patients were subjects with no known cardiopulmonary disease whose organs were listed but were unable to be placed at the time of organ recovery for heart transplantation and who consented to tissue for research purposes by the New York Organ Donor Network were included in this study. This study met all institutional guidelines of the Institutional Review Board of Columbia University and New York State organ donation guidelines regarding the use of clinical data, ethical treatment of patients adhering to the Declaration of Helsinki principles, and procurement of tissue for research. All subjects were recruited at the New York Presbyterian Hospital-Columbia University campus between 2008-2014, and informed consent was waived for use of discarded, de-identified tissue.

Analysis of cardiac function using echocardiography

Echocardiography was performed using the Vevo2100 system (Visual Sonics, MS550D transducer) as previously described [15]. Cardiac systolic functions of ejection fraction, fractional shortening and strain rate calcula-

Table 2. Sequences of QPCR primers

Gene Name	Primer Sequences
Murine	Forward 5'CAGAACATCATCCCCTGCATC3'
Gapdh	Reverse 5'CTGCTTCACCACCTTCTTGA3'
Murine	Forward 5'GGTCACCCATGGCACCATAA3'
Nfκb1	Reverse 5'AGCTGCAGAGCCTTCTCAAG3'
Murine	Forward 5'GCCACCTTTTGACAGTGATGAG3'
Il1β	Reverse 5'AAGGTCCACGGGAAAGACAC3'
Murine	Forward 5'GACACGAGTCCTGGTGACTT3'
Nlrp3	Reverse 5'GTCCACACAGAAAGTTCTCTTAGC3'
Murine	Forward 5'AACGCCATGGCTGACAAGA3'
Casp1	Reverse 5'TGATCACATAGGTCCCGTGC3'
Murine	Forward 5'CTG CGC TTG CAG AGA TTA AA3'
Tgfβ1	Reverse 5'GAA AGC CCT GTA TTC CGT CT3'
Rat	Forward 5'ATGTGCCGGACCTTGGAAG3'
Gapdh	Reverse 5'CCTCGGGTTAGCTGAGAGATCA3'
Rat	Forward 5'CACTGCTCAGGTCCACTGTC3'
Nfkb1	Reverse 5'CTGTCACTATCCCGGAGTTCA3'
Rat	Forward 5'CACCTCTCAAGCAGAGCACAG3'
Il1β	Reverse 5'GGGTTCCATGGTGAAGTCAAC3'
Rat	Forward 5'CCAGGGCTCTGTTCATTG3'
Nlrp3	Reverse 5'CCTTGGCTTTCACTTCG3'
Rat	Forward 5'AGGAGGGAATATGTGGG3'
Casp1	Reverse 5'AACCTTGGGCTTGTCTT3'

tion were based on M-mode images of the parasternal short-axis view at papillary level. All parameters were averaged over at least 3 cardiac cycles for analysis.

Histological analysis of cardiac structure

Animals were sacrificed and hearts were isolated and perfused with ice-cold cardioplegic solution (30 mM KCl in PBS) and stored in 10% neutral-buffered formalin 24 hours for further processing. Paraffin sections (5 μm) were prepared for trichrome staining and immunostaining using antibodies against HMGB1, desmin, vimentin or α-SMA as described previously [17].

Immunofluorescent analysis in cultured cells

Rat neonatal fibroblast cells were cultured in 12-well plates, after treatment with or without murine recombinant LCN2 (1 μg/ml) protein for 48 hours. Cells were fixed in 4% paraformaldehyde (PFA) for 15 minutes, quenched with 1% glycine for 10 minutes, and permeabilized with 0.1% Triton X-100 for one minute. After blocking with 3% BSA, cells were incubated with murine LCN2 (1:200) and HMGB1 primary antibody (1:100) overnight at 4°C, and incubated with Alexa Fluor 488 goat anti-rabbit IgG (Life Technologies) at 1:1000 for one hour at room temperature. Images were taken using a 60 objective with confocal microscope (Olympus, BX51).

Transmission electron microscopy (TEM)

TEM was performed as described previously [15]. In brief, LV myocardium was cut to 1 mm^3 and fixed with 2.5% glutaraldehyde in 0.1 M cacodylate buffer (pH 7.4) overnight at 4°C. After brief washing, the specimens were post-fixed in 1% osmium tetroxide, dehydrated, embedded in epoxy resin, and polymerized overnight at 60°C. Ultra-thin sections (100 nm) were cut and post-stained with Reynold's lead citrate and uranyl acetate to increase contrast. Sections were viewed and photographed using a P FEI CM100 TEM and Kodak Megaplus camera.

Western blot analysis

Heart tissue was snap frozen and then lysed in modified RIPA buffer by the Tissue Lyser II (Qiagen) for two minutes at full speed. The lysates were then centrifuged at full speed for 10 minutes. Supernatants were harvested and quantified by BCA assay. Tissue lysates (30 or 50 μg) were incubated with Laemmli sample buffer at 95°C for 10 minutes and then resolved by SDS-PAGE. After transferring to polyvinylidenedifluoride (PVDF) membranes, Western blotting was performed by incubating with antibodies. The following antibodies were used for immunoblot analysis: LC3-II (1:1000), BECLIN-1 (1:1000), Caspase-1 (1:1000), HMGB1 (1:1000), phospho-NF-κB p65 (Ser536) (1:750), NF-κB p65 (1:750), GAPDH (1:2000) and β-actin (1:2000) from Cell Signaling; p62 (1:1000) from BD Transduction Laboratories; LCN2 (1:2000) from Antibody and Immunoassay Services; IL-1β (1:1000) from R&D systems. IL-18 (1:1000) from MBL Life science. After incubation with secondary antibodies, the immune complexes were detected with enhanced chemiluminescence (ECL) reagents from GE Healthcare (Uppsala, Sweden).

Quantitative reverse-transcription polymerase chain reaction

The custom fibrosis PCR array was purchased from SABiosciences-61 (QIAGEN Inc.). Total

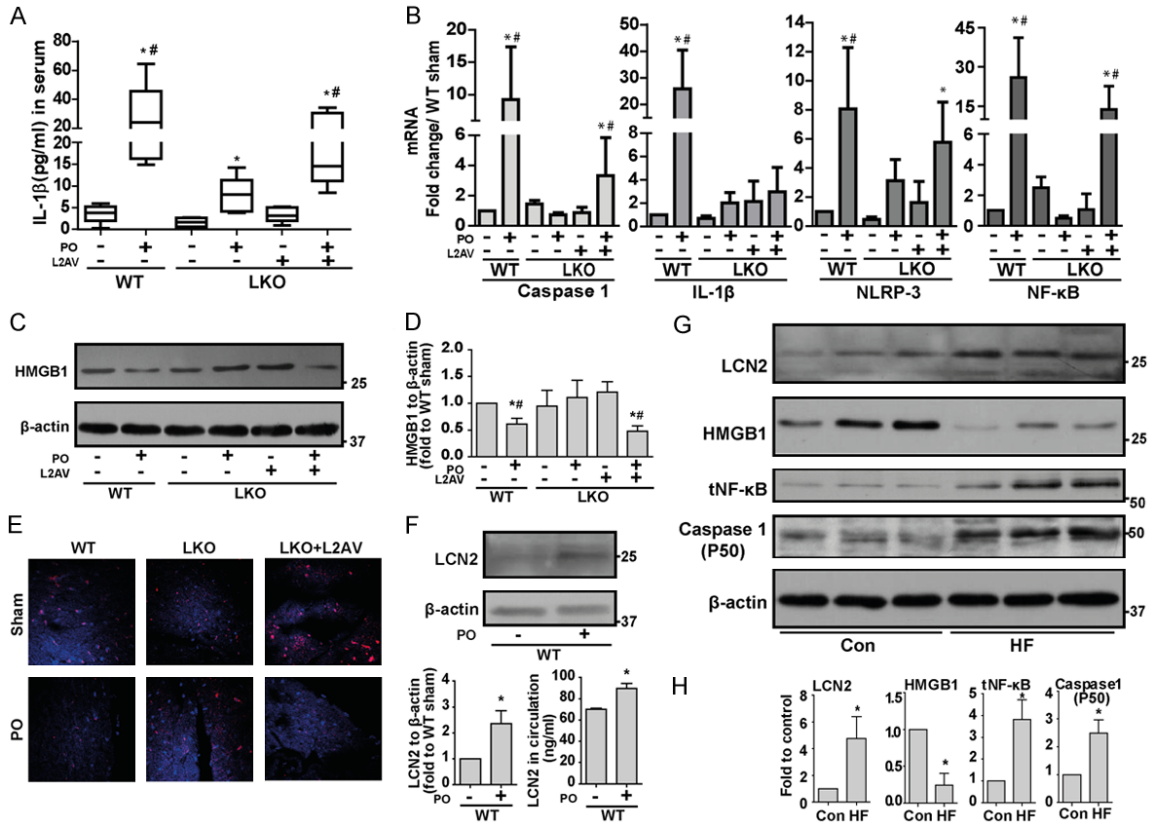

Figure 1. Inflammasome activation is attenuated in LKO mice challenged with PO. (A) IL-1β levels were determined by ELISA in serum collected from WT and LKO mice subjected to either sham or PO surgery. (B) qPCR was performed for gene expressions of inflammasome markers (Caspase-1, IL-1β, NLRP3 and NF-κB) in heart tissues collected from WT and LKO mice subjected to either sham or PO surgery. (C, D) Western blotting and densitometric quantifications was performed to analyze HMGB1 protein levels in the heart tissues from the above treated mice. (E) Immunofluorescence was performed for HMGB1 in heart tissue sections collected from WT and LKO mice subjected to either sham or PO surgery. Protein levels of LCN2 in heart tissue (F), densitometric quantification (F, left panel) and LCN2 level in circulation (F, right panel) were determined by Western blotting and ELISA, respectively. (G) Western blotting was performed to examine the protein levels of inflammation markers (LCN2, HMGB1, NF-κB and Caspase-1) in heart tissue lysates from healthy human subjects (Con) or patients with HF, with quantification shown in (H). *, P<0.05 vs. WT Sham or healthy human subjects and, #, vs. LKO PO, n=5-6.

RNA was isolated from heart tissues or cultured mice and rat fibroblasts using TRIzol® Reagent according to the manufacturer's instructions, and purified using the RNeasyMinElute Cleanup Kit to attain an A260/A280 ratio between 1.9 and 2.0. First-strand cDNA, synthesized from 0.5 μg RNA using the RT^2 First Strand kit, was used in a custom PCR array comprising of 96-well plates pre-coated with primers listed in **Table 1**. Quantitative real-time PCR was conducted using a Chromo4™ Detection system (Bio-Rad Laboratories Canada Ltd., Mississauga, ON, CA) according to cycling conditions outlined by the PCR array manufacturer. Data were analyzed using RT^2 Profiler PCR Array Data Analysis software (Version 3.5; QIAGEN Inc.) and normalized to GAPDH mRNA expression. For other genes detected listed in the **Table 2**, they were analyzed through real-time PCR using the following cycling conditions: 95°C/15 min, followed by 35 cycles of [95°C/30 sec, 55°C/30 sec, 72°C/30 sec], then 72°C/10 min. Melting curve analysis was used to ensure primer specificity. Data were then analyzed using the $2^{-\Delta\Delta Ct}$ method.

Cultured adult fibroblasts from mice, adult and neonatal rat fibroblasts from rats

Mice (male, 8 weeks) or rat heart (Wistar rats male, 6 months) was isolated from anesthetized animal and perfused with Ca^{2+} free K-H buffer for 6 minutes and then with LiberaseBlendyzme 4 (Roche) contained K-H

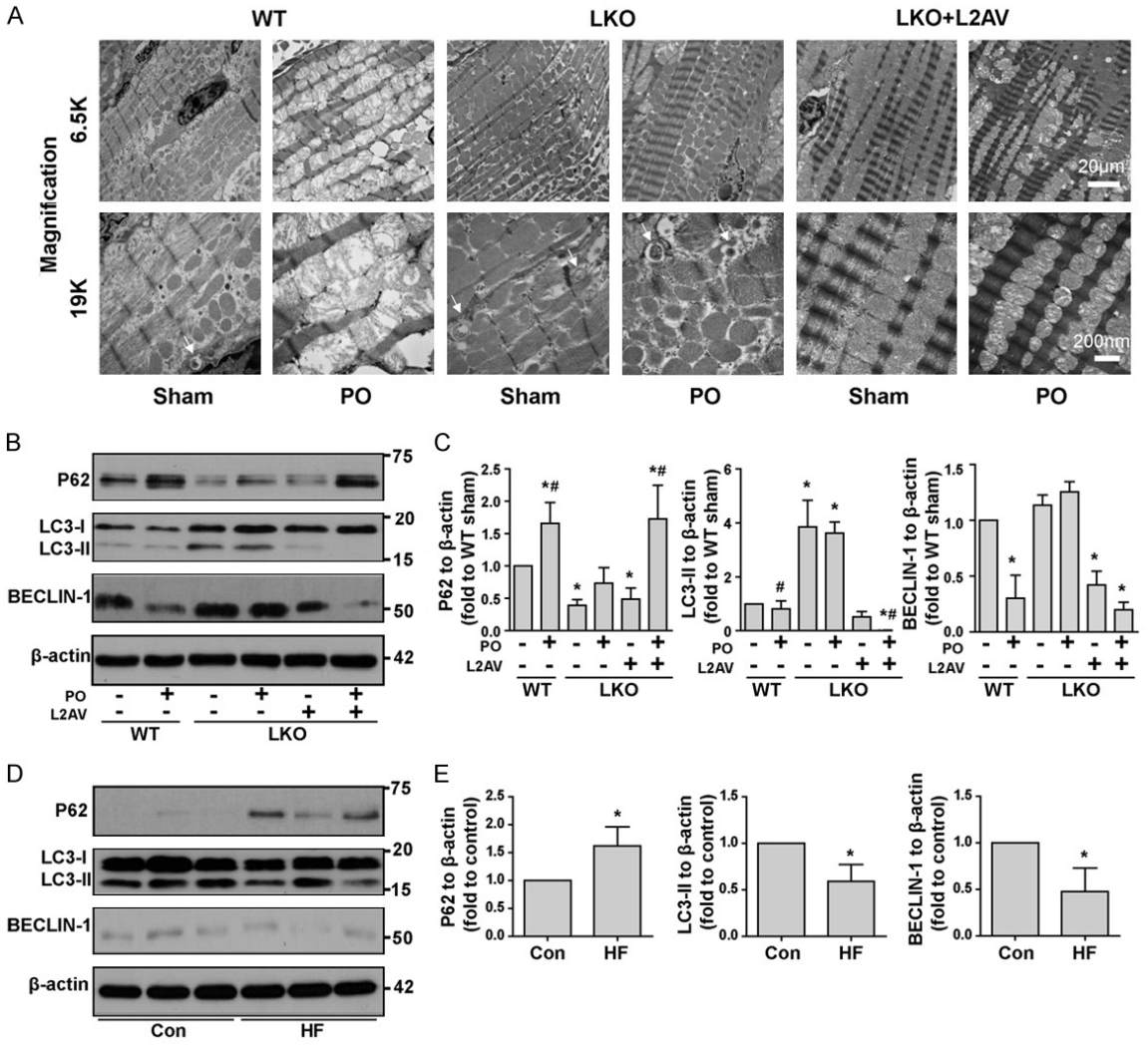

Figure 2. LCN2 deficiency protects against loss of mitochondrial morphology and autophagy flux disruption induced by PO. A: Mitochondria integrity was evaluated using TEM from heart tissue sections of WT and LKO (±L2AV) mice that had undergone either sham or pressure overload (PO) surgery. Autophagosomes were indicated by arrows. B: Autophagic flux was analyzed by examining the protein expression of P62, LC3-II and BECLIN-1 in heart tissue lysates from WT and LKO (±L2AV) mice that have undergone either sham or PO surgery. C: Densitometric quantifications of western blots in B. D: Autophagic flux was analyzed by examining the protein expression of P62, LC3-II, and BECLIN-1 in heart tissue lysates from healthy human subjects (Con) or patients with heart failure (HF). E: Densitometric quantifications of western blots in D. *, P<0.05 vs. WT Sham or healthy human subjects and, #, vs. LKO PO, n=5-6.

buffer for 3 times (10 ml per heart for mice, 20 ml per heart for rat). The hearts were perfused with 5% BSA K-H buffer before mincing. After stabilization for 3 hours, fibroblasts were stimulated with LCN2 (1 μg/ml) for 24 hours. Hearts were collected from 1- to 2-day-old neonatal rat pups, promptly after euthanasia by decapitation, and primary cultures of neonatal rat cardiomyocytes were performed as described previously [17]. After stabilization for 24 hours, neonatal rat fibroblasts were stimulated with LCN2 (1 μg/ml) for 48 hours. Samples were collected to examine the expression levels of HMGB1 by western blot analysis and mRNA by quantitative RT-PCR.

Statistical analysis

All results were derived from at least three sets of repeated experiments. The statistical calculations were performed by one-way analysis of variance followed by Tukey's multiple compari-

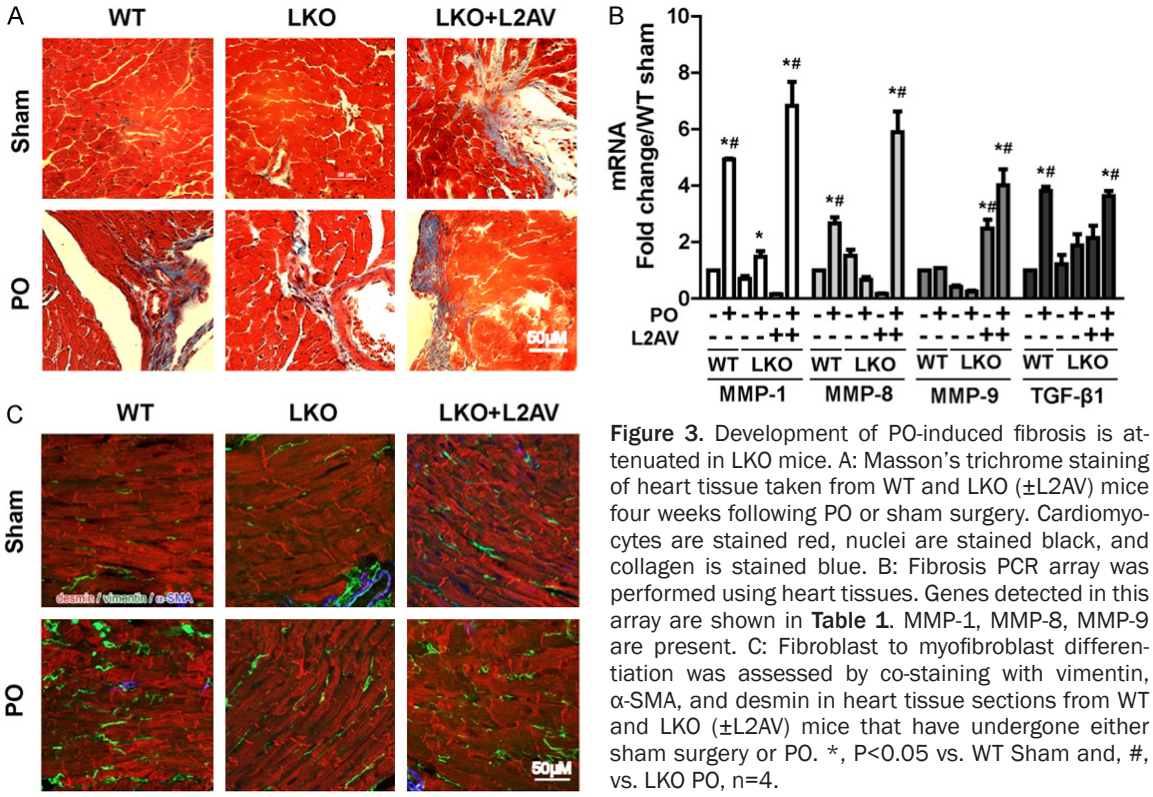

Figure 3. Development of PO-induced fibrosis is attenuated in LKO mice. A: Masson's trichrome staining of heart tissue taken from WT and LKO (±L2AV) mice four weeks following PO or sham surgery. Cardiomyocytes are stained red, nuclei are stained black, and collagen is stained blue. B: Fibrosis PCR array was performed using heart tissues. Genes detected in this array are shown in **Table 1**. MMP-1, MMP-8, MMP-9 are present. C: Fibroblast to myofibroblast differentiation was assessed by co-staining with vimentin, α-SMA, and desmin in heart tissue sections from WT and LKO (±L2AV) mice that have undergone either sham surgery or PO. *, P<0.05 vs. WT Sham and, #, vs. LKO PO, n=4.

son post-test using Prism version 5 (GraphPadSoftware; San Diego, CA, USA). Independent t tests were performed when there are comparisons between two groups. All values are presented as means ± SD and where arbitrary and not absolute value were involved the final graph displays fold over control values. For all statistical comparisons, a *P* value less than 0.05 was accepted to indicate significant differences.

Results

PO-induced inflammasome activation is attenuated in LKO mice

We examined NLRP3 inflammasome in WT and LKO (±LCN2 restoration using L2AV) mice four weeks after transverse aortic banding surgery. Serum interleukin (IL)-1β measurement by ELISA demonstrated increased IL-1β in WT and LKO+L2AV with PO, although IL-1β was increased in LKO, the magnitude of change under PO was greatly reduced (**Figure 1A**). Inflammasome-priming, measured via expression levels of caspase-1, NLPR3, IL-1β and nuclear factor kappa-light-chain-enhancer of activated B cells (NF-κB) showed similar significant increases in WT and LKO+L2AV after PO at the mRNA level (**Figure 1B**) [18]. Having shown that LCN2 positively regulates inflammasome activation in PO, we sought to decipher the mechanism of this action. NLRP3 inflammasome activation was previously shown to be regulated by the release of HMGB1 (high mobility group box chromosomal protein 1) from cells, after HMGB1-BECLIN-1 complex dissociation, via a mechanism involving toll-like receptor (TLR)4-mediated signaling [19-21]. Both Western blotting of heart homogenates (**Figure 1C** and **1D**) and immunofluorescent detection in tissue sections (**Figure 1E**) demonstrated that HMGB1 was significantly decreased in WT but not LKO mice after PO. Under PO, restoring LCN2 in LKO mice with L2AV decreased cellular HMGB1 to amount similar as WT mice (**Figure 1E**). After four weeks PO, a significant increase of LCN2 in both serum and heart tissue was detected in WT mice with PO (**Figure 1F**). In agreement with our mouse data, HMGB1 levels were significantly decreased in heart tissues of HF patients compared to healthy individuals (**Figure 1G** and **1H**). Furthermore, cardiac content of LCN2, NF-κB and Caspase-1 were all significantly increased in HF patients.

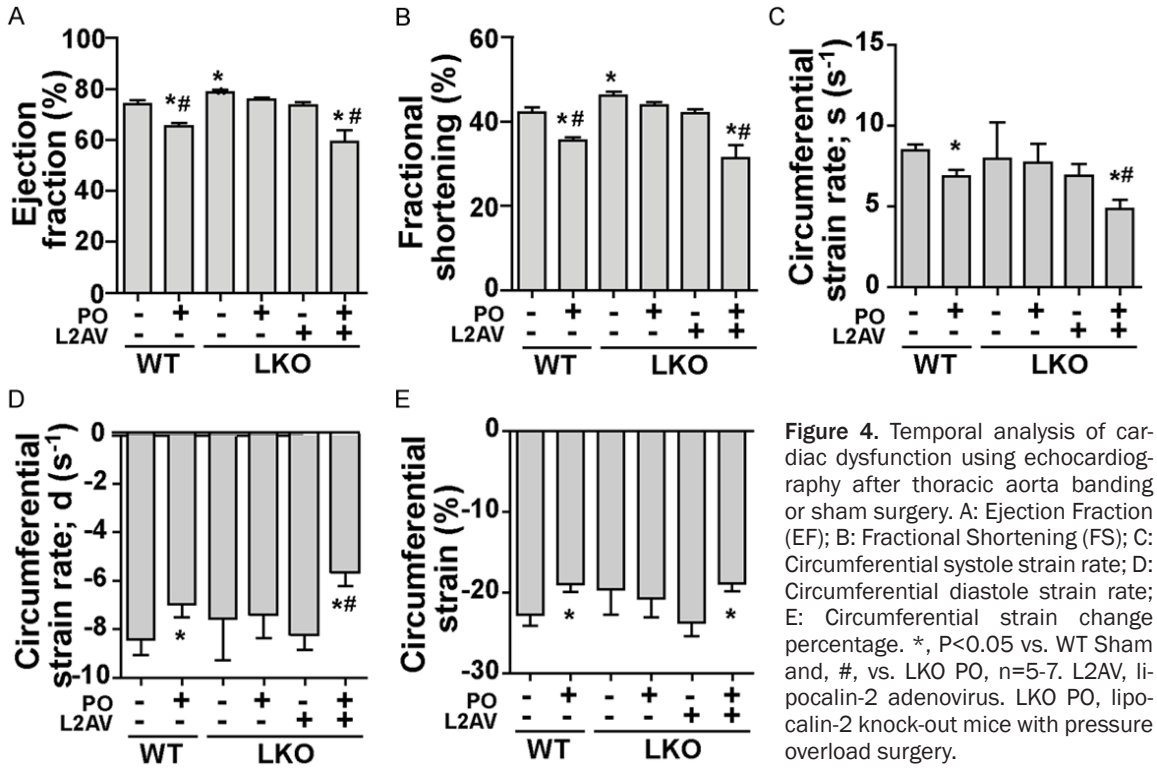

Figure 4. Temporal analysis of cardiac dysfunction using echocardiography after thoracic aorta banding or sham surgery. A: Ejection Fraction (EF); B: Fractional Shortening (FS); C: Circumferential systole strain rate; D: Circumferential diastole strain rate; E: Circumferential strain change percentage. *, P<0.05 vs. WT Sham and, #, vs. LKO PO, n=5-7. L2AV, lipocalin-2 adenovirus. LKO PO, lipocalin-2 knock-out mice with pressure overload surgery.

LCN2 exacerbates mitochondrial deterioration and attenuates autophagic flux in response to PO

Transmission electron microscopy indicated LCN2 deficiency greatly attenuated PO-induced mitochondria damage in cardiomyocytes, as shown by the presence of clear well-structured cristae in LKO mice before and after PO (**Figure 2A**). This protective effect was partially lost with the administration of L2AV (**Figure 2A**). Transmission electron microscopy is a gold-standard approach for analysis of autophagic structures, and our data indicated induction of autophagy in mice lacking LCN2 after PO-treatment (**Figure 2A**, arrow), with less observed in WT mice. Next, autophagic flux was evaluated by examining cardiac protein expression levels of P62, LC3-II, BECLIN-1. Western analysis showed increased protein expression of P62 and decreased LC3-II and BECLIN-1, suggesting less flux in WT versus LKO mice after PO (**Figure 2B** and **2C**). Analysis of cardiac biopsy tissue samples obtained from human subjects with or without HF indicated increased P62 plus decreased LC3-II and BECLIN-1 levels (**Figure 2D** and **2E**), indicative of less autophagy when compared with control. It is conceivable that signals such as reactive oxygen species or mitochondria DNA released from damaged mitochondria might be responsible for priming or activation of NLRP3 inflammasome [22, 23], whereas LCN-2 deficiency preserved mitochondria morphology and autophagic flux under PO.

LCN2 deficiency protects mice from PO-induced development of fibrosis

Fibrosis is an established component of ventricular remodeling in HF patients [14, 24]. Masson's trichrome staining revealed enhanced accumulation of collagen after PO in WT and LKO+L2AV, but not in LKO mice (**Figure 3A**). Assessing mRNA levels of fibrosis-related genes showed matrix metalloproteinases (MMP)-1, MMP-8 and TGF-β1 increased significantly after PO in WT and LKO+L2AV mice but not in LKO mice (**Figure 3B**). MMP-9 levels increased after restoring LCN2 in LKO with L2AV under both sham, and to a greater extent, PO conditions (**Figure 3B**). Immunofluorescence staining showed that LKO mice were somewhat protected against PO-induced occurrence of vimentin-positive fibroblasts (**Figure 3C**). Administration of L2AV to LKO mice negated these protective

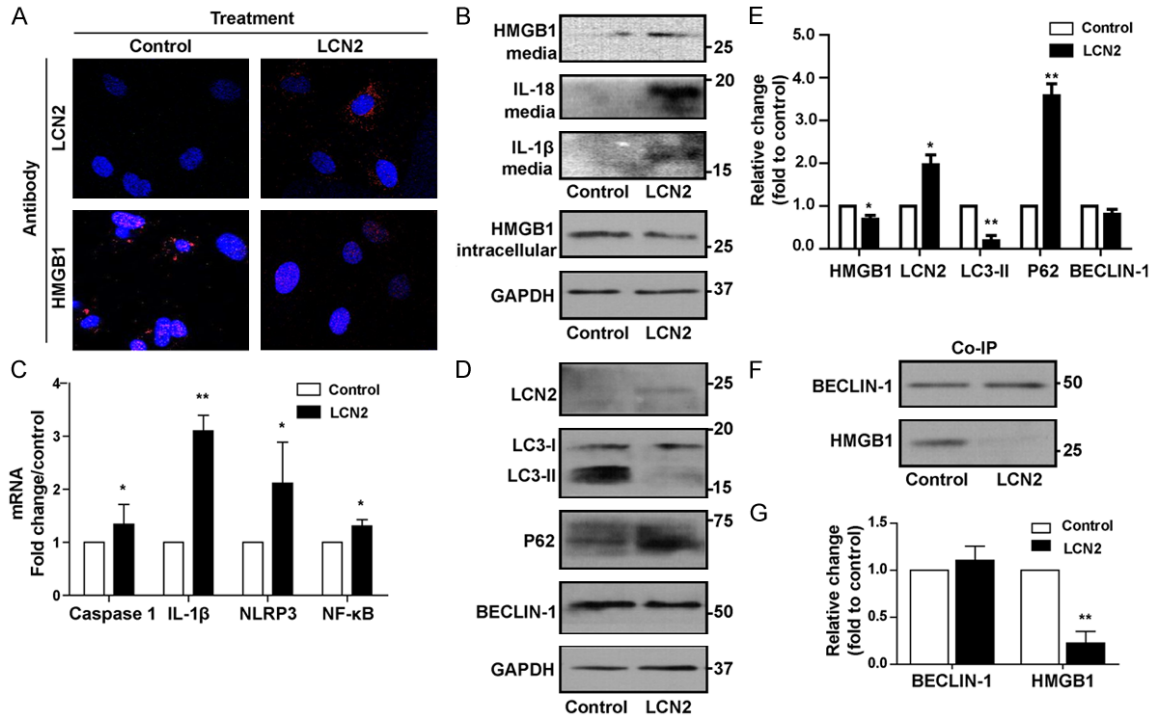

Figure 5. LCN2 treatment of rat neo-fibroblasts interrupts autophagic flux and induces inflammasome activation by releasing HMGB1. Rat neo-fibroblasts were isolated and treated with recombinant LCN2 (1 μg/ml) or control for 48 hours. Immunofluorescence (A) and Western blotting (B) were performed to examine the localization and protein expression levels of HMGB1 fibroblasts and IL-18 and IL-1β in medium. Expression levels of inflammasome markers showed in the graph (C) were examined by qPCR. (D) Western blotting was performed to examine the protein levels of autophagic markers (LCN2, LC3-II, P62 and BECLIN-1) with quantification shown in (E). (F, G) Co-immunoprecipitation (Co-IP) was performed in neonatal fibroblast cells to evaluate the binding status between BECLIN-1 and HMGB1. *, P<0.05, **, P<0.01 vs. corresponding control, n=3.

effects; however, there was much less accumulation of fibroblasts compared to WT mice with PO (**Figure 3C**). Immunostaining for smooth muscle actin (SMA) showed that there was no interstitial activation of myofibroblast after PO in all six groups, as expected from this model of mild PO (**Figure 3C**).

LCN2 deficiency protects mice from PO-induced development of cardiac dysfunction

Cardiac function of WT and LKO (±LCN2 restoration using L2AV) mice was evaluated by echocardiography four weeks after transverse aortic banding surgery. Consistent with previous reports [9], LKO mice demonstrated a higher ejection fraction (EF) and fractional shortening (FS) compared to age-matched WT mice that showed significant PO-induced cardiac dysfunction (**Figure 4A** and **4B**). This heart protective effect in LKO mice was abolished by administration of LCN2 (**Figure 4A** and **4B**) as the basal level of EF and ES in LKO mice treated with L2AV was similar to WT mice (**Figure 4A** and **4B**). Importantly, we validated the effectiveness of adenoviral LCN2 delivery by showing that circulating LCN2 produced by L2AV reached a peak above normal level observed in WT mice one week after virus injection (Supplementary Figure 1) [7]. An inherent limitation of this approach is that levels gradually decline after 2 and 4 weeks yet we did not perform a second adenovirus injection to avoid confounding effects from immune system activation and inflammation. As visualized in representative short axis images of M-mode and speckle tracking echocardiography (Supplementary Figure 2), ventricular wall constriction and both systole (**Figure 4C**) and diastole (**Figure 4D**) circumferential strain rate in WT and LKO+L2AV mice under PO dropped significantly four weeks after PO, but were preserved in LKO mice (**Figure 4E**; Supplementary Table 1). PO induced increased LV mass and the response was similar in both genotypes and in LKO with LCN2 replenishment (Supplementary

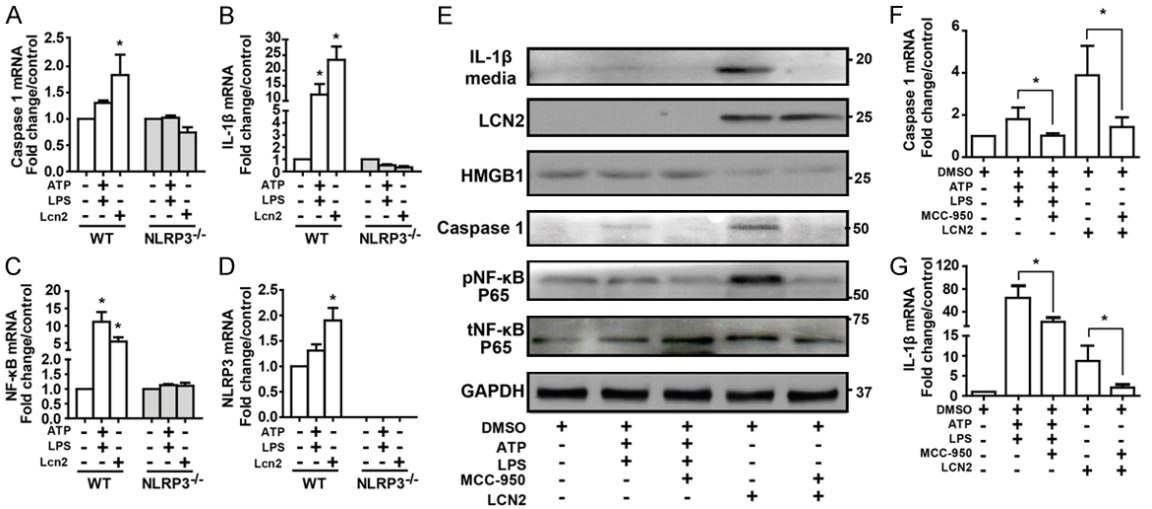

Figure 6. LCN2 induced inflammasome activation is attenuated by NLRP3 deficiency. Wild type and NLRP3-/- mice heart fibroblasts were isolated and treated with recombinant LCN2 (1 μg/ml) or ATP plus LPS for 24 hours. Expression levels of inflammasome markers, Caspase-1 (A), IL-1β (B), NF-κB (C) and NLRP3 (D) were examined by qPCR. Adult rat heart fibroblasts were isolated and treated with recombinant LCN2 (1 μg/ml) or ATP (5 μM) plus LPS (2.5 μg/ml) for 24 hours in the presence or absence of NLRP3 inhibitor MCC-950 (0.1 μM). (E) Western blotting was performed to examine the protein levels of LCN2 and inflammatory markers in medium (IL-1β) and fibroblasts (HMGB1, Caspase-1, pNF-κB, tNF-κB). Caspase-1 (F) and IL-1β (G) mRNA levels were checked by qPCR. *, P<0.05, **, P<0.01 vs. corresponding control, n=3.

Figure 3). In summary, these data indicate a detrimental role of LCN2 in the development of cardiac dysfunction.

LCN2 acts directly on primary cardiac fibroblasts to decrease intracellular HMGB1 levels, induce NLRP3 inflammasome activation and attenuate autophagy

During pathological conditions, cardiac fibroblasts play a crucial role in maintaining normal cardiac function by modulating the synthesis not only via deposition of extracellular matrix, but also upon autocrine and paracrine cell-to-cell communication [25]. We observed accumulation of fibroblasts after PO model and these may play a role in NLRP3 inflammasome complex formation. To test this possibility, we isolated primary cardiac fibroblasts from neonatal rats and treated with recombinant LCN2 for 48 hours. Immunofluorescent staining indicated increased LCN2 signal in the cytosol and reduced cytosolic HMGB1 levels in cells treated with LCN2 (**Figure 5A**). Western blotting data also confirmed that total cellular HMGB1 levels were decreased after LCN2 treatment (**Figure 5B**, lower). Meanwhile, HMGB1 was detected in concentrated conditioned medium after LCN2 treatment (**Figure 5B**, top). Protein levels of IL-1β and IL-18 were also increased in this medium after LCN2 treatment (**Figure 5B**, top). Gene expressions of Caspase-1, IL-1β, NLRP3 and NF-κB in fibroblasts (**Figure 5C**) were induced by LCN2 treatment. We found that LCN2 also had direct effects on protein markers of autophagy with decreased LC3-II and elevated P62 levels and a reduction in BECLIN-1 (**Figure 5D** and **5E**). HMGB1 also regulates autophagy by competing for BECLIN-1 binding with Bcl-2. To determine whether the interruption of autophagy is due to decreased binding between HMGB1 and BECLIN-1 after LCN2 treatment of cells, we immunoprecipitated BECLIN-1 and observed less association of HMGB1 after LCN2 treatment (**Figure 5F** and **5G**).

LCN2 induced inflammasome activation is attenuated by NLRP3 deficiency and TLR4 inhibition

Primary cardiac fibroblasts from WT and NLRP3 knockout (NLRP3-/-) adult mice were treated in culture with recombinant LCN2 or NLRP3 inflammasome activator lipopolysaccharide/adenosine triphosphate (LPS/ATP) for 24 h [26]. LCN2 treatment increased mRNA levels of inflammasome related genes Caspase-1 and IL-1β in WT mice but not in NLPR3-/- mice

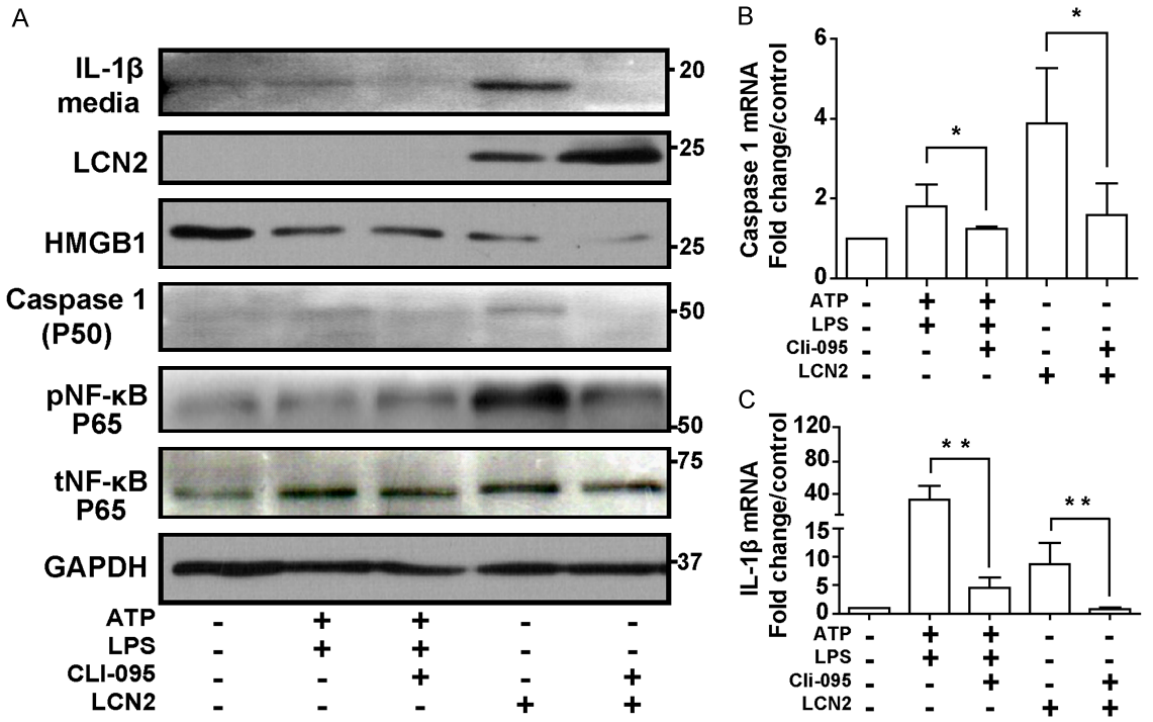

Figure 7. LCN2 induced inflammasome activation is attenuated by TLR4 inhibition. Adult rat heart fibroblasts were isolated and treated with recombinant LCN2 (1 μg/ml) or ATP (5 μM) plus LPS (2.5 μg/ml) for 24 hours in the presence or absence of TLR4 inhibitor Cli-095 (1 μg/ml). (A) Western blotting was performed to examine the protein levels of LCN2 and inflammatory markers in medium (IL-1β) and fibroblasts (HMGB1, Caspase-1, pNF-κB, tNF-κB). Caspase-1 (B) and IL-1β (C) mRNA levels were checked by qPCR. *, P<0.05, **, P<0.01 vs. corresponding control, n=3.

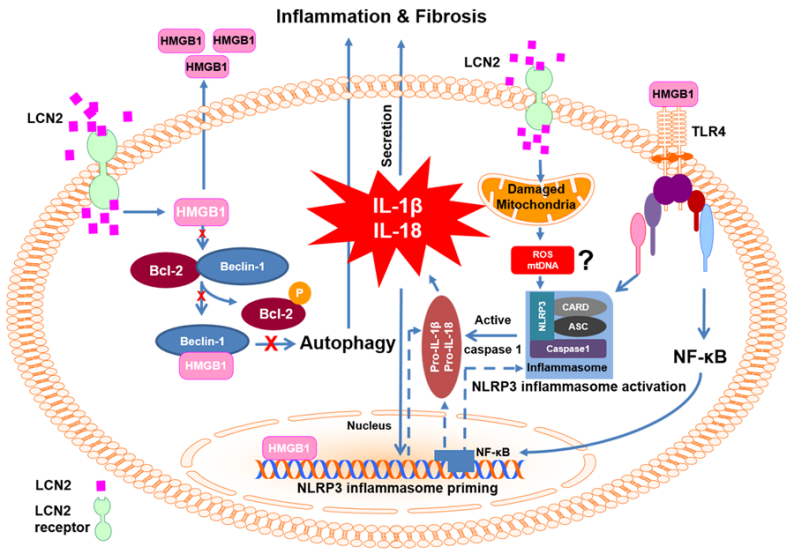

Figure 8. Schematic model depicting mechanisms via which LCN2 regulates NLRP3 inflammasome. LCN2 disrupts the association of BECLIN-1 and HMGB1, one consequence of which is altered autophagic flux (left side). Another is HMGB1 release from cells which can then induce an inflammatory response by binding to TLR4 receptors (right side). LCN2 also induced mitochondrial dysfunction and we propose that consequent increases in ROS or mtDNA may contribute to priming and activation of the NLRP3 inflammasome. The end result of NLRP3 inflammasome activation is production and cleavage of proinflammatory cytokines (IL-1 β and IL-18) via Caspase-1 activation. Together these effects may dictate cardiac remodeling events such as fibrosis. ASC, apoptosis-associated speck-like protein; Bcl-2, B-cell lymphoma 2; CARD, caspase activation and recruitment domain. IL-1β, interleukin-1β; IL-18, interleukin-18; NF-κB, transcription factor nuclear factor kappa-light chain-enhancer of activated B cells; NLRP3, NACHT, LRR and PYD domains-containing protein 3; TLR-4, toll-like receptor 4.

(**Figure 6A-D**). When treated with LCN2 and LPS/ATP in the presence or absence of NLRP3 inhibitor (MCC-950) or TLR4 inhibitor (Cli-095), mRNA levels of Caspase-1 and IL-1β were significantly attenuated (**Figures 6F**, **6G**, **7B** and **7C**).

MCC-950 and Cli-095 also attenuated the level of LCN2 induced IL-1β release into the media, as well as Caspase-1 and phospho-NF-κB p65 (Ser536) content in rat adult fibroblasts (**Figures 6E** and **7A**). Consistently, the protein expression level of HMGB1 decreased after LCN2 treatment, but not LPS/ATP treatment, indicating the role of LCN2 in releasing HMGB1 from the cytosol (**Figures 6E** and **7A**).

Discussion

Our analysis of the contribution by LCN2 to cardiac dysfunction, and in particular the discovery of novel mechanisms of LCN2 action has wide-ranging diagnostic and therapeutic implications, not only in heart failure but also other conditions such as kidney dysfunction. A principal novel discovery of this study was that LCN2 induced NLRP3 inflammasome activation via release of the danger-associated molecular pattern (DAMP) protein HMGB1 and subsequent TLR4-dependent signaling. Our results revealed that lack of LCN2 in mice mitigates maladaptive fibrotic remodeling and facilitates adequate induction of autophagic flux in response to PO, in keeping with our previous work indicating that LCN2 directly attenuated autophagic flux [13]. Thus, we have validated the functional consequences of cardiac LCN2 actions and provided new insight into the mechanisms involved (**Figure 8**).

An important impact of NLRP3 inflammasome activation in diabetes and cardiovascular disease is well documented [11, 27, 28]. Previous studies showed that serum LCN2 levels correlate positively with various cardiovascular diseases including HF [2]. Basal expression of LCN2 in heart tissue is low and we found that direct administration of LCN2 accelerated the progression of HF [6]. One of the best characterized DAMPs is HMGB1 which promotes NLRP3 inflammasome and NF-κB activation [29]. Effects of HMGB1 can be mediated via several mechanisms, including HMGB1 binding to receptor for advanced glycation end products (RAGE) and toll-like receptors TLR2 and TLR4 [21, 29]. In astrocytes, the inhibition of TLR4, rather than RAGE or TLR2 attenuated HMGB1-induced IL-18 production [30]. We found decreased intracellular HMGB1 levels in rat adult and neonatal fibroblasts treated with LCN2, suggesting that LCN2 induces release of HMGB1 into the extracellular space by an as yet unknown mechanism. Furthermore, we found decreased HMGB1 levels in WT and LKO+L2AV, but not LKO mice after PO as well as in cardiac biopsy samples of human HF patients. Our data indicated that NLRP3 inflammasome was initiated by LCN2 via the release of HMGB1 followed by TLR-4 activation and mitochondria damage, thus assembling various lines of evidence in the literature into a detailed cohesive mechanism of LCN2 action. The induction of the NLRP3 inflammasome complex and subsequent inflammatory effects are then reasonably considered to contribute to cardiac dysfunction.

Reciprocal crosstalk between NLRP3 inflammasome activation and LCN2 action was suggested by studies showing that stimulation of TLR4 induces the formation of the inflammasome complex and production of LCN2 [31]. Many studies have now indicated that the degree of autophagy changes in the failing heart although the functional significance is still contentious [32]. Disruption of autophagy by cardiac-specific knockdown of Atg5 in mice leads to cardiomyopathy [33]. We believe that LCN2 is an important suppressor of cardiac autophagy and have recently shown reduced autophagic flux in cardiomyoblast cells treated with LCN2 [13]. Our current study provides evidence that the increase in cardiac autophagy normally seen in response to PO, and which is generally regarded as a beneficial adaptive response, is enhanced in LKO mice and attenuated by adenoviral delivery of LCN2 to these mice. Together, these data indicate that LCN2 acts to suppress cardiac autophagic flux and this likely contributes to cardiac dysfunction. Interestingly, sustained autophagy upon transgenic Atg7 overexpression in mice decreased cardiac fibrosis and dysfunction [34]. We showed that LKO mice were somewhat protected against PO-induced induction of vimentin-positive fibroblasts and fibrosis, while administration of L2AV to LKO mice negated these protective effects. In addition to the classic role of extracellular matrix regulation, MMP-9 activity can also contribute to inflammation in the failing heart via activation of inflammatory cytokines such as IL-1β, IL-8 and tumor necrosis factor alpha (TNF-α) [35].

In conclusion, our study confirms the detrimental role of LCN2 in development of cardiac dysfunction and provides new mechanistic insight on mechanisms of LCN2 action. Indeed, the effects which we have observed in this study

could well be at least in part mediated via systemic effects of LCN2 in other tissues which causes crosstalk with the heart. A principal novel discovery of this study was that LCN2 induced NLRP3 inflammasome activation via release of the danger-associated molecular pattern (DAMP) protein HMGB1 and subsequent TLR4-dependent signaling. This study also provided further evidence that LCN2 acts to suppress stress-induced autophagic flux. Our focus was on the heart yet this data has potentially wide-ranging diagnostic and therapeutic implications, since the physiological significance of LCN2, also commonly referred to as NGAL, is perhaps most well established in kidney. Nevertheless, potential for suppressing neutrophil-derived LCN2-mediated inflammation must be balances by potential adverse effects of over-suppression due to the beneficial role of neutrophils in cardiac repair by polarizing macrophages towards a reparative phenotype [36]. This work will also likely stimulate interest in new avenues of research on the regulation of NLRP3 inflammasome, autophagy and fibrosis by LCN2 in other target tissues. In summary, we have characterized the cardiac functional consequences of LCN2 deletion, with or without readministration, in mice and provided new insight into the mechanisms involved.

Acknowledgements

This work was supported by Grant-in-aid and Career Investigator Award to GS from Heart & Stroke Foundation of Canada/Ontario. BH was supported by the Canadian Institutes of Health Research (grant #286920) and the E-Rare Joint Transnational Call 'Development of Innovative Therapeutic Approaches for Rare Diseases'. MC/AR were supported by NHMRC Project Grant APP1086786.

Disclosure of conflict of interest

None.

Address correspondence to: Gary Sweeney, Department of Biology, York University, M3J1P3, Toronto, ON, Canada. Tel: +1-416-736-2100; Fax: +1-416-736-5698; E-mail: gsweeney@yorku.ca

References

[1] Abel ED, Litwin SE and Sweeney G. Cardiac remodeling in obesity. Physiol Rev 2008; 88: 389-419.

[2] Wang Y, Lam KS, Kraegen EW, Sweeney G, Zhang J, Tso AW, Chow WS, Wat NM, Xu JY, Hoo RL and Xu A. Lipocalin-2 is an inflammatory marker closely associated with obesity, insulin resistance, and hyperglycemia in humans. Clin Chem 2007; 53: 34-41.

[3] Chan YK, Sung HK and Sweeney G. Iron metabolism and regulation by neutrophil gelatinase-associated lipocalin in cardiomyopathy. Clin Sci (Lond) 2015; 129: 851-862.

[4] Jang Y, Lee JH, Wang Y and Sweeney G. Emerging clinical and experimental evidence for the role of lipocalin-2 in metabolic syndrome. Clin Exp Pharmacol Physiol 2012; 39: 194-199.

[5] Berger T, Togawa A, Duncan GS, Elia AJ, You-Ten A, Wakeham A, Fong HE, Cheung CC and Mak TW. Lipocalin 2-deficient mice exhibit increased sensitivity to Escherichia coli infection but not to ischemia-reperfusion injury. Proc Natl Acad Sci U S A 2006; 103: 1834-1839.

[6] Song E, Fan P, Huang B, Deng HB, Cheung BM, Feletou M, Vilaine JP, Villeneuve N, Xu A, Vanhoutte PM and Wang Y. Deamidated lipocalin-2 induces endothelial dysfunction and hypertension in dietary obese mice. J Am Heart Assoc 2014; 3: e000837.

[7] Law IK, Xu A, Lam KSL, Berger T, Mak TW, Vanhoutte PM, Liu JT, Sweeney G, Zhou M, Yang B and Wang Y. Lipocalin-2 deficiency attenuates insulin resistance associated with aging and obesity. Diabetes 2010; 59: 872-882.

[8] Liu JT, Song E, Xu A, Berger T, Mak TW, Tse HF, Law IK, Huang B, Liang Y, Vanhoutte PM and Wang Y. Lipocalin-2 deficiency prevents endothelial dysfunction associated with dietary obesity: role of cytochrome P450 2C inhibition. Br J Pharmacol 2012; 165: 520-531.

[9] Yang B, Fan P, Xu A, Lam KS, Berger T, Mak TW, Tse HF, Yue JW, Song E, Vanhoutte PM, Sweeney G and Wang Y. Improved functional recovery to I/R injury in hearts from lipocalin-2 deficiency mice: restoration of mitochondrial function and phospholipids remodeling. Am J Transl Res 2012; 4: 60-71.

[10] Matsa R, Ashley E, Sharma V, Walden AP and Keating L. Plasma and urine neutrophil gelatinase-associated lipocalin in the diagnosis of new onset acute kidney injury in critically ill patients. Crit Care 2014; 18: R137.

[11] Butts B, Gary RA, Dunbar SB and Butler J. The Importance of NLRP3 Inflammasome in Heart Failure. J Card Fail 2015; 21: 586-593.

[12] Deretic V. Autophagy as an innate immunity paradigm: expanding the scope and repertoire of pattern recognition receptors. Curr Opin Immunol 2012; 24: 21-31.

[13] Chan YK, Sung HK, Jahng JW, Kim GH, Han M and Sweeney G. Lipocalin-2 inhibits autophagy and induces insulin resistance in H9c2 cells. Mol Cell Endocrinol 2016; 430: 68-76.

[14] Dadson K, Kovacevic V, Rengasamy P, Kim GH, Boo S, Li RK, George I, Schulze PC, Hinz B and Sweeney G. Cellular, structural and functional cardiac remodelling following pressure overload and unloading. Int J Cardiol 2016; 216: 32-42.
[15] Jahng JW, Turdi S, Kovacevic V, Dadson K, Li RK and Sweeney G. Pressure overload-induced cardiac dysfunction in aged male adiponectin knockout mice is associated with autophagy deficiency. Endocrinology 2015; 156: 2667-2677.
[16] Castillero E, Akashi H, Pendrak K, Yerebakan H, Najjar M, Wang C, Naka Y, Mancini D, Sweeney HL, J DA, Ali ZA, Schulze PC and George I. Attenuation of the unfolded protein response and endoplasmic reticulum stress after mechanical unloading in dilated cardiomyopathy. Am J Physiol Heart Circ Physiol 2015; 309: H459-470.
[17] Dadson K, Turdi S, Boo S, Hinz B and Sweeney G. Temporal and molecular analyses of cardiac extracellular matrix remodeling following pressure overload in adiponectin deficient mice. PLoS One 2015; 10: e0121049.
[18] Guo H, Callaway JB and Ting JP. Inflammasomes: mechanism of action, role in disease, and therapeutics. Nat Med 2015; 21: 677-687.
[19] Yu M, Wang H, Ding A, Golenbock DT, Latz E, Czura CJ, Fenton MJ, Tracey KJ and Yang H. HMGB1 signals through toll-like receptor (TLR) 4 and TLR2. Shock 2006; 26: 174-179.
[20] Tang D, Kang R, Livesey KM, Cheh CW, Farkas A, Loughran P, Hoppe G, Bianchi ME, Tracey KJ, Zeh HJ 3rd and Lotze MT. Endogenous HMGB1 regulates autophagy. J Cell Biol 2010; 190: 881-892.
[21] Klune JR, Dhupar R, Cardinal J, Billiar TR and Tsung A. HMGB1: endogenous danger signaling. Mol Med 2008; 14: 476-484.
[22] Heid ME, Keyel PA, Kamga C, Shiva S, Watkins SC and Salter RD. Mitochondrial ROS induces NLRP3-dependent lysosomal damage and inflammasome activation. J Immunol 2013; 191: 1-19.
[23] Shimada K, Crother TR, Karlin J, Dagvadorj J, Chiba N, Chen S, Ramanujan VK, Wolf AJ, Vergnes L, Ojcius DM, Rentsendorj A, Vargas M, Guerrero C, Wang Y, Fitzgerald KA, Underhill DM, Town T and Arditi M. Oxidized mitochondrial DNA activates the NLRP3 inflammasome during apoptosis. Immunity 2012; 36: 401-414.
[24] Segura AM, Frazier OH and Buja LM. Fibrosis and heart failure. Heart Fail Rev 2014; 19: 173-185.
[25] Souders CA, Bowers SL and Baudino TA. Cardiac fibroblast: the renaissance cell. Circ Res 2009; 105: 1164-1176.
[26] Juliana C, Fernandes-Alnemri T, Kang S, Farias A, Qin F and Alnemri ES. Non-transcriptional priming and deubiquitination regulate NLRP3 inflammasome activation. J Biol Chem 2012; 287: 36617-36622.
[27] Henriksbo BD and Schertzer JD. Is immunity a mechanism contributing to statin-induced diabetes? Adipocyte 2015; 4: 232-238.
[28] Henriksbo BD, Lau TC, Cavallari JF, Denou E, Chi W, Lally JS, Crane JD, Duggan BM, Foley KP, Fullerton MD, Tarnopolsky MA, Steinberg GR and Schertzer JD. Fluvastatin causes NLRP3 inflammasome-mediated adipose insulin resistance. Diabetes 2014; 63: 3742-3747.
[29] Pisetsky DS, Erlandsson-Harris H and Andersson U. High-mobility group box protein 1 (HMGB1): an alarmin mediating the pathogenesis of rheumatic disease. Arthritis Res Ther 2008; 10: 209.
[30] Banjara M. Lipocalin-2: a new regulator of non-pathogen-associated neuroinflammation. Int J Clin Exp Neurol 2014; 2: 8-15.
[31] Wang Y, Song E, Bai B and Vanhoutte PM. Toll-like receptors mediating vascular malfunction: Lessons from receptor subtypes. Pharmacol Ther 2016; 158: 91-100.
[32] Gottlieb RA and Mentzer RM Jr. Autophagy: an affair of the heart. Heart Fail Rev 2013; 18: 575-584.
[33] Nakai A, Yamaguchi O, Takeda T, Higuchi Y, Hikoso S, Taniike M, Omiya S, Mizote I, Matsumura Y, Asahi M, Nishida K, Hori M, Mizushima N and Otsu K. The role of autophagy in cardiomyocytes in the basal state and in response to hemodynamic stress. Nat Med 2007; 13: 619-624.
[34] Bhuiyan MS, Pattison JS, Osinska H, James J, Gulick J, McLendon PM, Hill JA, Sadoshima J and Robbins J. Enhanced autophagy ameliorates cardiac proteinopathy. J Clin Invest 2013; 123: 5284-5297.
[35] Rodriguez D, Morrison CJ and Overall CM. Matrix metalloproteinases: what do they not do? New substrates and biological roles identified by murine models and proteomics. Biochim Biophys Acta 2010; 1803: 39-54.
[36] Horckmans M, Ring L, Duchene J, Santovito D, Schloss MJ, Drechsler M, Weber C, Soehnlein O and Steffens S. Neutrophils orchestrate post-myocardial infarction healing by polarizing macrophages towards a reparative phenotype. Eur Heart J 2017; 38: 187-197.

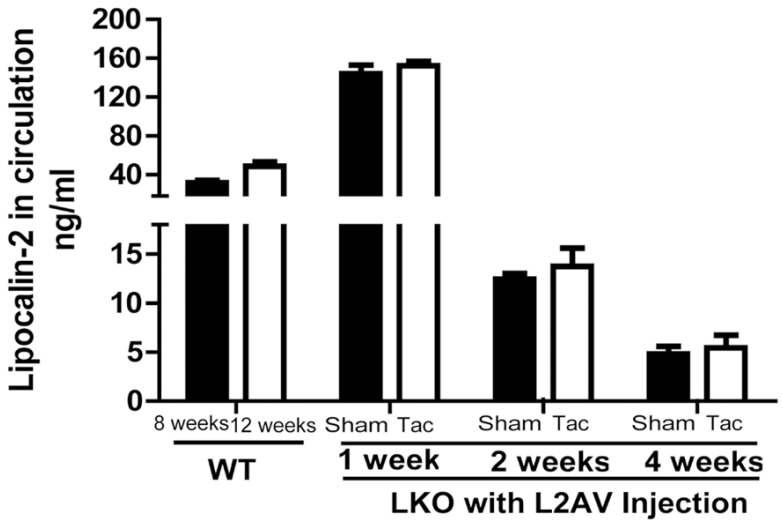

Supplementary Figure 1. Sera were collected in both 8- and 12-weeks-old WT mice and LKO mice with L2AV restoration for 1, 2 and 4 weeks. Sera LCN2 were evaluated by Elisa. n=3-5.

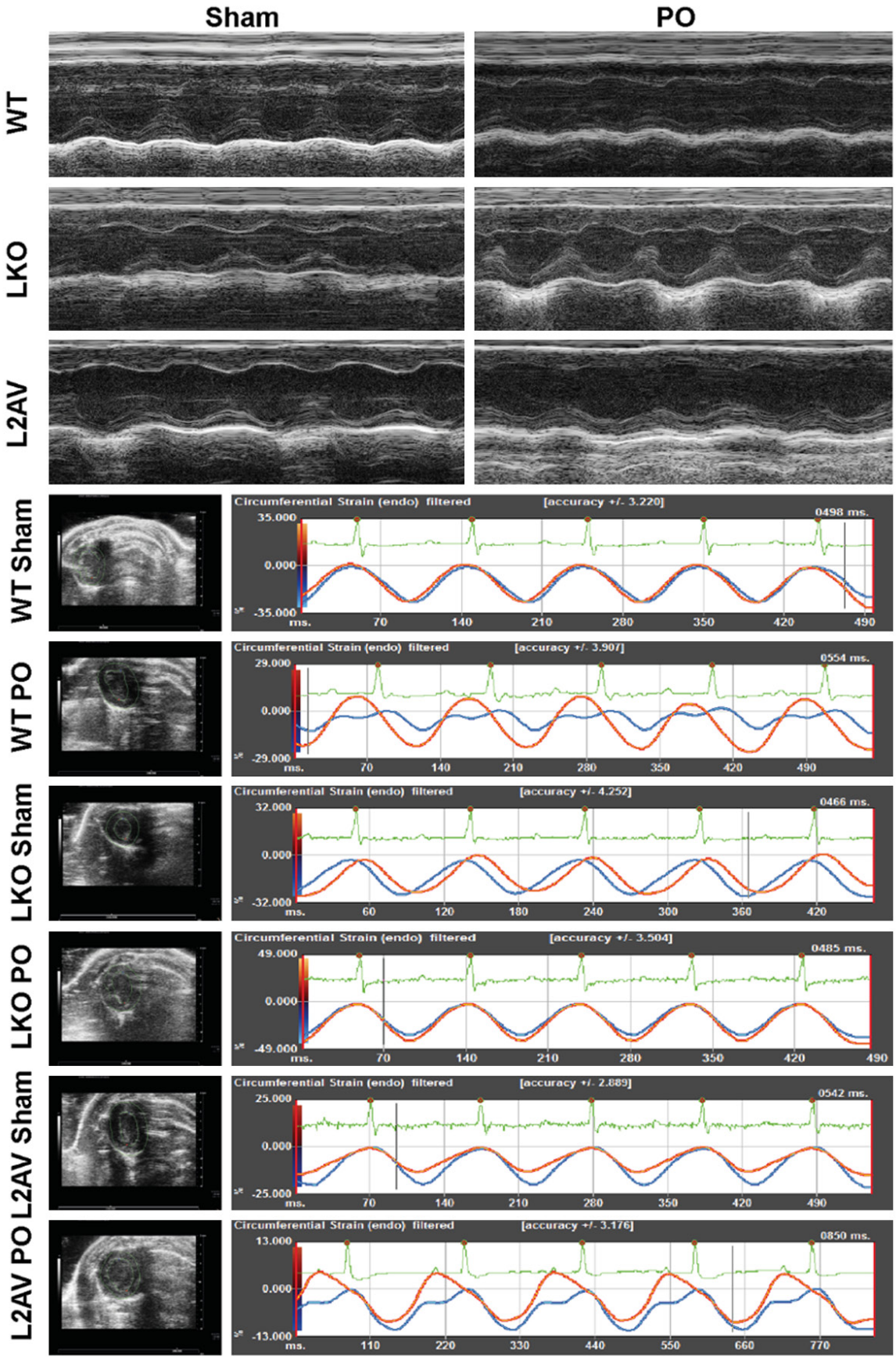
Sham
PO
WT
LKO
L2AV
WT Sham
WT PO
LKO Sham
LKO PO
L2AV Sham
L2AV PO
Circumferential Strain (endo) filtered
[accuracy +/- 3.220]
0498 ms.
35.000
0.000
-35.000
ms.
70
140
210
280
350
420
490
[accuracy +/- 3.907]
0554 ms.
29.000
-29.000
[accuracy +/- 4.252]
0466 ms.
32.000
-32.000
60
120
180
240
300
360
[accuracy +/- 3.504]
0485 ms.
49.000
-49.000
[accuracy +/- 2.889]
0542 ms.
25.000
-25.000
[accuracy +/- 3.176]
0850 ms.
13.000
-13.000
110
220
330
440
550
660
770

Supplementary Figure 2. Representative M-mode images of short-axis view of LV and representative images of circumferential strain rate during 5 cardiac cycles.

Supplementary Table 1. Analysis of cardiac parameters of mice heart four weeks after thoracic aorta banding surgery

	WT SHAM	WT PO	LKO SHAM	LKO PO	LKO+L2AV SHAM	LKO+L2AV PO
Cardiac output (ml/min)	21.12±3.16	21.14±4.24	21.98±3.97	22.26±6.79	20.83±3.14	17.35±3.20*
LVEDD (mm)	3.21±0.31	3.71±0.39*	3.23±0.32	3.66±0.32	3.51±0.29	3.87±0.31*
LVESD (mm)	1.86±0.25	2.42±0.29*	1.70±0.26	2.22±0.35	2.04±0.24	2.68±0.27*
LVEDV (μl)	42.23±9.77	59.25±14.35*	42.63±10.28	57.34±11.03*	51.96±10.98	65.72±12.56*
LVESV (μl)	11.22±3.75	23.15±4.83*	8.78±3.42	17.36±6.71*	13.88±4.20	27.90±11.56*,#
LV mass (mg)	89.03±17.01	117.85±6.72*	94.05±32.04	121.99±4.62*	88.99±18.50	114.02±8.77*
StrokeVolume (μl)	31.00±6.57	38.57±8.45*	33.85±6.86	39.96±7.51*	38.07±6.94*	37.80±3.10*

Left ventricular end-systolic diameter (LVESD); Left ventricular end-diastolic diameter (LVEDD); Left ventricular end-systolic volume (LVESV); Left ventricular end-systolic volume (LVEDV). *, P<0.05 vs. corresponding WT shamand, #, vs. LKO PO, n=5-7.

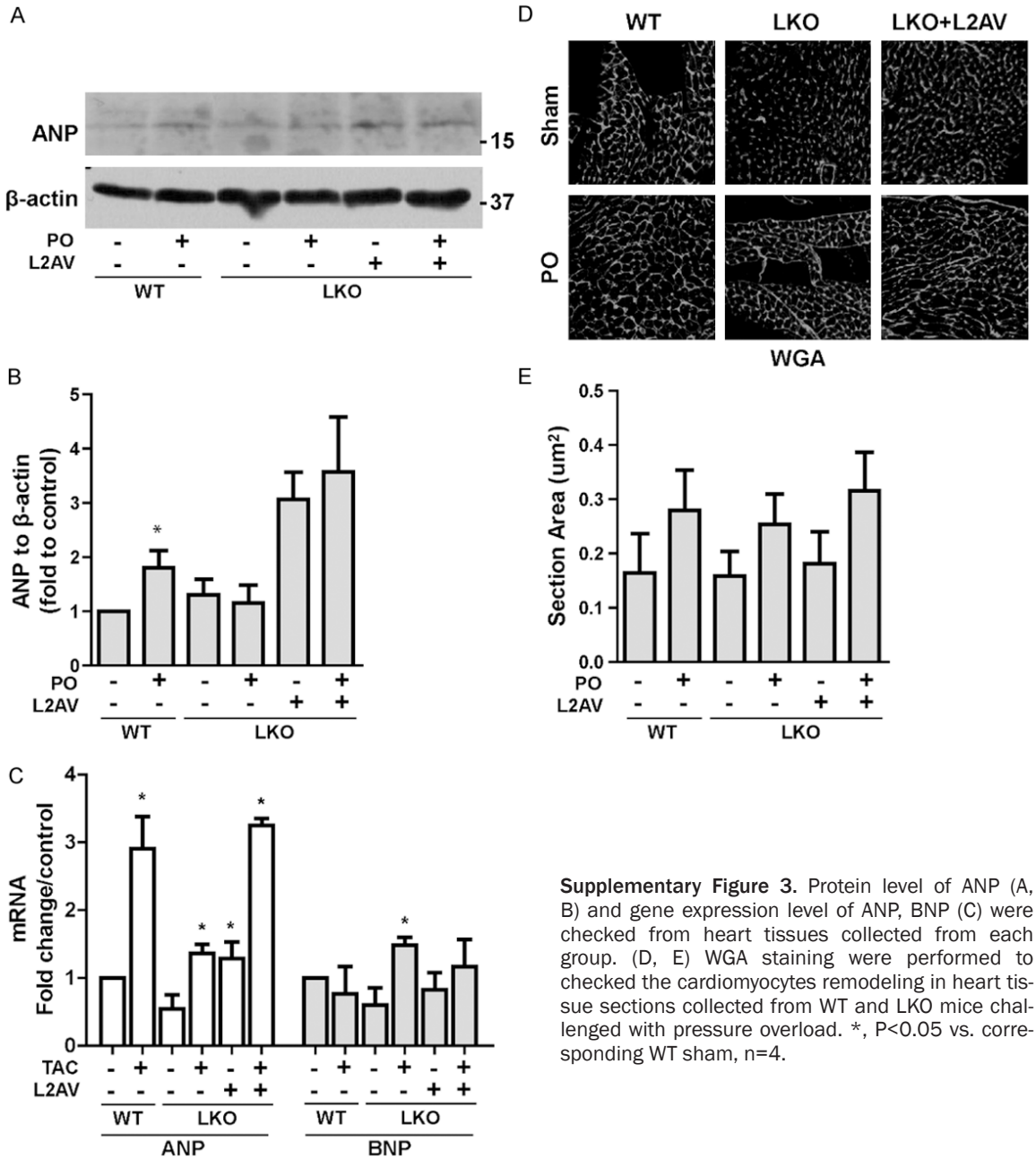

Supplementary Figure 3. Protein level of ANP (A, B) and gene expression level of ANP, BNP (C) were checked from heart tissues collected from each group. (D, E) WGA staining were performed to checked the cardiomyocytes remodeling in heart tissue sections collected from WT and LKO mice challenged with pressure overload. *, P<0.05 vs. corresponding WT sham, n=4.

Appendix E

COPYRIGHT PERMISSION

Copyright Permission to reproduce figure 1.2 & 1.3

JOHN WILEY AND SONS LICENSE TERMS AND CONDITIONS

Jul 05, 2017

This Agreement between York University -- Hye Kyoung Sung ("You") and John Wiley and Sons ("John Wiley and Sons") consists of your license details and the terms and conditions provided by John Wiley and Sons and Copyright Clearance Center.

License Number	4139010877270
License date	Jun 30, 2017
Licensed Content Publisher	John Wiley and Sons
Licensed Content Publication	Clinical and Experimental Pharmacology and Physiology
Licensed Content Title	Emerging clinical and experimental evidence for the role of lipocalin-2 in metabolic syndrome
Licensed Content Author	Yangsoo Jang,Jong Ho Lee,Yu Wang,Gary Sweeney
Licensed Content Date	Jan 30, 2012
Licensed Content Pages	6
Type of use	Dissertation/Thesis
Requestor type	University/Academic
Format	Electronic
Portion	Figure/table
Number of figures/tables	2
Original Wiley figure/table number(s)	Figure 1 and 2
Will you be translating?	No
Title of your thesis / dissertation	The effects of Lcn2 and iron on cardiac remodeling and the impact on cardiac function
Expected completion date	Sep 2017
Expected size (number of pages)	250
Requestor Location	York University 4700 keele st Toronto, ON M3J1P3 Canada Attn: BIOLOGY

Copyright Permission to reproduce figure 1.4

ELSEVIER LICENSE
TERMS AND CONDITIONS

Jul 05, 2017

This Agreement between York University -- Hye Kyoung Sung ("You") and Elsevier ("Elsevier") consists of your license details and the terms and conditions provided by Elsevier and Copyright Clearance Center.

License Number	4139020937510
License date	Jun 30, 2017
Licensed Content Publisher	Elsevier
Licensed Content Publication	Trends in Endocrinology & Metabolism
Licensed Content Title	Insulin resistance in the nervous system
Licensed Content Author	Bhumsoo Kim,Eva L. Feldman
Licensed Content Date	Mar 1, 2012
Licensed Content Volume	23
Licensed Content Issue	3
Licensed Content Pages	9
Start Page	133
End Page	141
Type of Use	reuse in a thesis/dissertation
Intended publisher of new work	other
Portion	figures/tables/illustrations
Number of figures/tables/illustrations	1
Format	electronic
Are you the author of this Elsevier article?	No
Will you be translating?	No
Order reference number	
Original figure numbers	figure 1
Title of your thesis/dissertation	The effects of Lcn2 and iron on cardiac remodeling and the impact on cardiac function

Copyright Permission to reproduce figure 1.5 & 1.6

NATURE PUBLISHING GROUP LICENSE TERMS AND CONDITIONS

Jul 05, 2017

This Agreement between York University -- Hye Kyoung Sung ("You") and Nature Publishing Group ("Nature Publishing Group") consists of your license details and the terms and conditions provided by Nature Publishing Group and Copyright Clearance Center.

License Number	4139021129869
License date	Jun 30, 2017
Licensed Content Publisher	Nature Publishing Group
Licensed Content Publication	Nature Reviews Molecular Cell Biology
Licensed Content Title	Self-consumption: the interplay of autophagy and apoptosis
Licensed Content Author	Guillermo Mariño, Mireia Niso-Santano, Eric H. Baehrecke, Guido Kroemer
Licensed Content Date	Jan 8, 2014
Licensed Content Volume	15
Licensed Content Issue	2
Type of Use	reuse in a dissertation / thesis
Requestor type	academic/educational
Format	print
Portion	figures/tables/illustrations
Number of figures/tables/illustrations	2
High-res required	no
Figures	Box1 and 2
Author of this NPG article	no
Your reference number	
Title of your thesis / dissertation	The effects of Lcn2 and iron on cardiac remodeling and the impact on cardiac function
Expected completion date	Sep 2017
Estimated size (number of pages)	250
Requestor Location	York University 4700 keele st

Copyright Permission to reproduce journal article:

Molecular and Cellular Endocrinology (2016) Jul 15; 430:68-76.

ELSEVIER LICENSE
TERMS AND CONDITIONS

Jul 05, 2017

This Agreement between York University -- Hye Kyoung Sung ("You") and Elsevier ("Elsevier") consists of your license details and the terms and conditions provided by Elsevier and Copyright Clearance Center.

License Number	4142120800217
License date	Jul 04, 2017
Licensed Content Publisher	Elsevier
Licensed Content Publication	Molecular and Cellular Endocrinology
Licensed Content Title	Lipocalin-2 inhibits autophagy and induces insulin resistance in H9c2 cells
Licensed Content Author	Yee Kwan Chan,Hye Kyoung Sung,James Won Suk Jahng,Grace Ha Eun Kim,Meng Han,Gary Sweeney
Licensed Content Date	Jul 15, 2016
Licensed Content Volume	430
Licensed Content Issue	n/a
Licensed Content Pages	9
Start Page	68
End Page	76
Type of Use	reuse in a thesis/dissertation
Portion	full article
Format	electronic
Are you the author of this Elsevier article?	Yes
Will you be translating?	No
Order reference number	
Title of your thesis/dissertation	The effects of Lcn2 and iron on cardiac remodeling and the impact on cardiac function
Expected completion date	Sep 2017
Estimated size (number of	250

Copyright Permission to reproduce journal article:

Journal of Cellular Physiology (2017) Aug; 232(8): 2125-2134

JOHN WILEY AND SONS LICENSE TERMS AND CONDITIONS

Jul 05, 2017

This Agreement between York University -- Hye Kyoung Sung ("You") and John Wiley and Sons ("John Wiley and Sons") consists of your license details and the terms and conditions provided by John Wiley and Sons and Copyright Clearance Center.

License Number	4142121024194
License date	Jul 04, 2017
Licensed Content Publisher	John Wiley and Sons
Licensed Content Publication	Journal of Cellular Physiology
Licensed Content Title	Lipocalin-2 (NGAL) Attenuates Autophagy to Exacerbate Cardiac Apoptosis Induced by Myocardial Ischemia
Licensed Content Author	Hye Kyoung Sung,Yee Kwan Chan,Meng Han,James Won Suk Jahng,Erfei Song,Eric Danielson,Thorsten Berger,Tak W. Mak,Gary Sweeney
Licensed Content Date	Mar 24, 2017
Licensed Content Pages	10
Type of use	Dissertation/Thesis
Requestor type	Author of this Wiley article
Format	Electronic
Portion	Full article
Will you be translating?	No
Title of your thesis / dissertation	The effects of Lcn2 and iron on cardiac remodeling and the impact on cardiac function
Expected completion date	Sep 2017
Expected size (number of pages)	250
Requestor Location	York University 4700 keele st Toronto, ON M3J1P3 Canada Attn: BIOLOGY
Publisher Tax ID	EU826007151

Copyright Permission to reproduce journal article:

Clinical Science (2015) 129(10):851-62

Dear Hye,

Thank you for your email.

I am pleased to say that you have permission to reuse the figure in your thesis as long as the original work is correctly cited in texgt and as part of a bibliography.

If you have any further questions, please do not hesitate to contact us.

Kind Regards,